Copy 1

NASA TM X-428

12/14/66
Code 5A
Page 151
X66.85067

NASA TM X-428

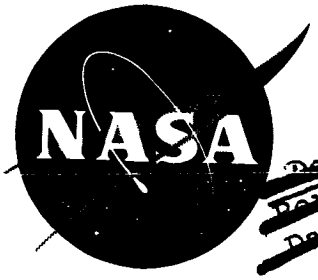

CON

TECHNICAL MEMORANDUM

X-428

DOWNGRADED TO
BY AUTHORITY OF NASA CLASSIFICATION
CHANGE NOTICE NO. 74 DATED
ITEM

SPECIAL RELEASE
On
referenced, or given further
distribution without approval of NASA

INVESTIGATION OF THE STATIC AERODYNAMIC CHARACTERISTICS OF A MODEL OF A BOMBER IN SIMULATED REFUELING POSITIONS BEHIND A TANKER MODEL AT MACH NUMBERS OF 1.57, 2.16, AND 2.87

By Royce L. McKinney, Julia A. Lancaster, and H. Norman Silvers

Langley Research Center
Langley Field, Va.

Downgraded
GROUP III
DOWNGRADED AT 12 YEAR INTERVALS; NOT AUTOMATICALLY DECLASSIFIED

REVIEW COPY

NASA HDQRTS. DOCMTN.
This document consists of ____ pages
Available to NASA Offices and No. 1 of 16 Copies; Series: A
Research Centers Only.

This material contains information affecting the National Defense of the United States
to an unauthorized person is prohibited by law.

FILE COPY
To be returned to

NATIONAL AERONAUTICS AND SPACE ADMINISTRATION
Washington, D. C.

(NASA-TM-X-428) INVESTIGATION OF THE STATIC AERODYNAMIC CHARACTERISTICS OF A MODEL OF A BOMBER IN SIMULATED REFUELING POSITIONS BEHIND A TANKER MODEL AT MACH NUMBERS OF 1.57, 2.16, AND (NASA) 151 p
71-71

CONFIDENTIAL

65 AS1-58

[redacted]

NATIONAL AERONAUTICS AND SPACE ADMINISTRATION

TECHNICAL MEMORANDUM X-428

INVESTIGATION OF THE

STATIC AERODYNAMIC CHARACTERISTICS OF A MODEL OF A BOMBER

IN SIMULATED REFUELING POSITIONS BEHIND A TANKER MODEL AT

MACH NUMBERS OF 1.57, 2.16, AND 2.87*

By Royce L. McKinney, Julia A. Lancaster,
[redacted] H. Norman Silvers

L 5 9 1

CLASSIFICATION CHANGE CONF
TO = UNCLASSIFIED

By authority of T.D. No. 24-126
Changed by C. L. Merritt Date 1/10/74

ABSTRACT

An investigation has been conducted in the Langley Unitary Plan wind tunnel to determine the effect of the flow field of a model of a supersonic bomber configuration, simulating a tanker aircraft, on the static forces and moments of a similar configuration, simulating the receiver aircraft. Tests were made with the receiver model at various combinations of longitudinal, lateral, and vertical positions relative to the tanker model for a range of angles of attack and sideslip of the receiver model. Reynolds number for the tests, based on the wing mean geometric chord of the receiver model, was 2.1×10^6.

[redacted]

CLASSIFICATION
BY AUTHO
CHANGE NOTICES NO.
NO.

NOTE: This document contains information
the national defense of the
United
within the meaning of the
Espionage Laws,
Sections
793 and 794. The transmission
revelation of its contents in any manner
to an unauthorized person is prohibited
by law.

[redacted]

Available to NASA Offices and

[redacted]

NATIONAL AERONAUTICS AND SPACE ADMINISTRATION

TECHNICAL MEMORANDUM X-428

INVESTIGATION OF THE STATIC AERODYNAMIC CHARACTERISTICS OF A MODEL OF A BOMBER IN SIMULATED REFUELING POSITIONS BEHIND A TANKER MODEL AT MACH NUMBERS OF 1.57, 2.16, AND 2.87*

By Royce L. McKinney, Julia A. Lancaster, and H. Norman Silvers

L 5 9 1

SUMMARY

Measurements were made of the forces and moments acting on a model of a supersonic canard bomber configuration while in and approaching possible refueling positions relative to a similar model. The receiver-model controls, based on estimates of control effectiveness, appear capable of trimming the moment coefficients experienced at all test positions. Relatively large changes in the static-stability parameters due to the tanker flow field were observed.

INTRODUCTION

An investigation has been conducted in the Langley Unitary Plan wind tunnel to determine the static aerodynamic characteristics of a model of a high-speed bomber configuration in the presence of a model considered to represent a high-speed tanker configuration. The investigation was made to obtain data with which an evaluation of the feasibility of supersonic refueling, based on experimental results, could be made. A complete evaluation would consist of the static effects of the tanker flow field on the receiver and, in addition, the dynamic behavior of the receiver as it approaches, occupies, and leaves typical refueling positions.

The present paper considers briefly only the effects of the tanker flow field on the static aerodynamic characteristics of the receiver. The control deflections required to trim the receiver model at any given

[redacted]

CONFIDENTIAL

position are used to evaluate the effect of the tanker flow field on the static aerodynamic characteristics of the receiver since the ability of the receiver to maintain position is a deciding factor in determining the possibility of supersonic in-flight refueling.

SYMBOLS

The aerodynamic force and moment data are referred to axes with their origin in the wing-chord plane and the plane of symmetry at the quarter-mean-geometric-chord point of the receiver model. The longitudinal data are referred to the stability axes and the lateral data, to the body axes (fig. 1). The coordinate system used to define the location of the receiver model has its origin at the quarter-mean-geometric-chord point in the wing-chord plane and the plane of symmetry of the tanker model. The wing geometry is based on a straight trailing edge without a cutout.

L 5 9 1

b wing span, in.

c local chord, in.

$\bar{c}$ mean geometric chord, in.

C_D' drag coefficient, $\frac{\text{Drag}}{qS}$

C_L lift coefficient, $\frac{\text{Lift}}{qS}$

C_l rolling-moment coefficient, $\frac{\text{Rolling moment}}{qSb}$

C_{l_β} lateral-stability parameter, $\partial C_l/\partial\beta$, per deg

C_m pitching-moment coefficient, $\frac{\text{Pitching moment}}{qS\bar{c}}$

$C_{m_{C_L}}$ longitudinal-stability parameter, $\partial C_m/\partial C_L$

C_n yawing-moment coefficient, $\frac{\text{Yawing moment}}{qSb}$

CONFIDENTIAL

C_{n_β} directional-stability parameter, $\partial C_m/\partial\beta$, per deg

C_Y side-force coefficient, $\frac{\text{Side force}}{qS}$

$C_{m_{\delta_c}}$ pitch control effectiveness, $\partial C_m/\partial\delta_c$, per deg

$C_{n_{\delta_r}}$ yaw control effectiveness, $\partial C_n/\partial\delta_r$, per deg

$C_{l_{\delta_a}}$ roll control effectiveness, $\partial C_l/\partial\delta_a$, per deg

L 5 9 1

l length of model, in.

M free-stream Mach number

q free-stream dynamic pressure, lb/sq ft

S wing area, sq ft

t wing thickness, in.

x distance, parallel to relative wind, between the 0.25$\bar{c}$ projections on the planes of symmetry of the tanker and the receiver models, positive downstream, in. (fig. 2)

y horizontal distance, perpendicular to the relative wind, between the 0.25$\bar{c}$ projections on the planes of symmetry of the tanker and the receiver models, positive to the left when viewed from the rear, in. (fig. 2)

z vertical distance, perpendicular to the relative wind, between the 0.25$\bar{c}$ projections on the planes of symmetry of the tanker and the receiver models, positive downward, in. (fig. 2)

α angle of attack, deg

β angle of sideslip, deg

δ_a roll-control-surface deflection angle relative to wing-chord plane, positive when trailing edge down for right aileron, deg

δ_c canard-surface deflection angle relative to wing-chord plane, positive when trailing edge down, deg

CONFIDENTIAL

δ_r rudder-control-surface deflection angle relative to fuselage center line, positive when trailing edge left, deg

Subscript:

nom nominal

APPARATUS AND TESTS

Tunnel

The investigation was conducted in the low Mach number test section of the Langley Unitary Plan wind tunnel, which is a variable-pressure continuous-flow tunnel. The nozzle leading to the test section is of the asymmetric sliding-block type, which permits a continuous variation in test-section Mach number from 1.5 to 2.9.

L 5 9 1

Models and Support Systems

The models used in this test consisted of two slightly different models of a supersonic bomber configuration. The two models were similar in configuration and size and were considered to be representative of possible supersonic bomber-tanker configurations. A drawing of the receiver model is shown in figure 3, and dimensions of both models are given in table I. Photographs of the models and support systems in the test section are shown in figure 4. The models have uncambered delta wings, canard control surfaces, twin vertical tails, and simulated engine housings with faired inlets below the wings.

The tanker model was supported by a sting and a vertical support strut that was rigidly attached to the tunnel ceiling (fig. 4). Vertical location of the tanker could be manually adjusted, thus, effectively changing the distance between the tanker and receiver models. Roll orientation of the tanker on the support sting could also be manually adjusted in 90° intervals through 360°. The sting of the tanker model was intended to simulate the boundary created by the exhaust flow from the tanker engines for the average conditions of thrust and Mach number of this investigation.

The receiver model was attached to an internally mounted six-component strain-gage balance, which was in turn attached to a sting mounted on a mechanism which allowed the angle of attack (wings horizontal attitude) to be remotely varied while keeping the vertical motion of the model reference point to a minimum. The angle-of-attack

CONFIDENTIAL

mechanism was attached to the main support sting which is remotely variable in longitudinal and lateral position, as well as angle of sideslip. Thus, the receiver model could be continuously varied in angle of attack, sideslip, and longitudinal and lateral position.

Test Conditions and Procedure

The tests were conducted at Mach numbers of 1.57, 2.16, and 2.87 and at stagnation pressures that were varied in order to provide a constant test Reynolds number of 2.1×10^6 based on the wing mean geometric chord of the receiver model. The stagnation temperature was 125° F. The dewpoint, measured at stagnation pressure, was maintained below -30° F in order to assure negligible condensation effects. The angle of attack of the receiver model varied from about -3° to 9° and the angle of sideslip varied from about -6° to 5°.

L 5 9 1

Pitch and sideslip runs without the tanker and tanker support system installed were made to determine the free-stream aerodynamic characteristics of the receiver. For each run made with the receiver-tanker combination, the angles of attack and sideslip of the tanker were constant. Two types of runs were made with the receiver in the presence of the tanker. One type of run, called a survey run, was made with the angles of attack and sideslip of the receiver held constant while the receiver position was varied. The receiver positions were varied longitudinally for several lateral positions and laterally for several longitudinal positions. The longitudinal survey runs were made at a nominal angle of attack of 3° and at an angle of sideslip of 0°. The lateral survey runs were made at a nominal angle of attack of 0° and several angles of sideslip.

The other type run made consisted of a variation in either angle of attack, called pitch runs, or sideslip, called sideslip runs, while both longitudinal, lateral, and vertical positions of the receiver were held constant. Most of the results were obtained with the models in the wings horizontal attitude (fig. 4(a)); however, some of the desired lateral positions of the receiver model relative to the tanker model could not be obtained with the models in the wings horizontal attitude and with the available strut settings. As a consequence, some tests were made with both models in the wings vertical attitude (fig. 4(b)) where the desired positions were available.

Corrections and Accuracy

All angles of attack, angles of sideslip, and distances between the two models have been corrected for deflection of the model support systems due to aerodynamic forces and moments. Since forces and moments

CONFIDENTIAL

were not measured on the tanker model, the forces and moments used to determine the deflections of the tanker-model support system were estimated from the measured results on the receiver model.

Balance-chamber pressure and base pressures were measured on the receiver model and the drag data were corrected to correspond to a balance chamber and base pressure equal to free-stream static pressure.

The maximum deviation of local Mach number from the average values presented in the data was ±0.020. A flow angularity exists in the vertical plane in the test section. The angles of attack for the wings horizontal attitude and the angles of sideslip for the wings vertical attitude have been corrected for this flow angularity.

Based on pretest calibration and balance accuracies, the accuracy of the force and moment coefficients, distances presented, and angles are estimated to be within the following limits:

C_D'	±0.0006
C_L	±0.004
C_l	±0.0007
C_m	±0.0007
C_n	±0.0003
C_Y	±0.001
x, in.	±0.05
y, in.	±0.2
z, in.	±0.2
α, deg	±0.1
β, deg	±0.1

PRESENTATION OF RESULTS

Schlieren photographs of the tanker-receiver combination are presented in figure 5. The data from the receiver-alone tests, representing free-stream receiver characteristics, and the data obtained with the receiver model in the flow field of the tanker model are presented in figures 6 to 21 as follows:

	Figure
Aerodynamic characteristics in pitch:	
Receiver alone	6
Receiver in presence of tanker	7 to 11
Longitudinal survey	14 to 17
Lateral survey	18

CONFIDENTIAL

Figure

Aerodynamic characteristics in sideslip:
Receiver alone 12
Receiver in presence of tanker 13
Lateral survey . . . . . 19 to 21

The angles of attack and sideslip of the tanker model varied with roll orientation and Mach number. These are presented as follows:

Figures	α, deg	β, deg	α, deg	β, deg	α, deg	β, deg
	at M = 1.57		at M = 2.16		at M = 2.87	
7 to 10; 14 to 16; 18 to 21	3.67	0	4.82	0	2.44	0
11 to 13; 17	3.13	-0.45	3.10	-1.51	2.94	0.45

DISCUSSION OF RESULTS

Basic Results

The basic data as presented in figures 7 to 11 and 13 to 21 were obtained, using the run types previously described, in the octant to the left of, behind, and below the tanker model defined by the following ranges of displacement variables:

$\frac{x}{l/4}$ . . . . . 0 to 6

$\frac{y}{b/4}$ . . . . . -0.4 to 5

$\frac{z}{b/4}$ . . . . . 0 to 4

These data represent a mapping of the effects of the tanker flow field on the receiver characteristics over the region defined in the preceding table. In order to maintain a position relative to the tanker, the receiver would be required to trim at some lift coefficient with all other force and moment coefficients equal to zero. For this reason, the ability of the receiver to trim the moments induced by the tanker becomes the deciding factor in determining the feasibility of supersonic in-flight refueling when considered from a static viewpoint.

CONFIDENTIAL

Trim Characteristics

An indication of the severity of the changes which occur in moment coefficients of the receiver due to the effects of the tanker flow field may be obtained from the receiver control deflections required to trim at a constant lift coefficient. In order to determine these trim control deflections it is necessary to know the various control effectiveness values. Since no tests were made to determine these values for the present configuration, they were estimated from references 1, 2, and 3. Control effectiveness was assumed to be proportional to the ratios of control surface area to wing area and distance to the centroid of the control surface to mean geometric chord for longitudinal and directional control. For estimation of lateral control, mean geometric chord was replaced by wing span. It was also assumed that longitudinal trim was furnished solely by canard deflection; directional trim, by all-movable vertical tails; and lateral trim, by flap-type control surfaces at the wing trailing edge. The resulting estimated values of control effectiveness are presented in the following table:

	M = 1.57	M = 2.16	M = 2.87
Control type:			
Longitudinal, $C_{m_{\delta_c}}$, per deg	0.0042	0.0031	0.0017
Lateral, $C_{l_{\delta_a}}$, per deg	-0.00086	-0.00064	-0.00035
Directional, $C_{n_{\delta_r}}$, per deg	-0.00092	-0.00069	-0.00047

A lift coefficient $(C_L = 0.15)$ near that for maximum lift-drag ratio was selected for estimation of trim control deflections. With the use of this constant lift coefficient, curves of pitching-moment coefficient versus longitudinal position were prepared for those combinations of lateral and vertical position at which the maximum untrimmed pitching moments occurred (fig. 22). By using the longitudinal control effectiveness values presented in the preceding table, it was found that the largest control deflection required would be about 13° (M = 2.87), which is well within the range where the canard-type control used for the present configuration remains effective.

A similar analysis was made for yawing-moment coefficient and rolling-moment coefficient, using figures 19 to 21 and the values of yaw and roll control effectiveness appearing in the preceding table. It was found that the receiver could be trimmed about the yaw and roll axes with control deflections less than 10° for all those positions investigated.

CONFIDENTIAL

Stability Characteristics

Although the analysis of the trim-control requirements made in the preceding section includes the effects of the flow field of the tanker on the static-stability characteristics of the receiver, it is felt to be of interest to summarize separately the longitudinal-stability parameter $C_{m_{C_L}}$, directional-stability parameter C_{n_β}, and the lateral-stability parameter C_{l_β} for the positions used in the foregoing analysis. These results are presented in figure 23.

L
5
9
1

The largest change in aerodynamic-center location due to change in longitudinal position was about 11.5 percent of the mean geometric chord. The maximum change in the directional-stability parameter is 0.0008, which is 80 percent of the directional stability of the receiver alone at a Mach number of 2.16. The maximum change in the lateral-stability parameter is equivalent to a change in effective dihedral of about 10° (assuming 1° of effective dihedral is equivalent to a C_{l_β} of 0.00008 (ref. 4)). These changes are felt to be serious; however, static instability was not encountered for any test condition.

CONCLUDING REMARKS

Measurements were made of the forces and moments acting on a model of a supersonic canard bomber while approaching and in possible refueling positions relative to a similar model. The results indicate that the receiver-model controls, based on estimates of control effectiveness, appear capable of trimming the moment coefficients experienced at all test positions. Relatively large changes which were observed in the static-stability parameter due to the tanker flow field should receive attention in the design of an aircraft intended to have supersonic-refueling capabilities.

Langley Research Center,
National Aeronautics and Space Administration,
Langley Field, Va., September 19, 1960.

REFERENCES

1. Church, James D., and Taylor, Nancy L.: An Investigation of a 0.05-Scale Model of the XSM-64A Navaho Missile and Booster at Supersonic Mach Numbers. Part I - Force Study. NASA TM X-16, 1959.

2. Carmel, Melvin M., Kelly, Thomas C., and Gregory, Donald T.: Aerodynamic Characteristics at Mach Numbers From 2.5 to 3.5 of a Canard Bomber Configuration Designed for Supersonic Cruise Flight. NACA RM L58G16, 1958.

3. Kelly, Thomas C., Carmel, Melvin M., and Gregory, Donald T.: An Exploratory Investigation at Mach Numbers of 2.50 and 2.87 of a Canard Bomber-Type Configuration Designed for Supersonic Cruise Flight. NACA RM L58B28, 1958.

4. Purser, Paul E.: An Approximation to the Effect of Geometric Dihedral on the Rolling Moment Due to Sideslip for Wings at Transonic and Supersonic Speeds. NACA RM L52B01, 1952.

L 5 9 1

CONFIDENTIAL

TABLE I.- GEOMETRIC CHARACTERISTICS OF THE MODELS

(a) Receiver model

Wing[1]:	
Airfoil section parallel to root chord:	
66-series forward of 0.45c; constant thickness 0.45c to constant-angle trailing edge defined by: t/c = 0.02 at 1.488-in. span location; t/c = 0.025 at 3.686-in. span location; zero thickness at wing tip	
Type	Delta
Span, in.	10.27
Total area, including wing cutout, sq ft	0.390
Aspect ratio	1.88
Taper ratio	0
Sweepback of quarter-chord line, deg	57.80
Dihedral angle, deg	0
Incidence angle, deg	0
Geometric twist, deg	0
Tip-chord length, in.	0
Root-chord length, in.	10.94
Length of $\bar{c}$, in.	7.30
Vertical location of 0.25$\bar{c}$, in.	0
Span location of $\bar{c}$, in.	1.71
Longitudinal location of 0.25$\bar{c}$, in. from nose	12.86
Fuselage:	
Upper:	
Length, in.	17.84
Maximum height, in.	0.83
Maximum width, in.	0.83
Frontal area, sq in.	0.54
Lower:	
Length, in.	10.44
Maximum height, in.	0.85
Maximum width, in.	1.83
Frontal area, sq in.	1.18
Base area, sq in.	0.40
Cavity area, sq in.	0.40
Vertical tail:	
Airfoil section parallel to root chord:	
0.30c to 0.70c hexagonal; t/c = 0.037 at root; t/c = 0.026 at tip	
Span, in.	1.44
Area, sq in.	2.07
Aspect ratio	1.00
Taper ratio	0.30
Sweepback of quarter-chord line, deg	45.00
Dihedral angle, deg	0
Incidence angle, deg	0
Geometric twist, deg	0
Tip-chord length, in.	0.66
Root-chord length, in.	2.22
Length of $\bar{c}$, in.	1.58
Vertical location of 0.25$\bar{c}$, in.	0.65
Span location of $\bar{c}$, in.	1.38
Longitudinal location of 0.25$\bar{c}$, in. from nose	16.72
Canard surface:	
Airfoil section parallel to root chord:	
0.30c to 0.70c hexagonal; t/c = 0.02 at root; t/c = 0.0375 at tip	
Span, in.	2.88
Total area, sq in.	5.22
Exposed area, sq in.	3.05
Aspect ratio	1.59
Taper ratio	0.29
Sweepback of quarter-chord line, deg	38.00
Dihedral angle, deg	0
Incidence angle, deg	0
Geometric twist, deg	0
Tip-chord length, in.	0.81
Root-chord length, in.	2.82
Length of $\bar{c}$, in.	2.00
Vertical location of 0.25$\bar{c}$, in.	0.59
Span location of $\bar{c}$, in.	0.59
Longitudinal location of 0.25$\bar{c}$, in. from nose	3.62

[1]Wing geometry based on straight trailing edge with no cutout.

CONFIDENTIAL

CONFIDENTIAL

TABLE I.- GEOMETRIC CHARACTERISTICS OF THE MODELS - Concluded

(b) Tanker model

Wing:	
Airfoil section parallel to root chord: 66-series; t/c = 0.025 to 0.45c; 0.45c to 0.70c constant thickness; 0.70c to 1.00c wedge	
Type	Delta
Span, in.	10.15
Total area, including wing cutout, sq ft	0.391
Aspect ratio	1.88
Taper ratio	0
Sweepback of quarter-chord line, deg	58.00
Dihedral angle, deg	0
Incidence angle, deg	0
Geometric twist, deg	0
Tip-chord length, in.	0
Root-chord length, in.	10.80
Length of $\bar{c}$, in.	7.20
Vertical location of 0.25$\bar{c}$, in.	0
Span location of $\bar{c}$, in.	1.69
Longitudinal location of 0.25$\bar{c}$, in. from nose	12.87
Fuselage:	
Upper:	
Length, in.	13.80
Maximum height, in.	0.73
Maximum width, in.	0.82
Lower:	
Length, in.	10.27
Maximum height, in.	0.74
Maximum width, in.	2.11
Vertical tail:	
Airfoil section parallel to root chord: 0.30c to 0.70c hexagonal; t/c = 0.0325 at root; t/c = 0.0250 at tip	
Span, in.	1.44
Total area, sq in.	2.07
Aspect ratio	1.00
Taper ratio	0.30
Sweepback of quarter-chord line, deg	45.00
Dihedral angle, deg	0
Incidence angle, deg	0
Geometric twist, deg	0
Tip-chord length, in.	0.66
Root-chord length, in.	2.22
Length of $\bar{c}$, in.	1.58
Vertical location of 0.25$\bar{c}$, in.	0.60
Span location of $\bar{c}$, in.	1.77
Longitudinal location of 0.25$\bar{c}$, in. from nose	17.12
Canard surfaces:	
Airfoil section parallel to root chord: Designated by the manufacturer as 66A003; t/c = 0.03	
Span, in.	2.69
Total area, sq in.	4.48
Exposed area, sq in.	2.85
Aspect ratio	1.61
Taper ratio	0.28
Sweepback of quarter-chord line, deg	38.00
Dihedral angle, deg	0
Incidence angle, deg	0
Geometric twist, deg	0
Tip-chord length, in.	0.73
Root-chord length, in.	2.60
Length of $\bar{c}$, in.	1.85
Vertical location of 0.25$\bar{c}$, in.	0.49
Span location of $\bar{c}$, in.	0.55
Longitudinal location of 0.25$\bar{c}$, in. from nose	4.75

CONFIDENTIAL

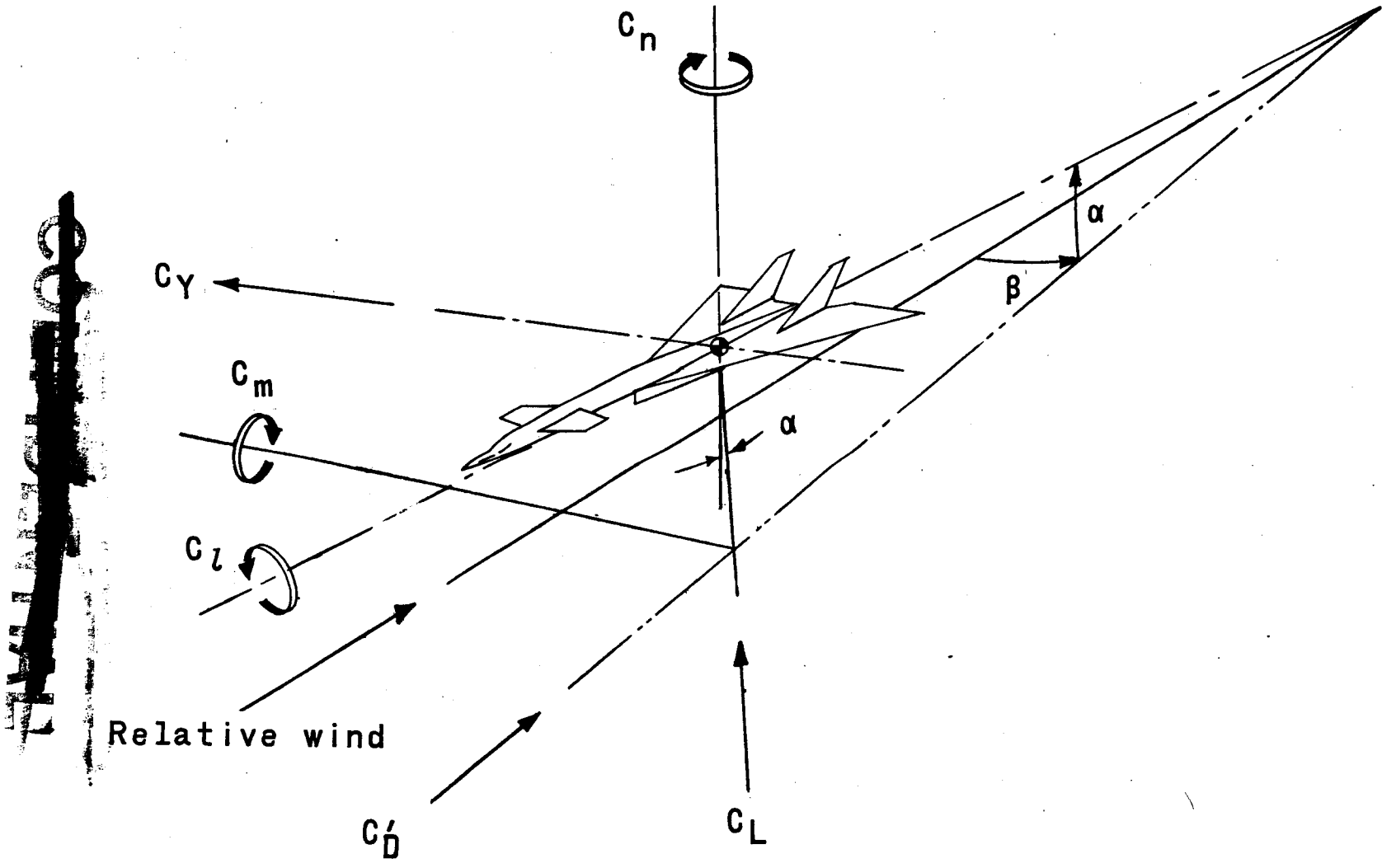

Figure 1.- Axes system. (Positive directions are indicated by arrows.)

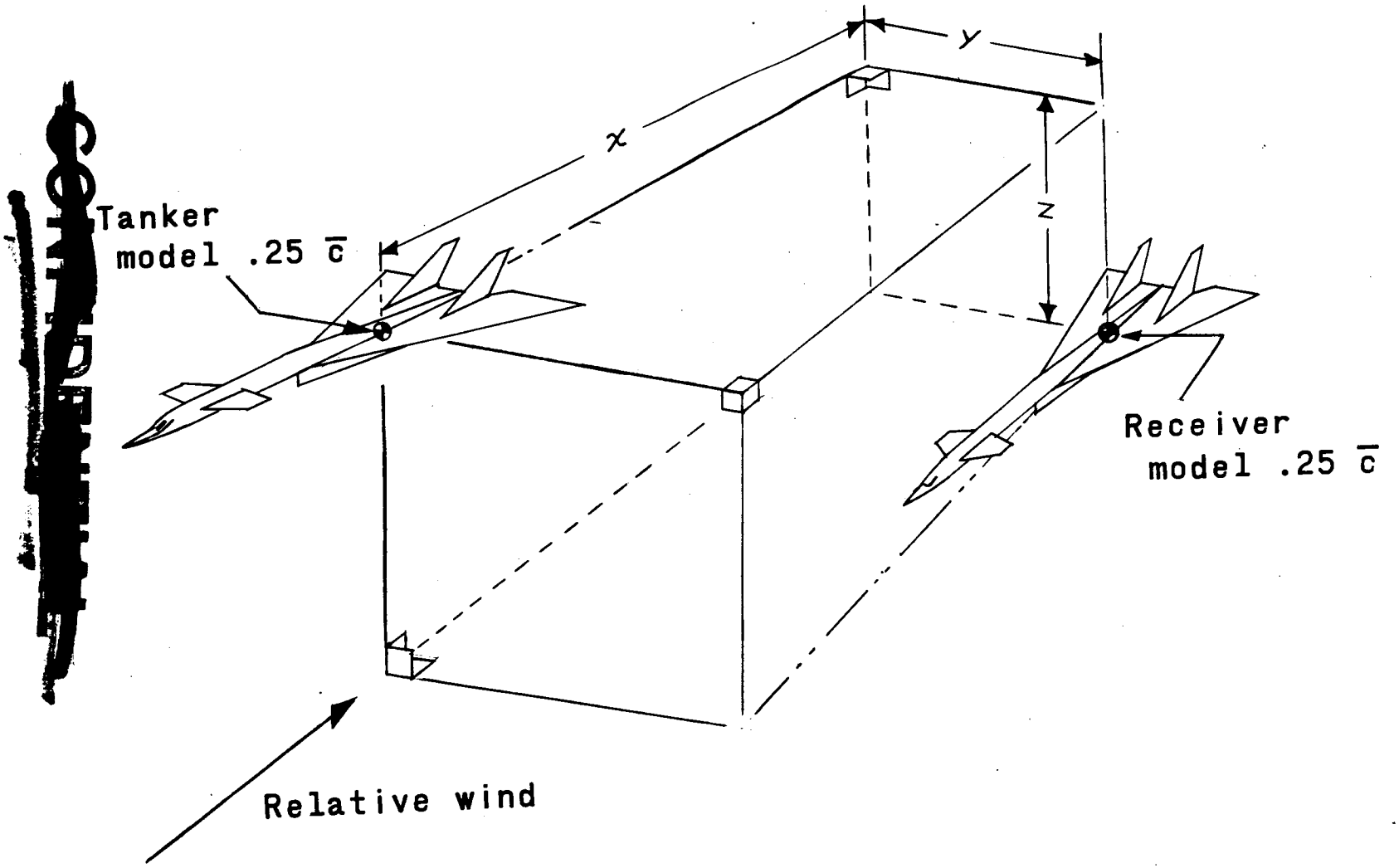

Figure 2.- Orthogonal axes system, displacement data.

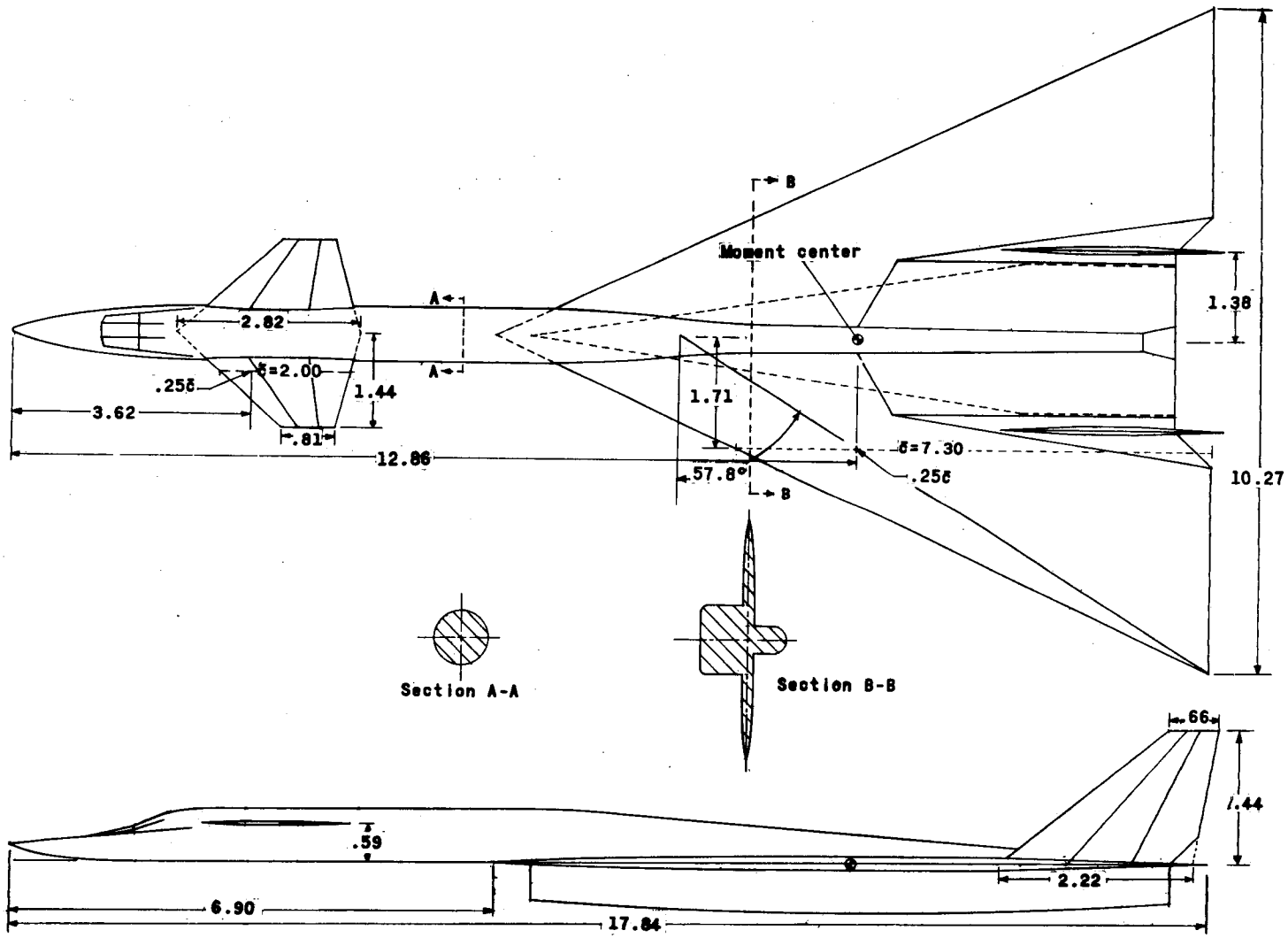

Figure 3.- Receiver-model details. All dimensions in inches unless otherwise noted.

CONFIDENTIAL SECRET

(a) Wings horizontal. L-58-909a

Figure 4.- Photographs of the receiver and tanker models mounted in Unitary Plan wind tunnel.

CONFIDENTIAL SECRET

CONFIDENTIAL SECRET

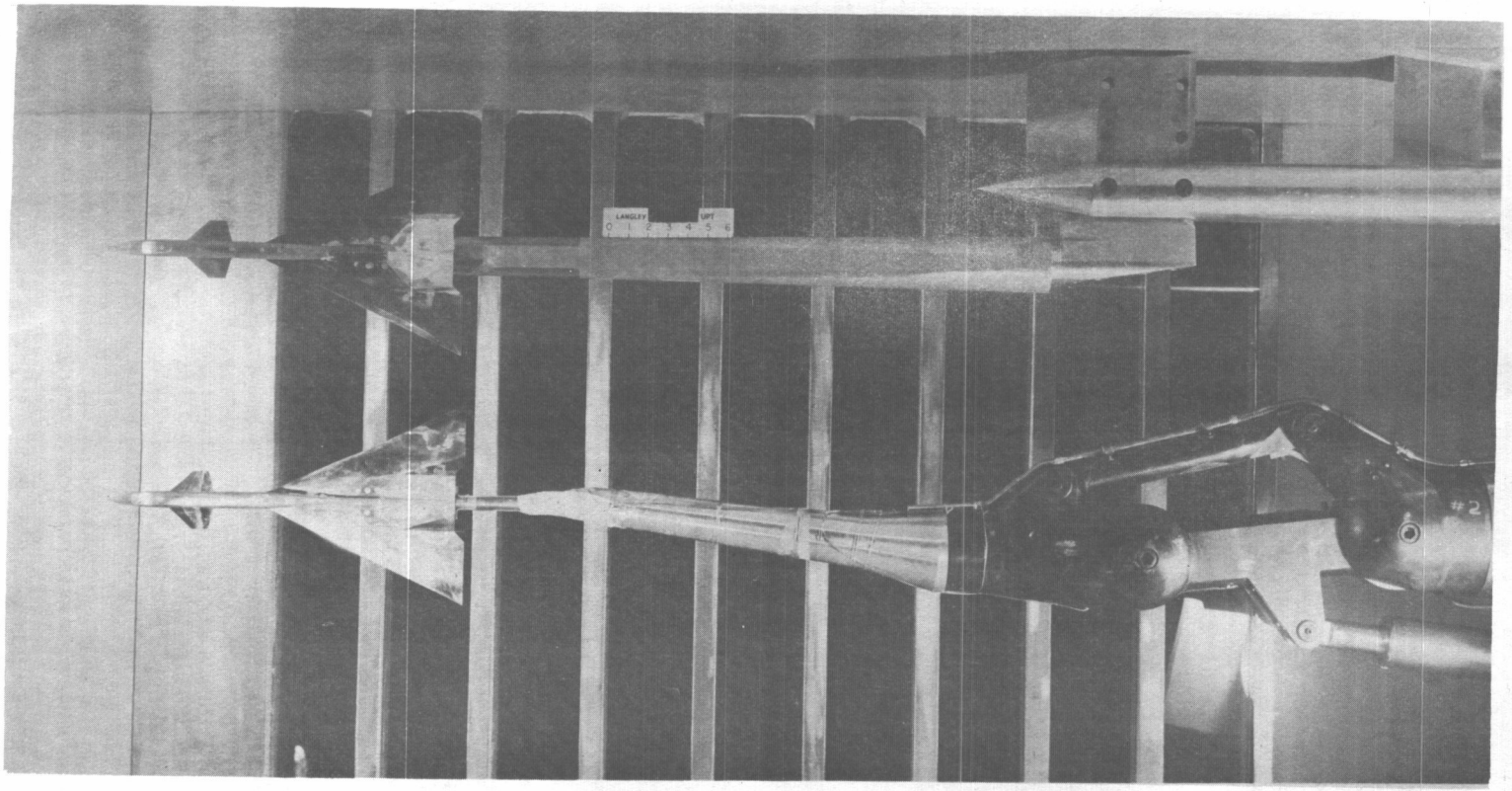

(b) Wings vertical. L-58-913a

Figure 4.- Concluded.

CONFIDENTIAL SECRET

CONFIDENTIAL SECRET

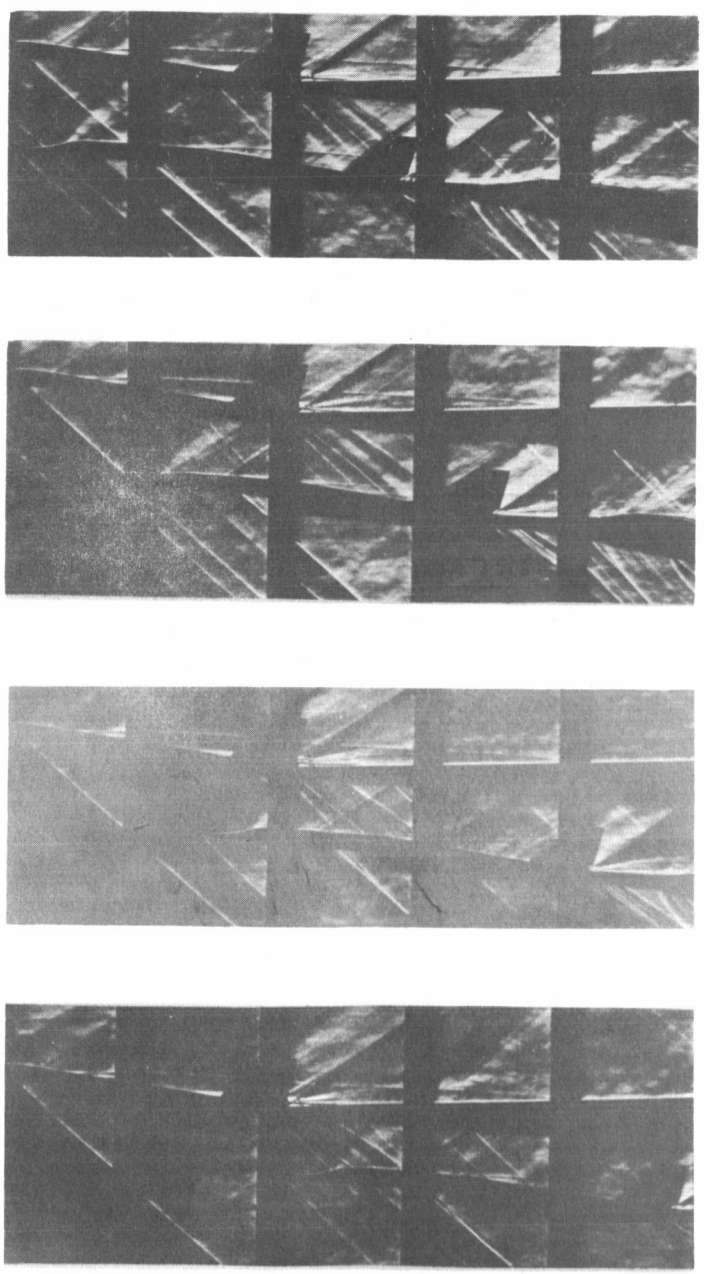

(a) $\left(\frac{z}{b/4}\right)_{nom} = 2$; M = 1.57. L-60-6901

Figure 5.- Typical schlieren photographs of the receiver and tanker models. α_{nom} of receiver = 3°; β = 0°; $\frac{y}{b/4} = 0$.

CONFIDENTIAL SECRET

CONFIDENTIAL SECRET

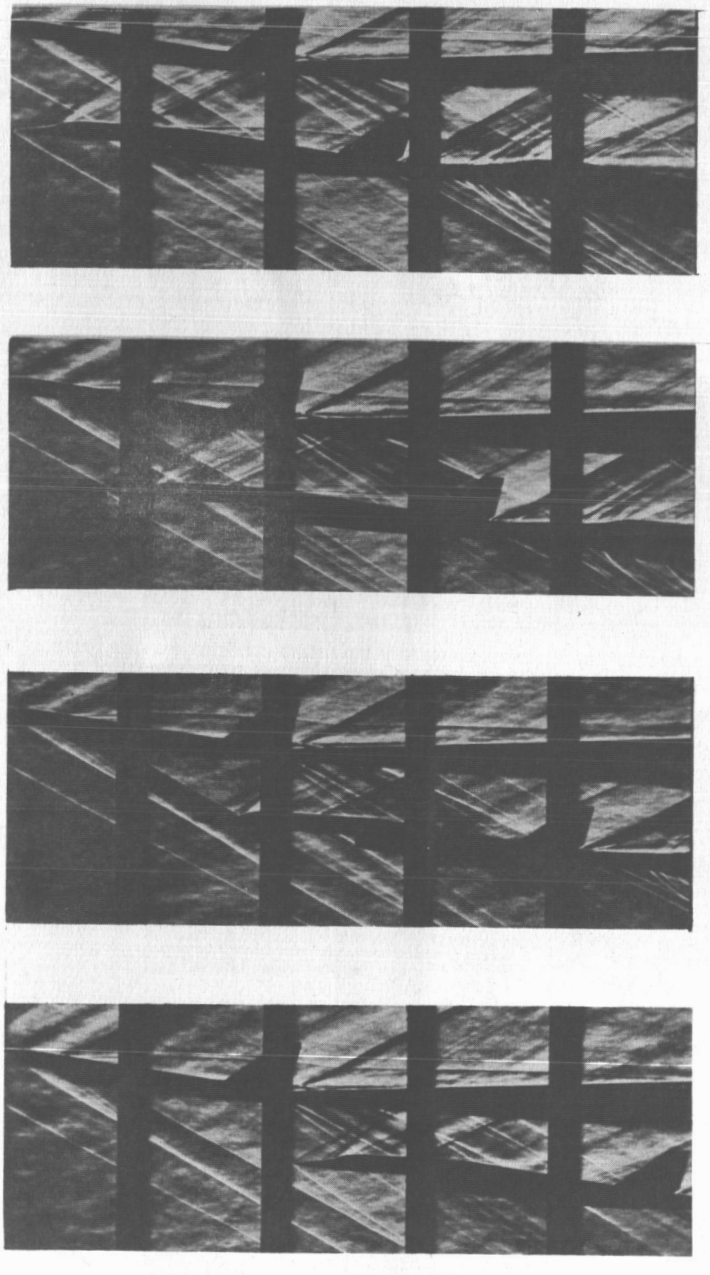

(b) $\left(\frac{z}{b/4}\right)_{nom} = 2$; M = 2.16. L-60-6902

Figure 5.- Continued.

CONFIDENTIAL SECRET

CONFIDENTIAL SECRET

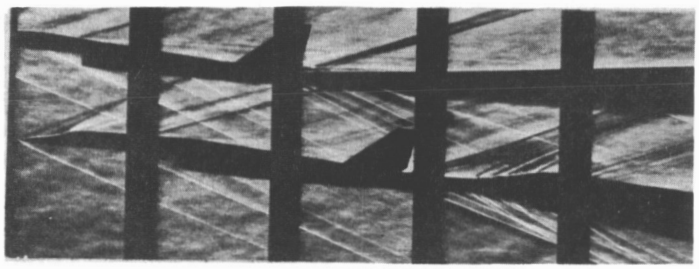

$\left(\frac{x}{l/4}\right)_{nom}$

1

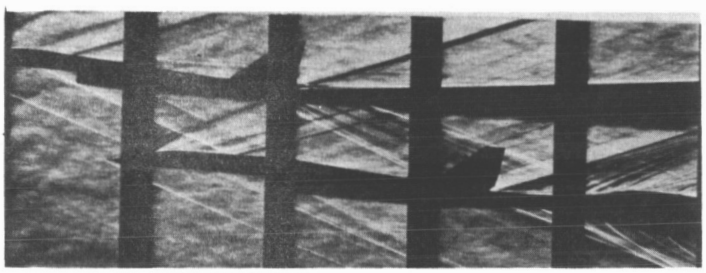

2

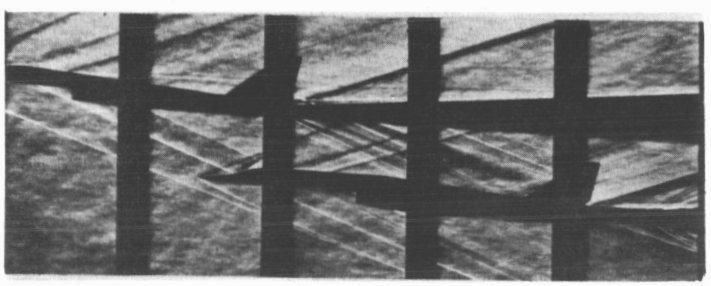

3

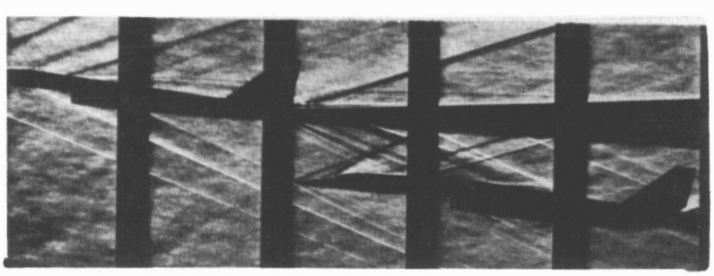

4

(c) $\left(\frac{z}{b/4}\right)_{nom} = 2$; M = 2.87. L-60-6903

Figure 5.- Continued.

CONFIDENTIAL SECRET

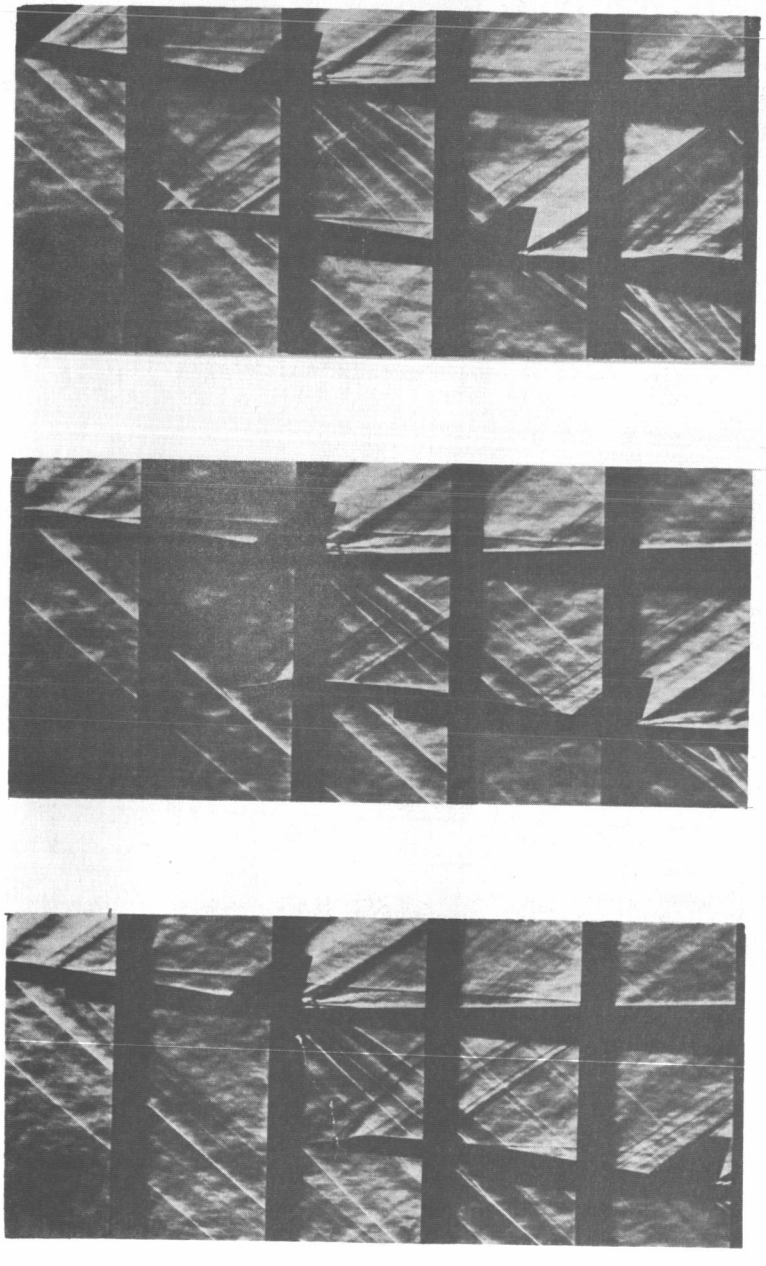

(d) $\left(\frac{z}{b/4}\right)_{nom} = 3$; M = 1.57.

L-60-6904

Figure 5.- Continued.

L-591

CONFIDENTIAL SECRET

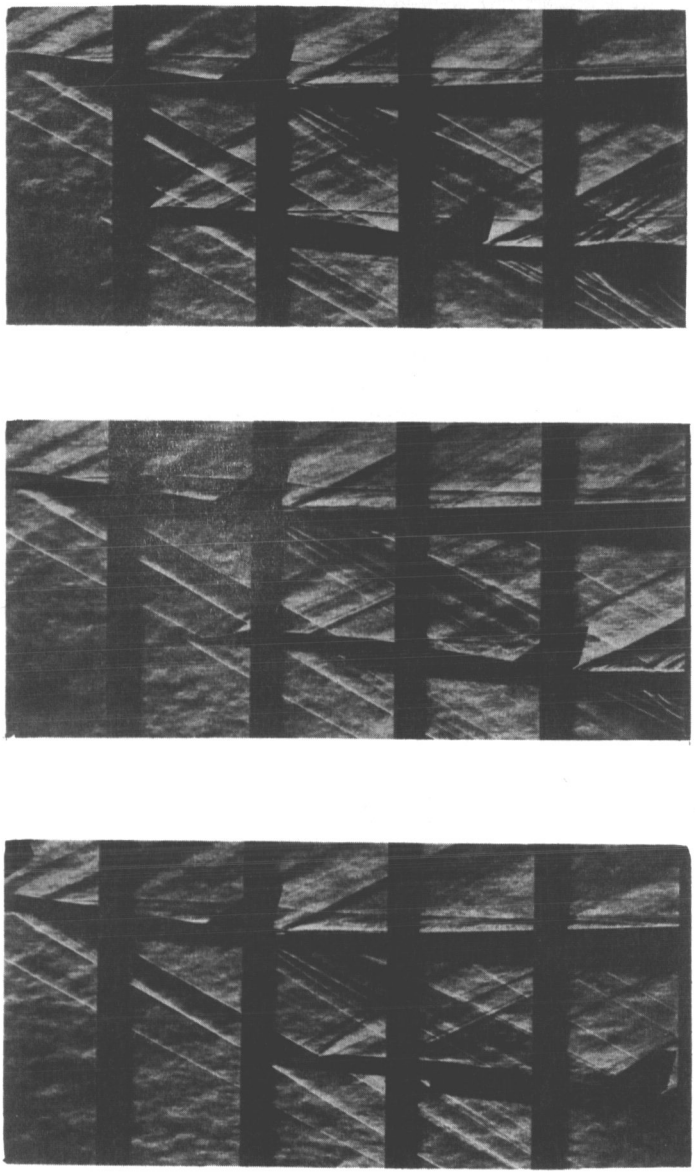

$\left(\frac{x}{l/4}\right)_{nom}$

2

3

4

(e) $\left(\frac{z}{b/4}\right)_{nom} = 3$; M = 2.16. L-60-6905

Figure 5.- Continued.

CONFIDENTIAL SECRET

CONFIDENTIAL SECRET

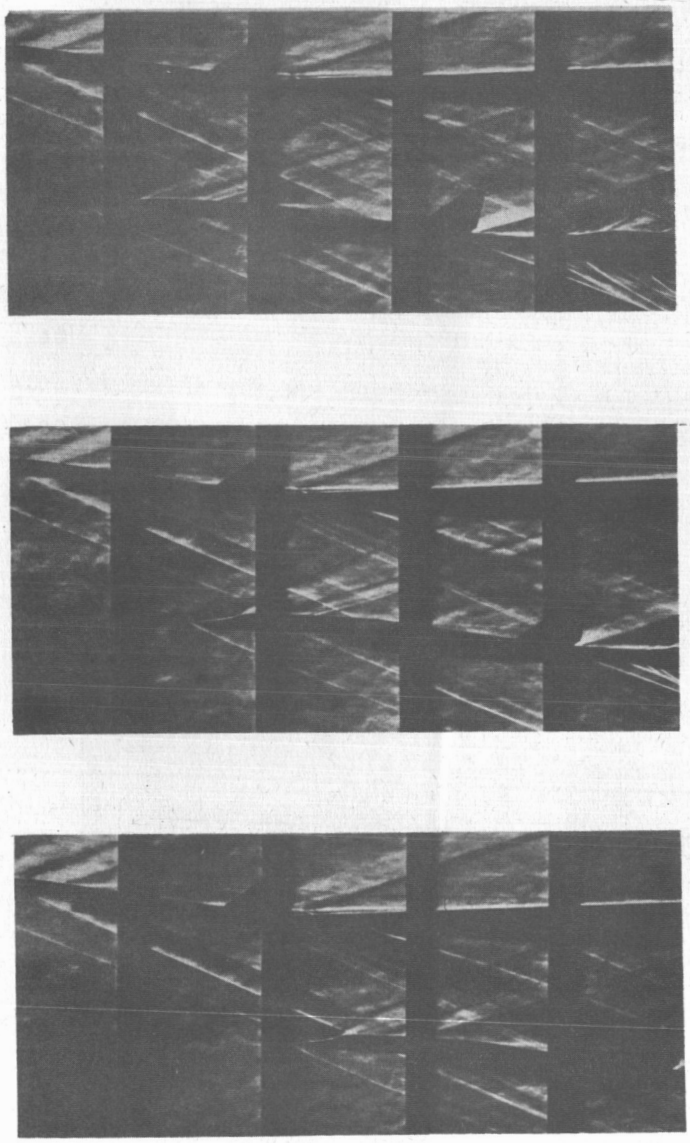

$\left(\frac{x}{l/4}\right)_{nom}$

2

3

4

(f) $\left(\frac{z}{b/4}\right)_{nom} = 3$; M = 2.87. L-60-6906

Figure 5.- Concluded.

CONFIDENTIAL SECRET

CONFIDENTIAL SECRET

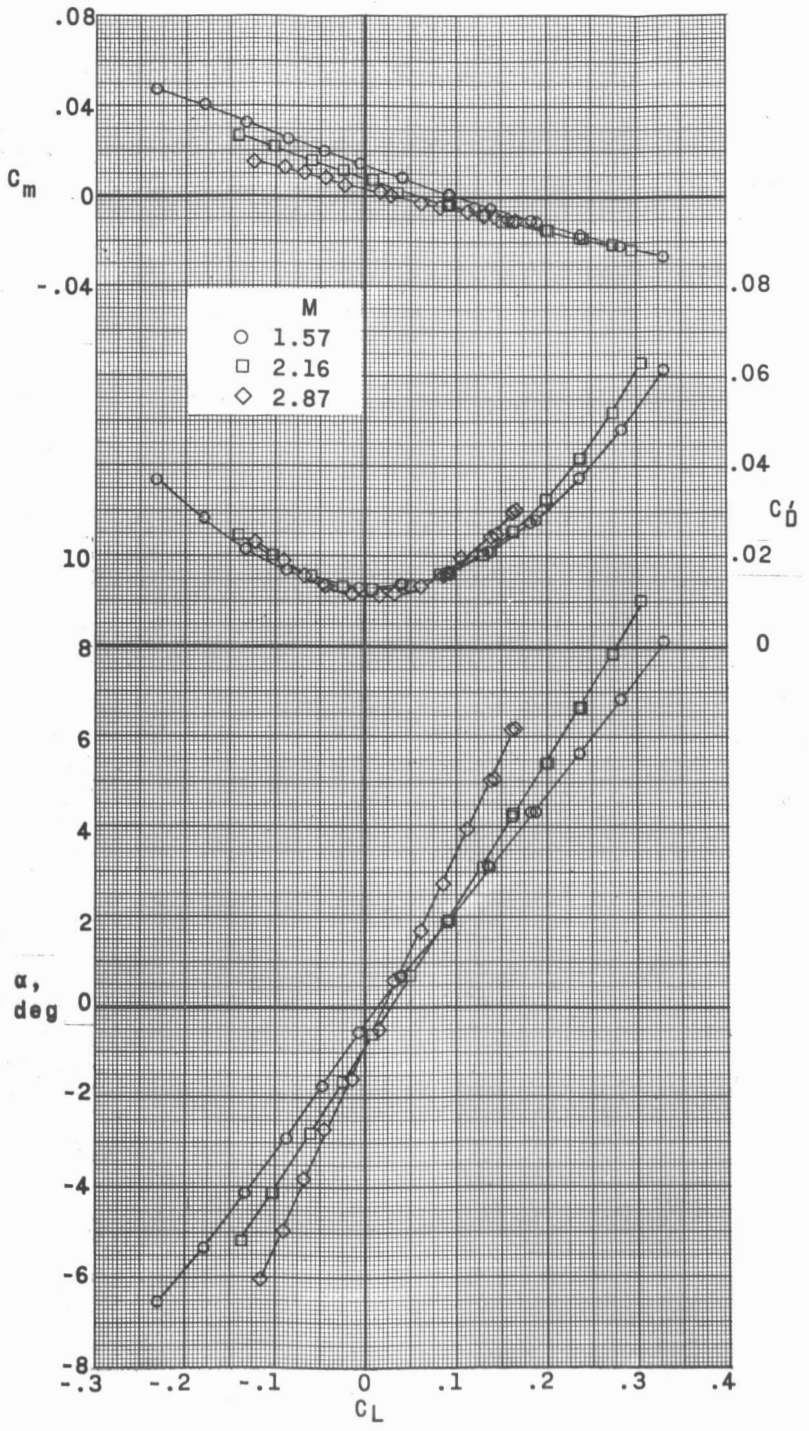

Figure 6.- Aerodynamic characteristics in pitch of the receiver model alone. $\beta = 0^{o}$.

CONFIDENTIAL SECRET

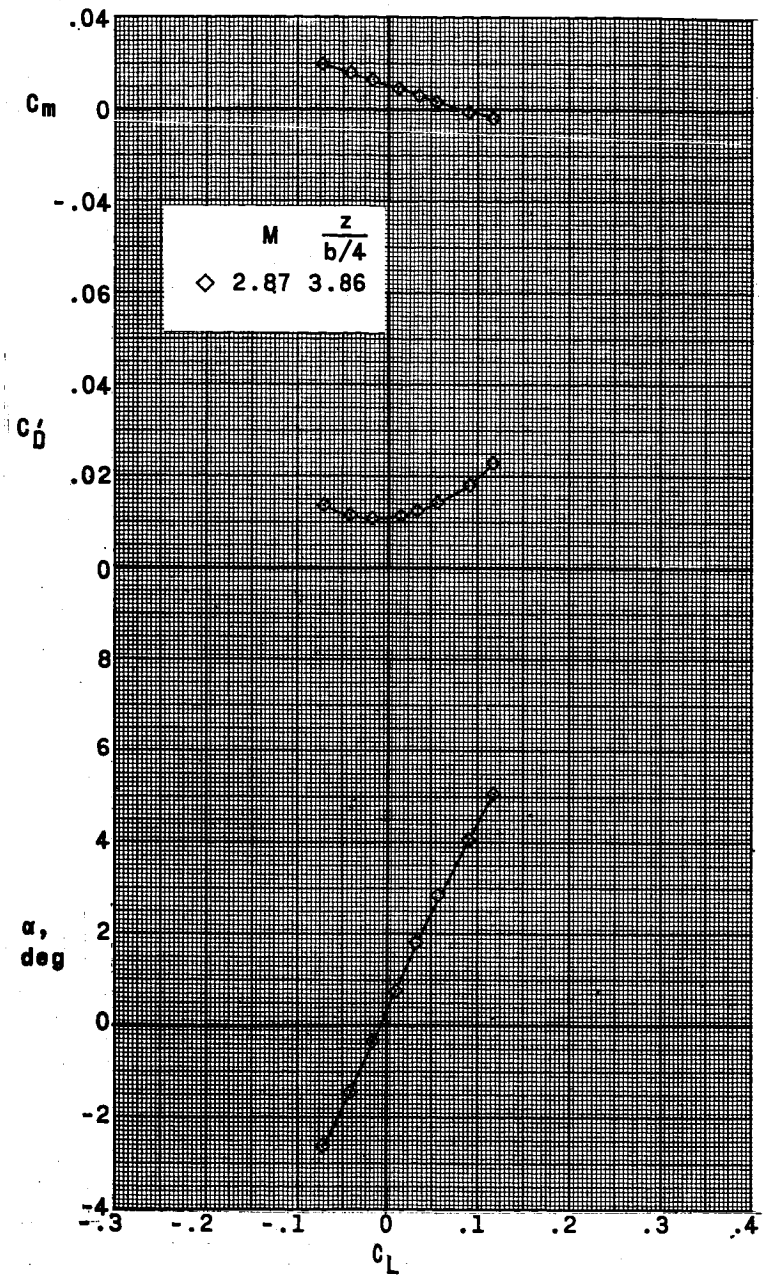

(a) $\left(\frac{z}{b/4}\right)_{nom} = 4.0$; $\frac{x}{l/4} = 4.02$.

Figure 7.- Aerodynamic characteristics in pitch of the receiver model in presence of tanker model. $\beta = 0^\circ$; $\frac{y}{b/4} = -0.4$.

L-591

CONFIDENTIAL

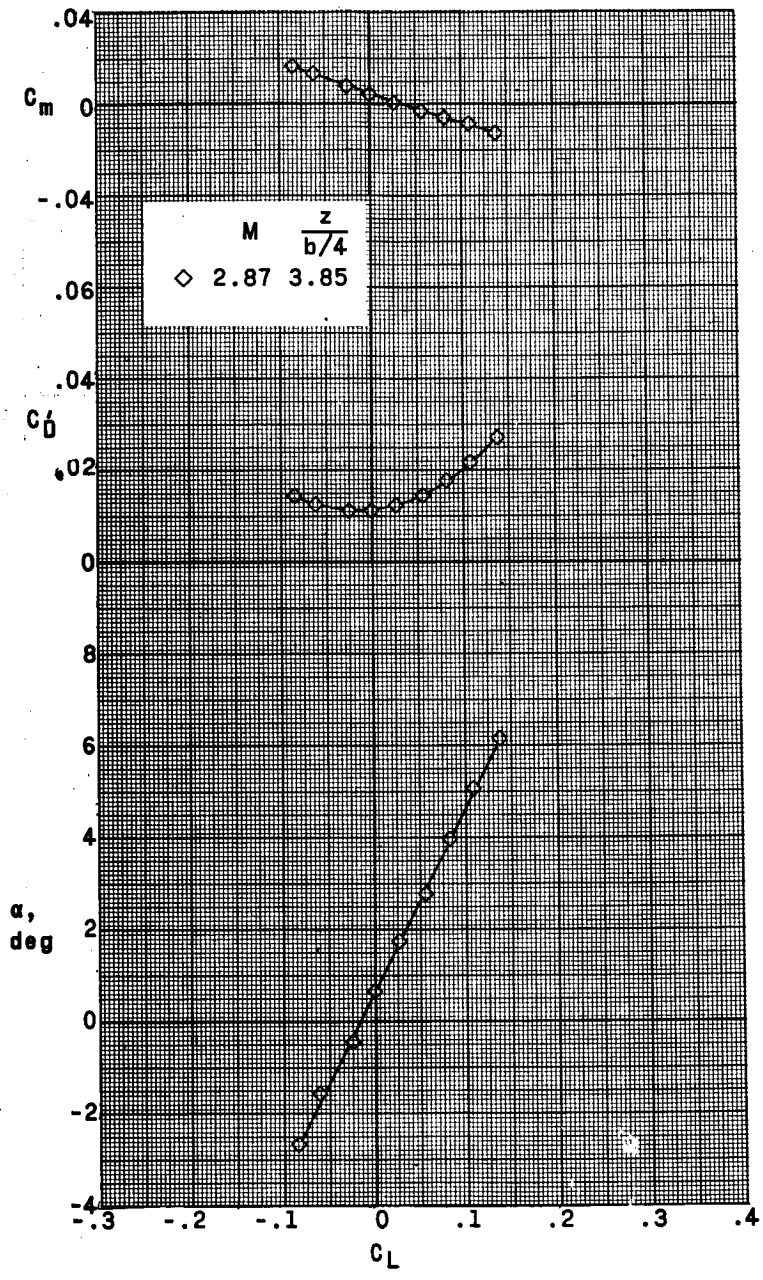

(b) $\left(\frac{z}{b/4}\right)_{nom} = 4.0; \frac{x}{l/4} = 5.02.$

Figure 7.- Continued.

CONFIDENTIAL

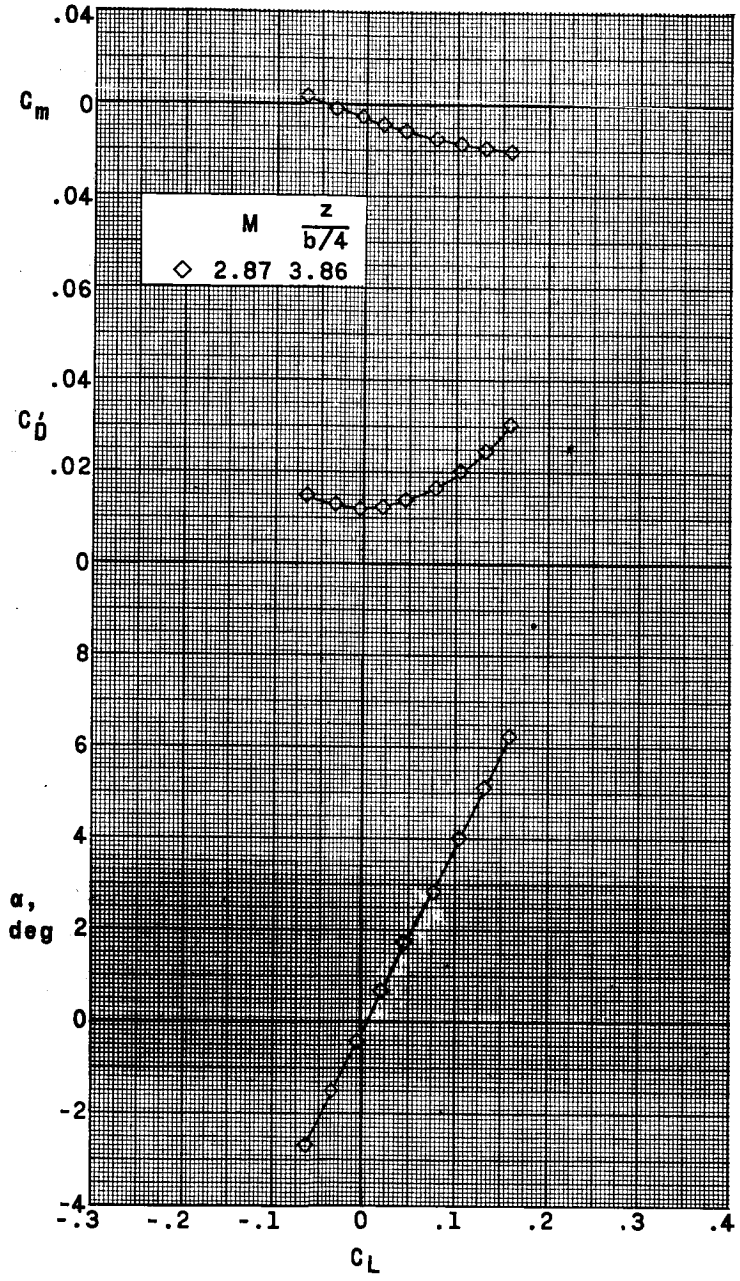

(c) $\left(\frac{z}{b/4}\right)_{nom} = 4.0$; $\frac{x}{l/4} = 6.02$.

Figure 7.- Concluded.

CONFIDENTIAL

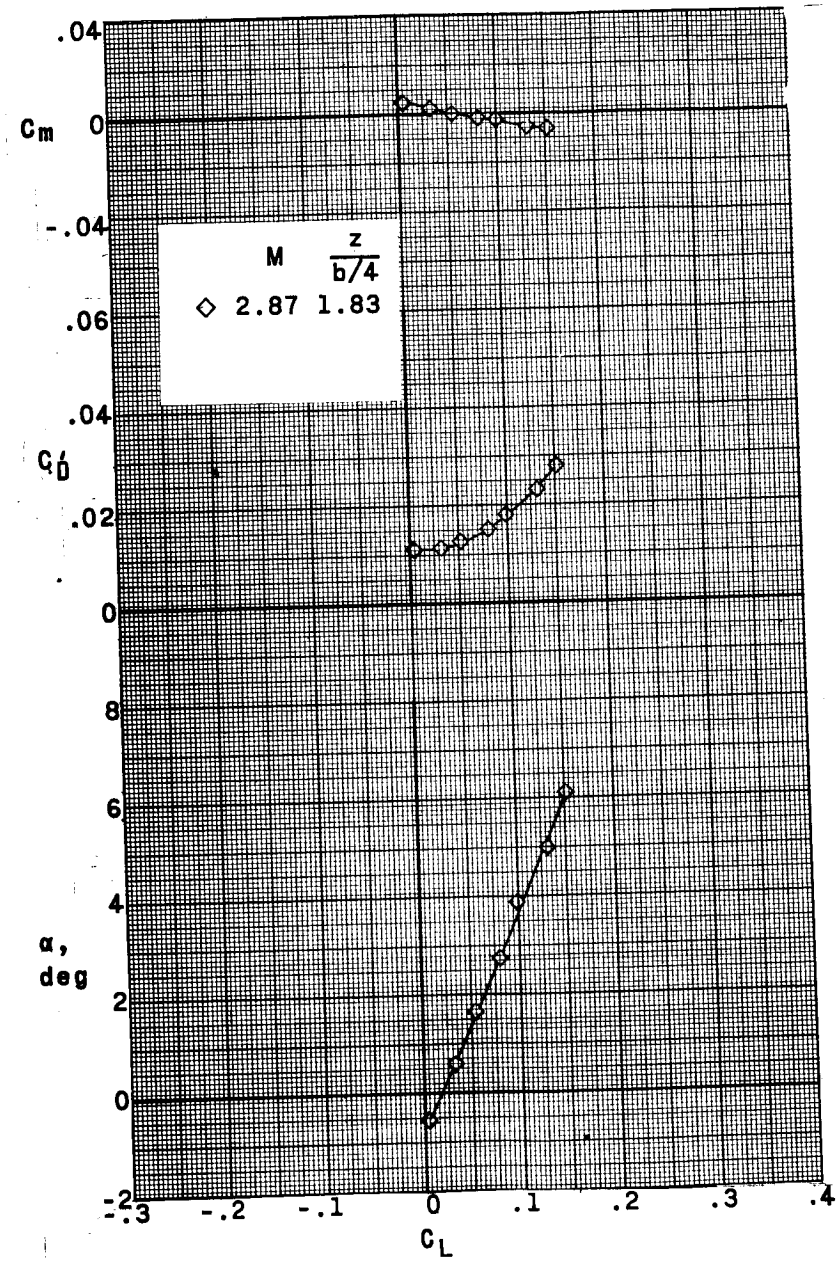

(a) $\left(\frac{z}{b/4}\right)_{nom} = 2.0$; $\frac{x}{l/4} = 0.02$.

Figure 8.- Aerodynamic characteristics in pitch of the receiver model in presence of tanker model. $\beta = 0^{\circ}$; $\frac{y}{b/4} = 0$.

CONFIDENTIAL

L-791

CONFIDENTIAL

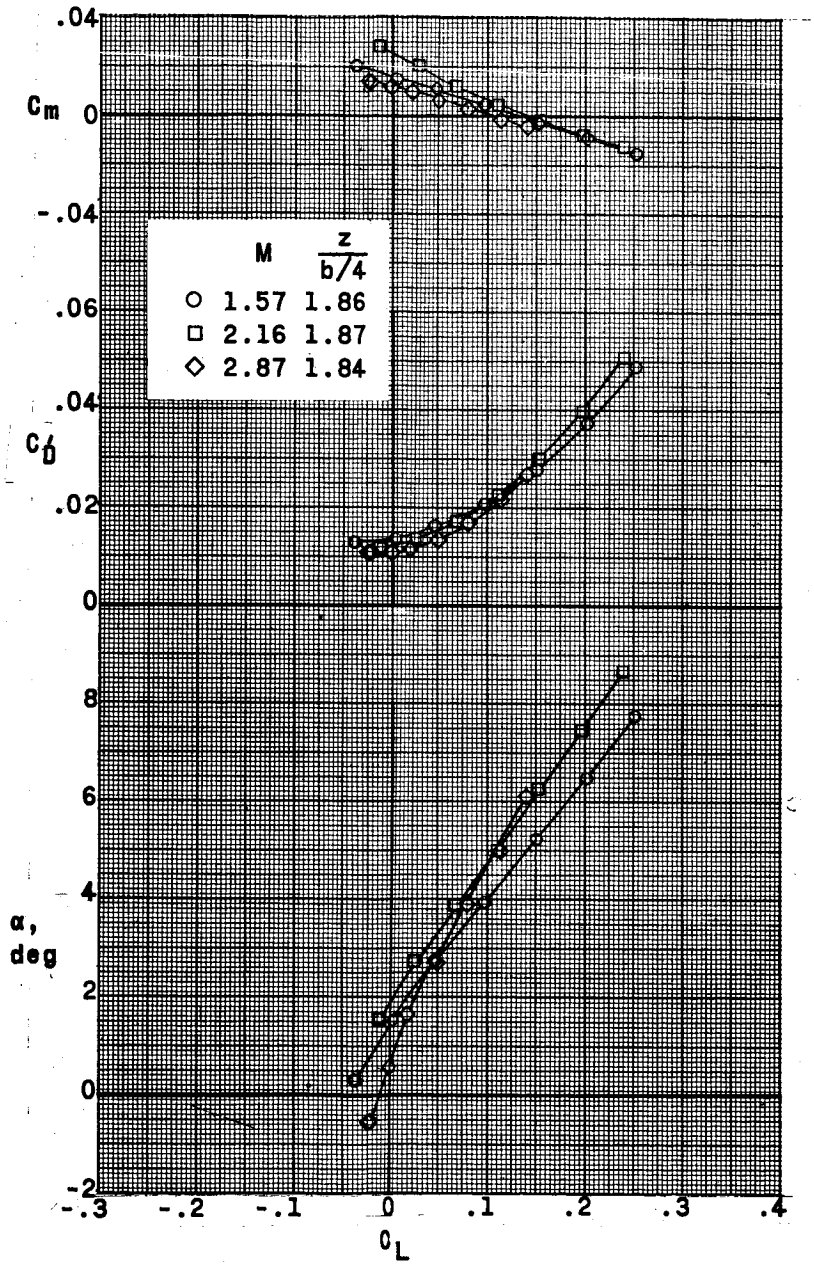

(b) $\left(\frac{z}{b/4}\right)_{nom} = 2.0$; $\frac{x}{l/4} = 1.02$.

Figure 8.- Continued.

CONFIDENTIAL

CONFIDENTIAL

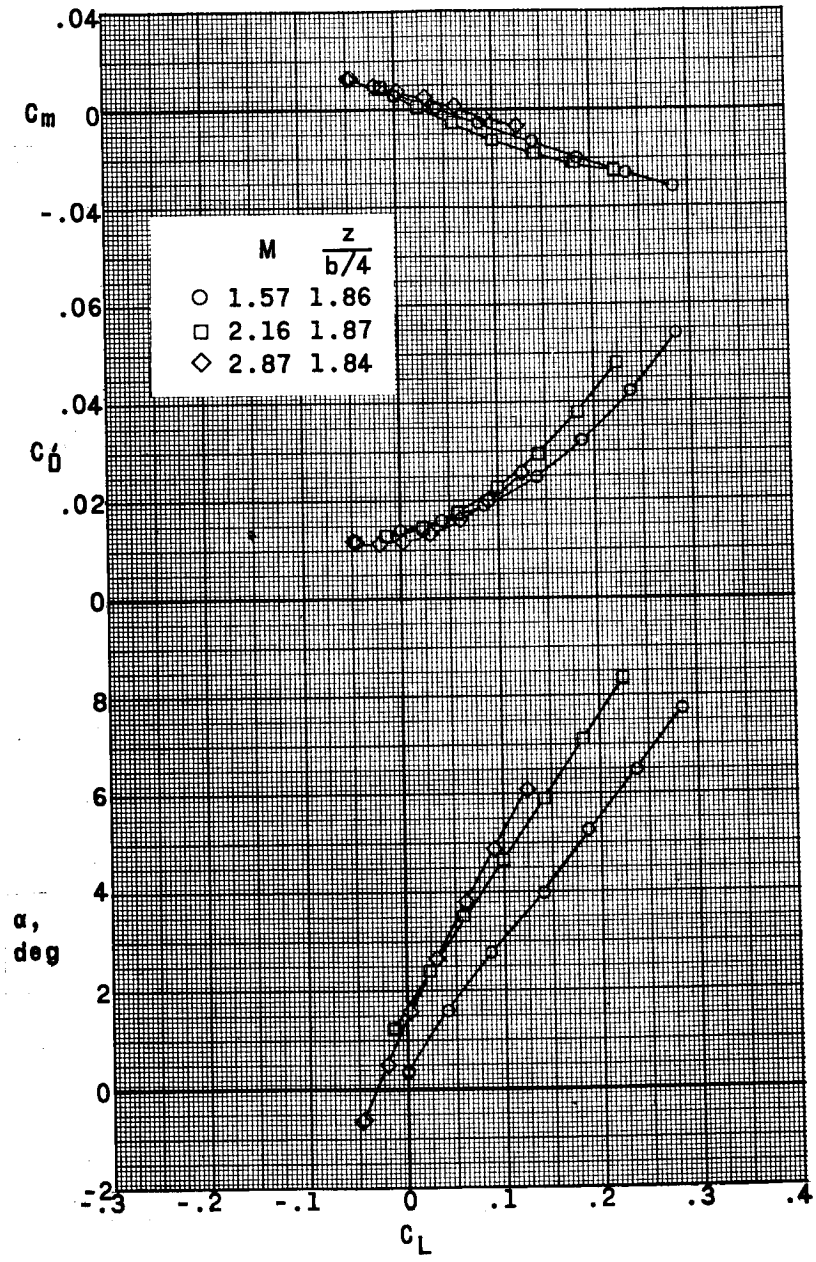

(c) $\left(\frac{z}{b/4}\right)_{nom} = 2.0$; $\frac{x}{l/4} = 2.02$.

Figure 8.- Continued.

CONFIDENTIAL

L-591

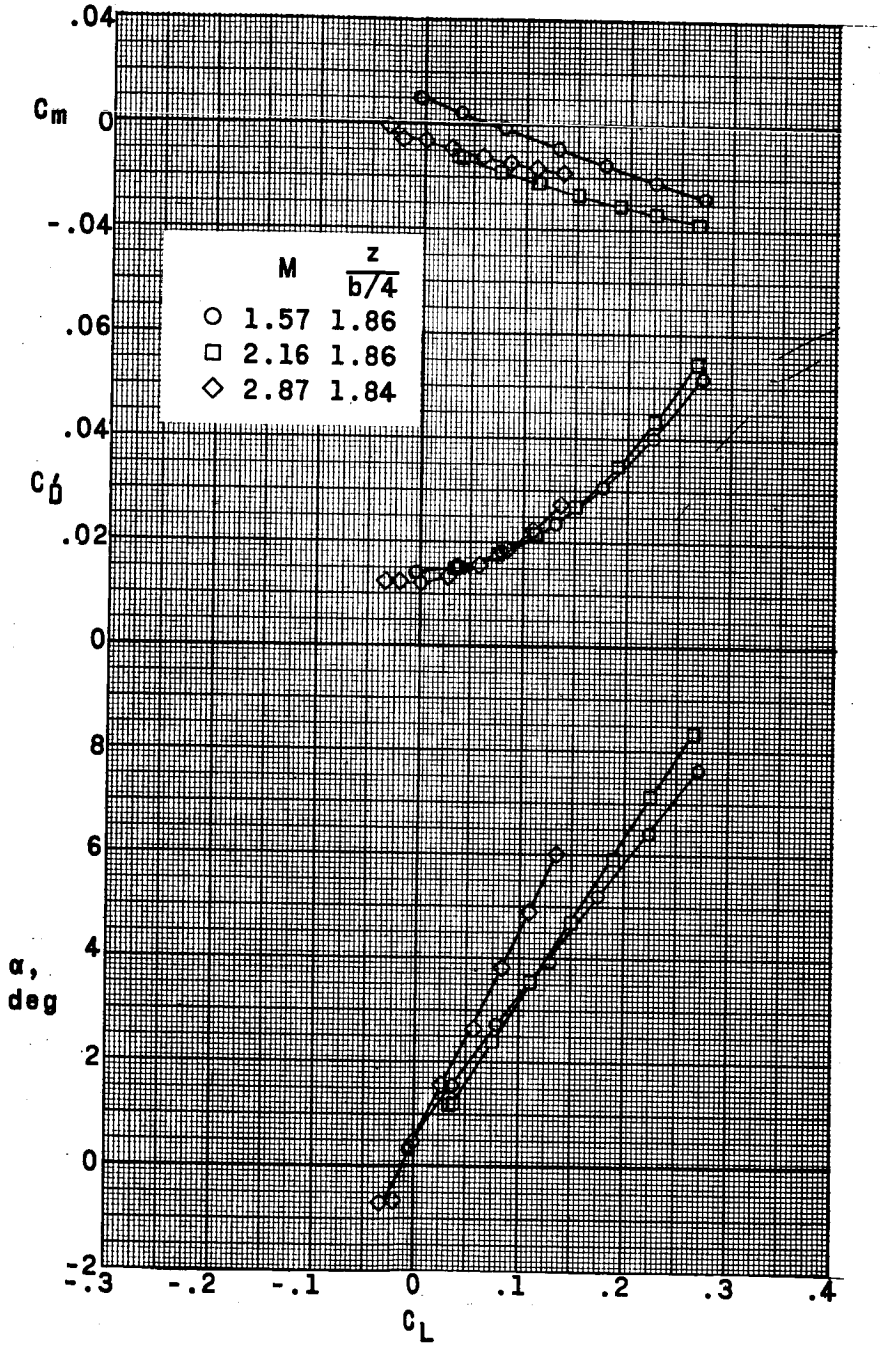

(d) $\left(\frac{z}{b/4}\right)_{nom} = 2.0$; $\frac{x}{l/4} = 3.02$.

Figure 8.- Continued.

CONFIDENTIAL

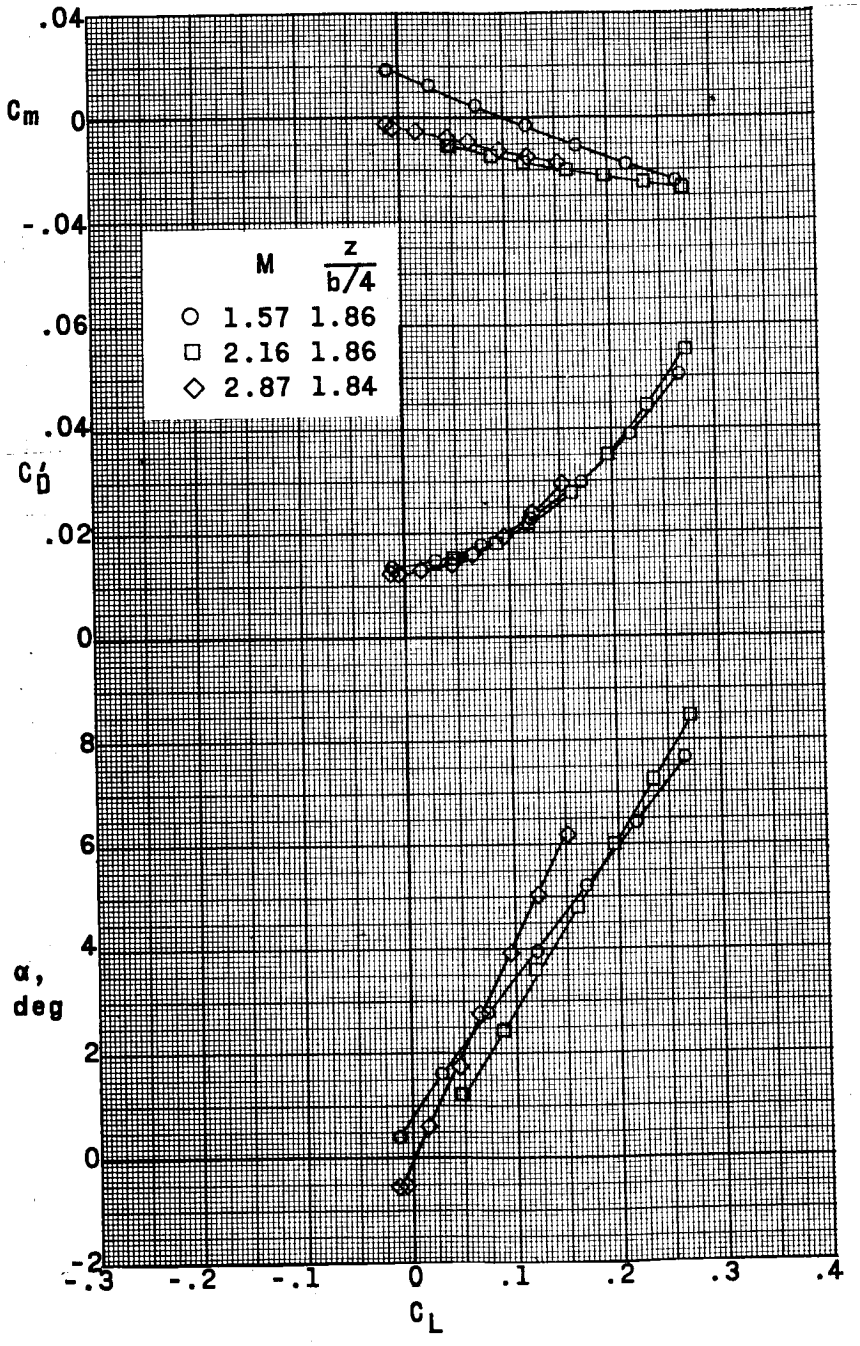

(e) $\left(\frac{z}{b/4}\right)_{nom} = 2.0$; $\frac{x}{l/4} = 4.02$.

Figure 8.- Continued.

CONFIDENTIAL

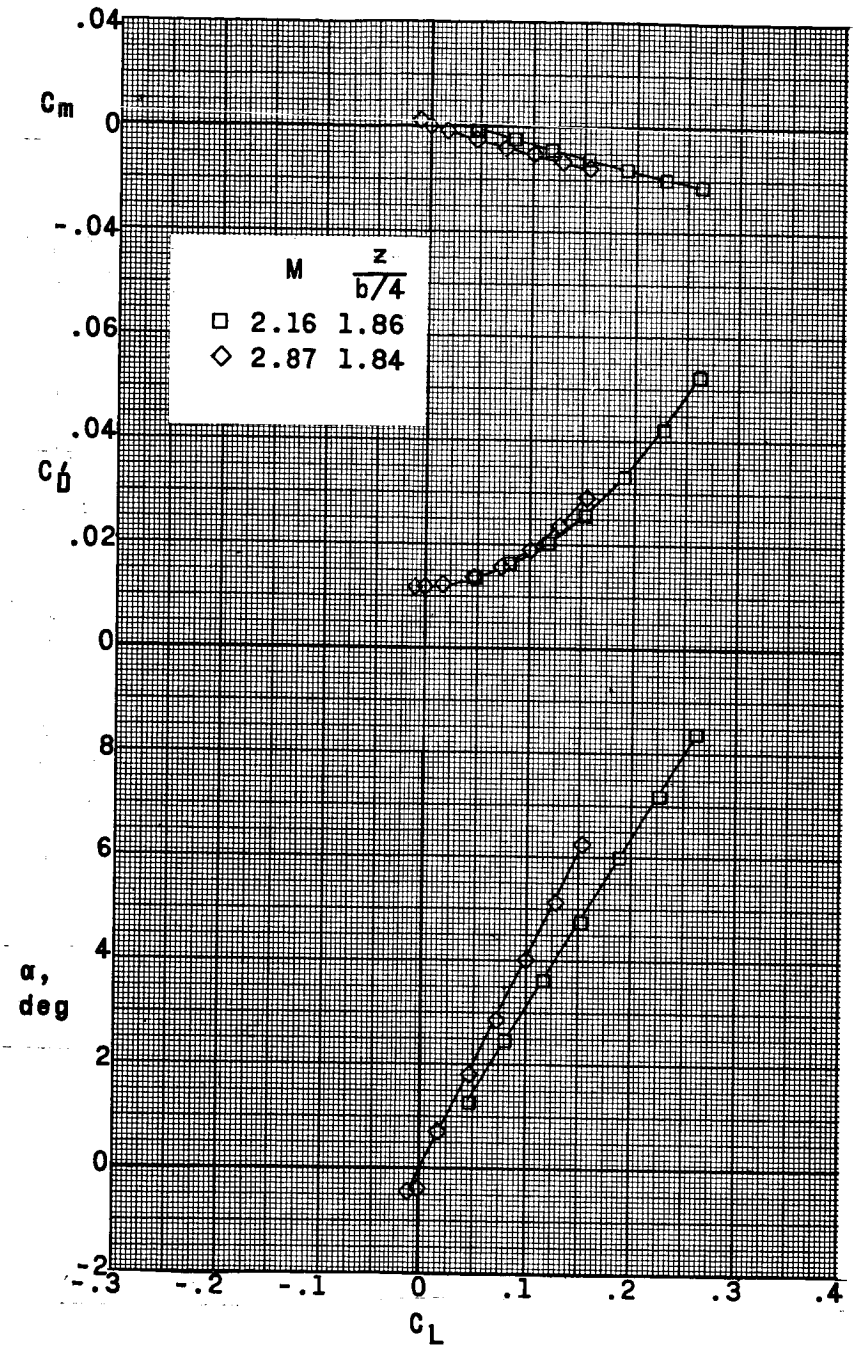

(f) $\left(\frac{z}{b/4}\right)_{nom} = 2.0$; $\frac{x}{l/4} = 5.02$.

Figure 8.- Continued.

L-591

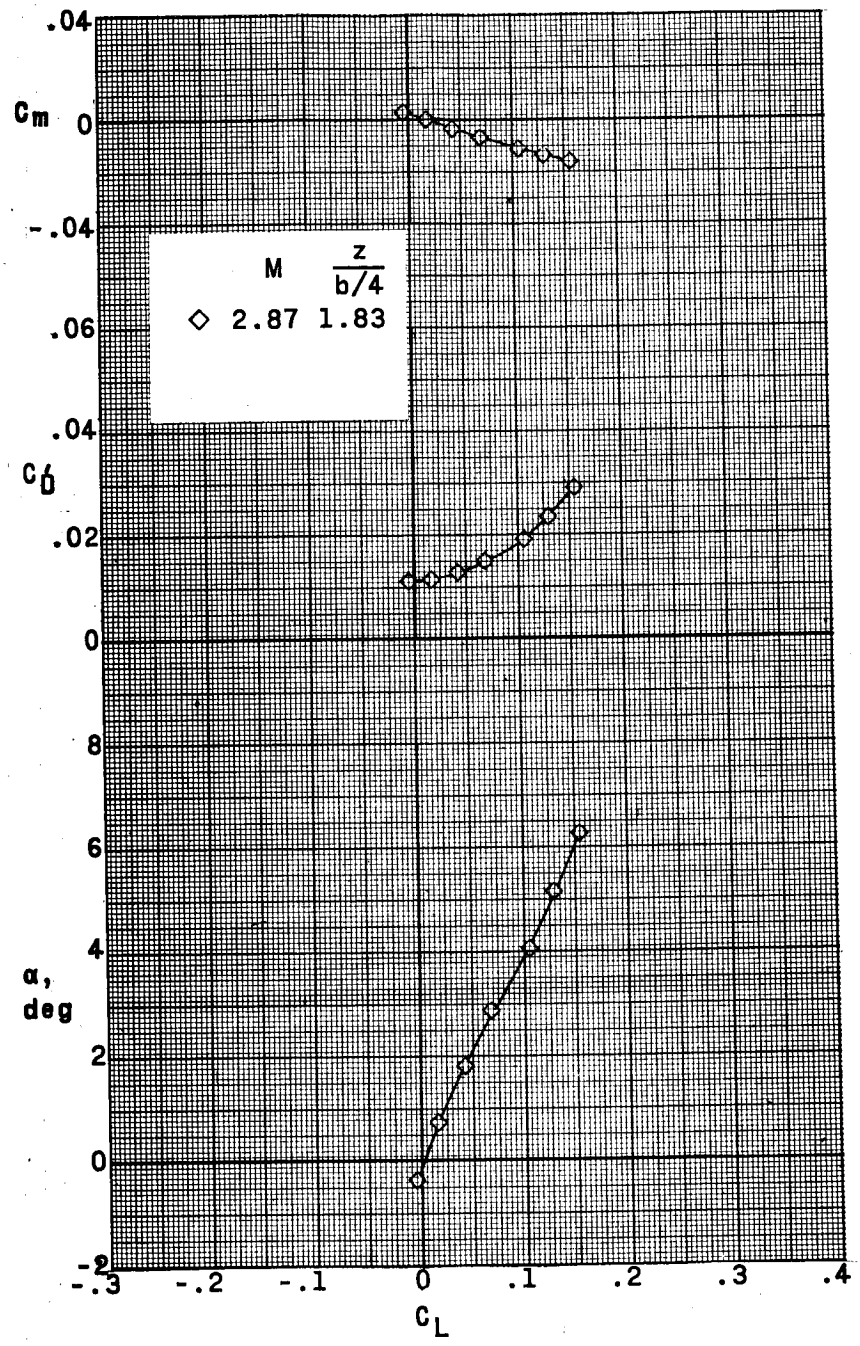

(g) $\left(\frac{z}{b/4}\right)_{nom} = 2.0; \frac{x}{l/4} = 6.02.$

Figure 8.- Continued.

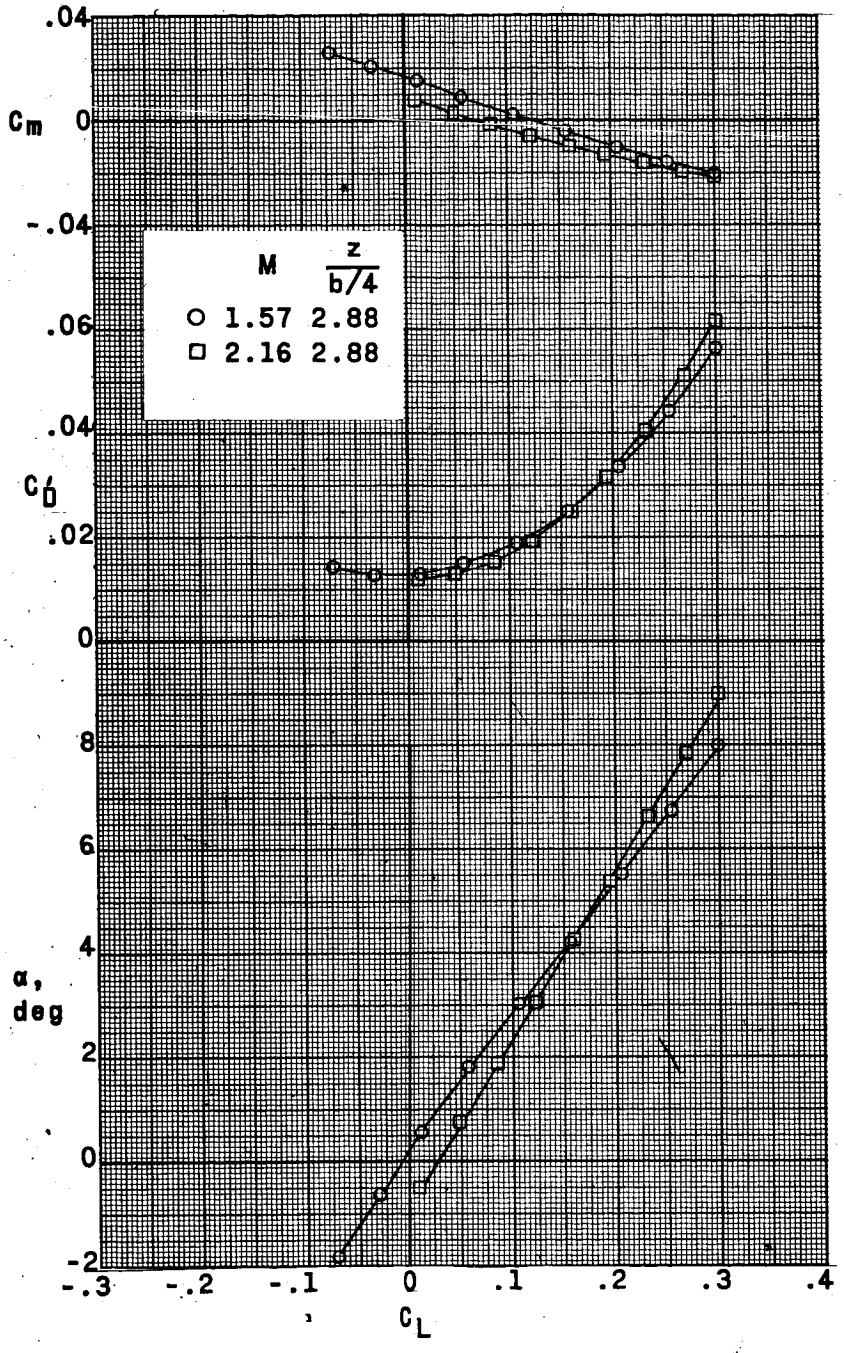

(h) $\left(\frac{z}{b/4}\right)_{nom} = 3.0; \frac{x}{l/4} = 0.03.$

Figure 8.- Continued.

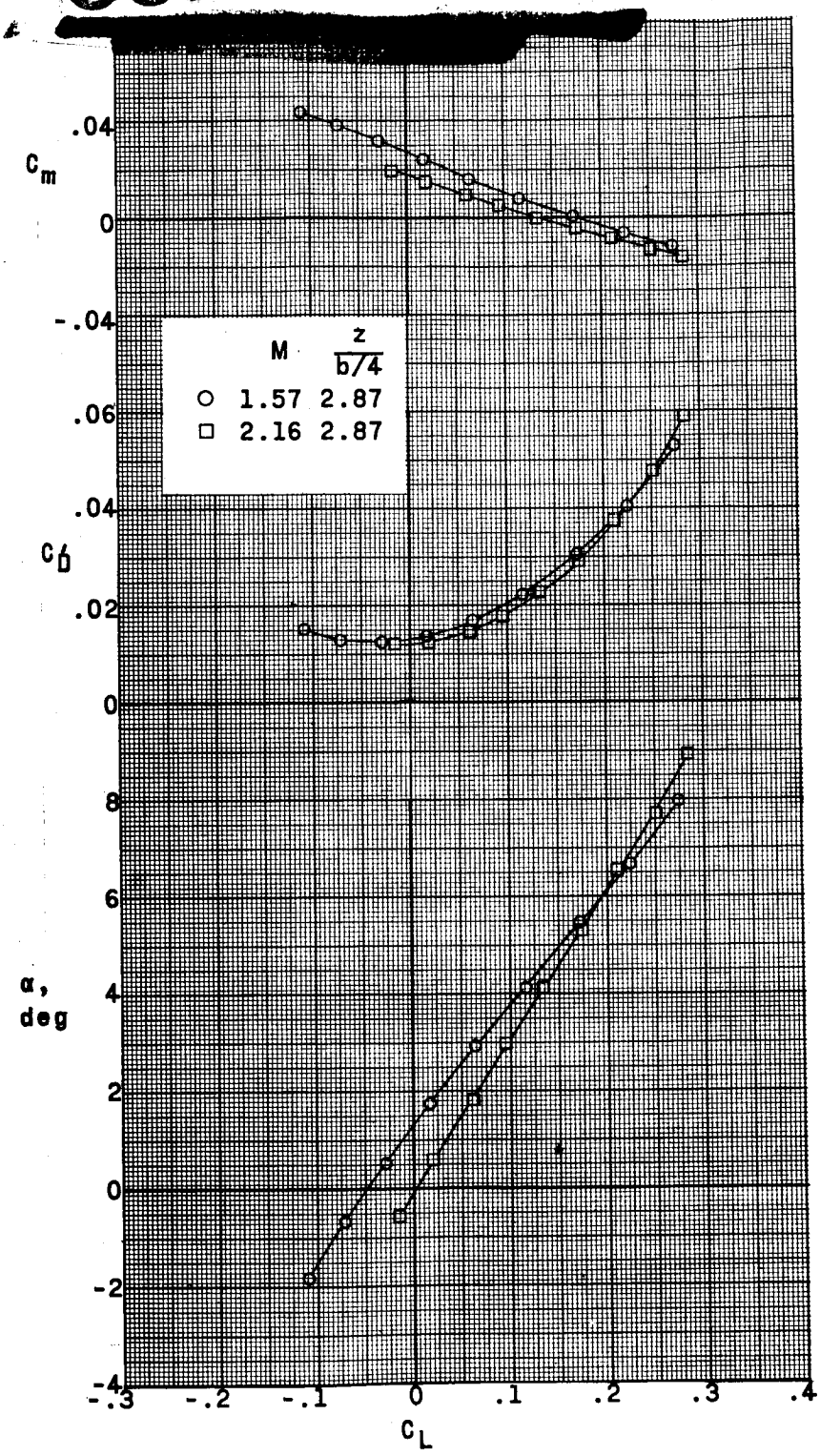

(i) $\left(\frac{z}{b/4}\right)_{nom} = 3.0; \frac{x}{l/4} = 1.02.$

Figure 8.- Continued.

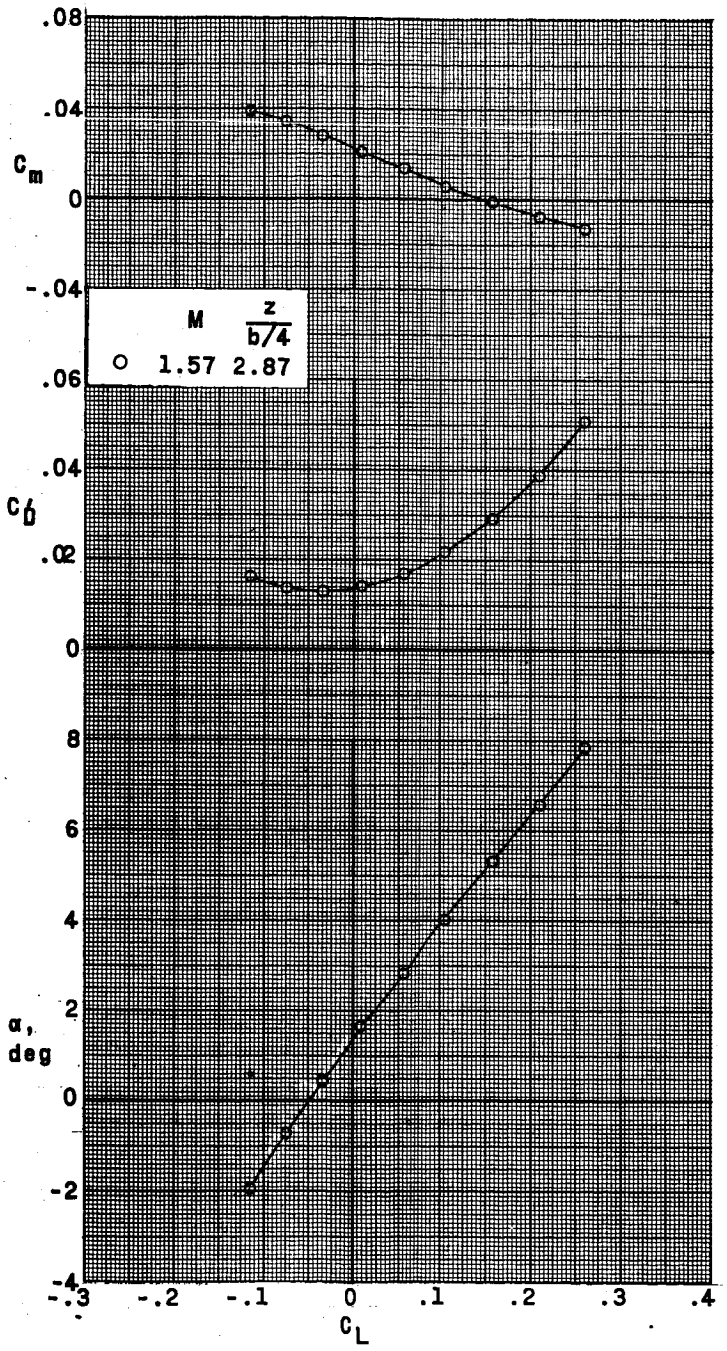

(j) $\left(\frac{z}{b/4}\right)_{nom} = 3.0; \frac{x}{l/4} = 1.52.$

Figure 8.- Continued.

CONFIDENTIAL

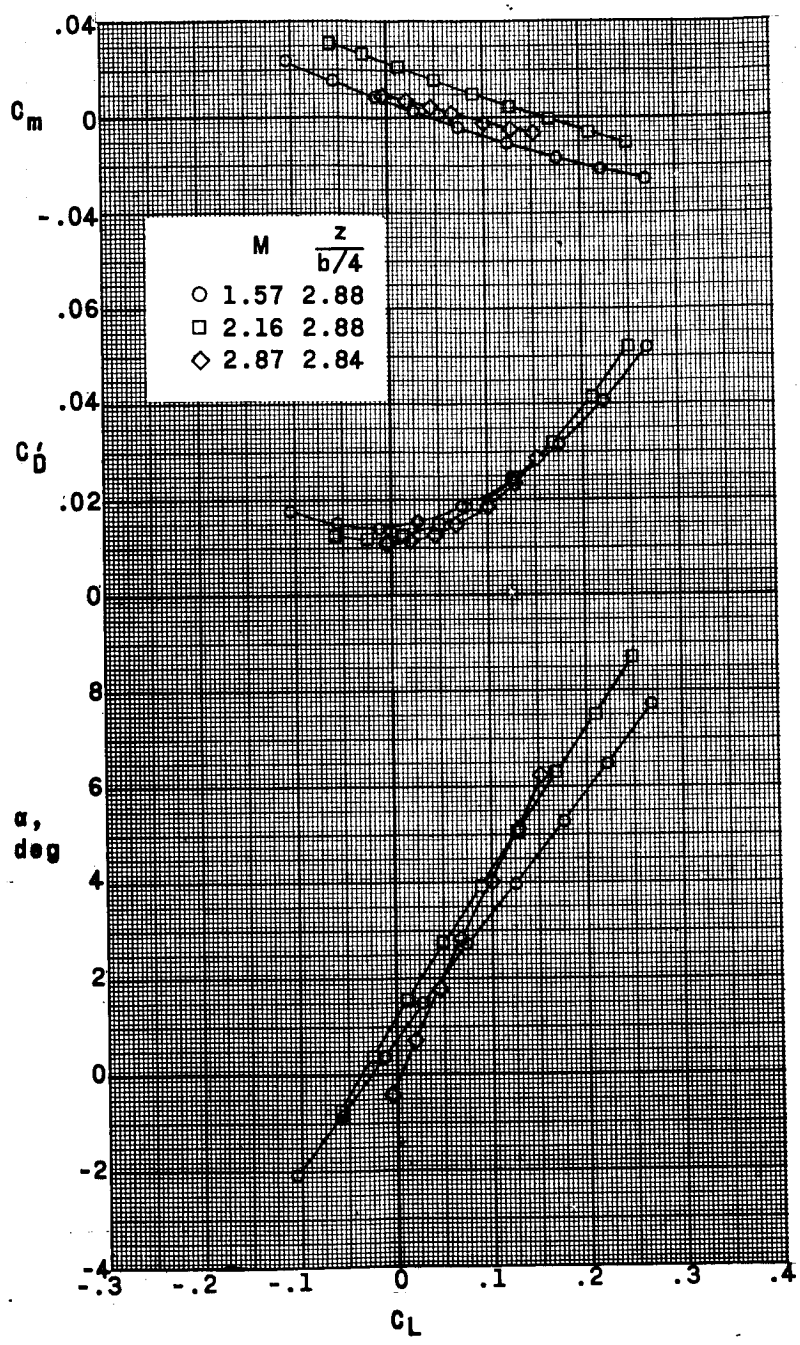

(k) $\left(\frac{z}{b/4}\right)_{nom} = 3.0; \frac{x}{l/4} = 2.02.$

Figure 8.- Continued.

CONFIDENTIAL

L-591

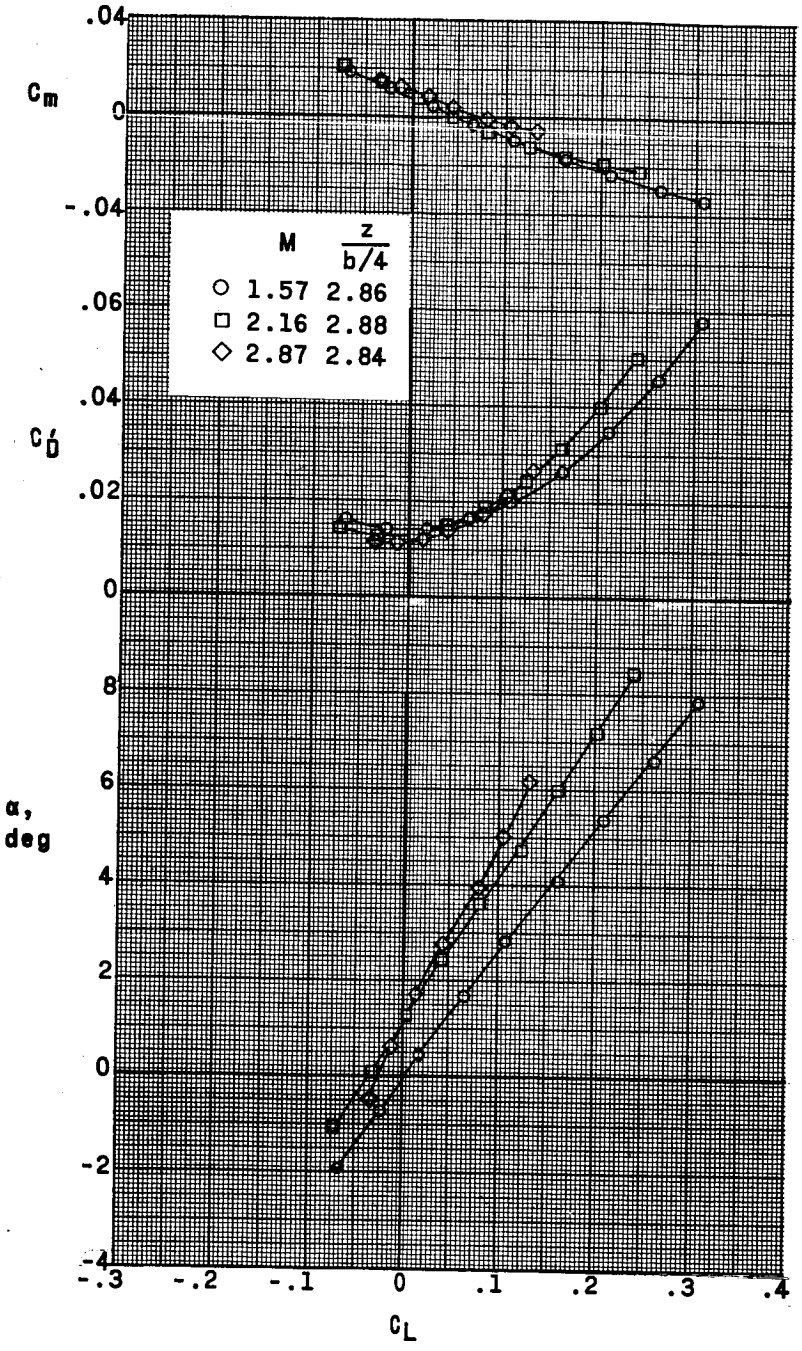

(l) $\left(\frac{z}{b/4}\right)_{nom} = 3.0$; $\frac{x}{l/4} = 3.02$.

Figure 8.- Continued.

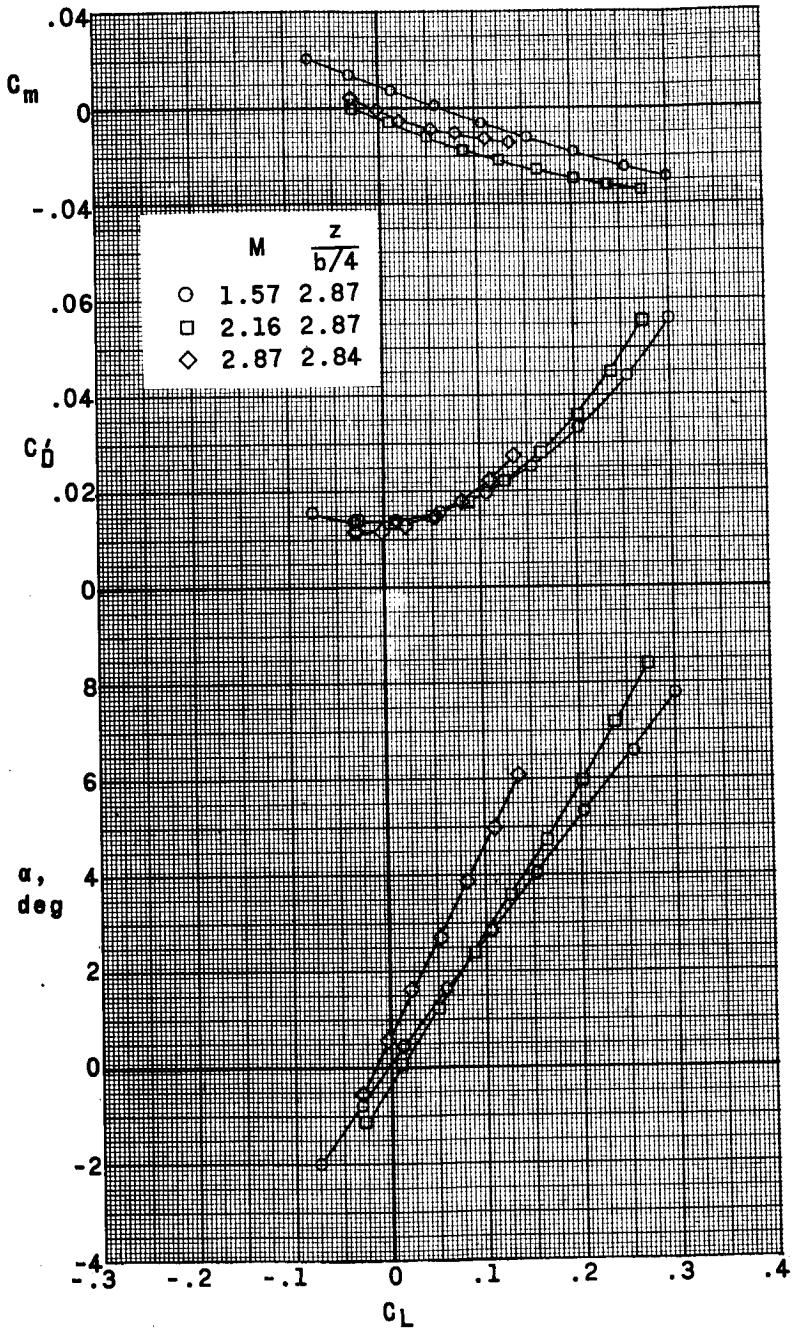

(m) $\left(\frac{z}{b/4}\right)_{nom} = 3.0; \frac{x}{l/4} = 4.02.$

Figure 8.- Continued.

L-591

CONFIDENTIAL

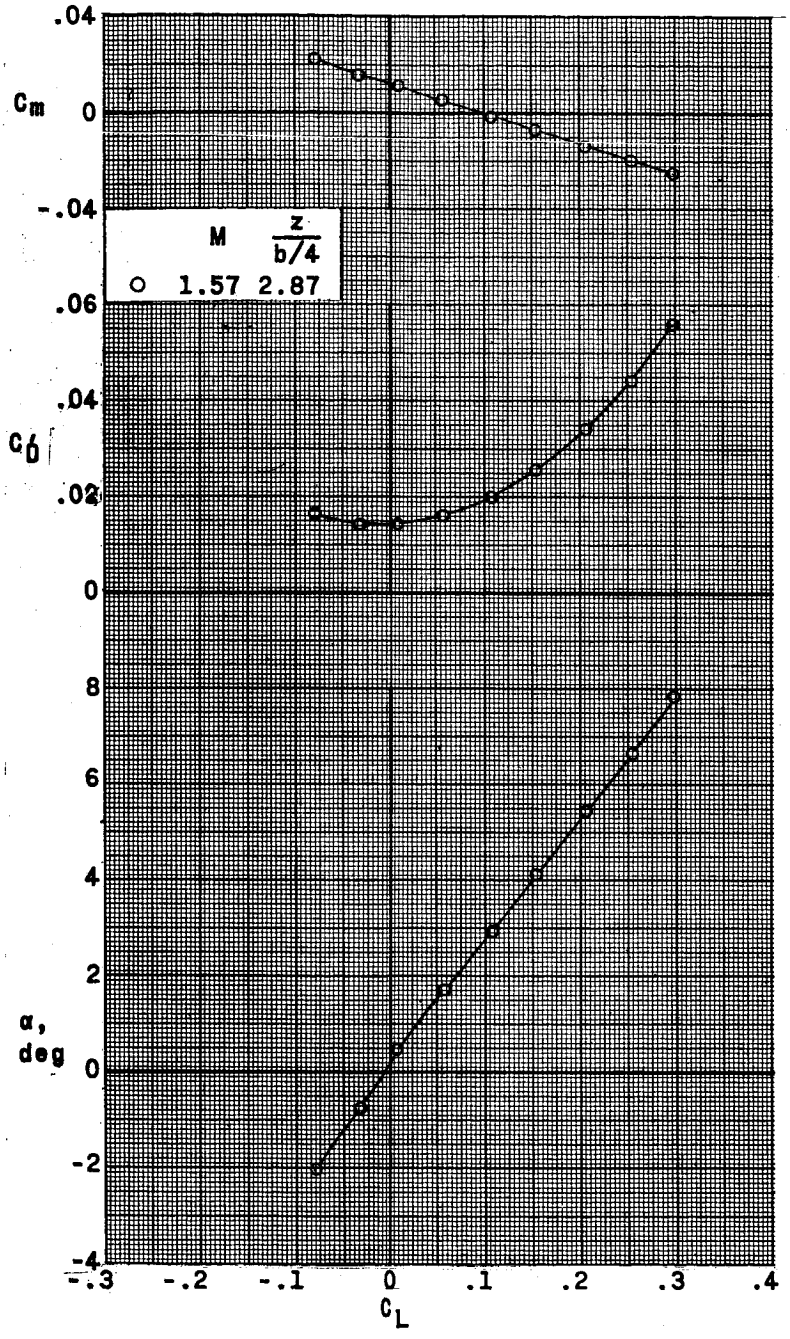

(n) $\left(\frac{z}{b/4}\right)_{nom} = 3.0; \frac{x}{l/4} = 4.53.$

Figure 8.- Continued.

CONFIDENTIAL

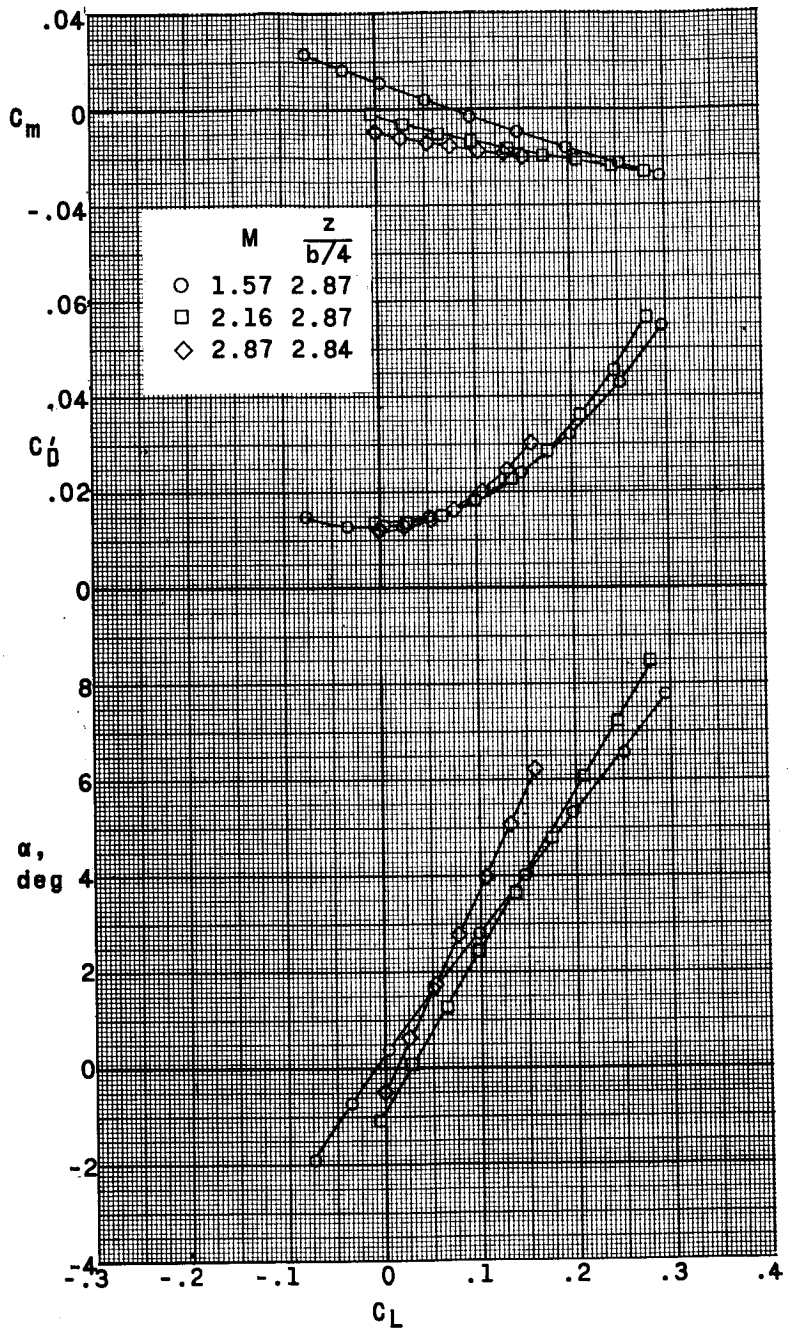

(o) $\left(\frac{z}{b/4}\right)_{nom} = 3.0; \frac{x}{l/4} = 5.02.$

Figure 8.- Continued.

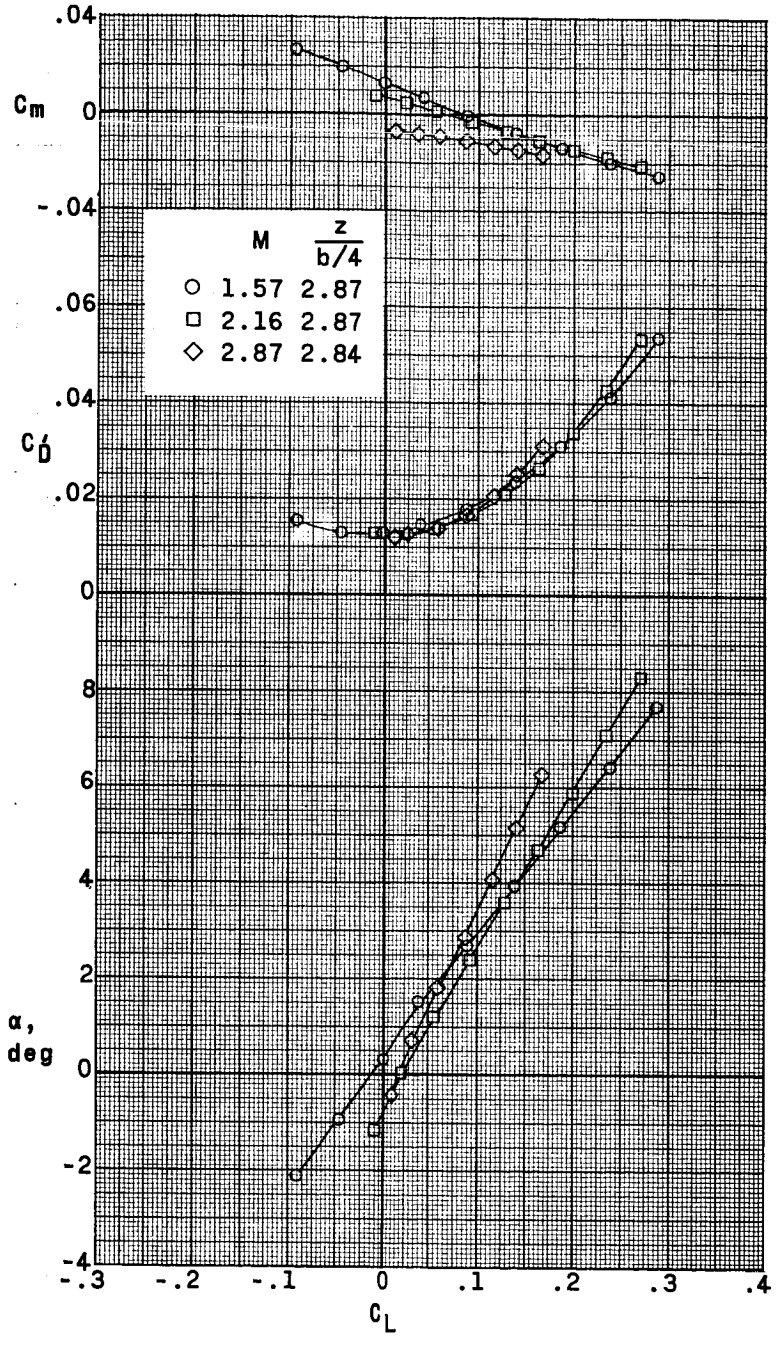

(p) $\left(\frac{z}{b/4}\right)_{nom} = 3.0$; $\frac{x}{l/4} = 6.02$.

Figure 8.- Continued.

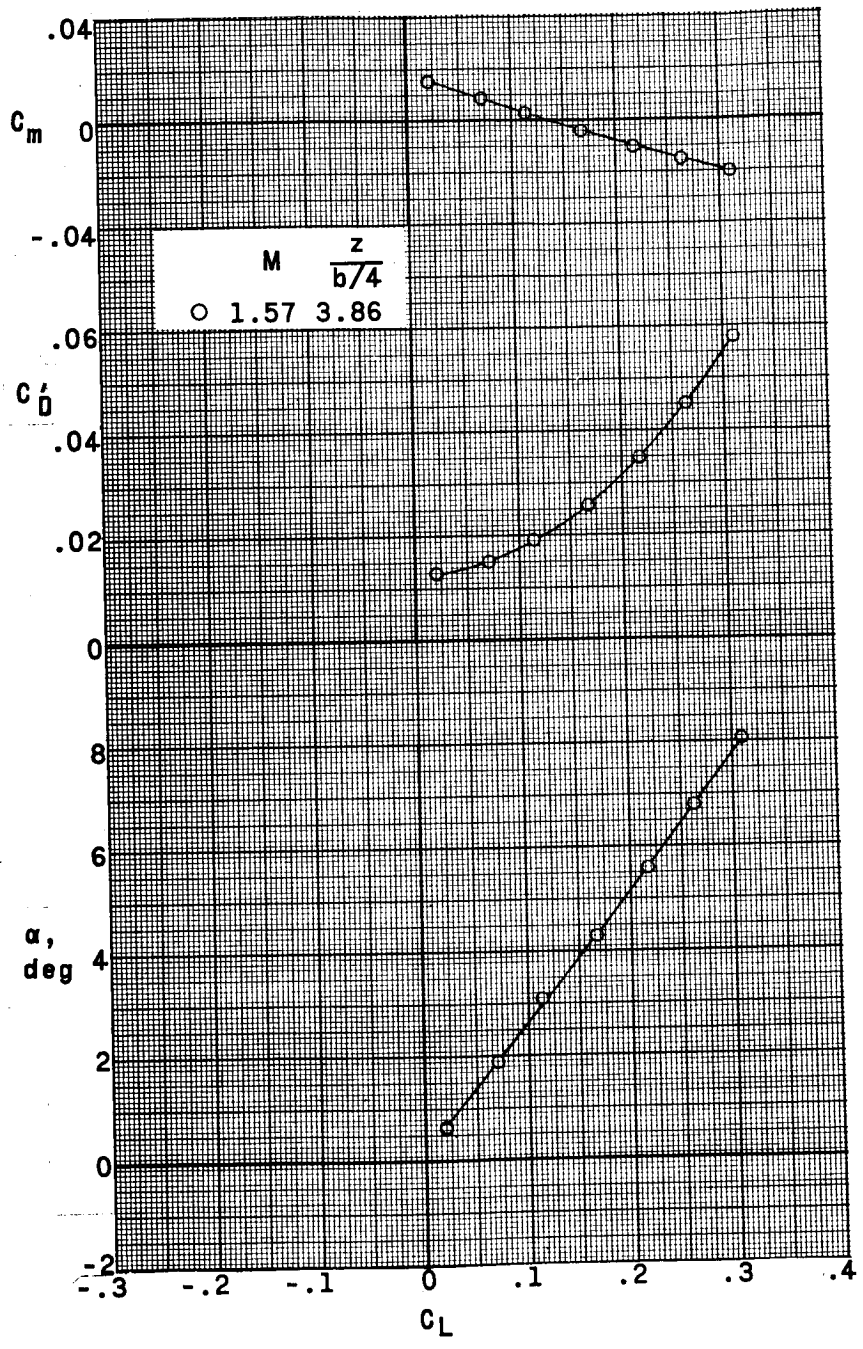

(q) $\left(\frac{z}{b/4}\right)_{nom} = 4.0$; $\frac{x}{l/4} = 0.02$.

Figure 8.- Continued.

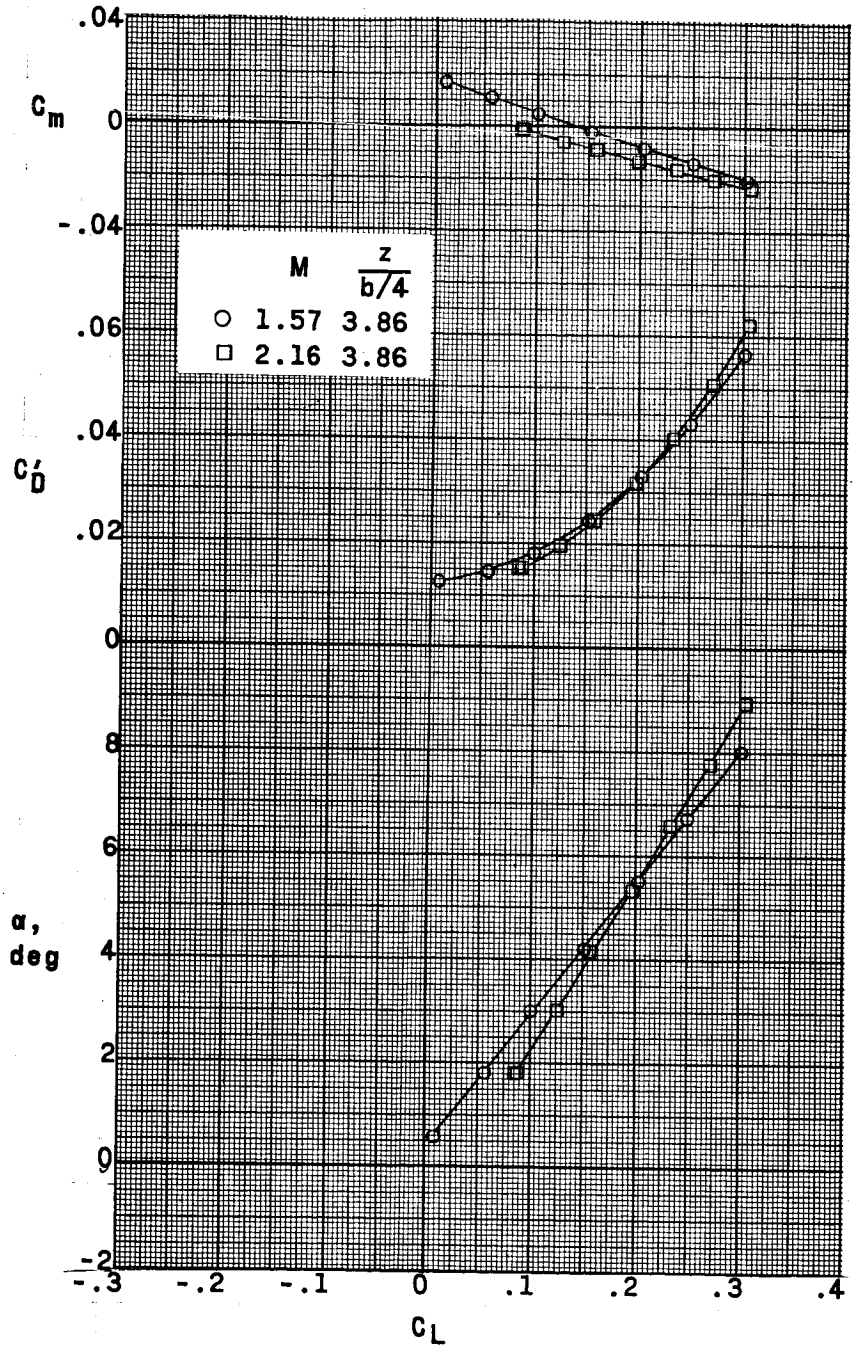

(r) $\left(\frac{z}{b/4}\right)_{nom} = 4.0; \frac{x}{l/4} = 1.02.$

Figure 8.- Continued.

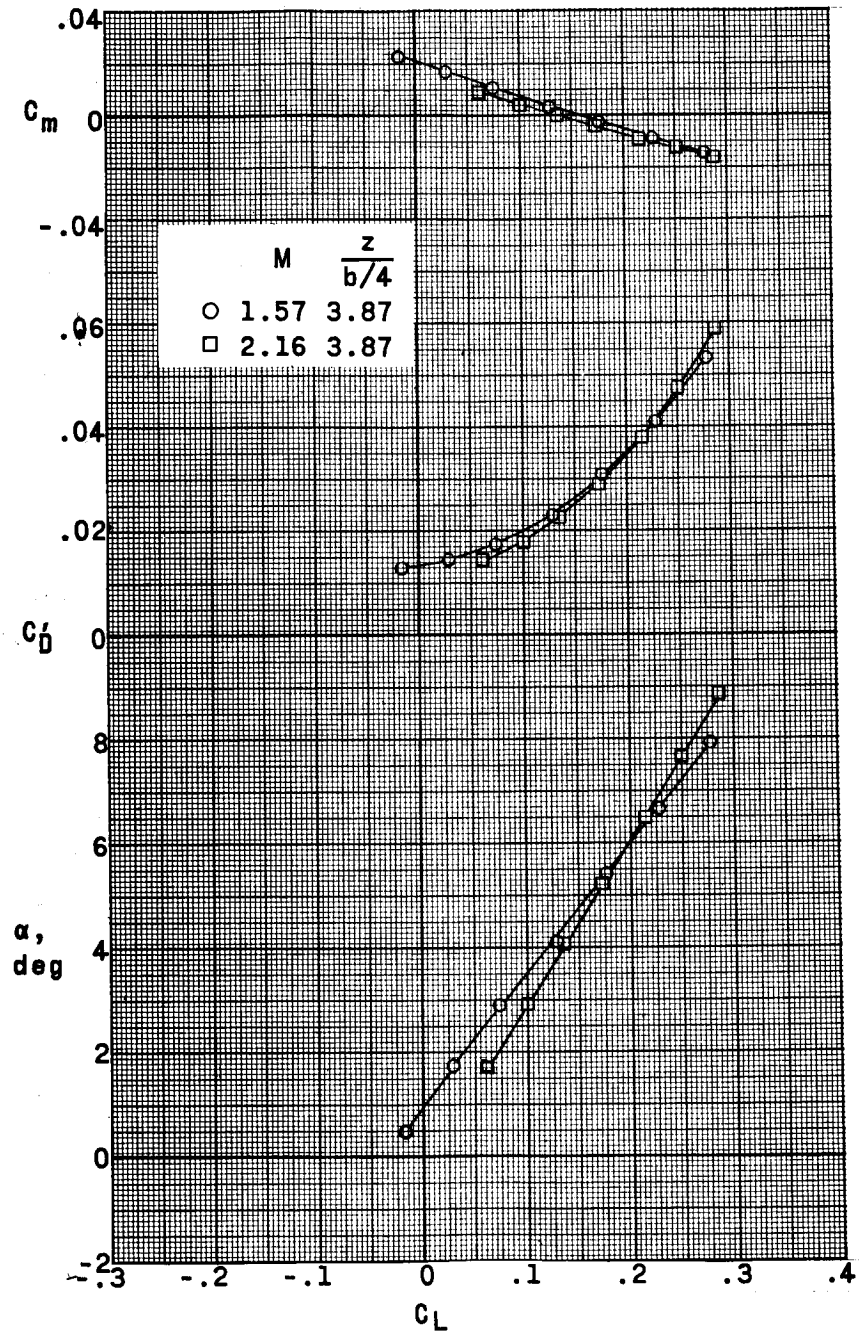

(s) $\left(\frac{z}{b/4}\right)_{nom} = 4.0; \frac{x}{l/4} = 2.02.$

Figure 8.- Continued.

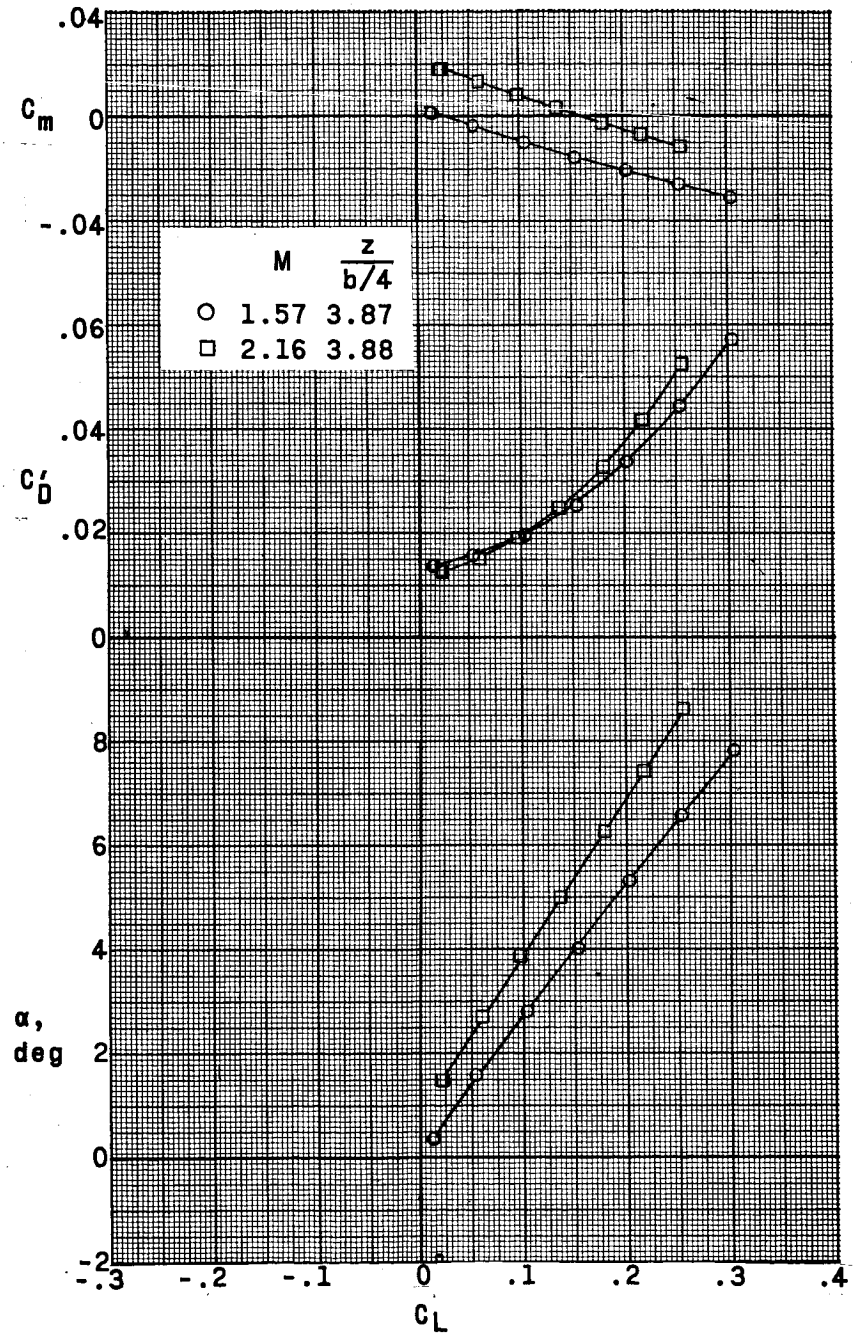

(t) $\left(\frac{z}{b/4}\right)_{nom} = 4.0; \frac{x}{l/4} = 3.02.$

Figure 8.- Continued.

CONFIDENTIAL

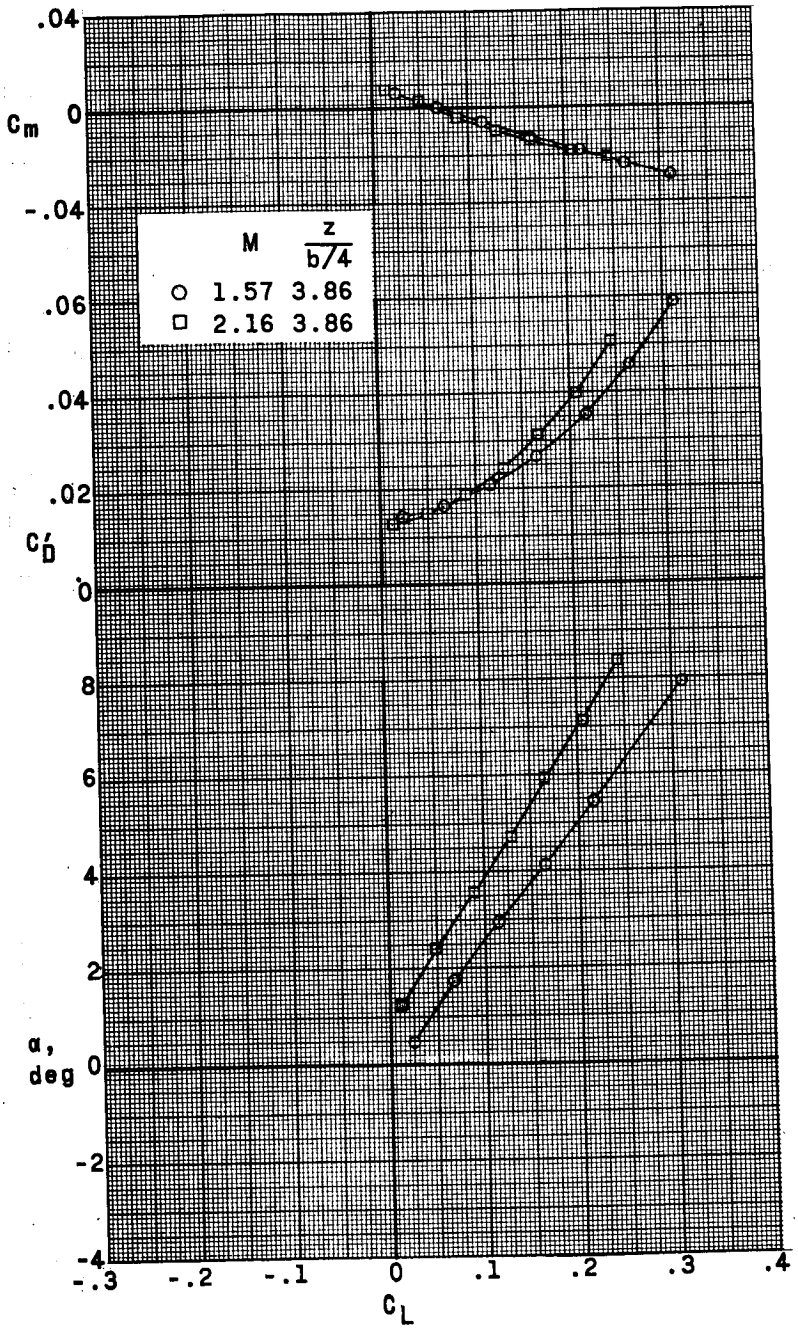

(u) $\left(\frac{z}{b/4}\right)_{nom} = 4.0; \frac{x}{l/4} = 4.02.$

Figure 8.- Concluded.

CONFIDENTIAL

CONFIDENTIAL

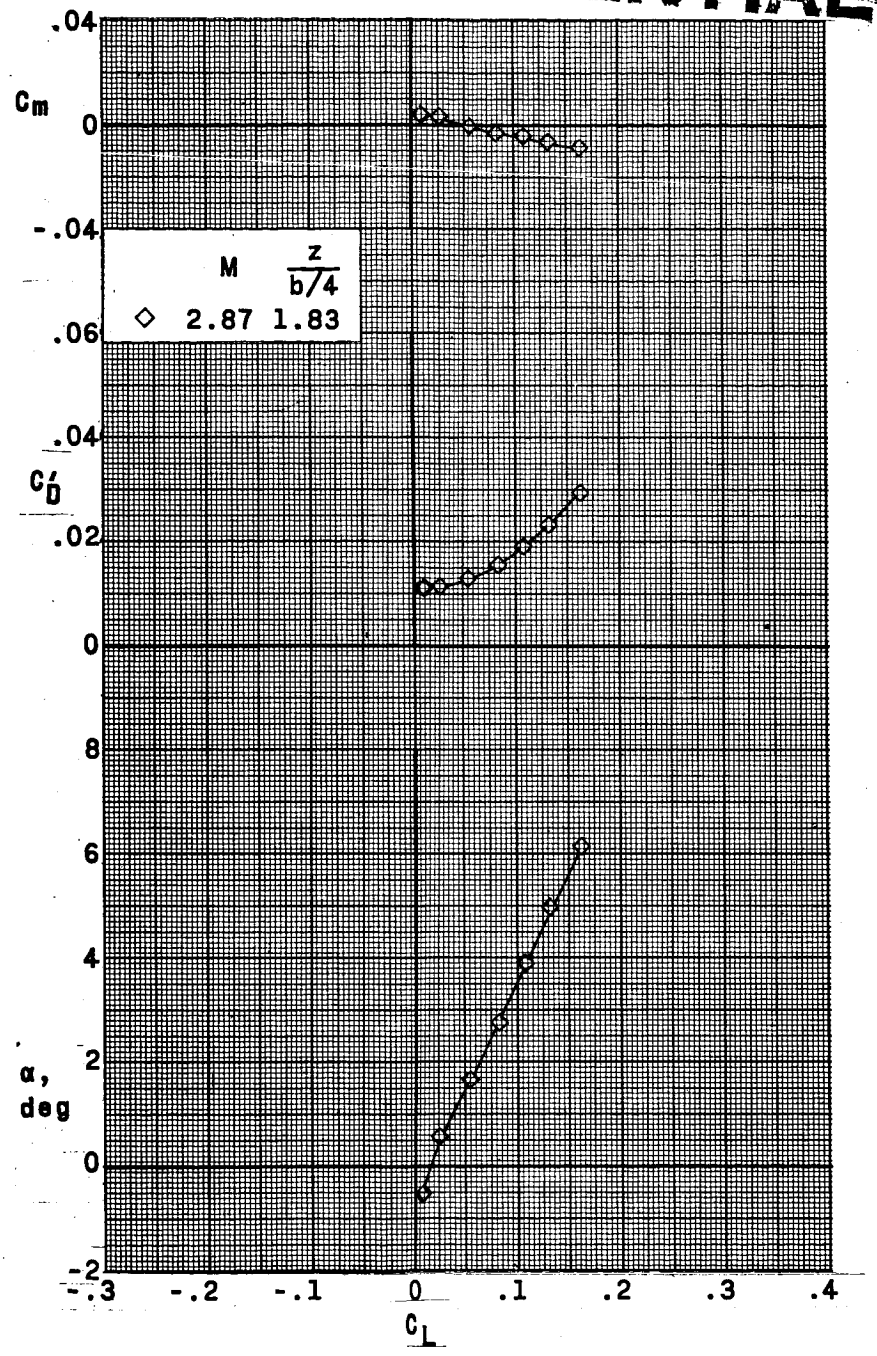

(a) $\left(\frac{z}{b/4}\right)_{nom} = 2.0$; $\frac{x}{l/4} = 0.02$.

Figure 9.- Aerodynamic characteristics in pitch of the receiver model in the presence of tanker model. $\beta = 0^{\circ}$; $\frac{y}{b/4} = 1.00$.

CONFIDENTIAL

L-591

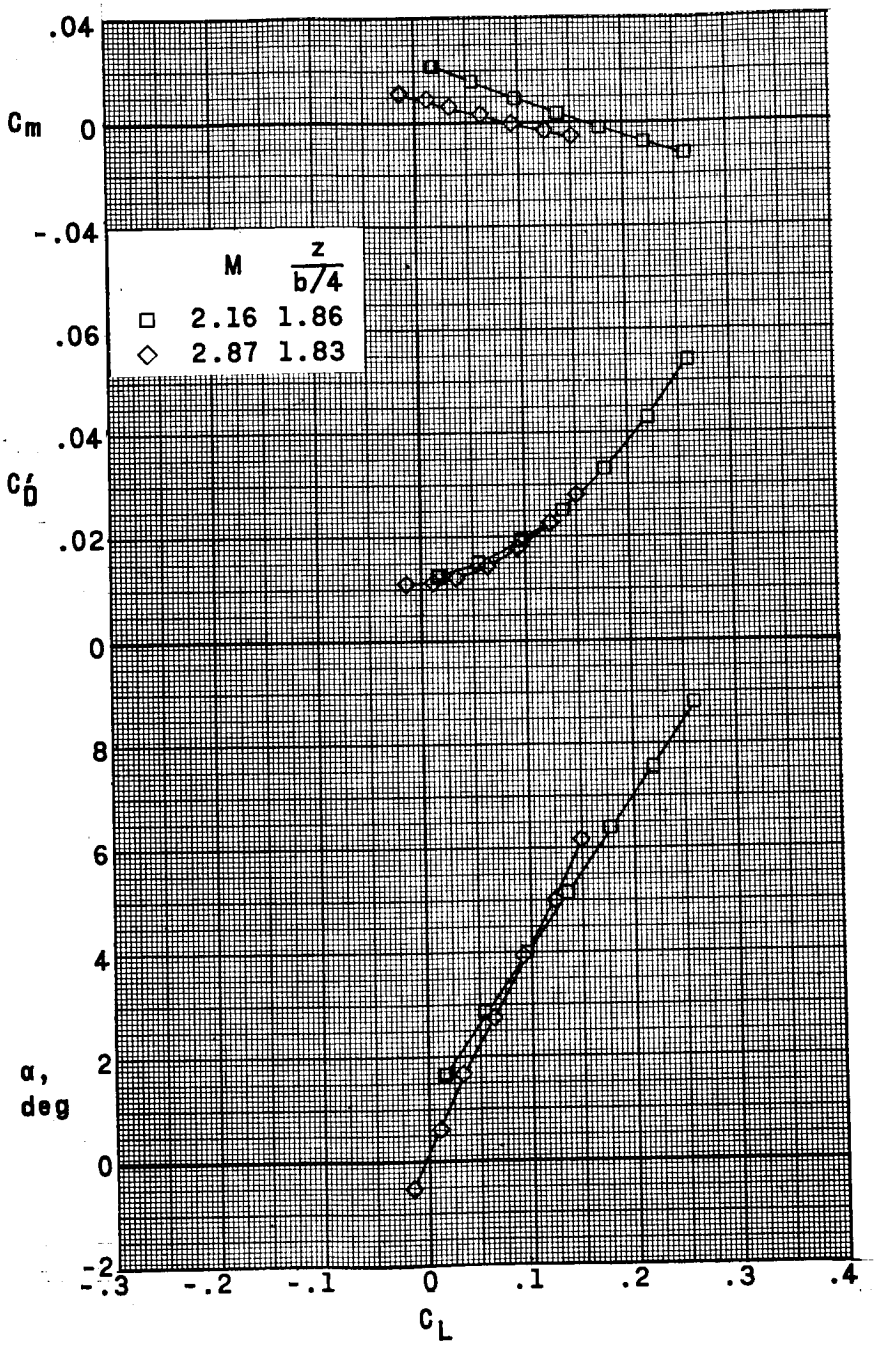

(b) $\left(\frac{z}{b/4}\right)_{nom}$ = 2.0; $\frac{x}{l/4}$ = 1.02.

Figure 9.- Continued.

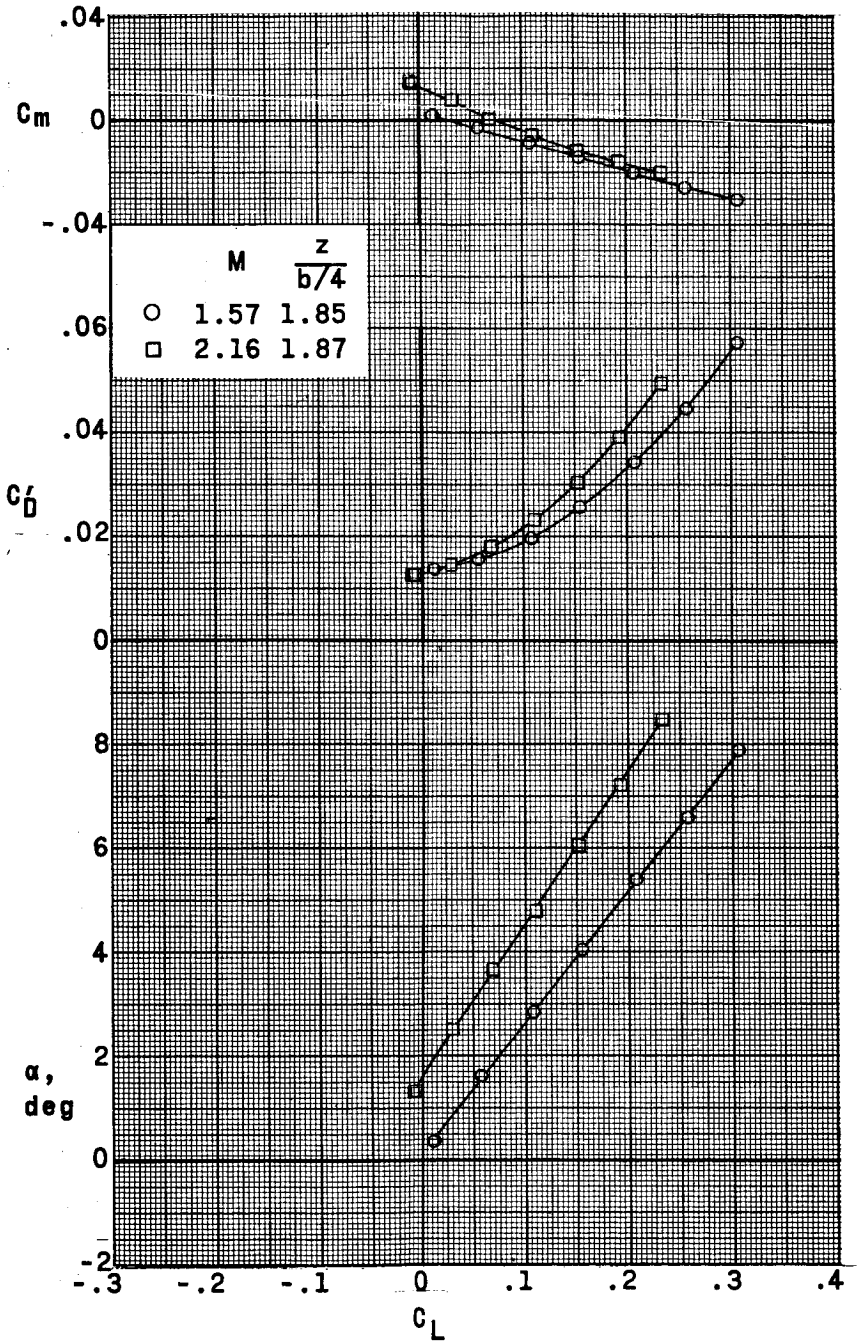

(c) $\left(\frac{z}{b/4}\right)_{nom} = 2.0$; $\frac{x}{l/4} = 2.02$.

Figure 9.- Continued.

CONFIDENTIAL

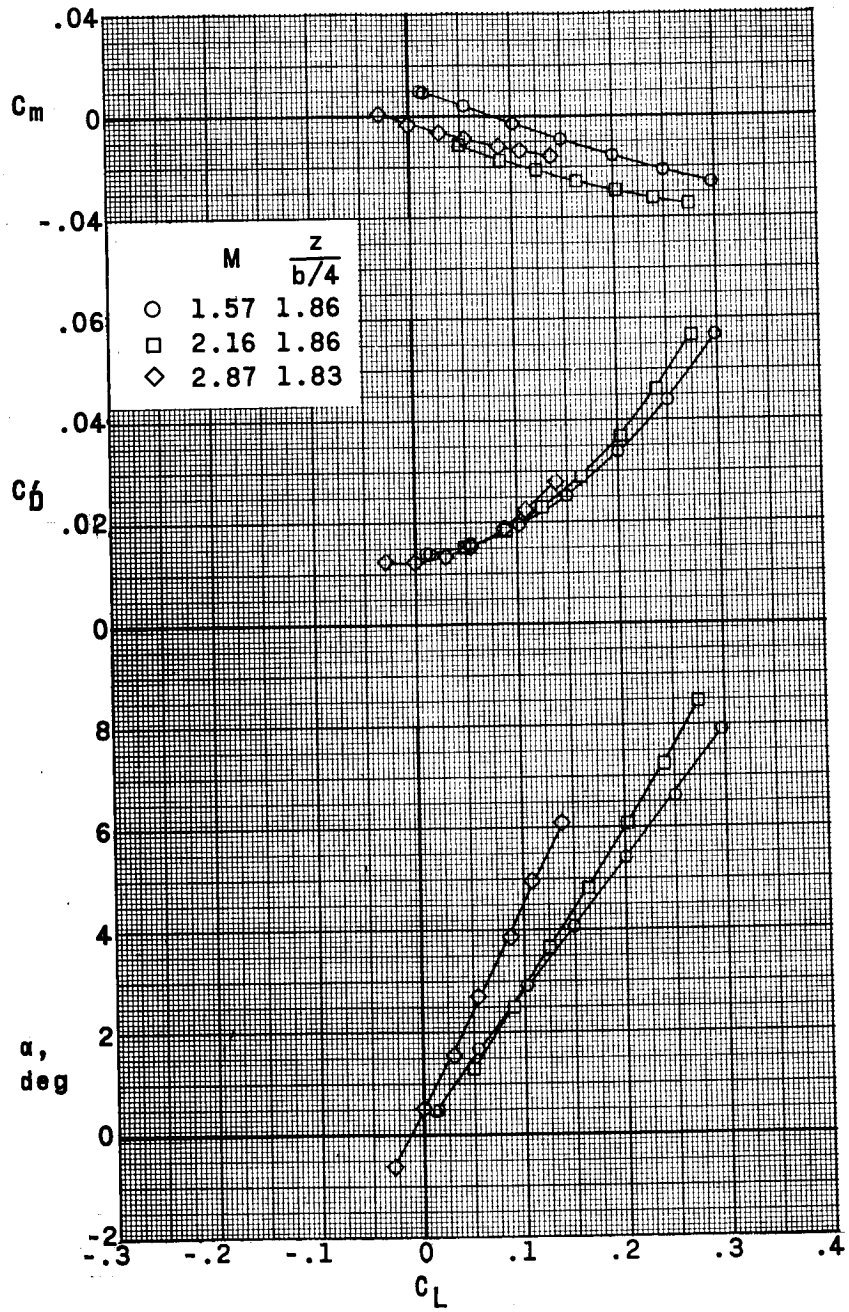

(d) $\left(\frac{z}{b/4}\right)_{nom} = 2.0$; $\frac{x}{l/4} = 3.02$.

Figure 9.- Continued.

CONFIDENTIAL

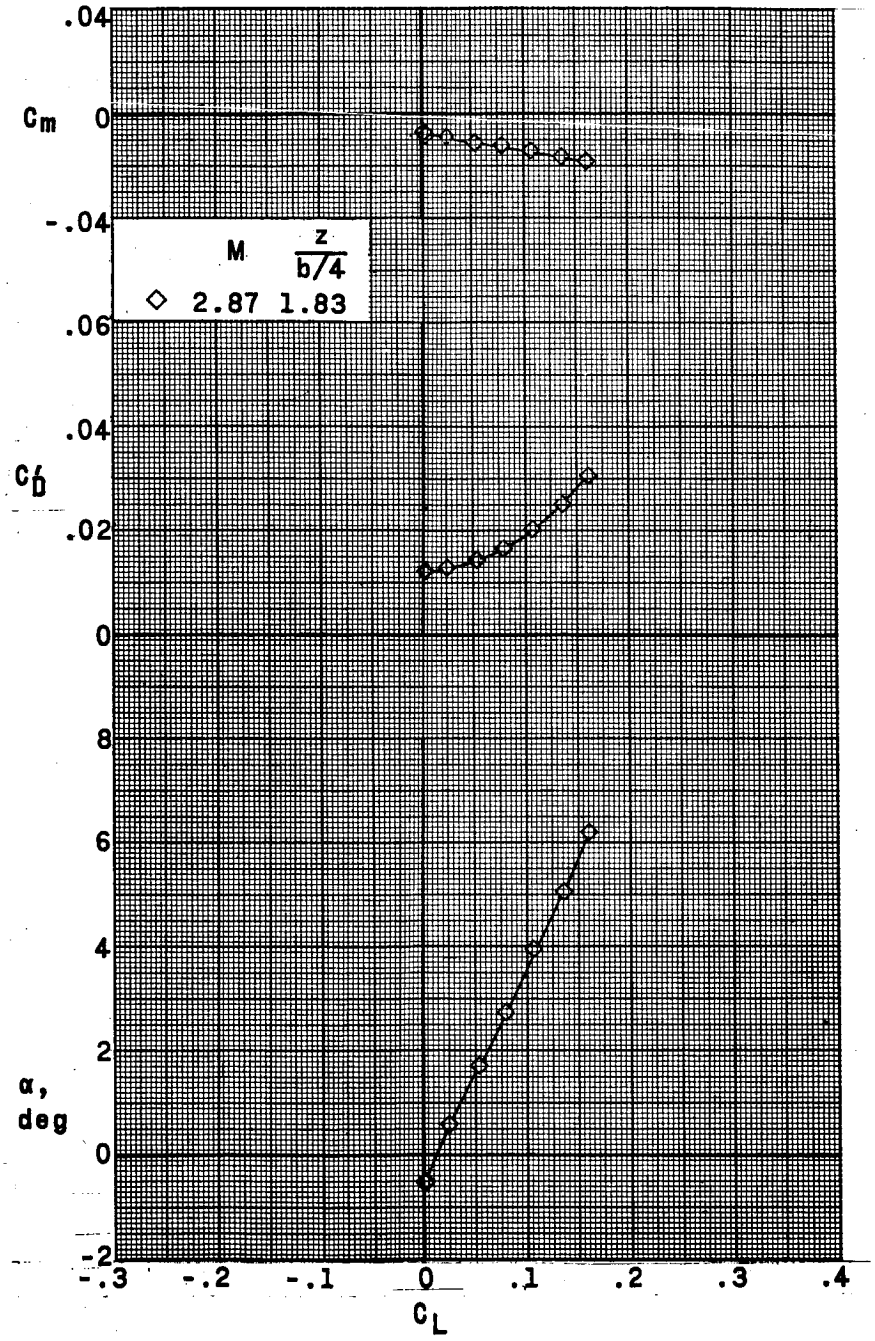

(e) $\left(\frac{z}{b/4}\right)_{nom} = 2.0; \frac{x}{l/4} = 4.02.$

Figure 9.- Continued.

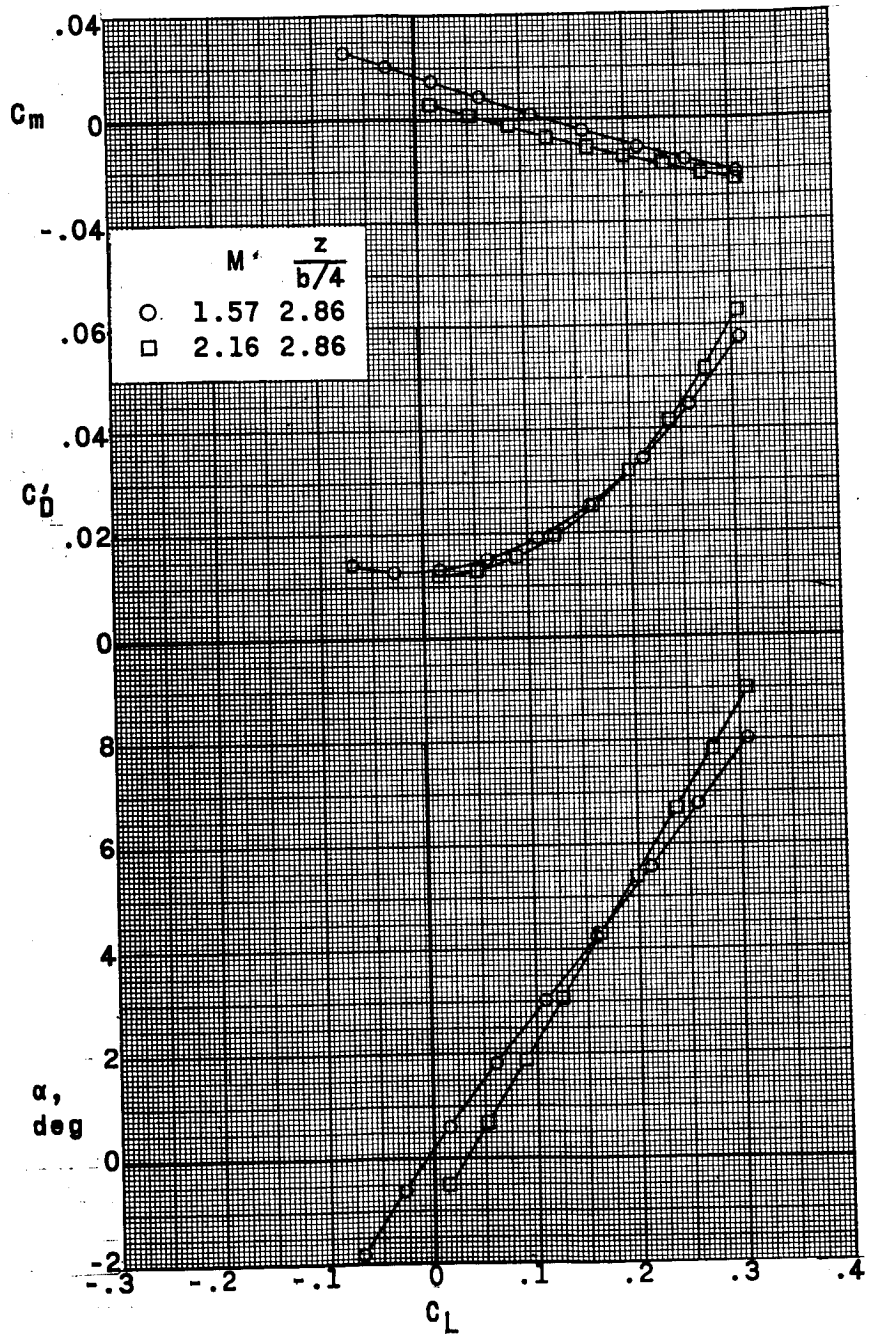

(f) $\left(\frac{z}{b/4}\right)_{nom} = 3.0; \frac{x}{l/4} = 0.02.$

Figure 9.- Continued.

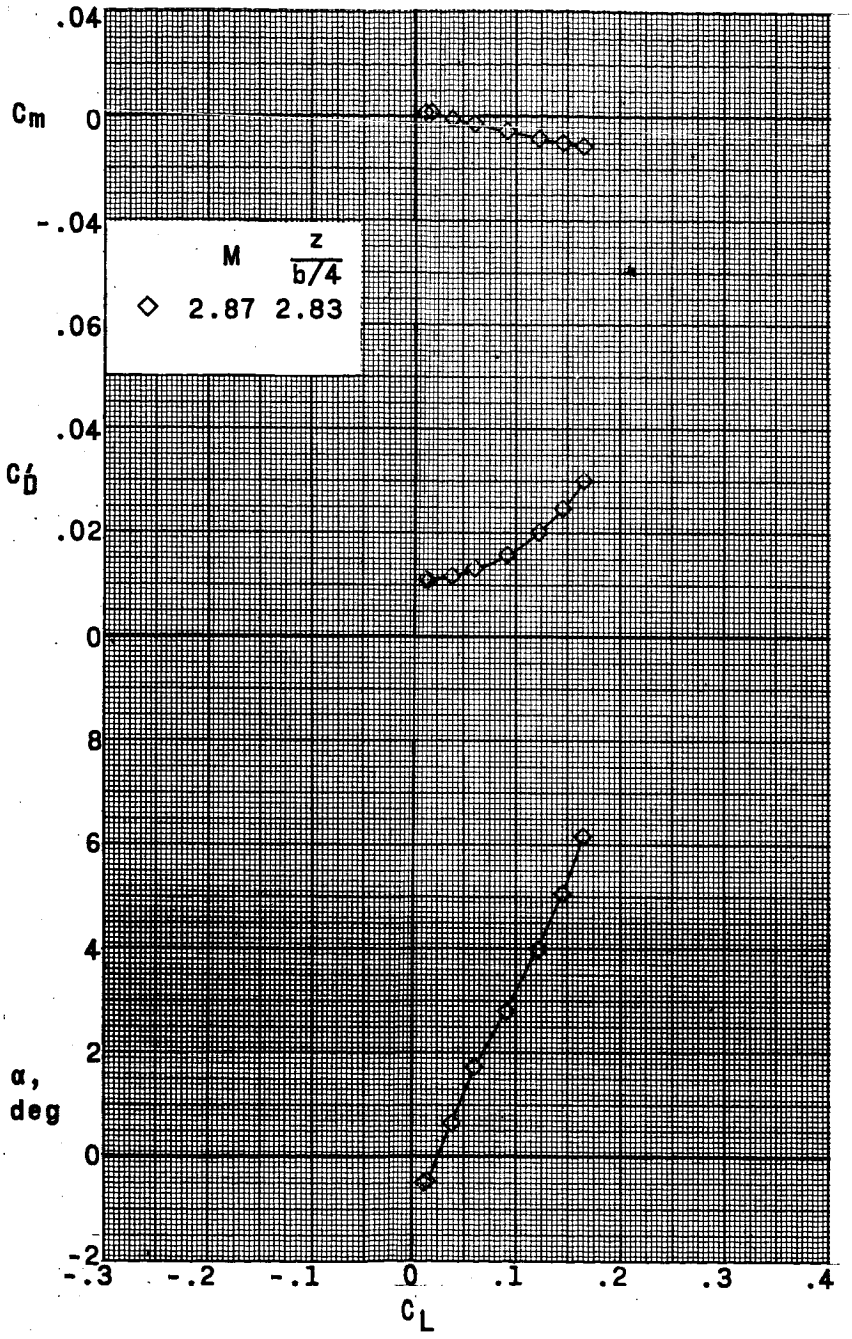

(g) $\left(\frac{z}{b/4}\right)_{nom} = 3.0; \frac{x}{l/4} = 1.02.$

Figure 9.- Continued.

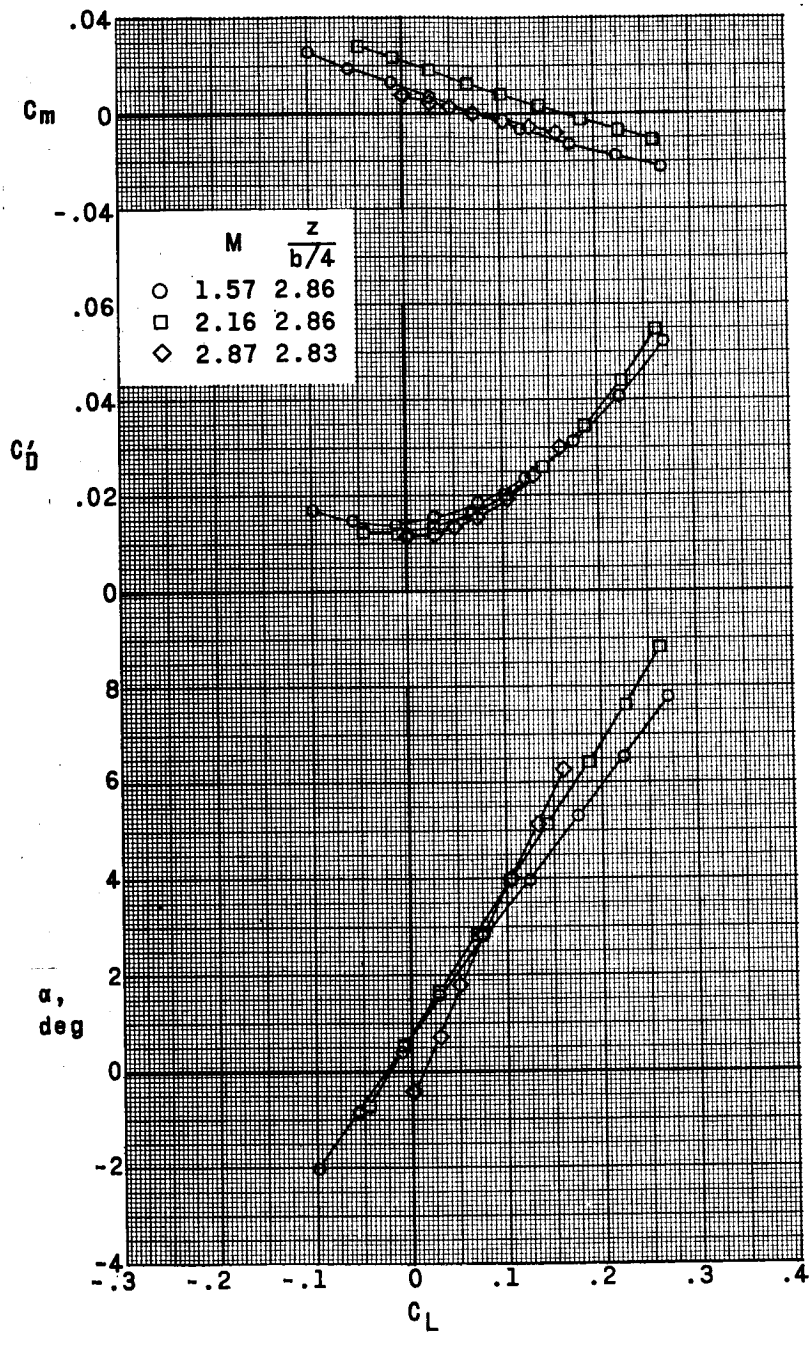

(h) $\left(\frac{z}{b/4}\right)_{nom} = 3.0; \frac{x}{l/4} = 2.02.$

Figure 9.- Continued.

[redacted]

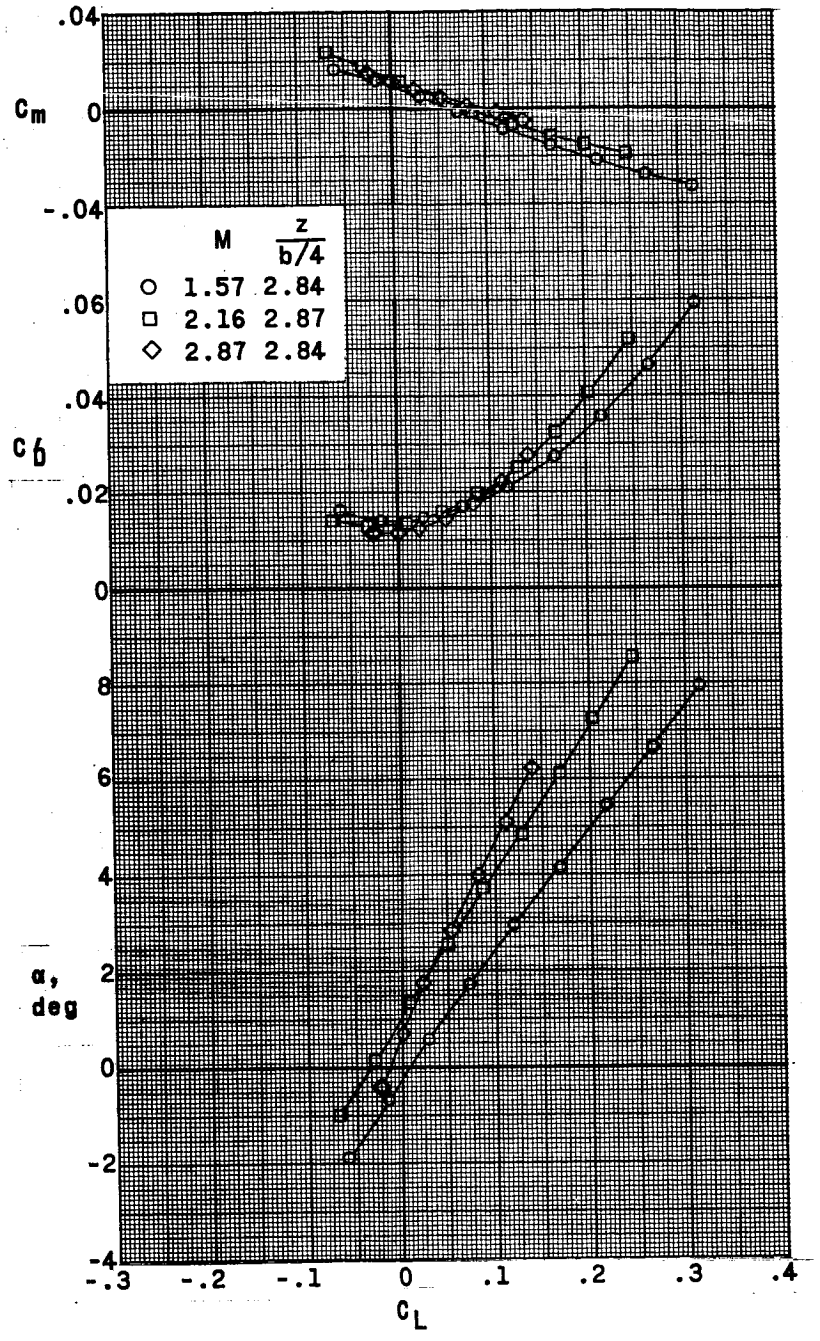

(i) $\left(\frac{z}{b/4}\right)_{nom} = 3.0; \frac{x}{l/4} = 3.02.$

Figure 9.- Continued.

[redacted]

I-591

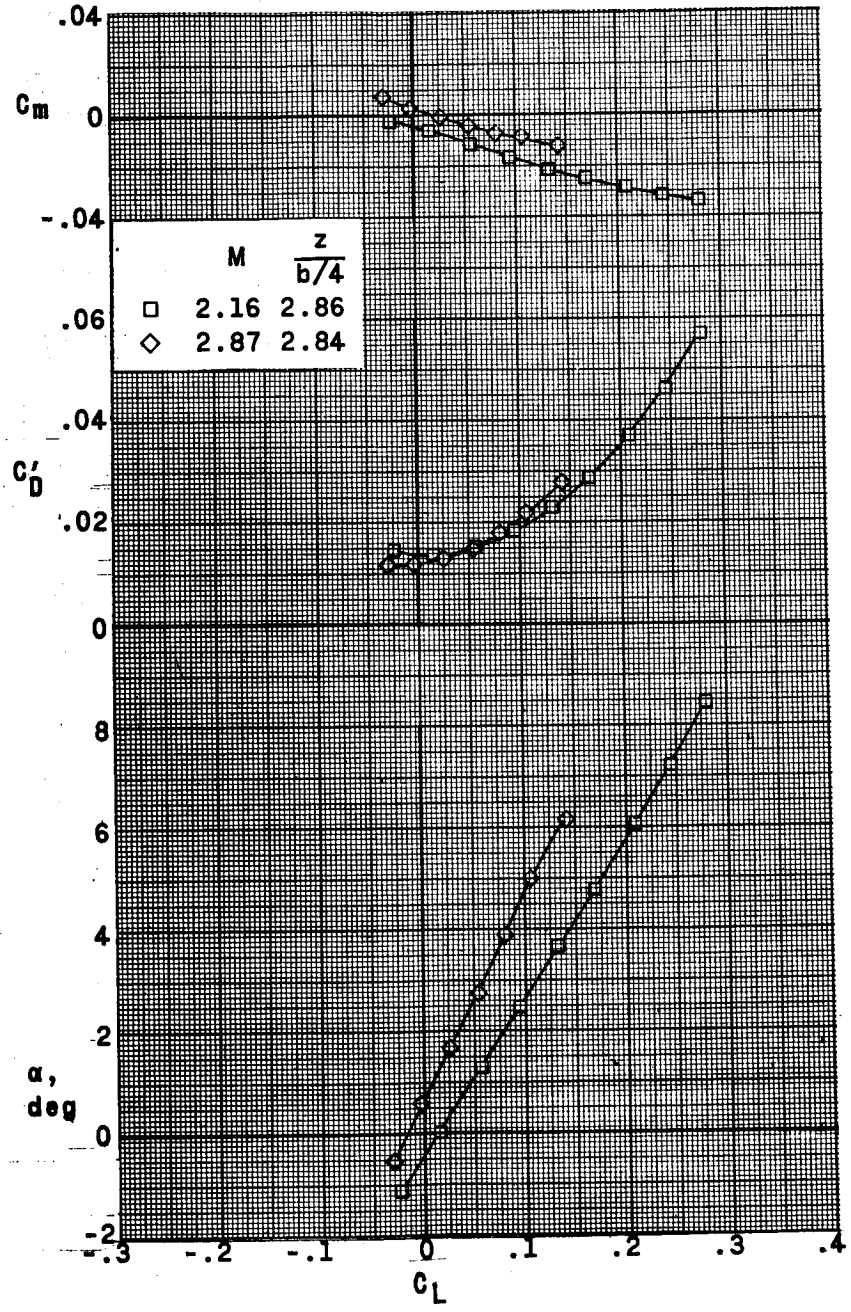

(j) $\left(\frac{z}{b/4}\right)_{nom} = 3.0; \frac{x}{l/4} = 4.02.$

Figure 9.- Continued.

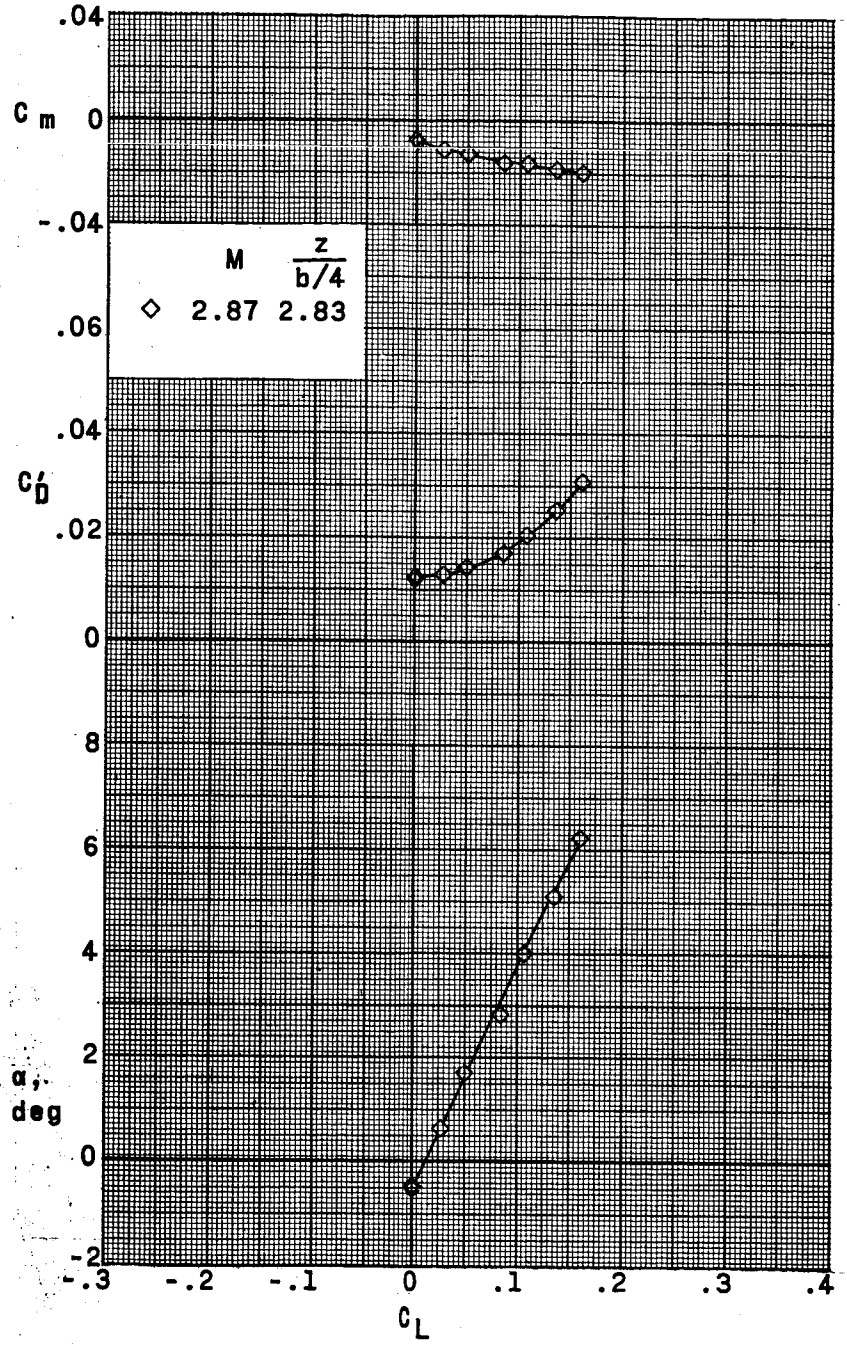

(k) $\left(\frac{z}{b/4}\right)_{nom} = 3.0; \frac{x}{l/4} = 5.02.$

Figure 9.- Continued.

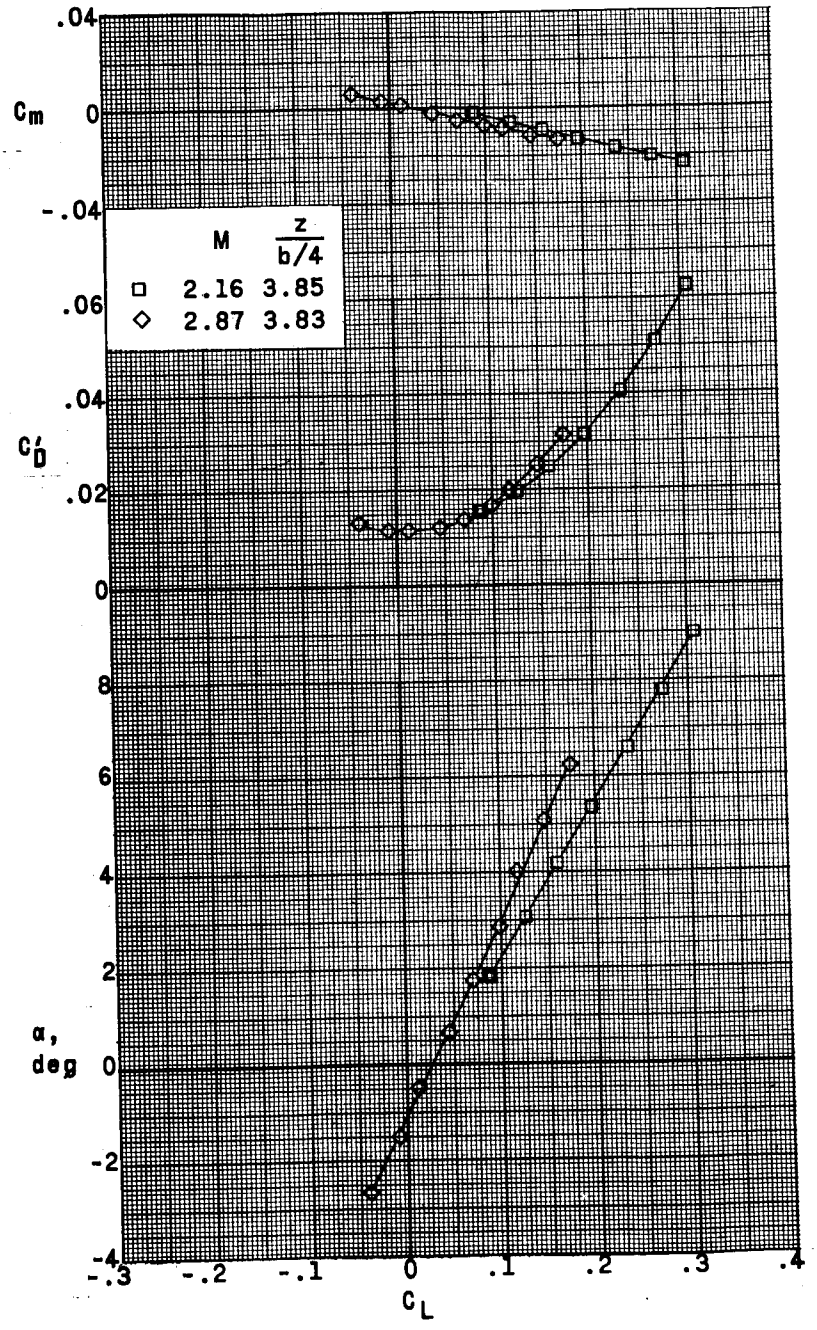

(l) $\left(\frac{z}{b/4}\right)_{nom} = 4.0; \frac{x}{l/4} = 1.02.$

Figure 9.- Continued.

CONFIDENTIAL

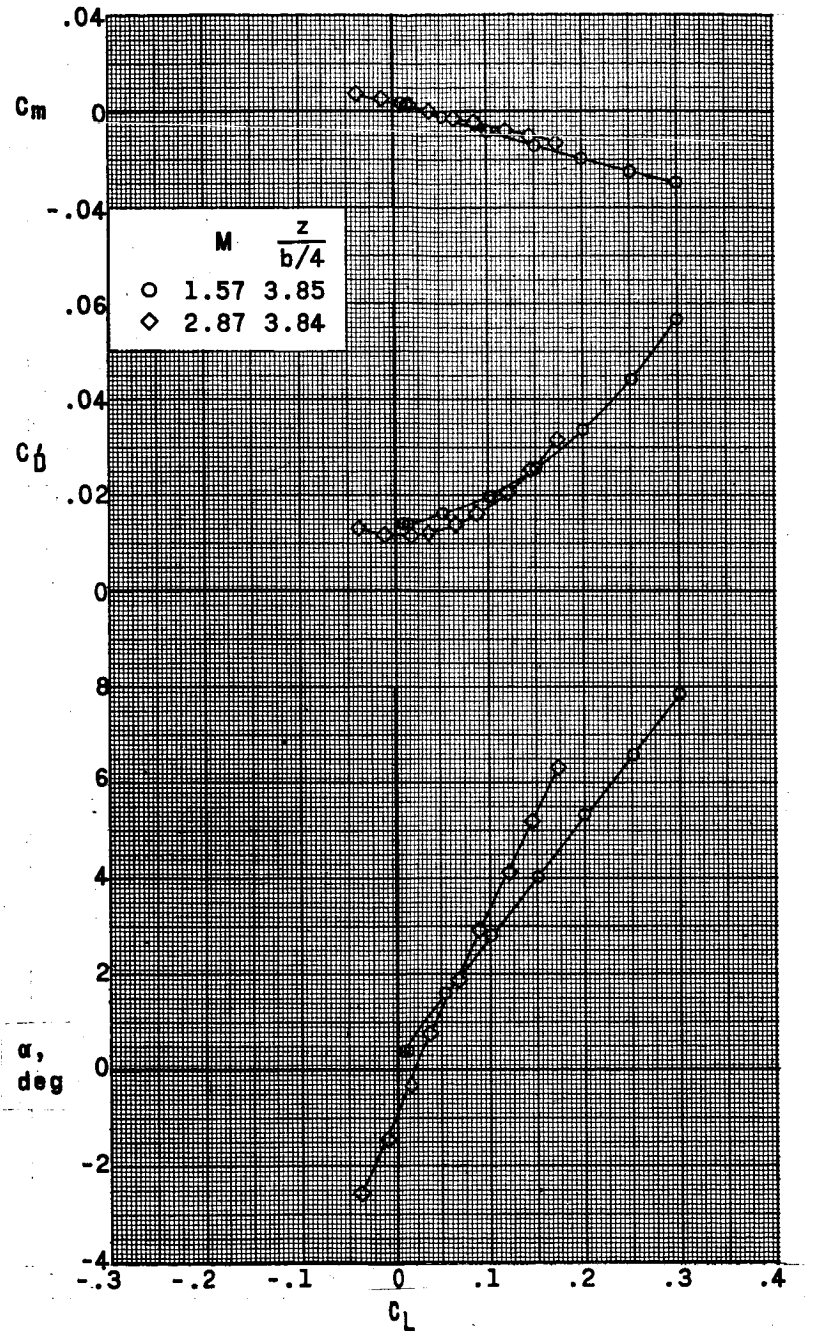

(m) $\left(\frac{z}{b/4}\right)_{nom} = 4.0; \frac{x}{l/4} = 3.02.$

Figure 9.- Continued.

CONFIDENTIAL

CONFIDENTIAL

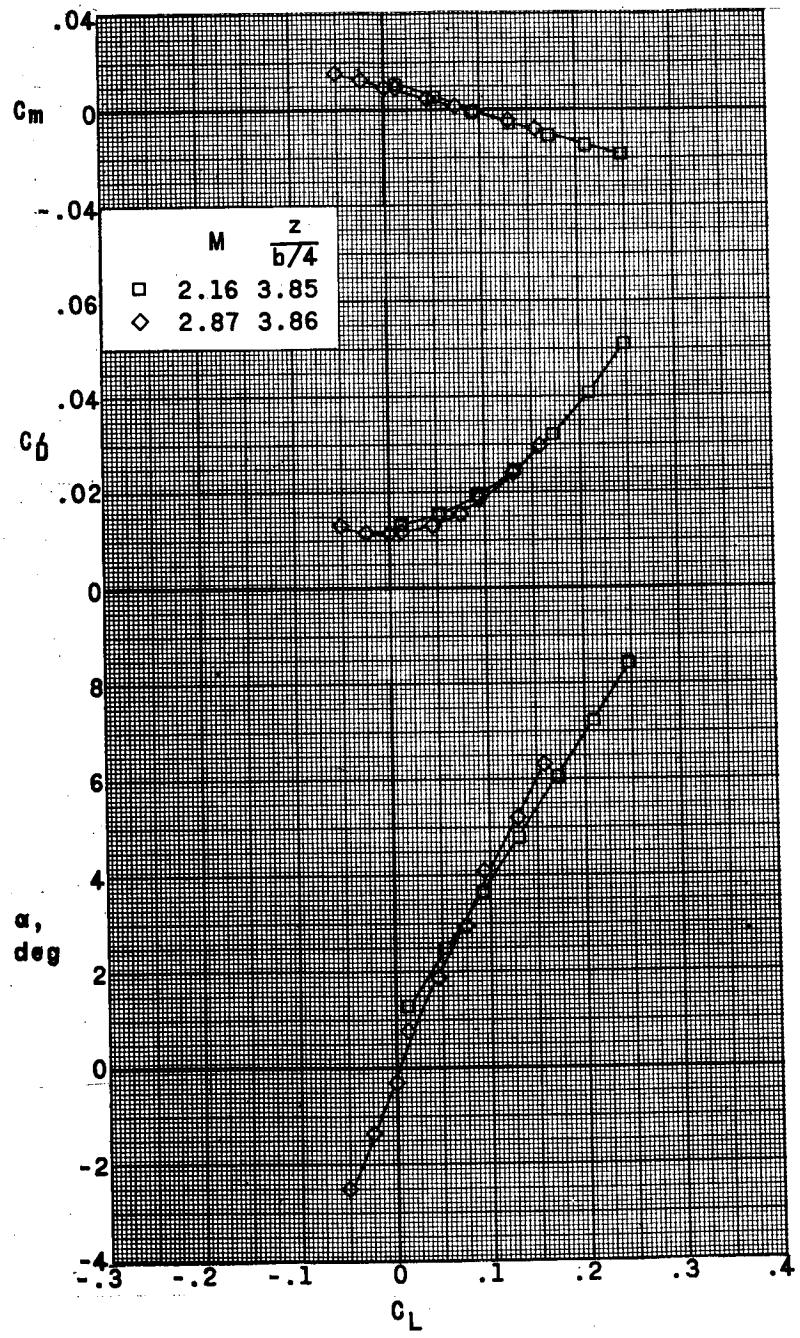

(n) $\left(\frac{z}{b/4}\right)_{nom} = 4.0; \frac{x}{l/4} = 4.02.$

Figure 9.- Continued.

CONFIDENTIAL

L-591

CONFIDENTIAL

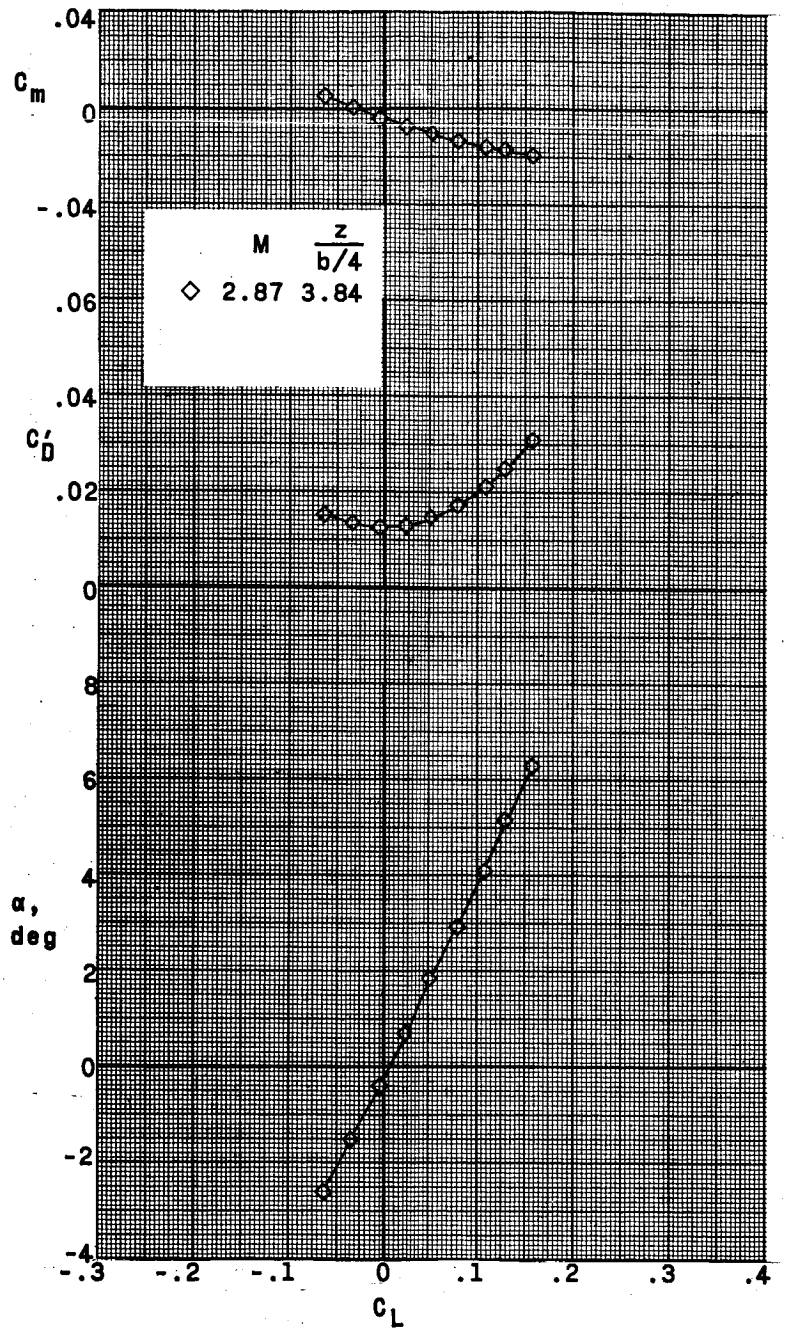

(o) $\left(\frac{z}{b/4}\right)_{nom} = 4.0$; $\frac{x}{l/4} = 6.02$.

Figure 9.- Concluded.

CONFIDENTIAL

CONFIDENTIAL

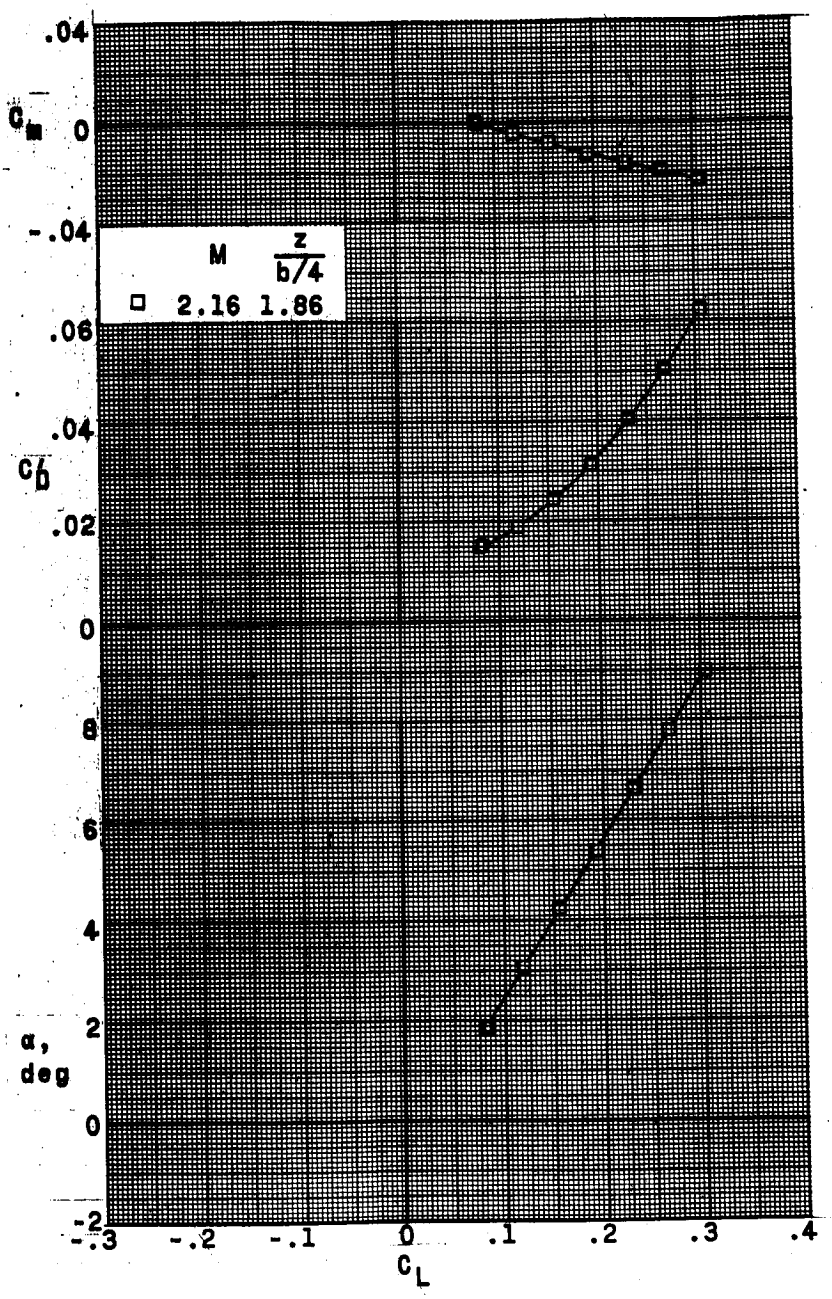

(a) $\left(\frac{z}{b/4}\right)_{nom} = 2.0$; $\frac{x}{l/4} = 0.02$.

Figure 10.- Aerodynamic characteristics in pitch of the receiver model in presence of tanker model. $\beta = 0^{\circ}$; $\frac{y}{b/4} = 2.0$.

CONFIDENTIAL

CONFIDENTIAL

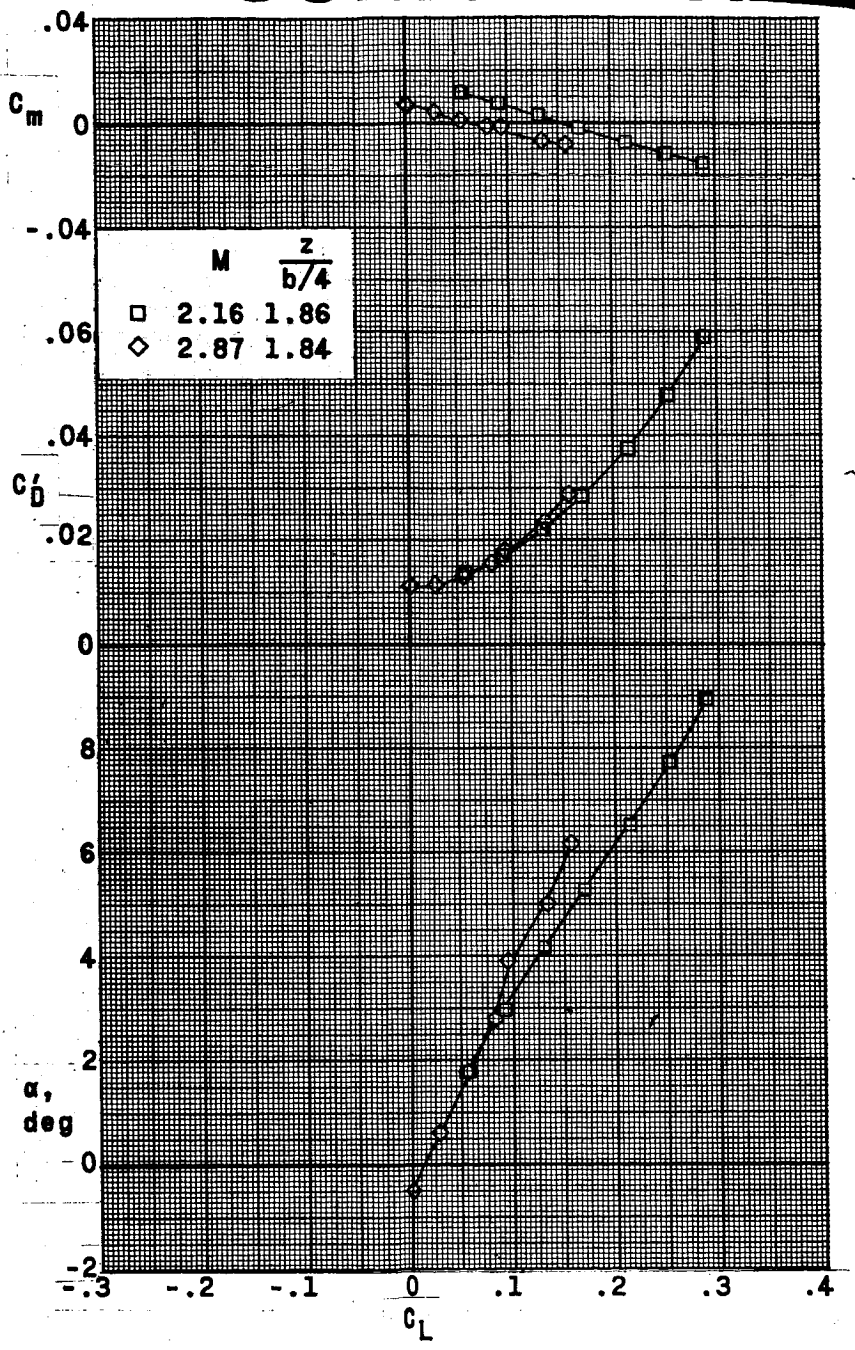

(b) $\left(\frac{z}{b/4}\right)_{nom} = 2.0$; $\frac{x}{l/4} = 1.02$.

Figure 10.- Continued.

CONFIDENTIAL

CONFIDENTIAL

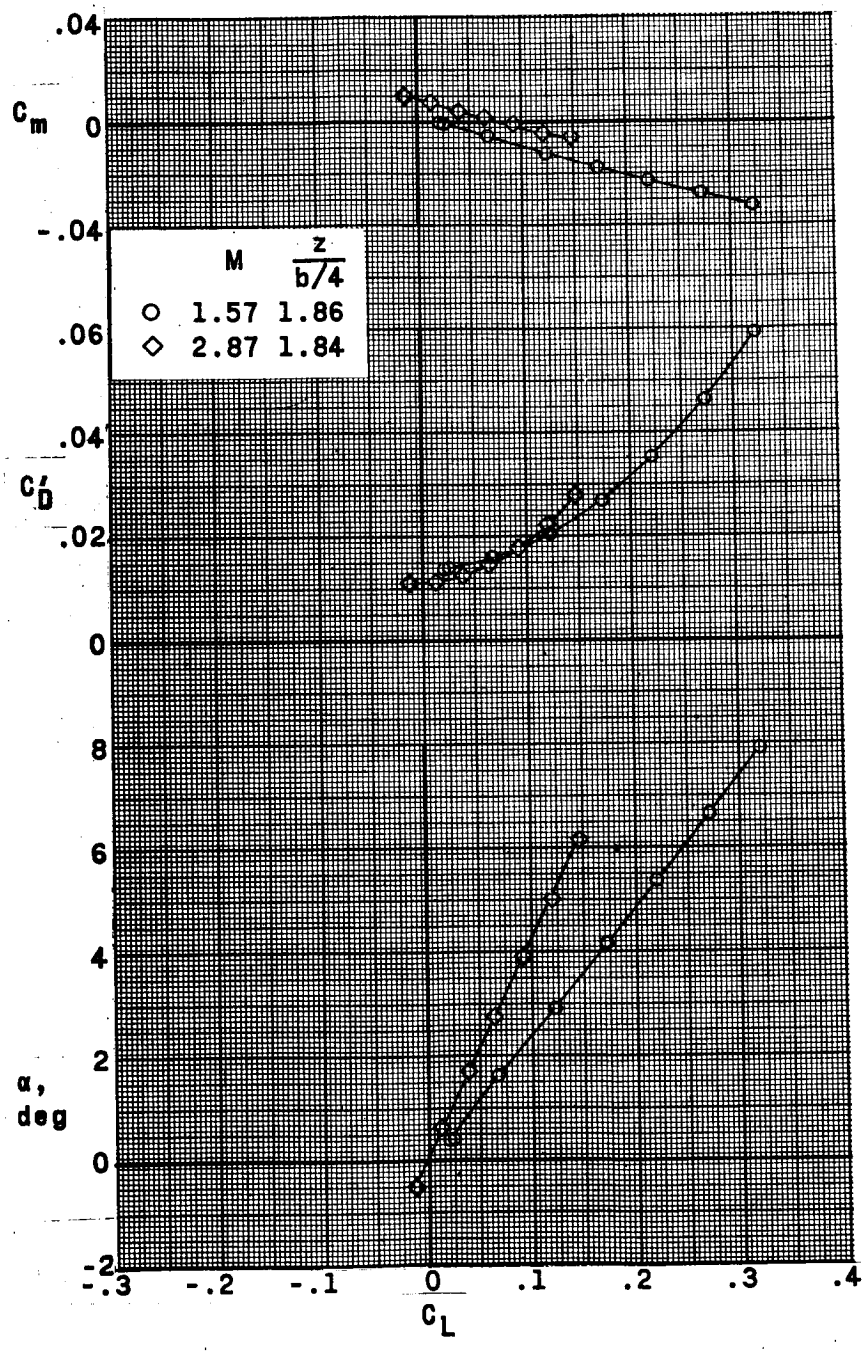

(c) $\left(\frac{z}{b/4}\right)_{nom} = 2.0$; $\frac{x}{l/4} = 2.02$.

Figure 10.- Continued.

CONFIDENTIAL

L-591

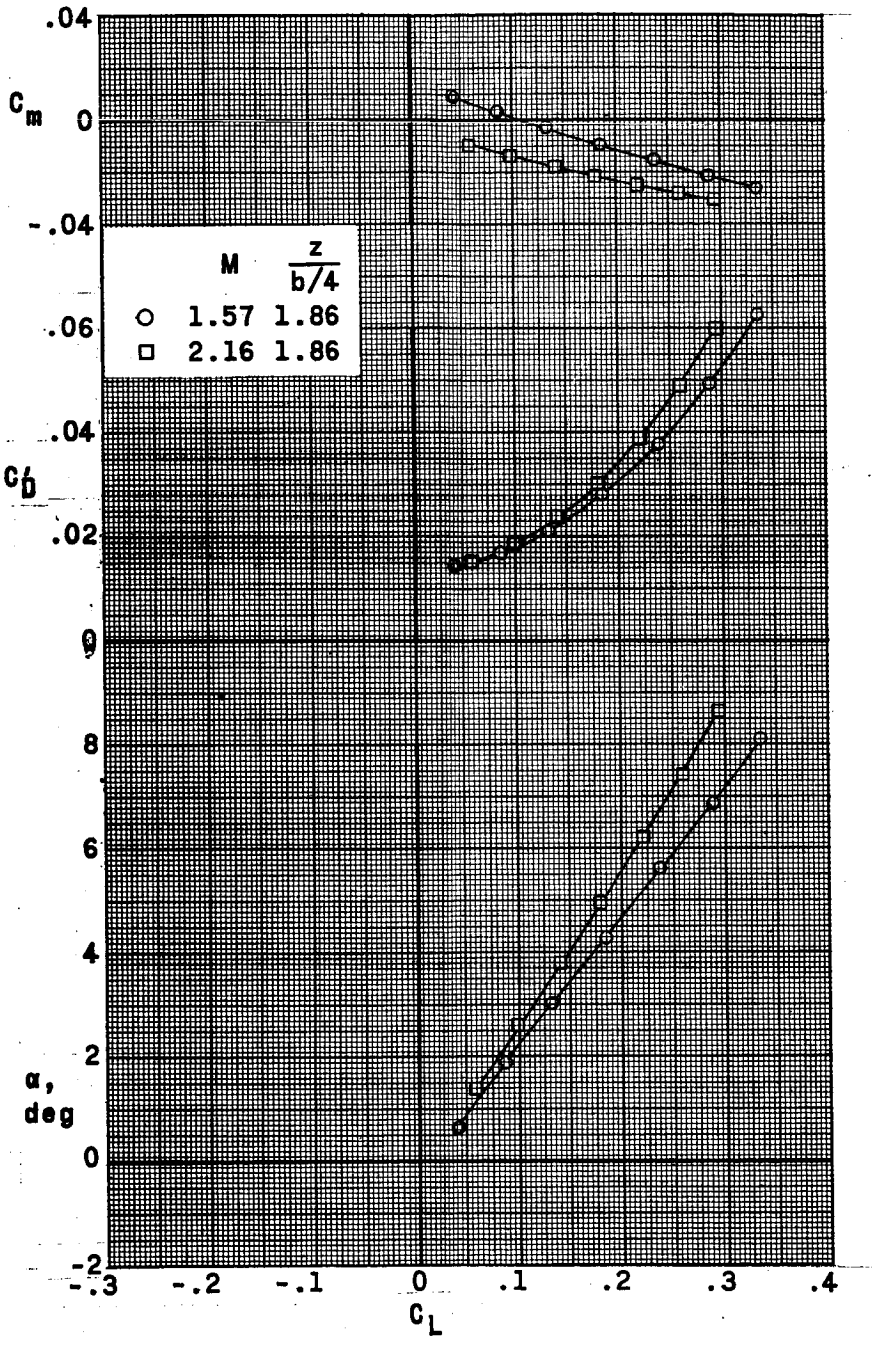

(d) $\left(\frac{z}{b/4}\right)_{nom} = 2.0; \frac{x}{l/4} = 3.02.$

Figure 10.- Continued.

L-591

CONFIDENTIAL

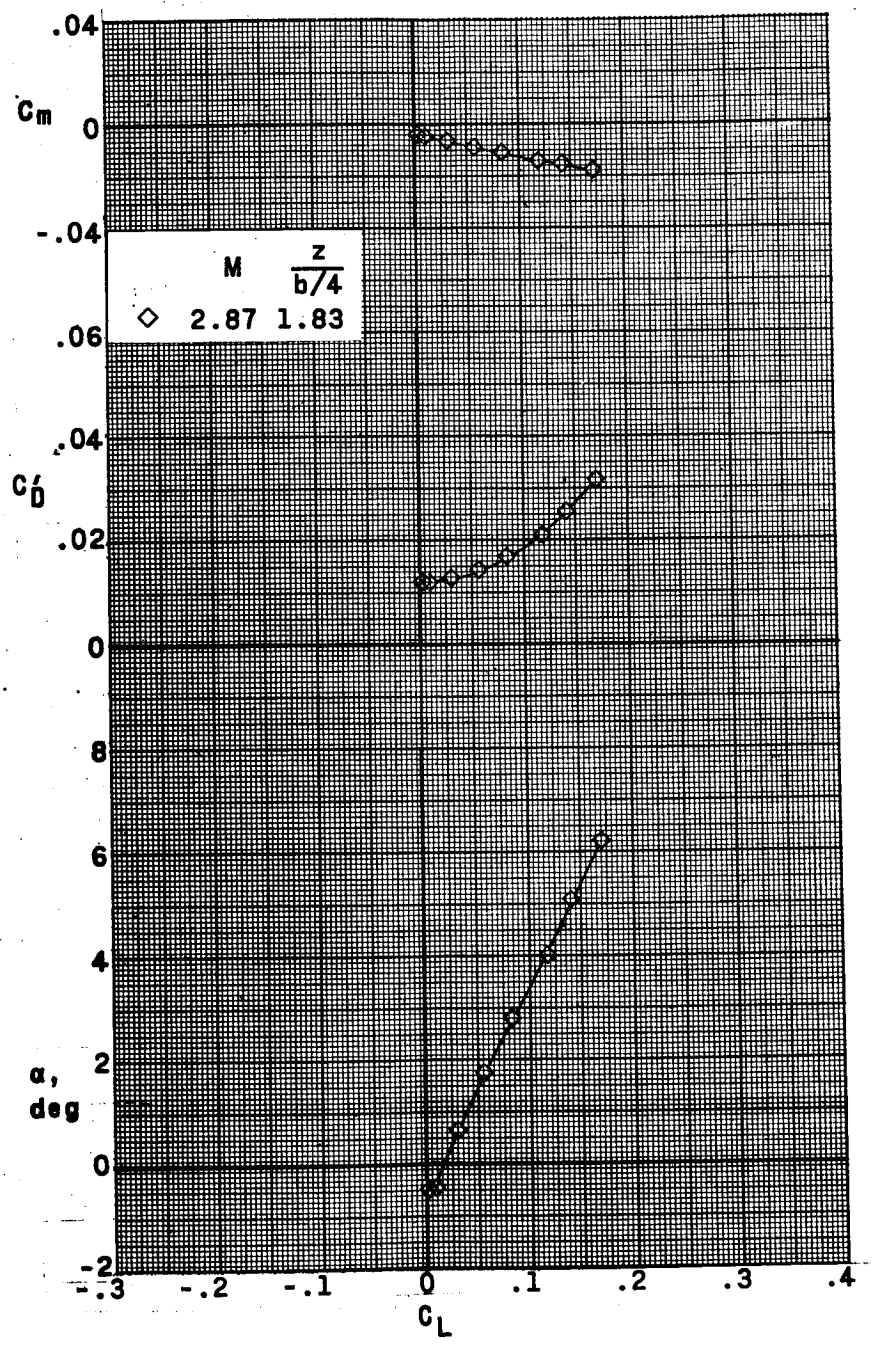

(e) $\left(\frac{z}{b/4}\right)_{nom} = 2.0; \frac{x}{l/4} = 4.02.$

Figure 10.- Continued.

CONFIDENTIAL

CONFIDENTIAL

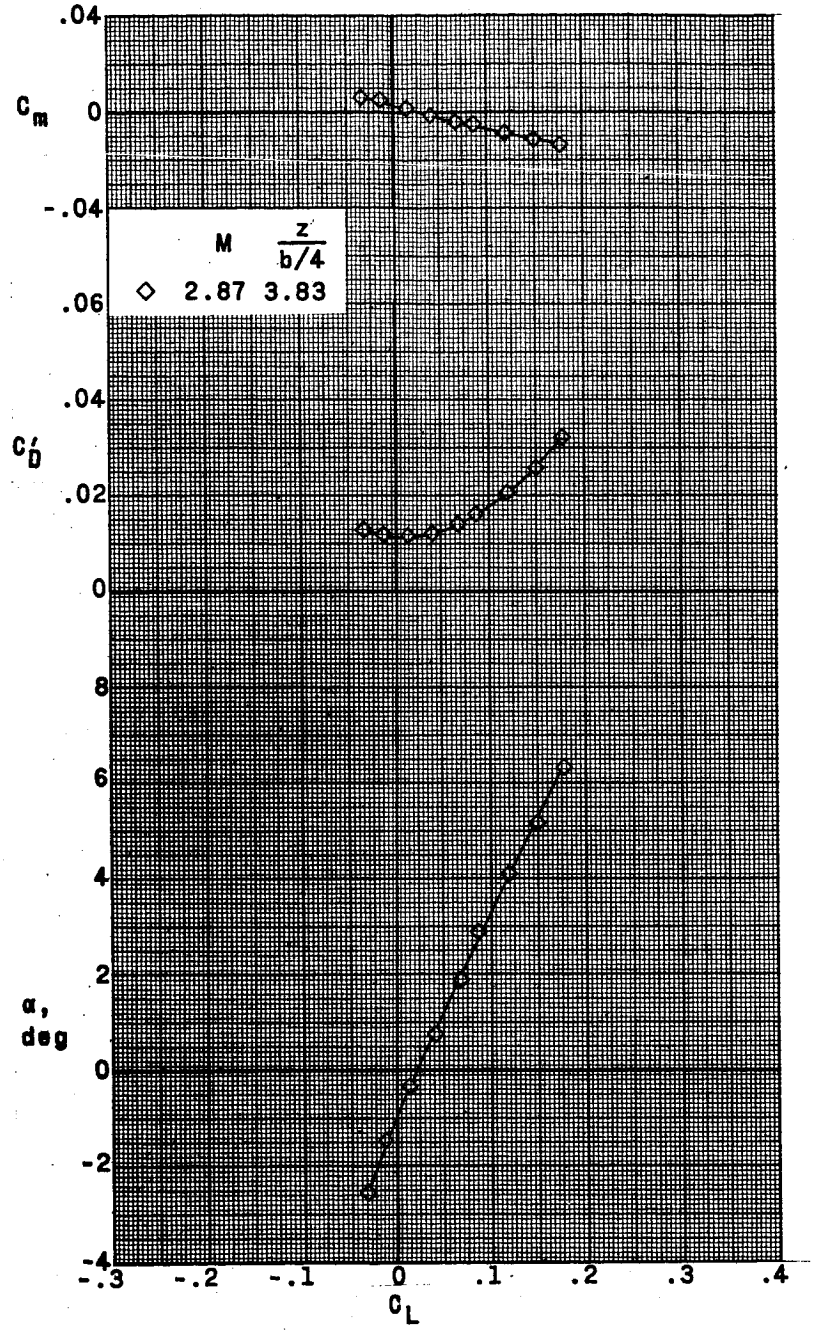

(f) $\left(\frac{z}{b/4}\right)_{nom} = 4.0; \frac{x}{l/4} = 3.02.$

Figure 10.- Concluded.

CONFIDENTIAL

CONFIDENTIAL

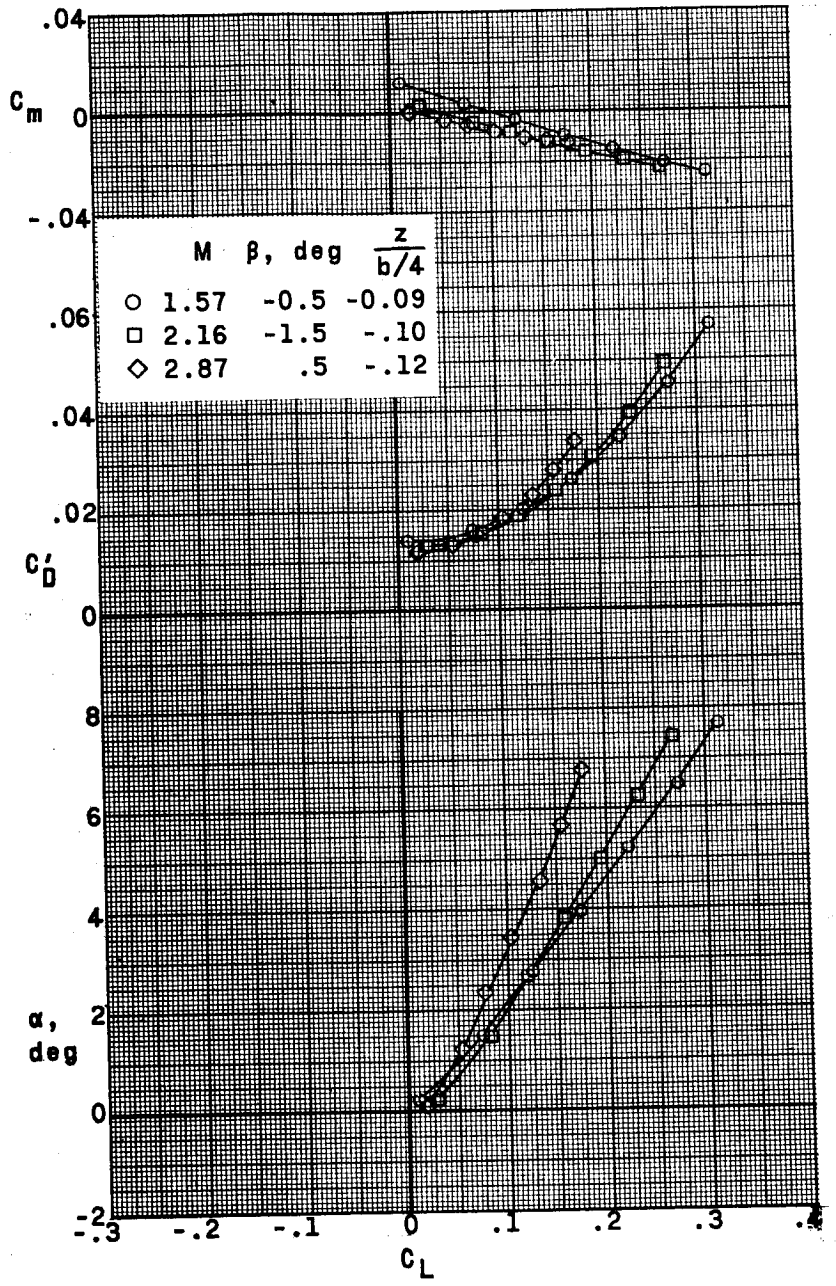

(a) $\left(\frac{z}{b/4}\right)_{nom} = 0$; $\frac{x}{l/4} = 0.02$.

Figure 11.- Aerodynamic characteristics in pitch of the receiver model in presence of tanker model. $\frac{y}{b/4} = 4.75$; $\beta_{nom} = 0^o$.

CONFIDENTIAL

L-591

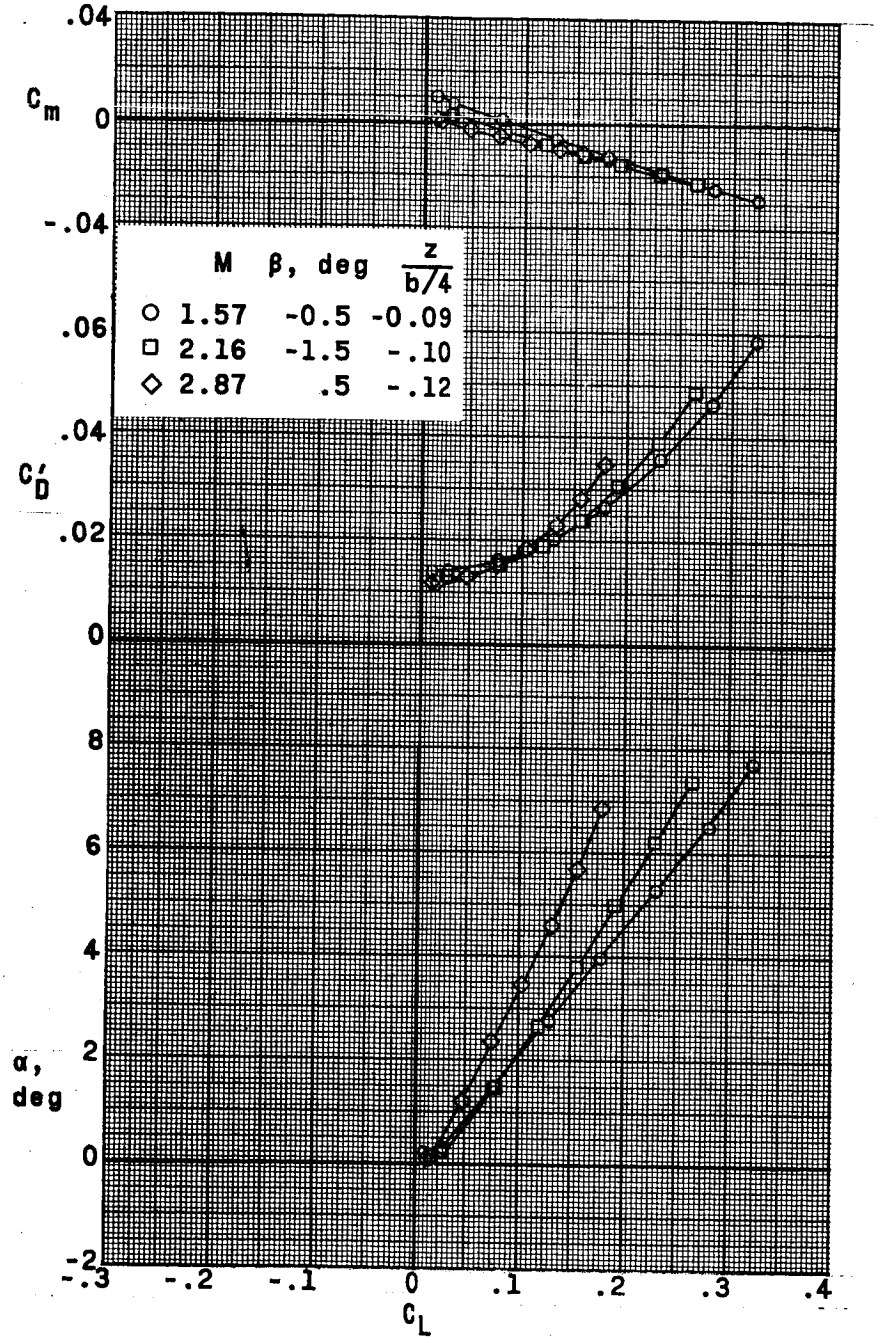

(b) $\left(\frac{z}{b/4}\right)_{nom} = 0$; $\frac{x}{l/4} = 1.03$.

Figure 11.- Continued.

CONFIDENTIAL

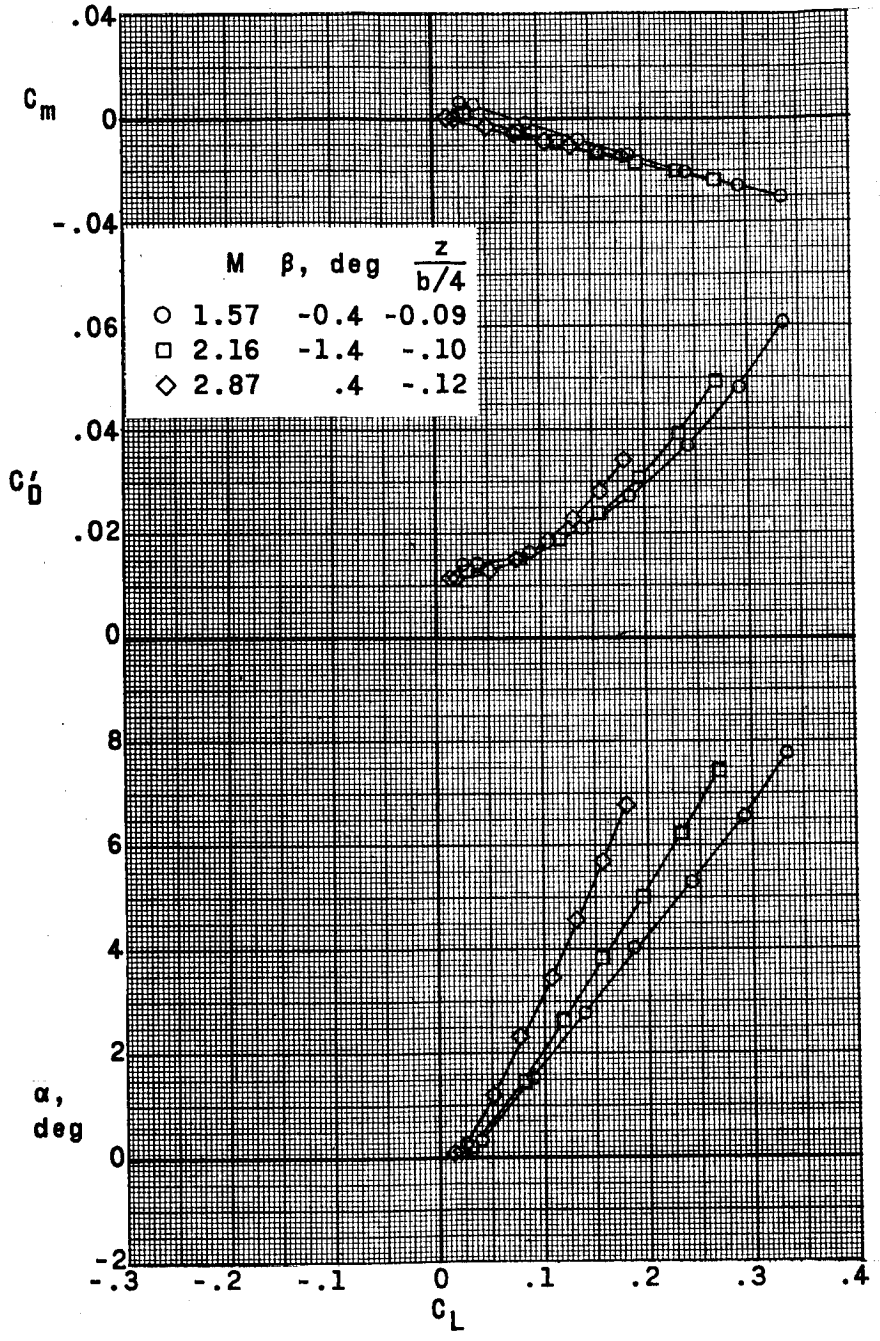

(c) $\left(\frac{z}{b/4}\right)_{nom} = 0$; $\frac{x}{l/4} = 2.03$.

Figure 11.- Continued.

CONFIDENTIAL

L-591

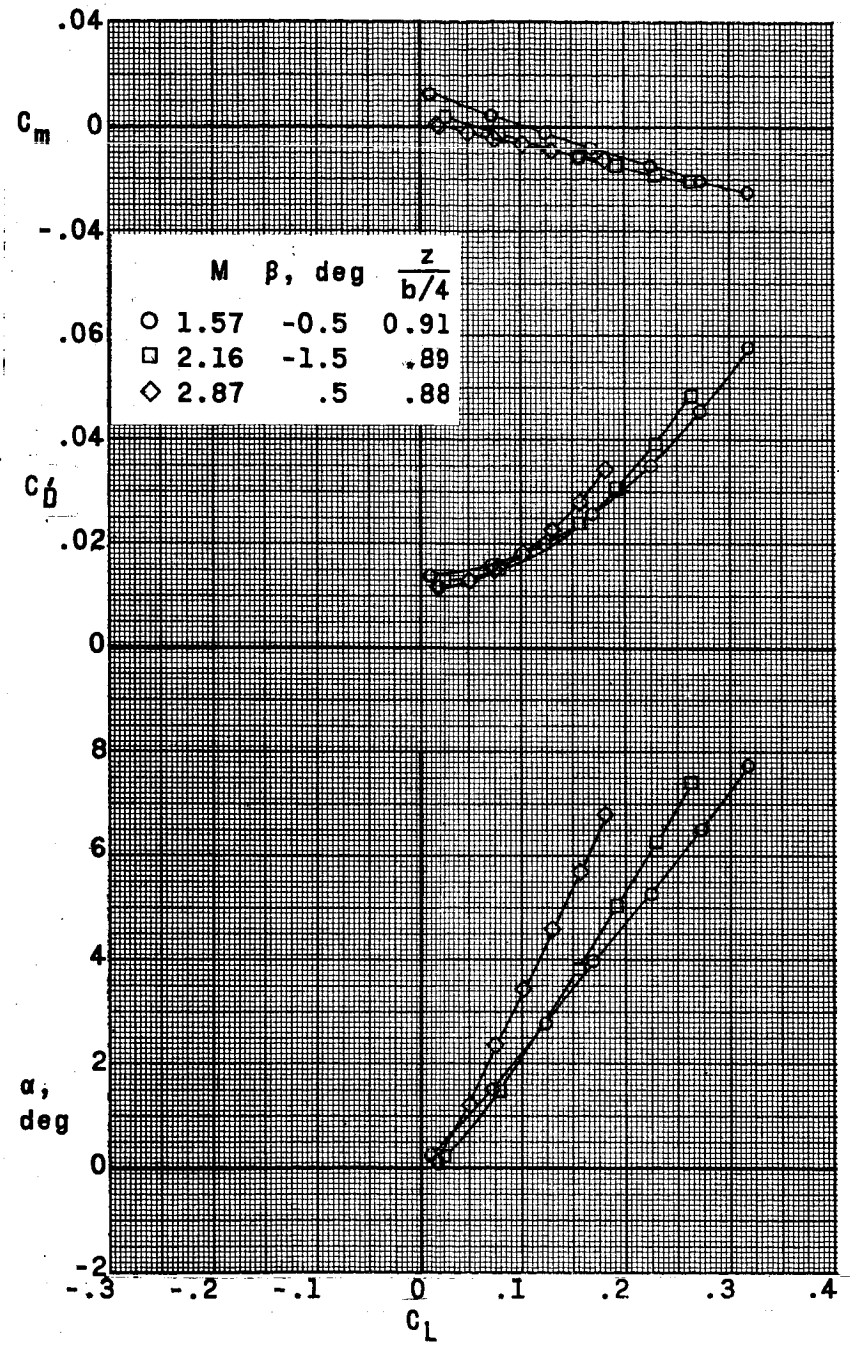

(d) $\left(\frac{z}{b/4}\right)_{nom} = 1.0; \frac{x}{l/4} = 0.03.$

Figure 11.- Continued.

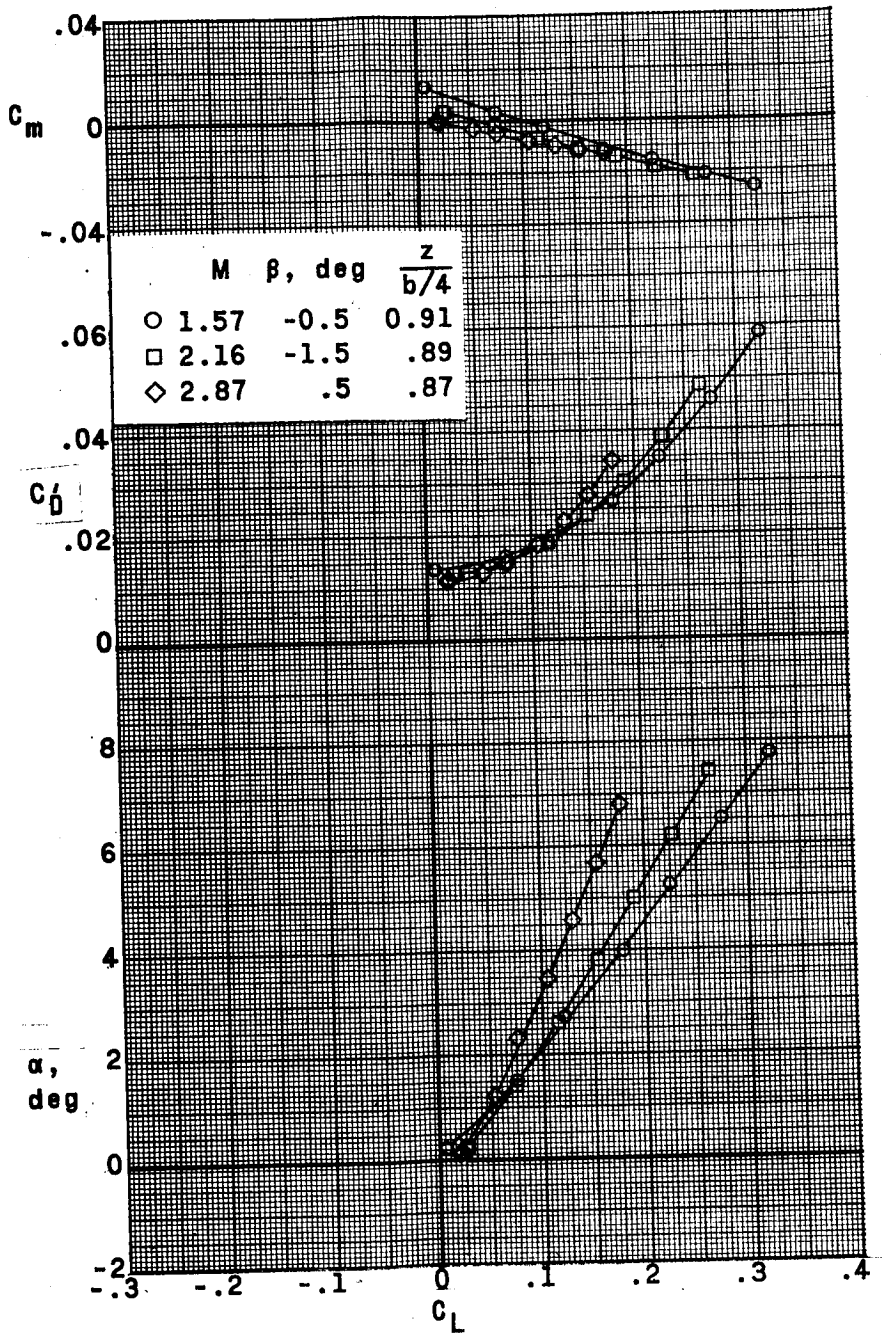

(e) $\left(\frac{z}{b/4}\right)_{nom} = 1.0; \frac{x}{l/4} = 1.03.$

Figure 11.- Continued.

CONFIDENTIAL

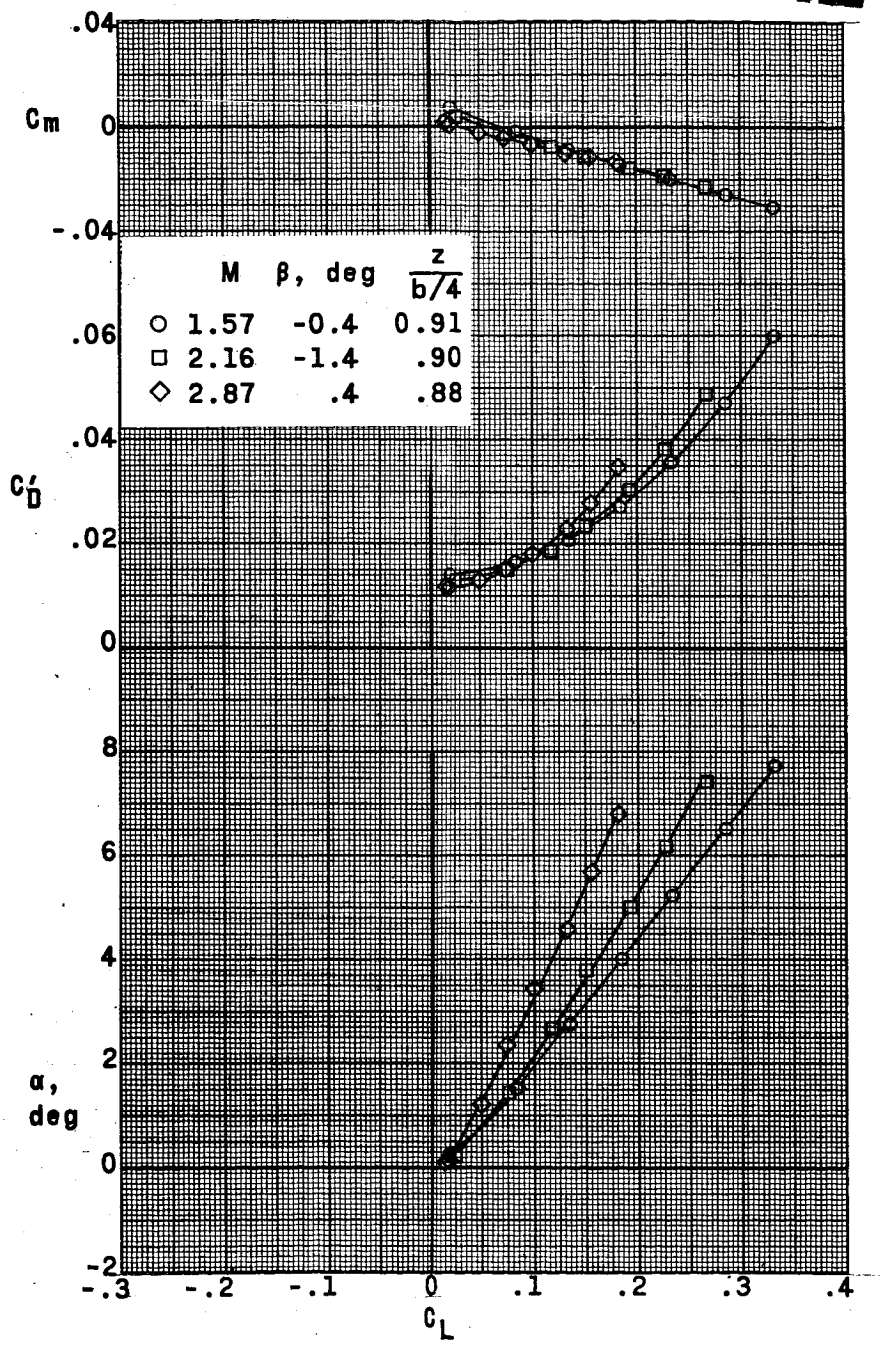

(f) $\left(\frac{z}{b/4}\right)_{nom} = 1.0; \frac{x}{l/4} = 2.03.$

Figure 11.- Concluded.

CONFIDENTIAL

L-591

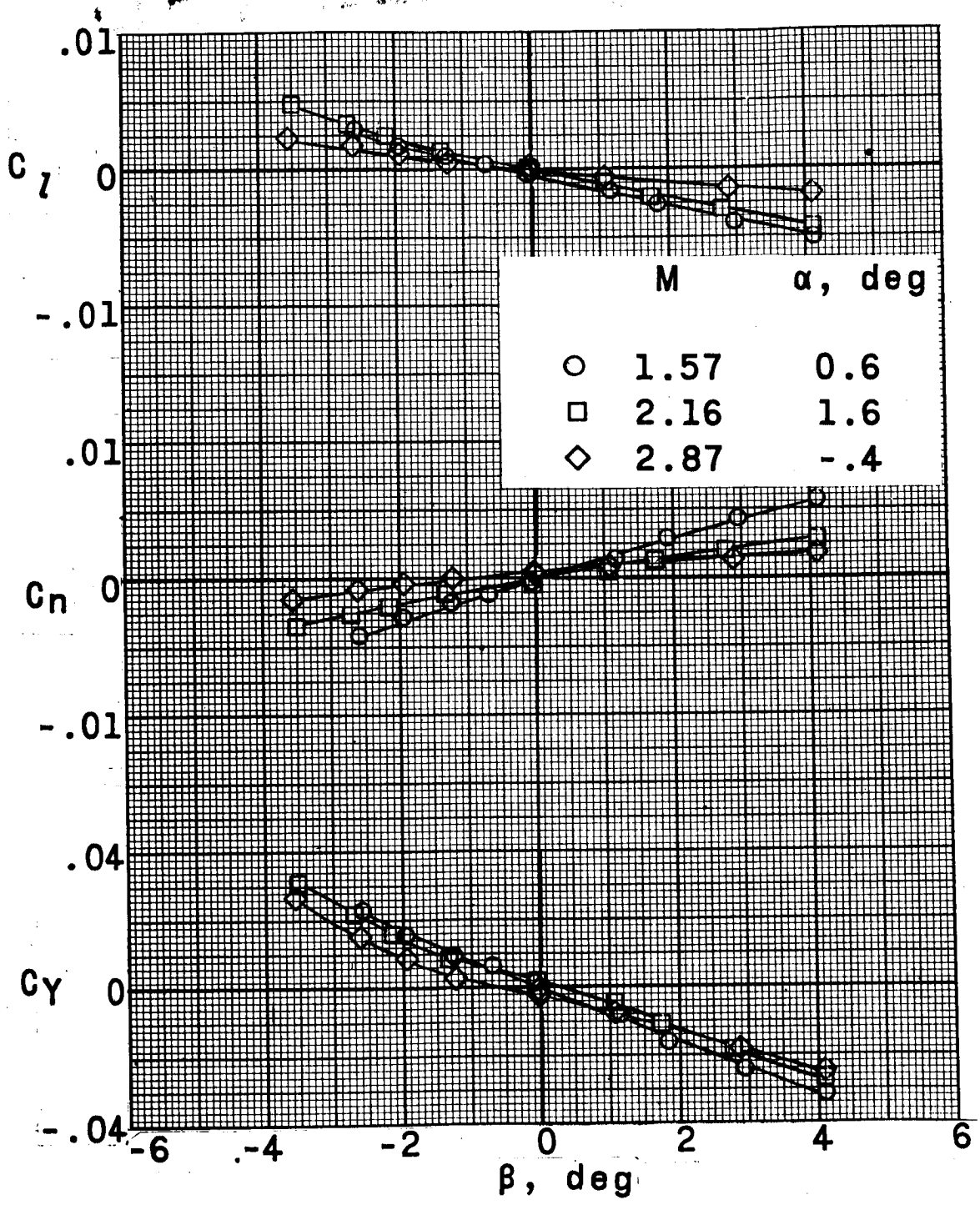

Figure 12.- Aerodynamic characteristics in sideslip of the receiver model alone. $\alpha_{nom} = 0^{\circ}$.

CONFIDENTIAL

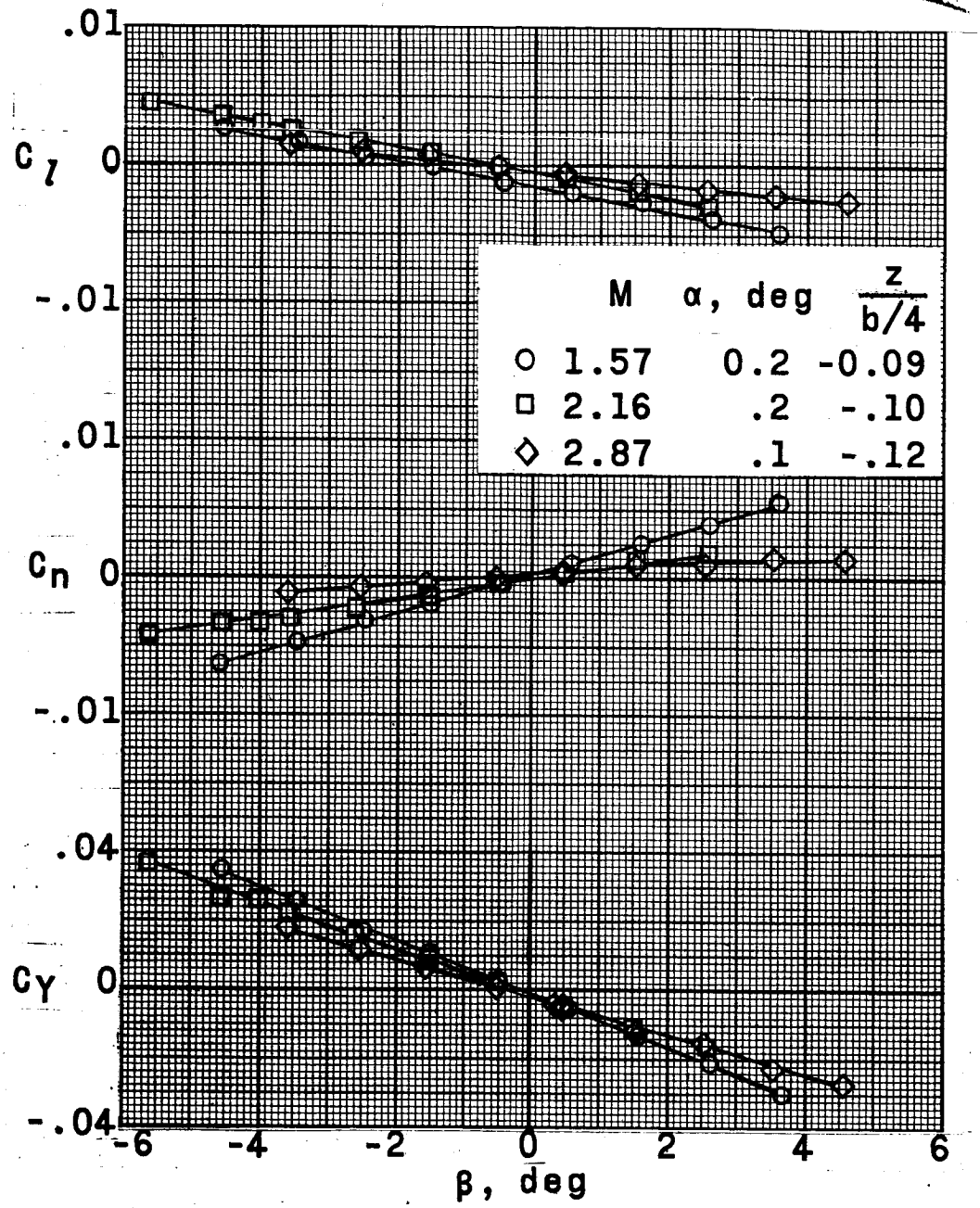

(a) $\left(\frac{z}{b/4}\right)_{nom} = 0$; $\frac{x}{l/4} = 0.02$.

Figure 13.- Aerodynamic characteristics in sideslip of the receiver model in presence of tanker model. $\frac{y}{b/4} = 4.80$.

CONFIDENTIAL

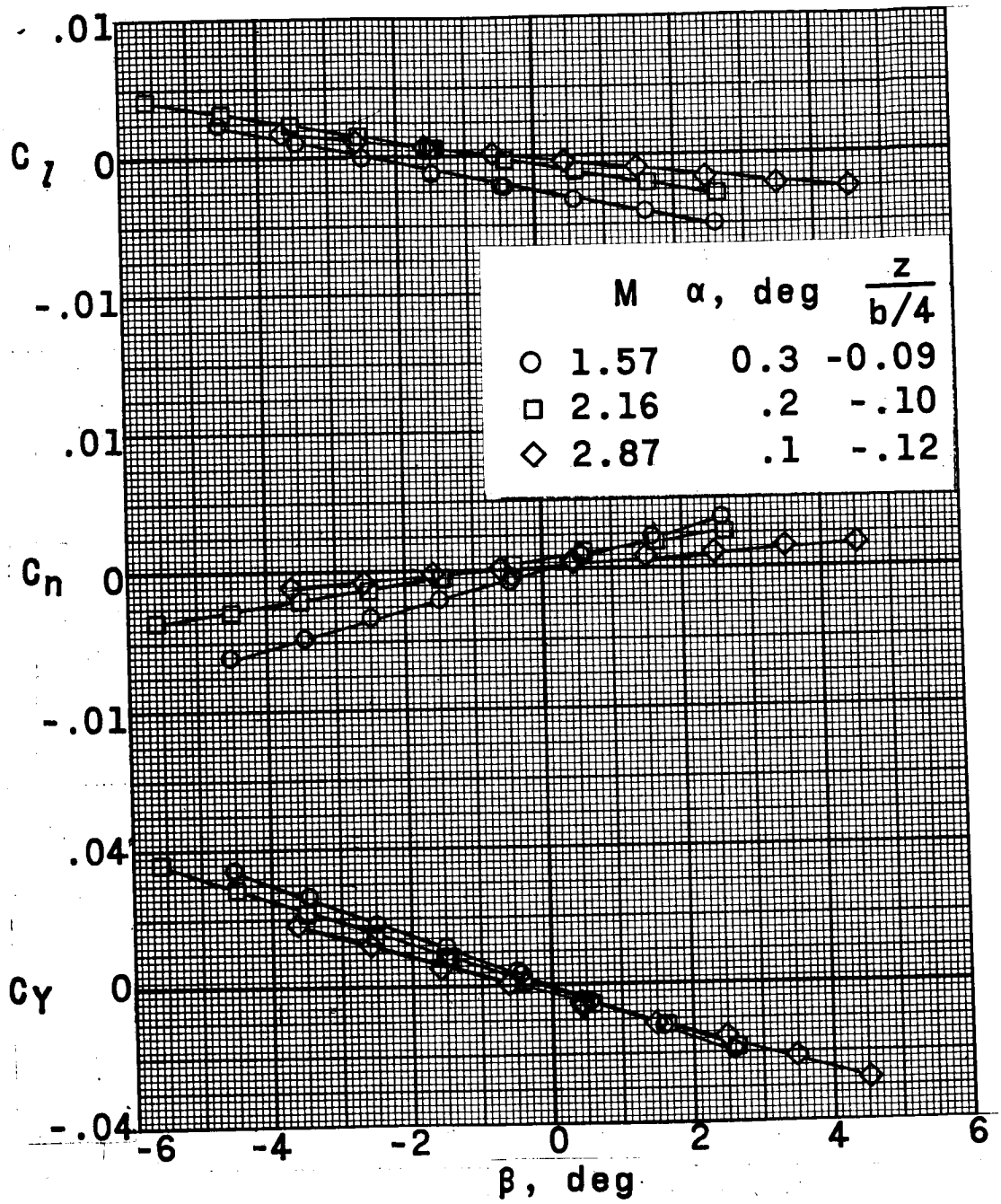

(b) $\left(\frac{z}{b/4}\right)_{nom} = 0; \frac{x}{l/4} = 1.02.$

Figure 13.- Continued.

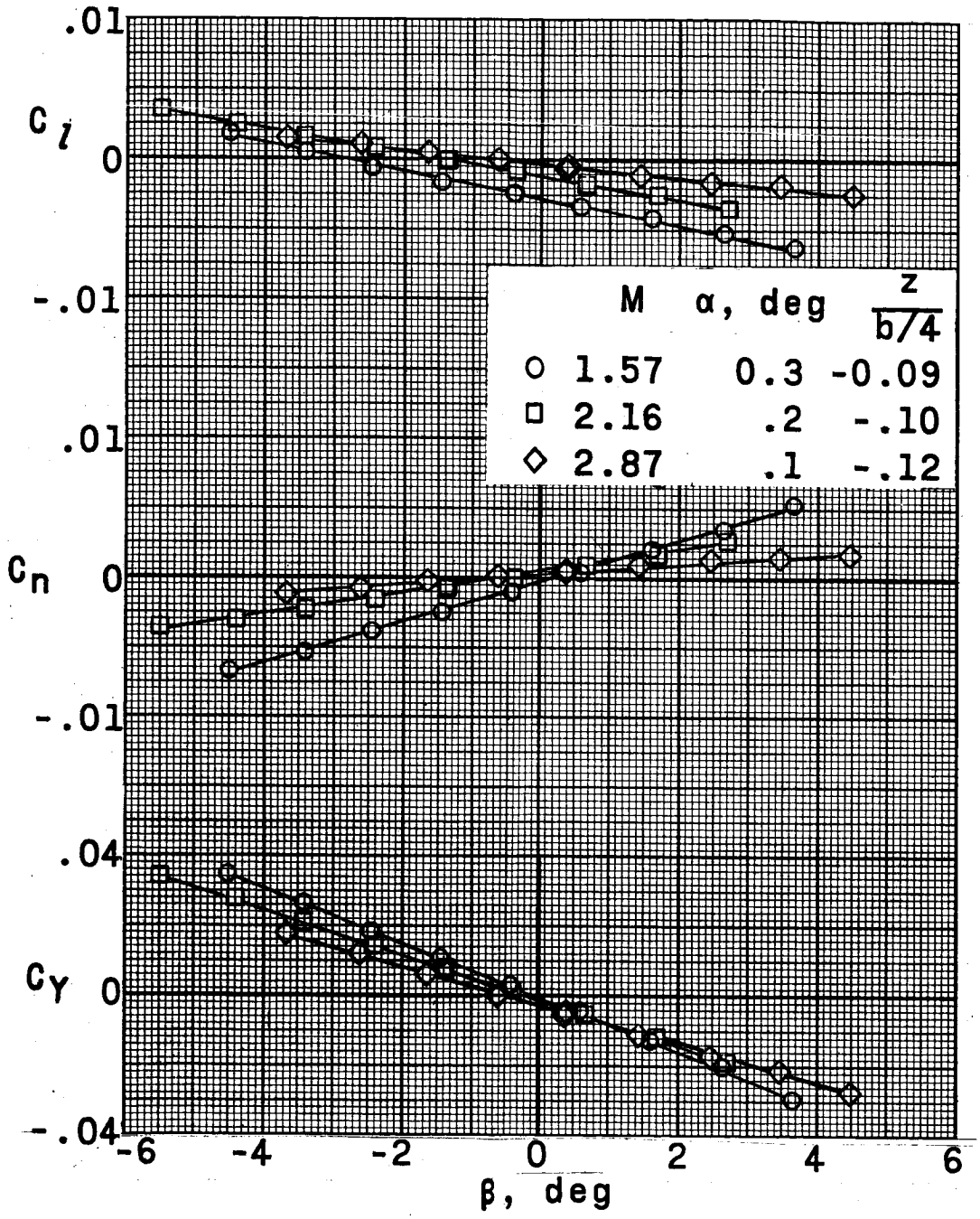

(c) $\left(\frac{z}{b/4}\right)_{nom} = 0$; $\frac{x}{l/4} = 2.03$.

Figure 13.- Continued.

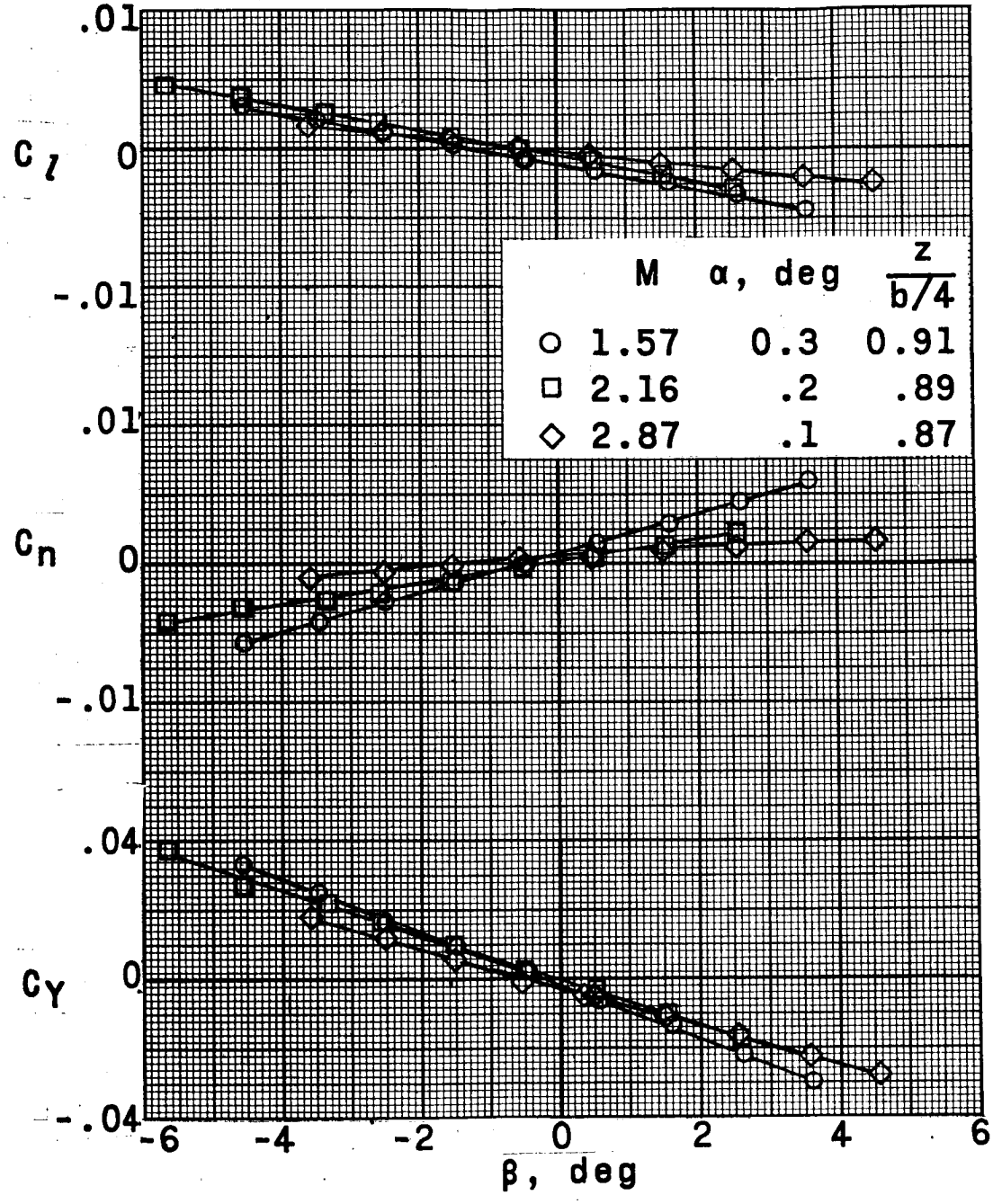

(d) $\left(\frac{z}{b/4}\right)_{nom} = 1.0; \frac{x}{l/4} = 0.02.$

Figure 13.- Continued.

CONFIDENTIAL

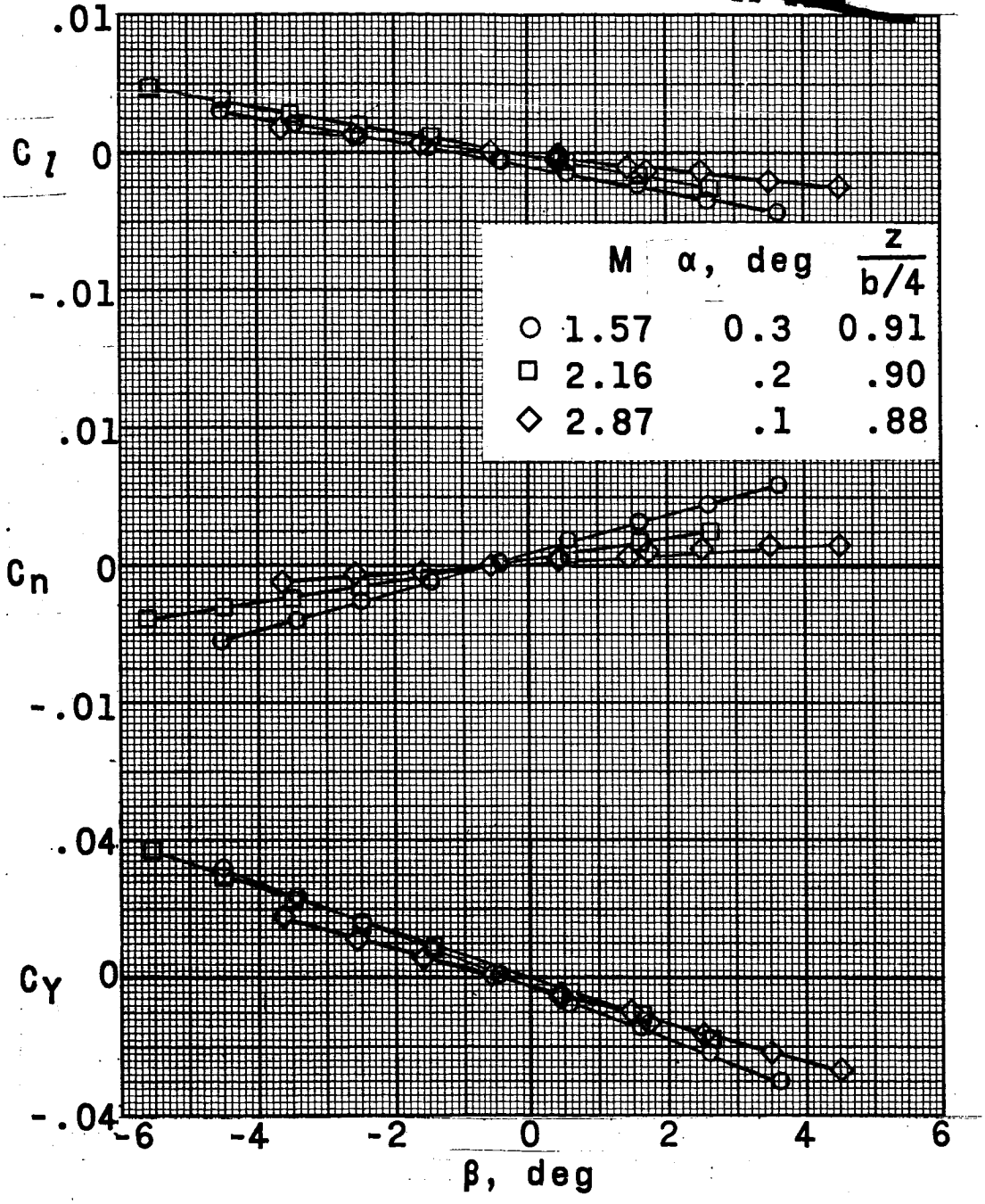

(e) $\left(\frac{z}{b/4}\right)_{nom} = 1.0$; $\frac{x}{l/4} = 1.02$.

Figure 13.- Continued.

CONFIDENTIAL

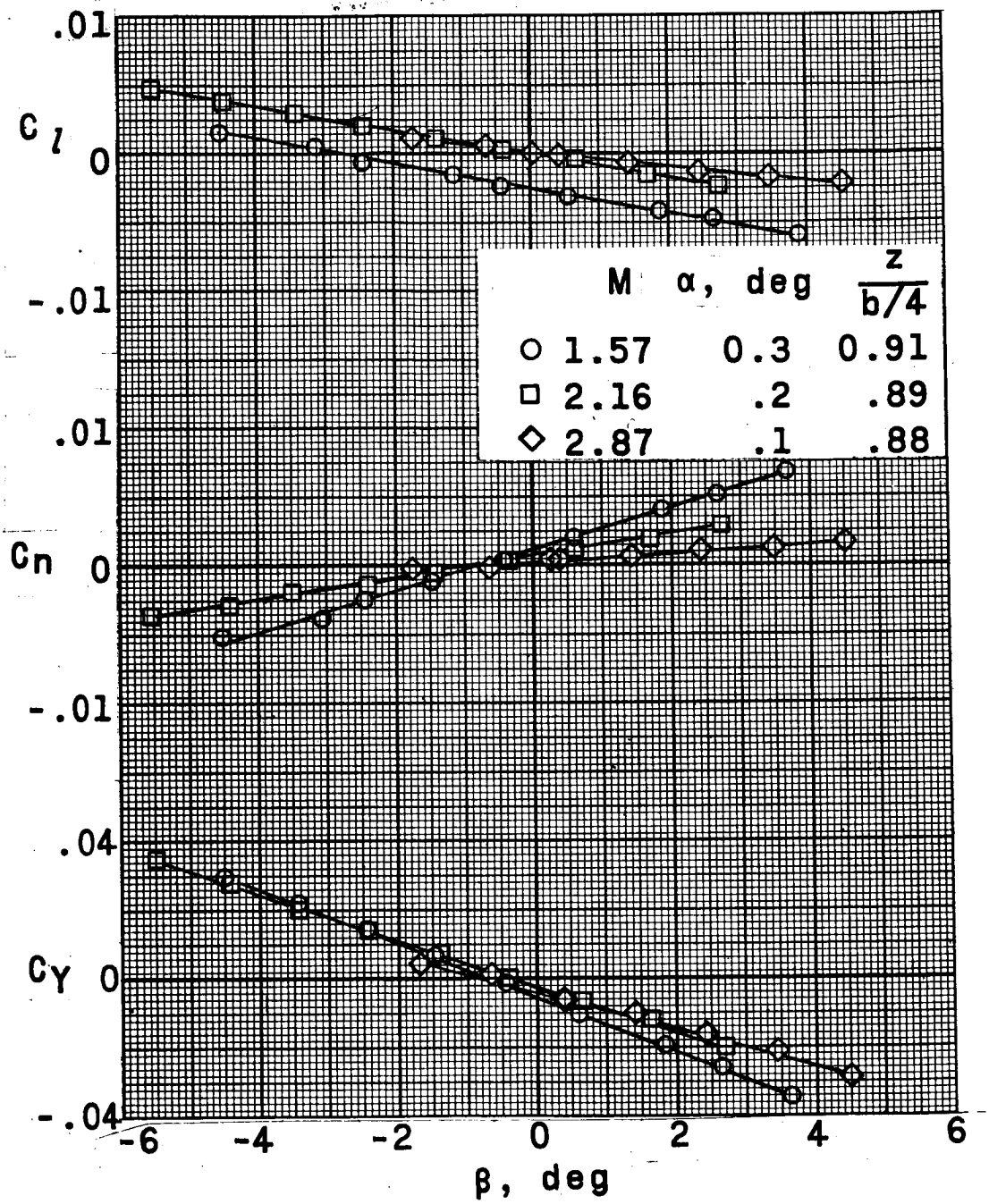

(f) $\left(\frac{z}{b/4}\right)_{nom} = 1.0$; $\frac{x}{l/4} = 2.02$.

Figure 13.- Concluded.

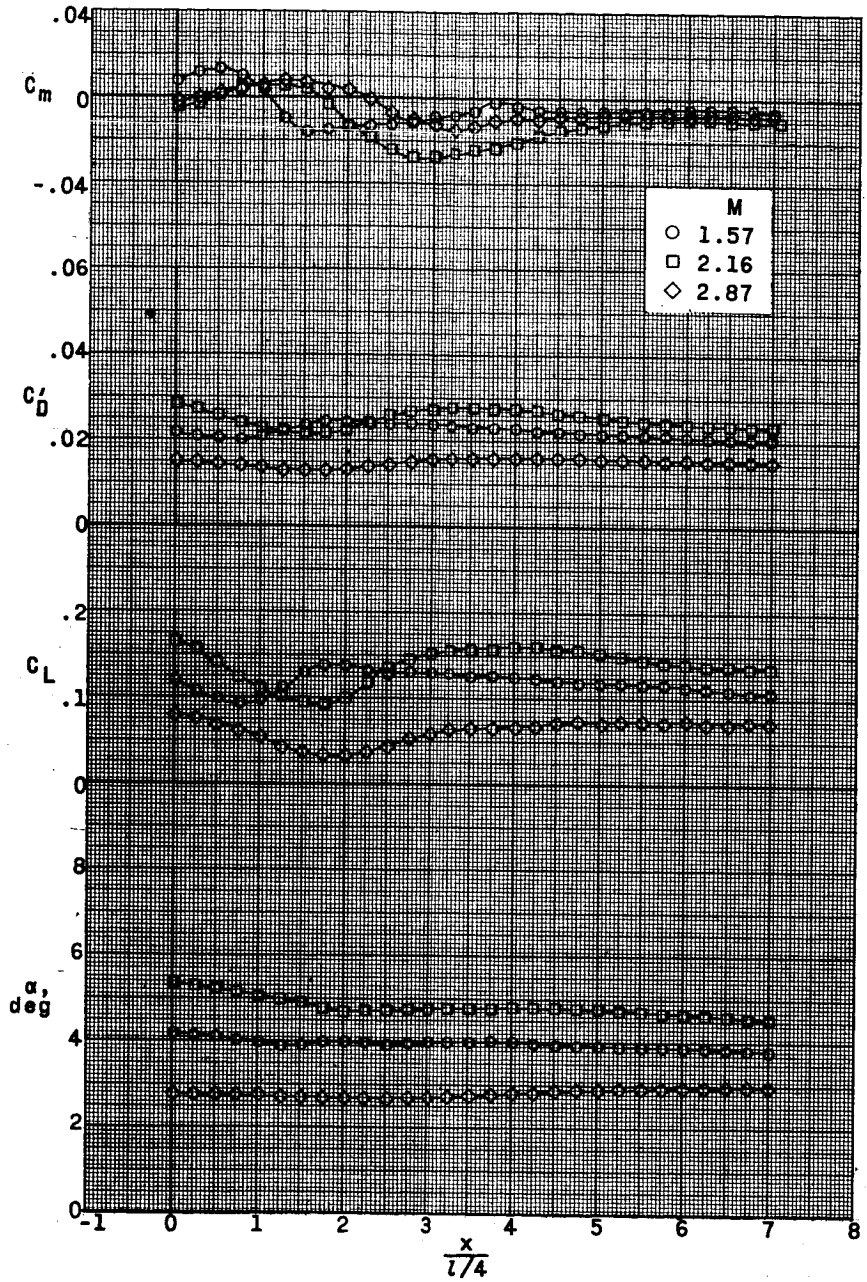

(a) $\frac{z}{b/4} = 1.83$.

Figure 14.- The variation of aerodynamic pitch characteristics with longitudinal position of the receiver model in presence of tanker model. $\beta = 0^{\circ}$; $\frac{y}{b/4} = 0$.

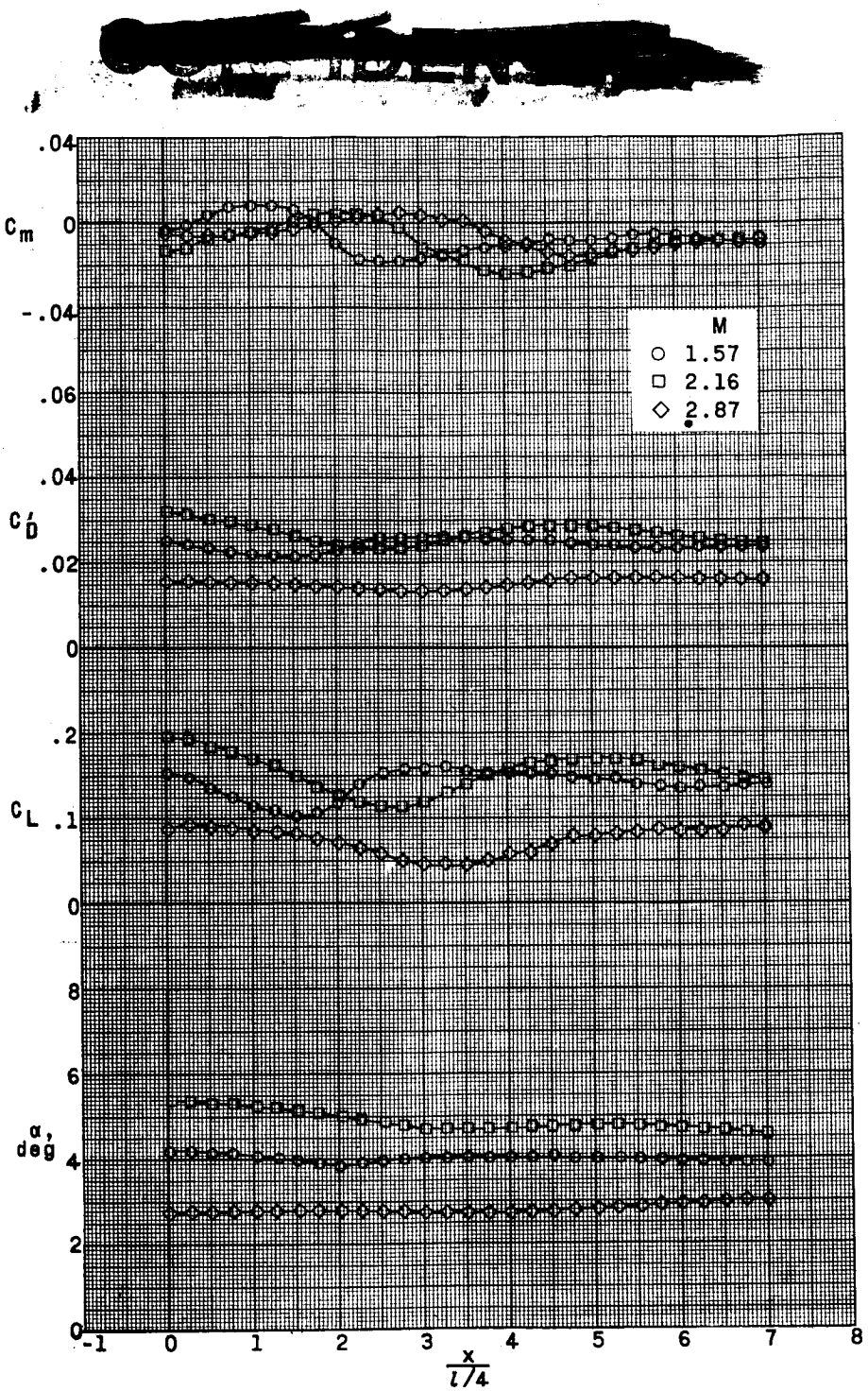

(b) $\frac{z}{b/4} = 2.82.$

Figure 14.- Continued.

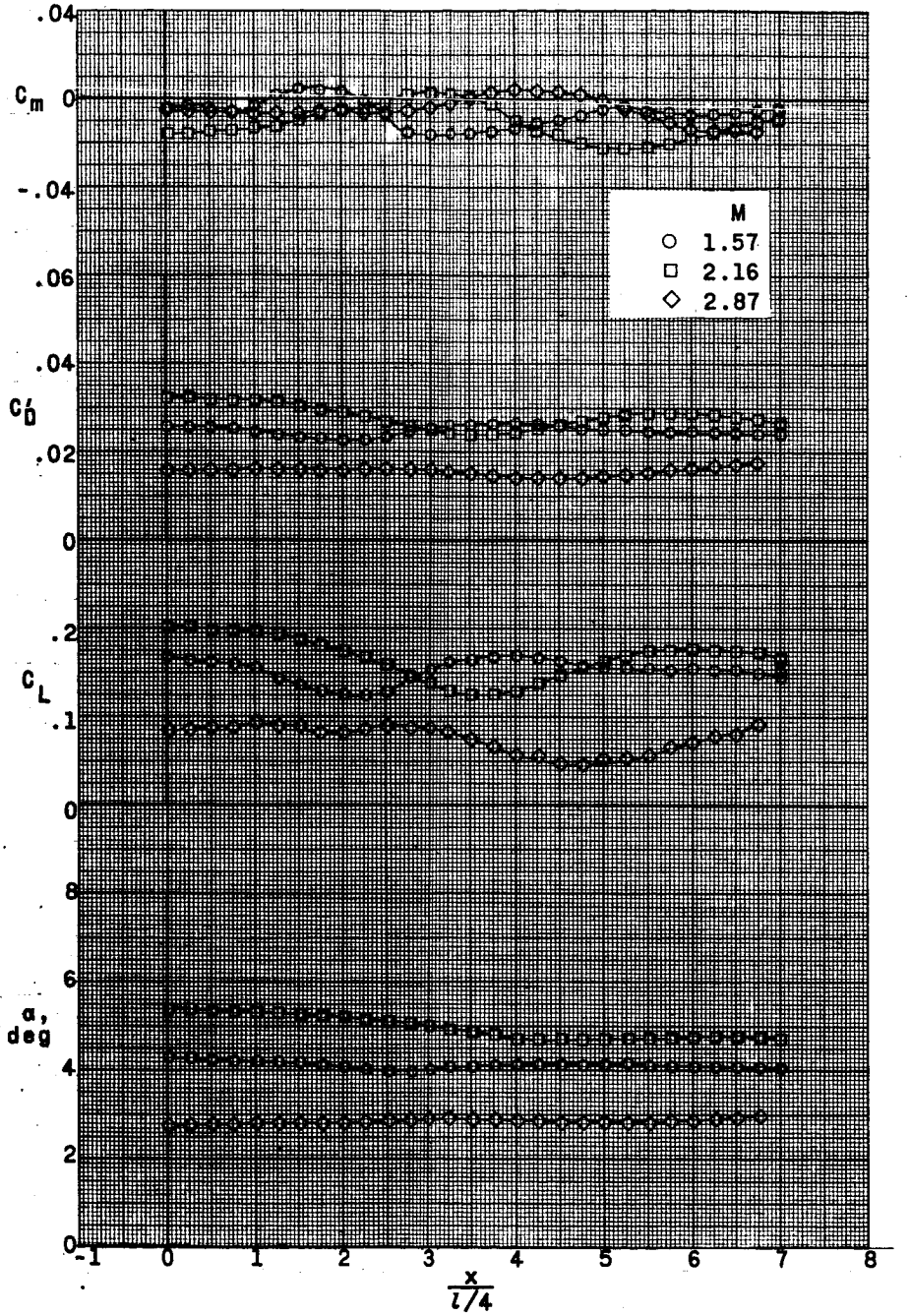

(c) $\frac{z}{b/4} = 3.82.$

Figure 14.- Concluded.

CONFIDENTIAL

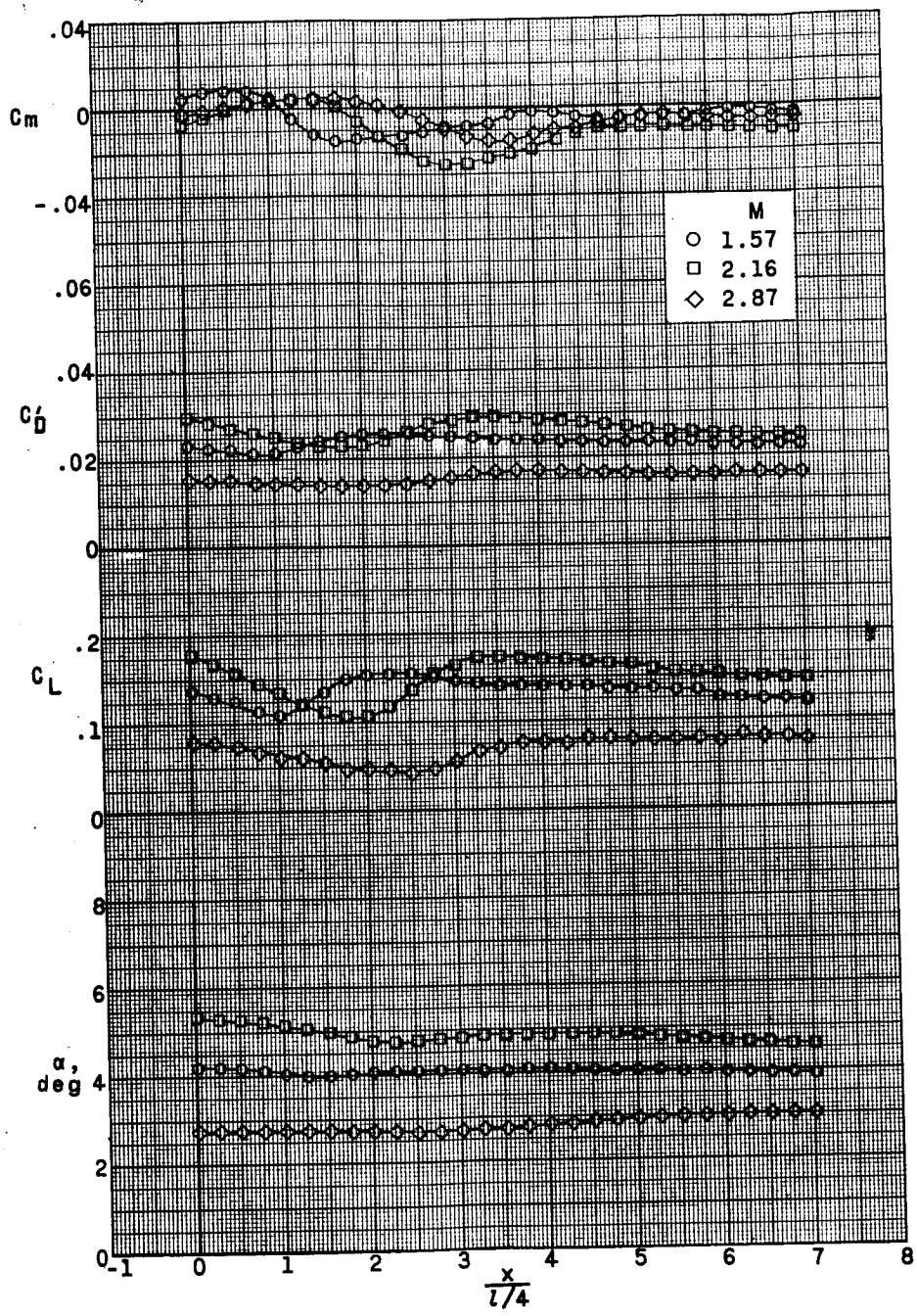

(a) $\frac{z}{b/4} = 1.82.$

Figure 15.- The variation of aerodynamic pitch characteristics with longitudinal position of the receiver model in presence of tanker model. $\beta = 0^{\circ}$; $\frac{y}{b/4} = 1.0$.

CONFIDENTIAL

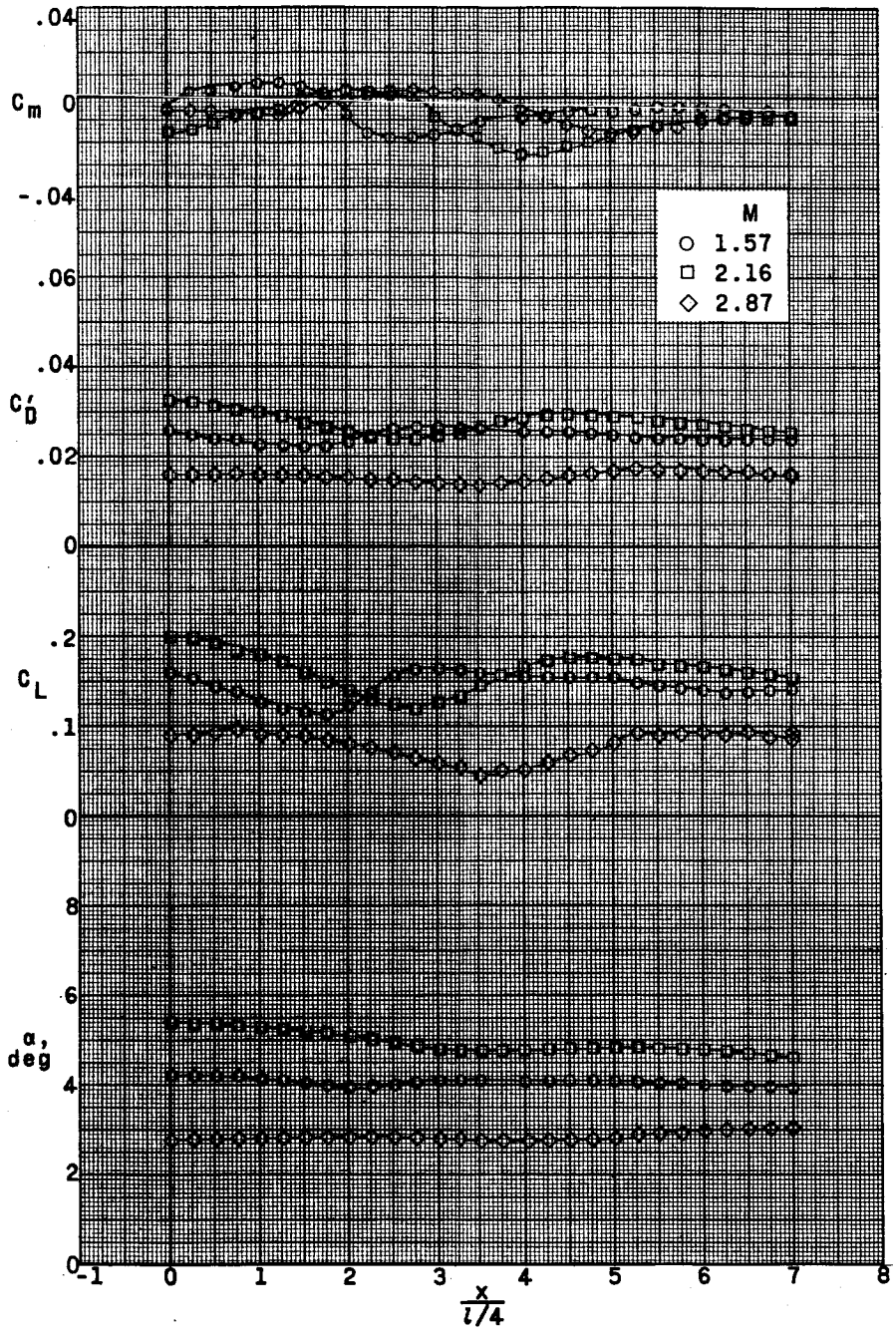

(b) $\frac{z}{b/4} = 2.82.$

Figure 15.- Continued.

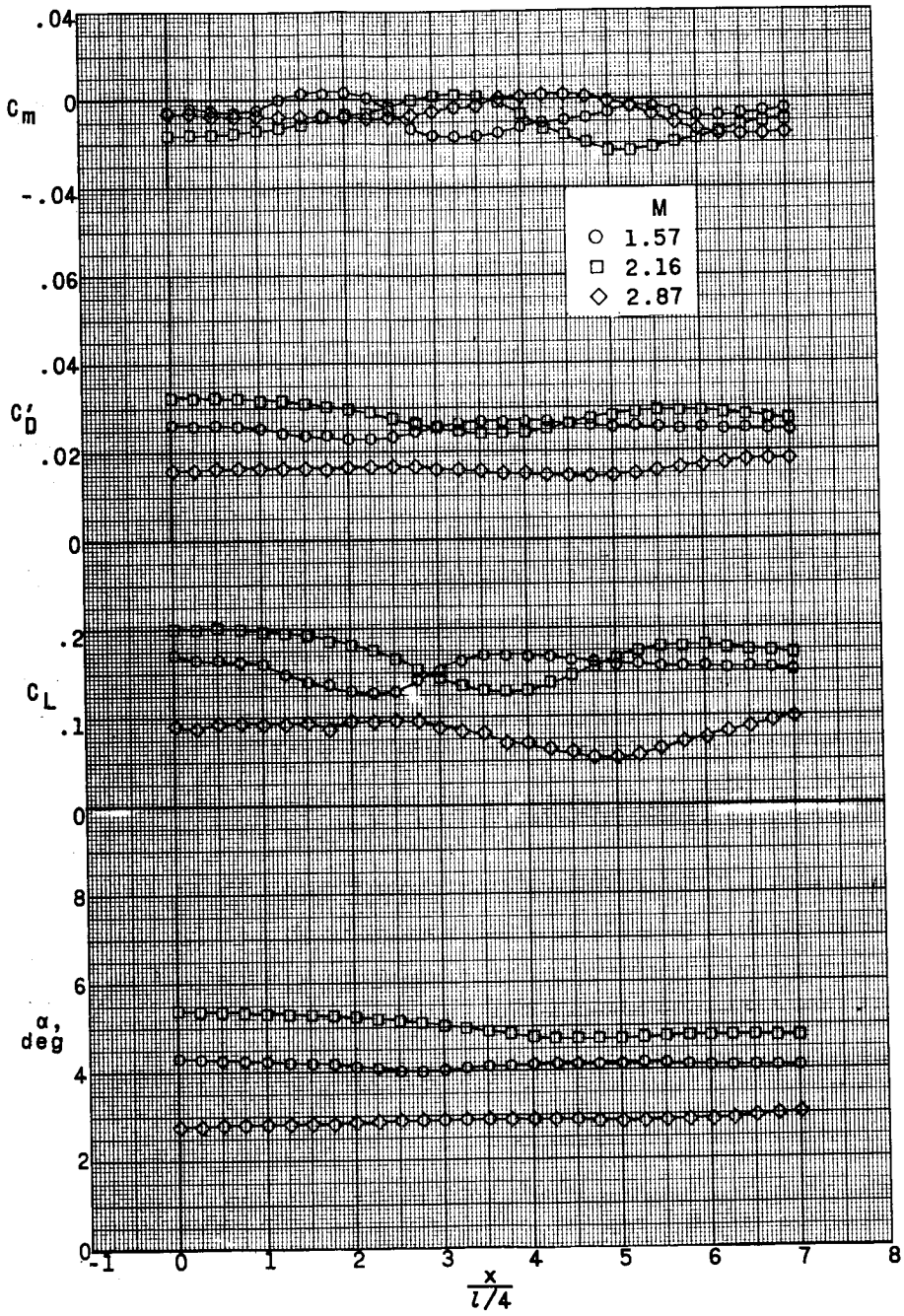

(c) $\frac{z}{b/4} = 3.82.$

Figure 15.- Concluded.

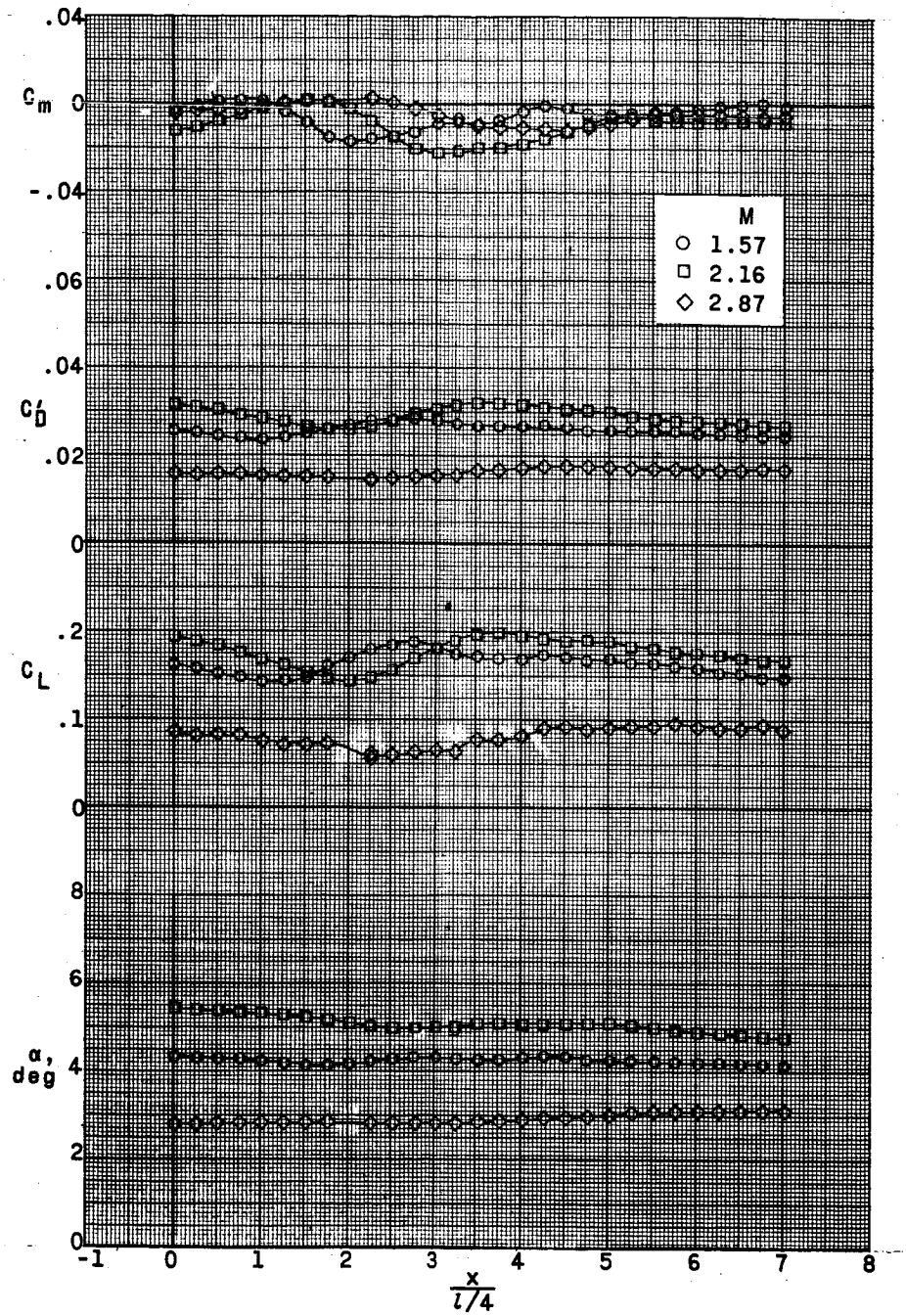

Figure 16.- The variation of aerodynamic pitch characteristics with longitudinal position of receiver model in presence of tanker model. $\beta = 0^{\circ}$; $\frac{y}{b/4} = 2.0$; $\frac{z}{b/4} = 1.82$.

CONFIDENTIAL

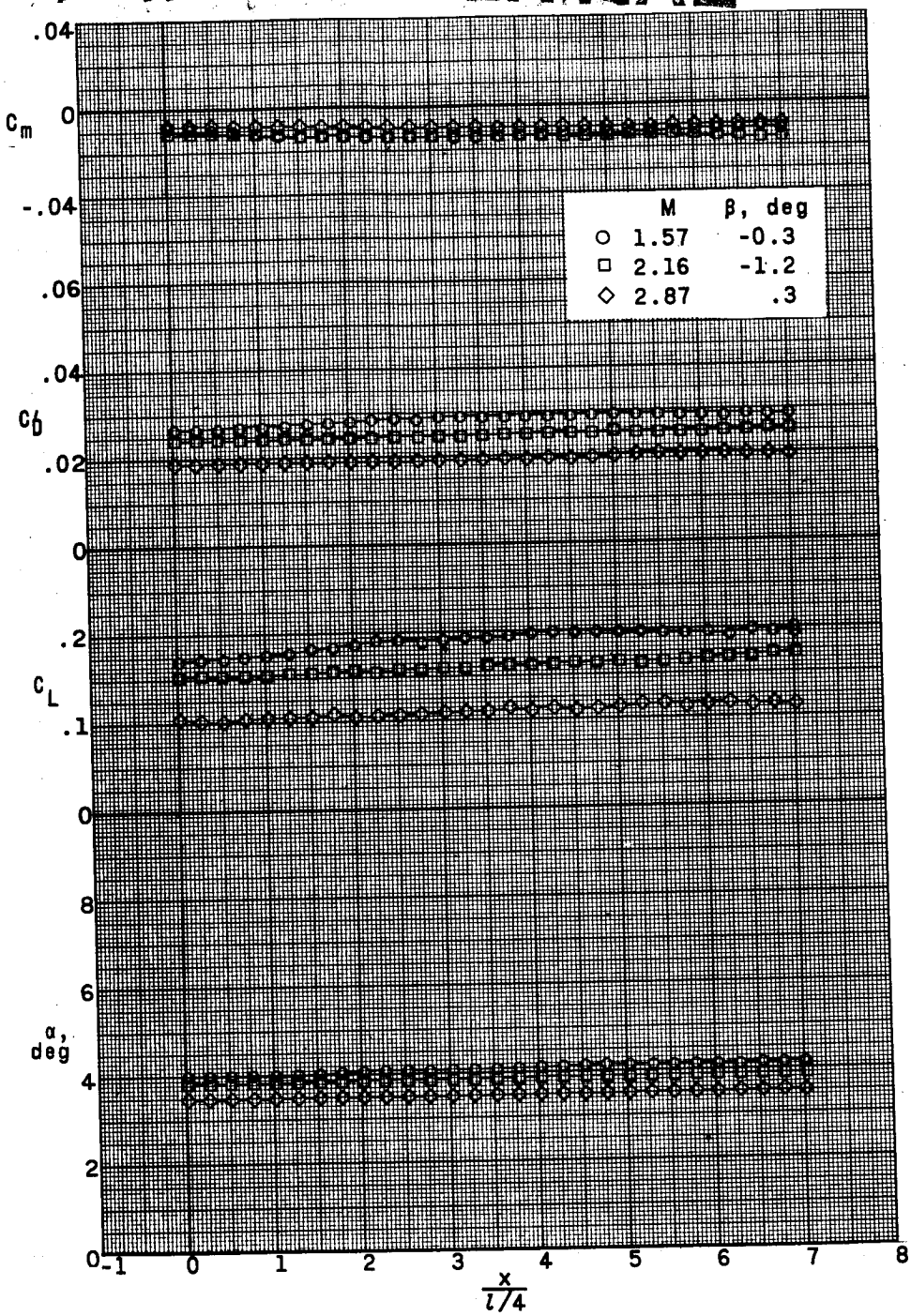

(a) $\frac{z}{b/4} = -0.11$.

Figure 17.- The variation of aerodynamic pitch characteristics with longitudinal position of the receiver model in presence of tanker model. $\frac{y}{b/4} = 1.75$, $\beta_{c.g.} = 0^{\circ}$.

CONFIDENTIAL

CONFIDENTIAL

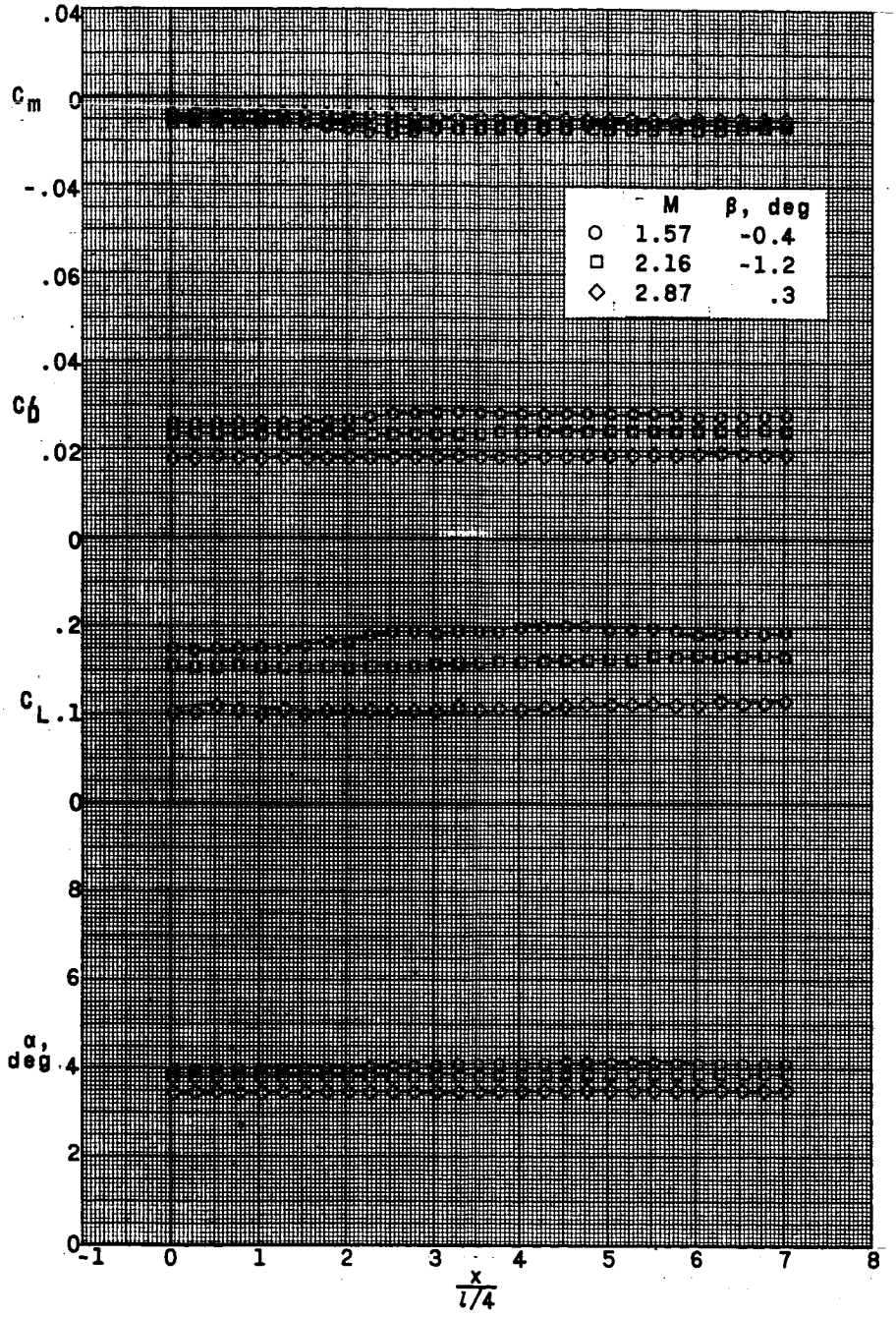

(b) $\frac{z}{b/4} = 0.89$.

Figure 17.- Concluded.

CONFIDENTIAL

CONFIDENTIAL

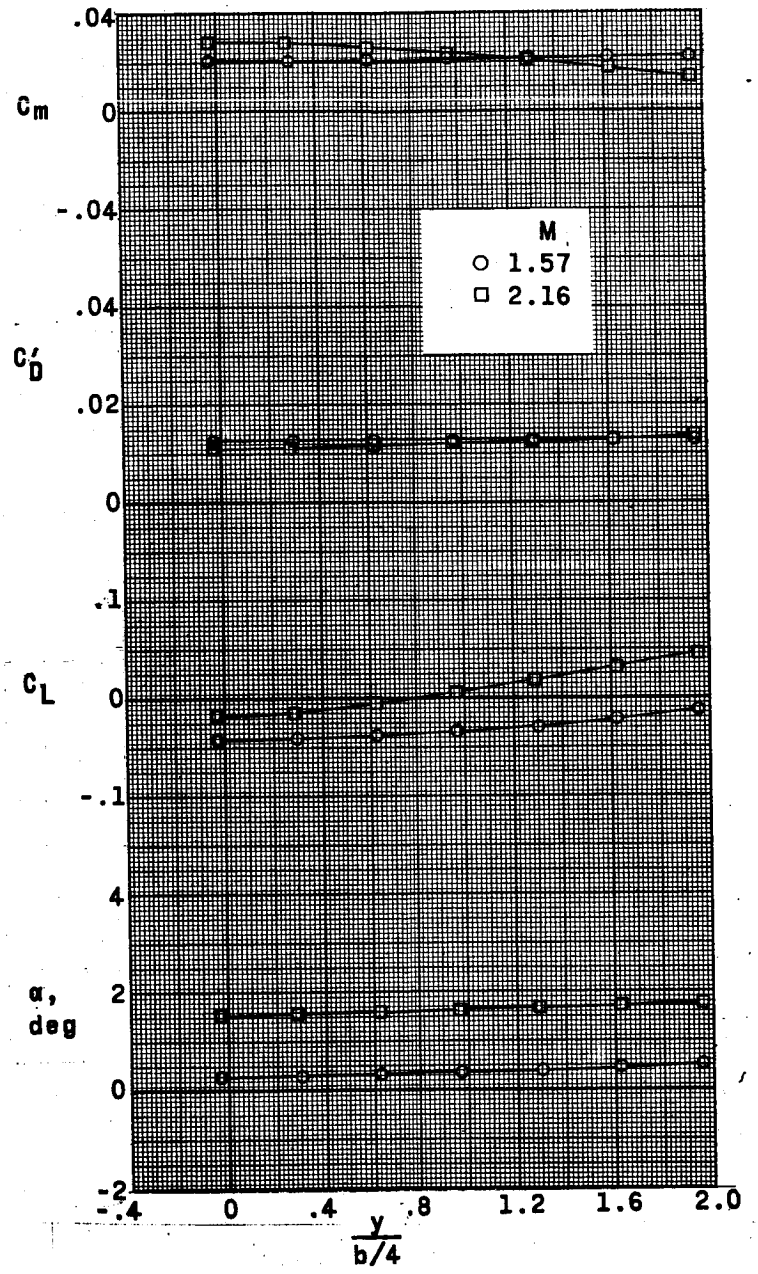

(a) $\frac{z}{b/4} = 1.90$; $\frac{x}{l/4} = 1.02$.

Figure 18.- The variation of aerodynamic pitch characteristics with lateral position of the receiver model in presence of tanker model. $\beta = 0^{o}$.

CONFIDENTIAL

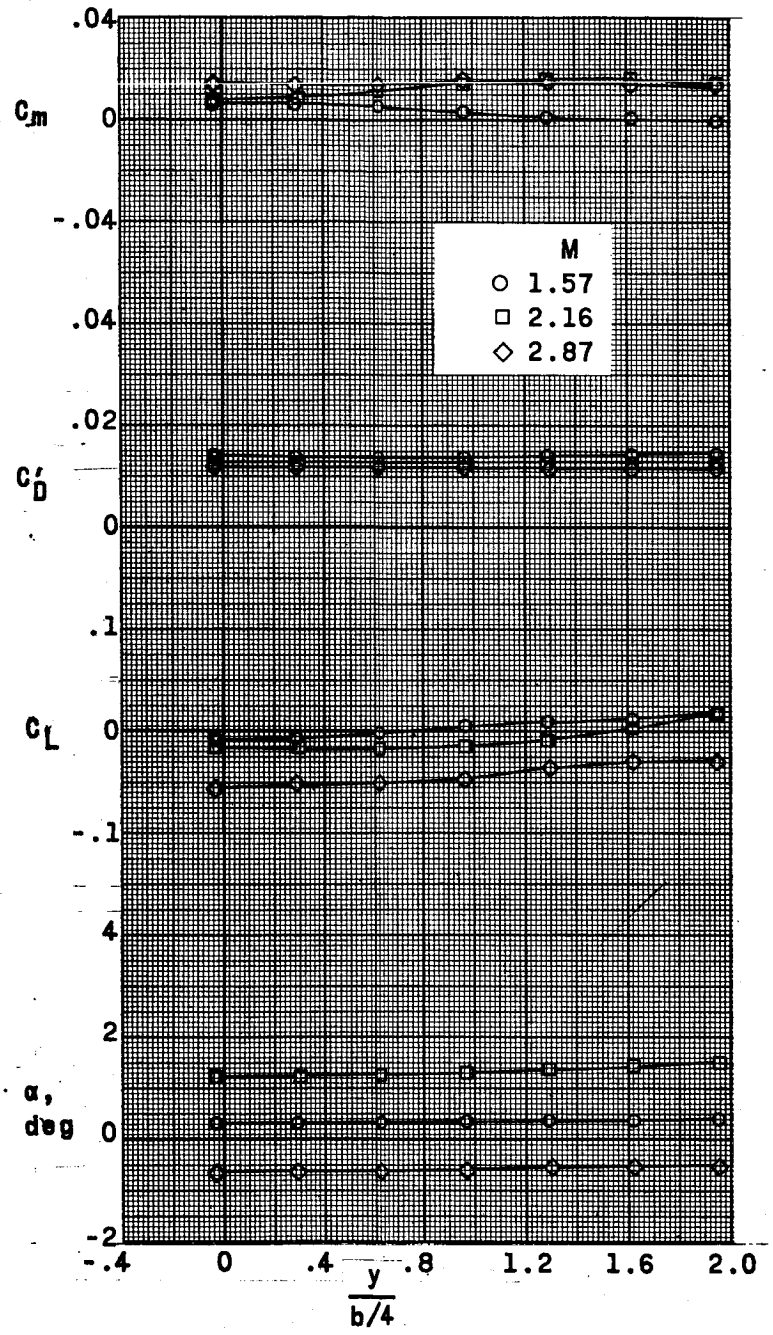

(b) $\frac{z}{b/4} = 1.90$; $\frac{x}{l/4} = 2.02$.

Figure 18.- Continued.

CONFIDENTIAL

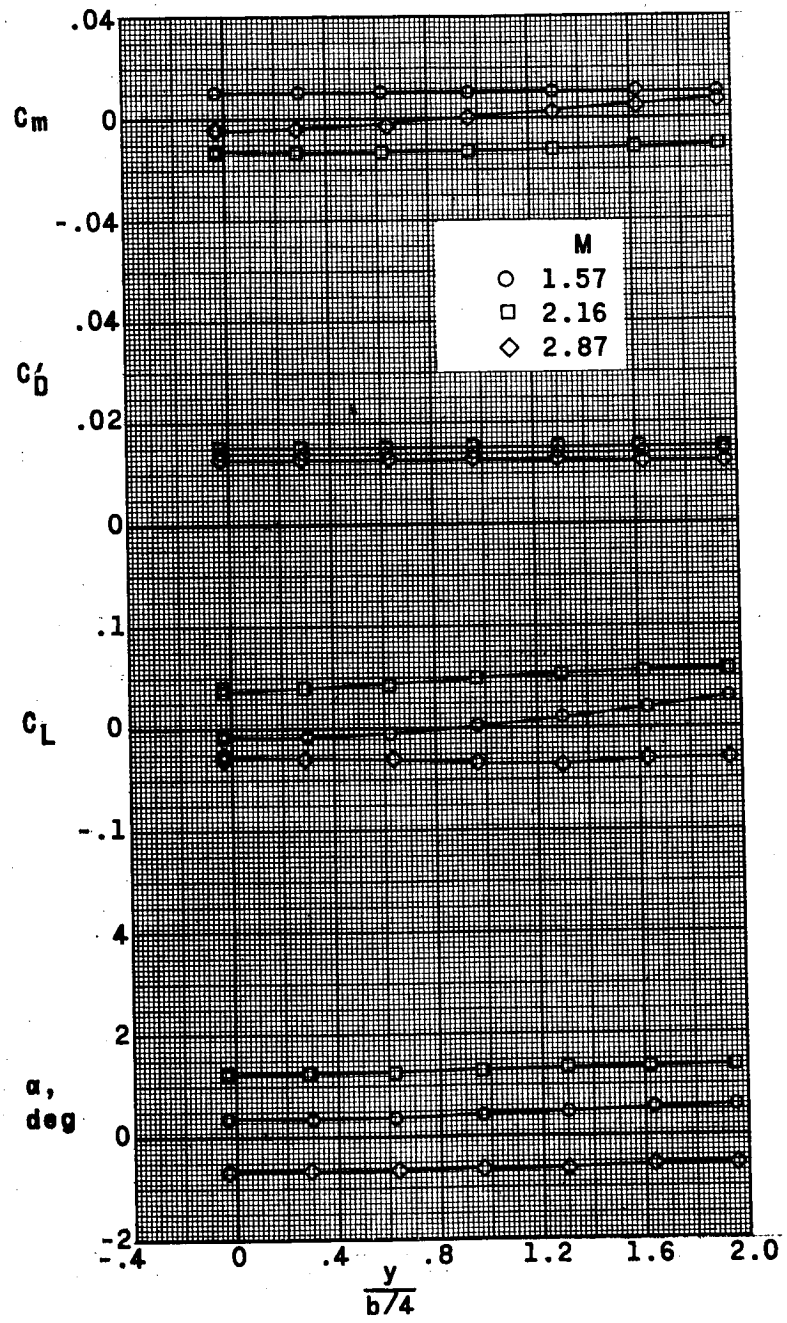

(c) $\frac{z}{b/4} = 1.90$; $\frac{x}{l/4} = 3.02$.

Figure 18.- Continued.

CONFIDENTIAL

L-591

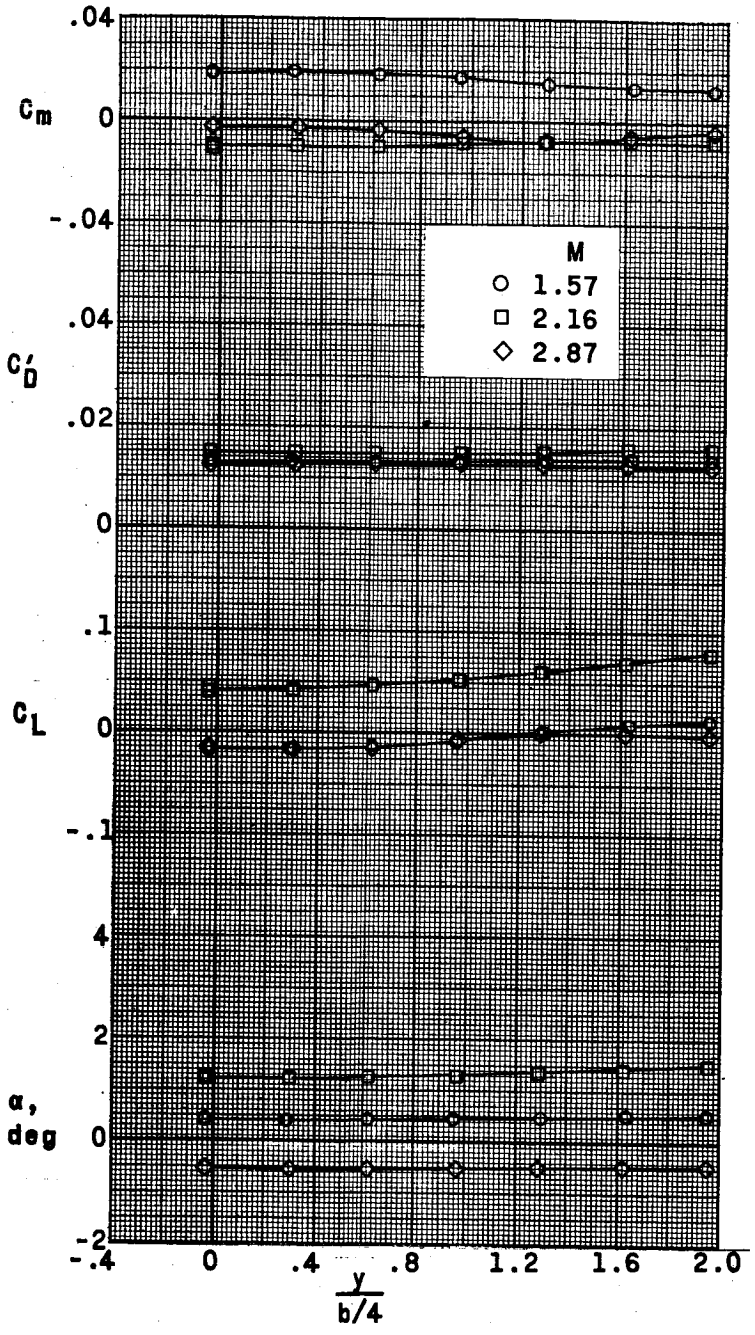

(d) $\frac{z}{b/4} = 1.90$; $\frac{x}{l/4} = 4.02$.

Figure 18.- Continued.

[redacted]

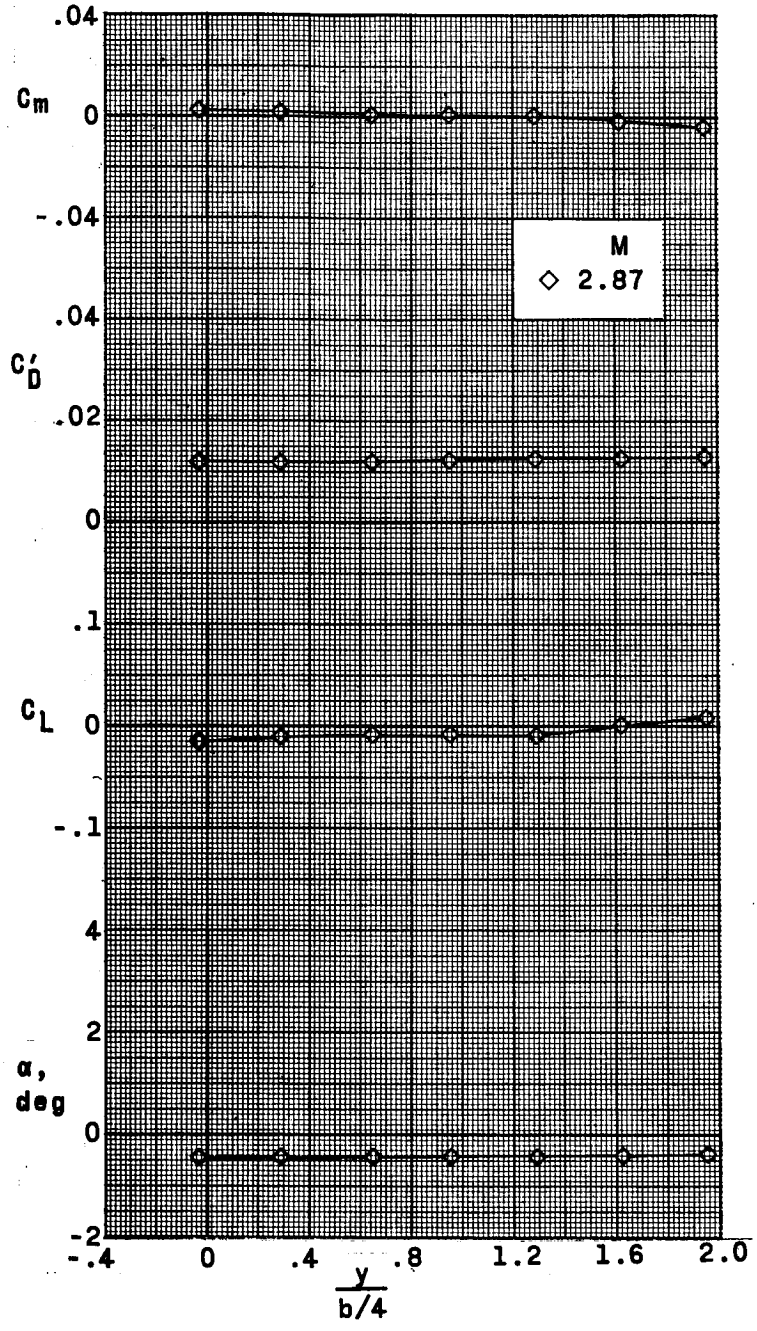

(e) $\frac{z}{b/4} = 1.90$; $\frac{x}{l/4} = 5.02$.

Figure 18.- Continued.

[redacted]

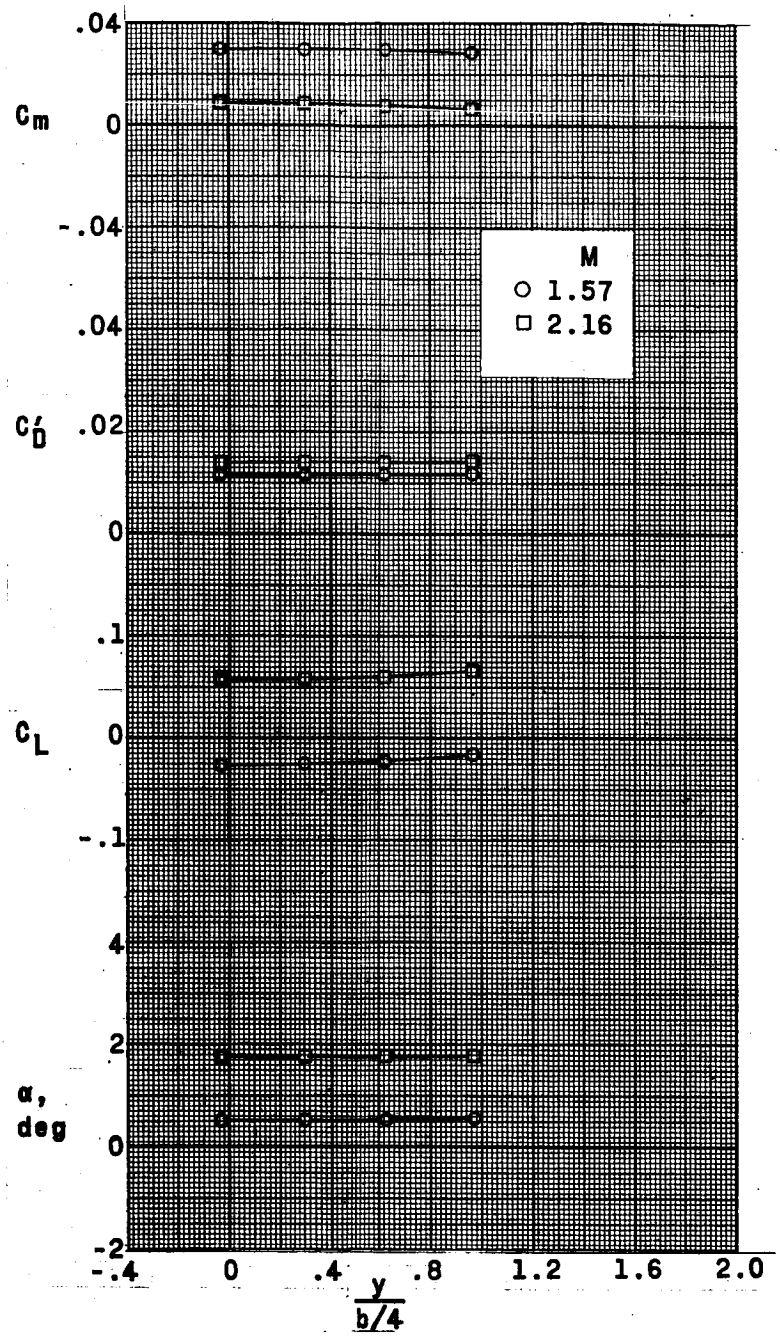

(f) $\frac{z}{b/4} = 2.90$; $\frac{x}{l/4} = 1.02$.

Figure 18.- Continued.

CONFIDENTIAL

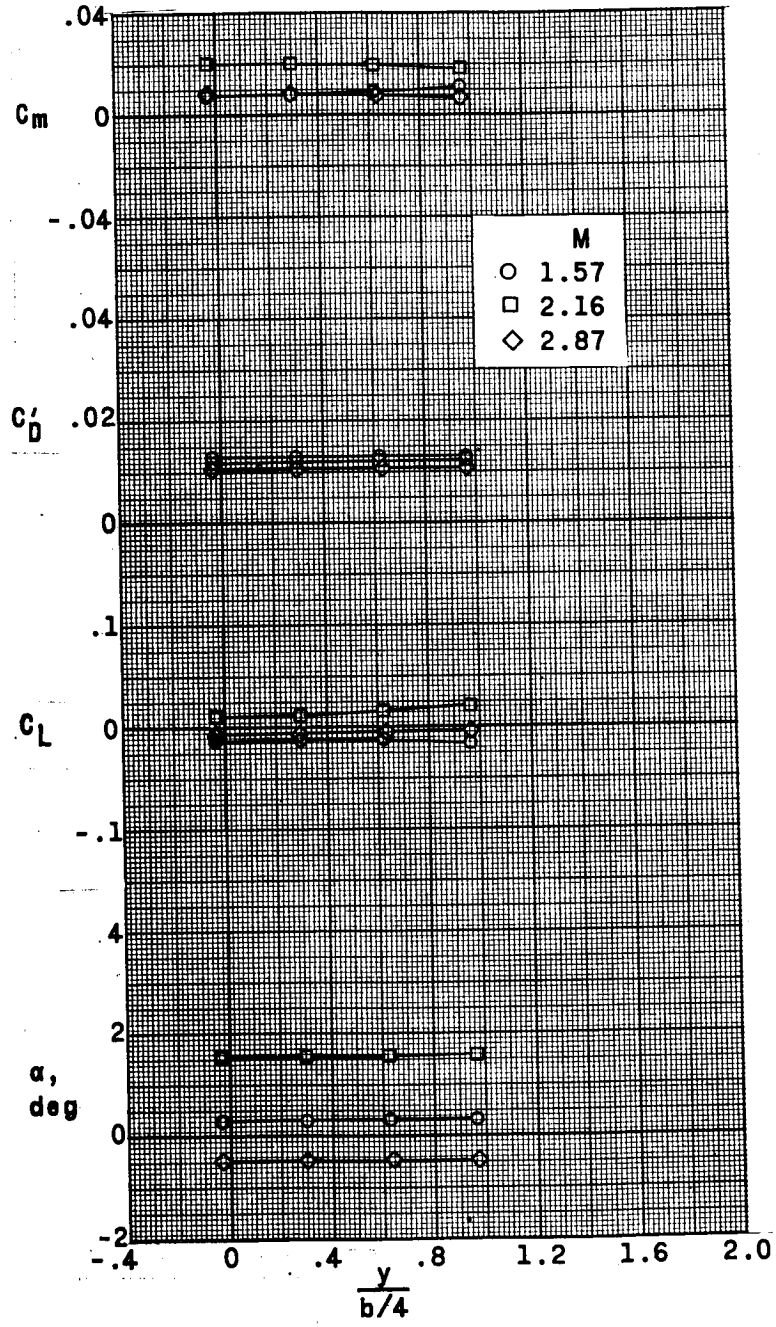

(g) $\frac{z}{b/4} = 2.90$; $\frac{x}{l/4} = 2.02$.

Figure 18.- Continued.

CONFIDENTIAL

CONFIDENTIAL

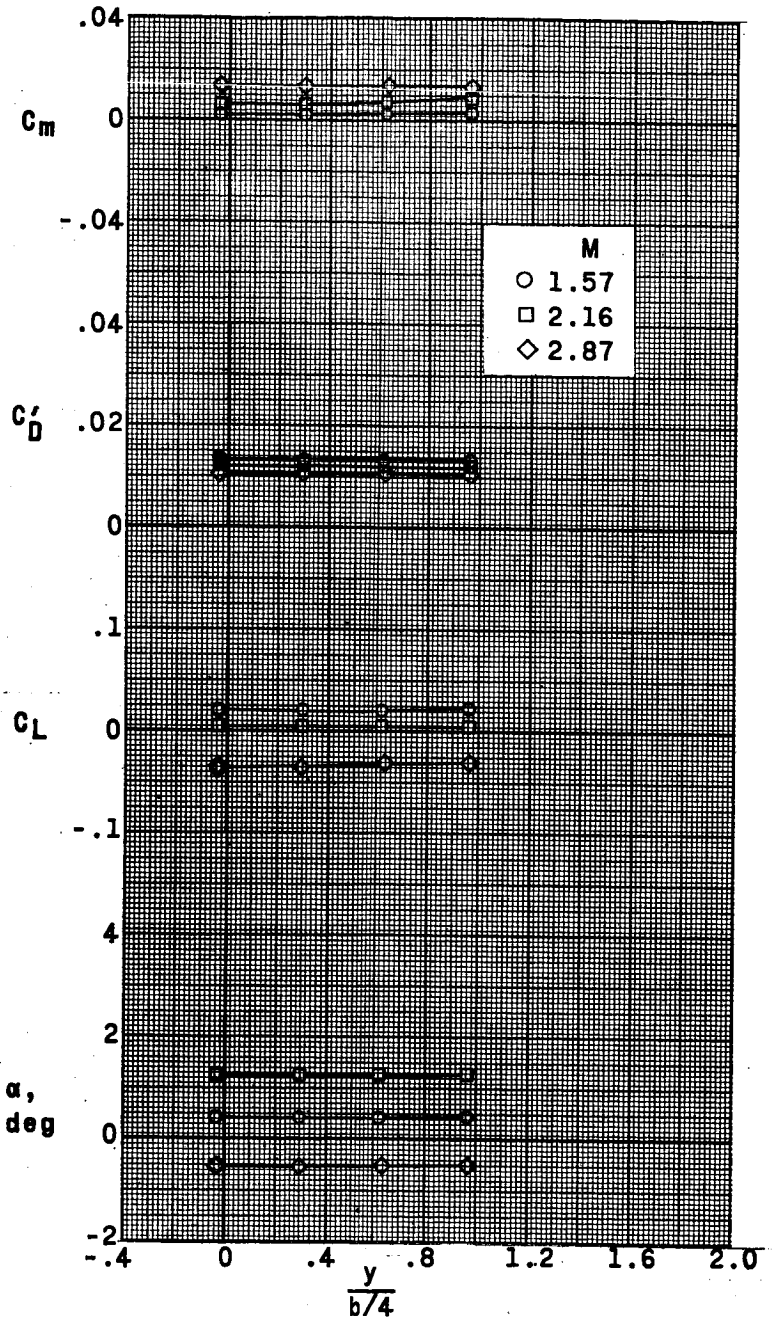

(h) $\frac{z}{b/4} = 2.90$; $\frac{x}{l/4} = 3.02$.

Figure 18.- Continued.

CONFIDENTIAL

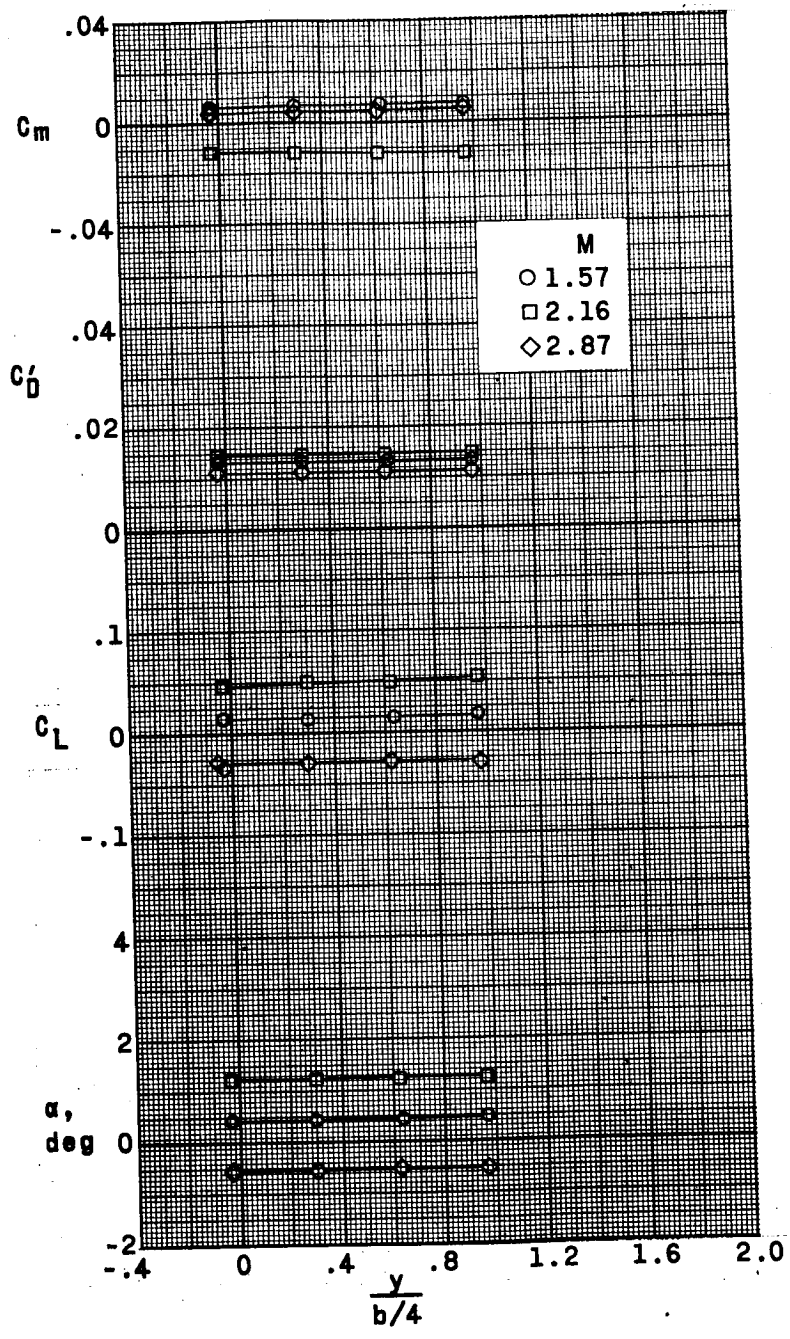

(i) $\frac{z}{b/4} = 2.90$; $\frac{x}{l/4} = 4.02$.

Figure 18.- Continued.

CONFIDENTIAL

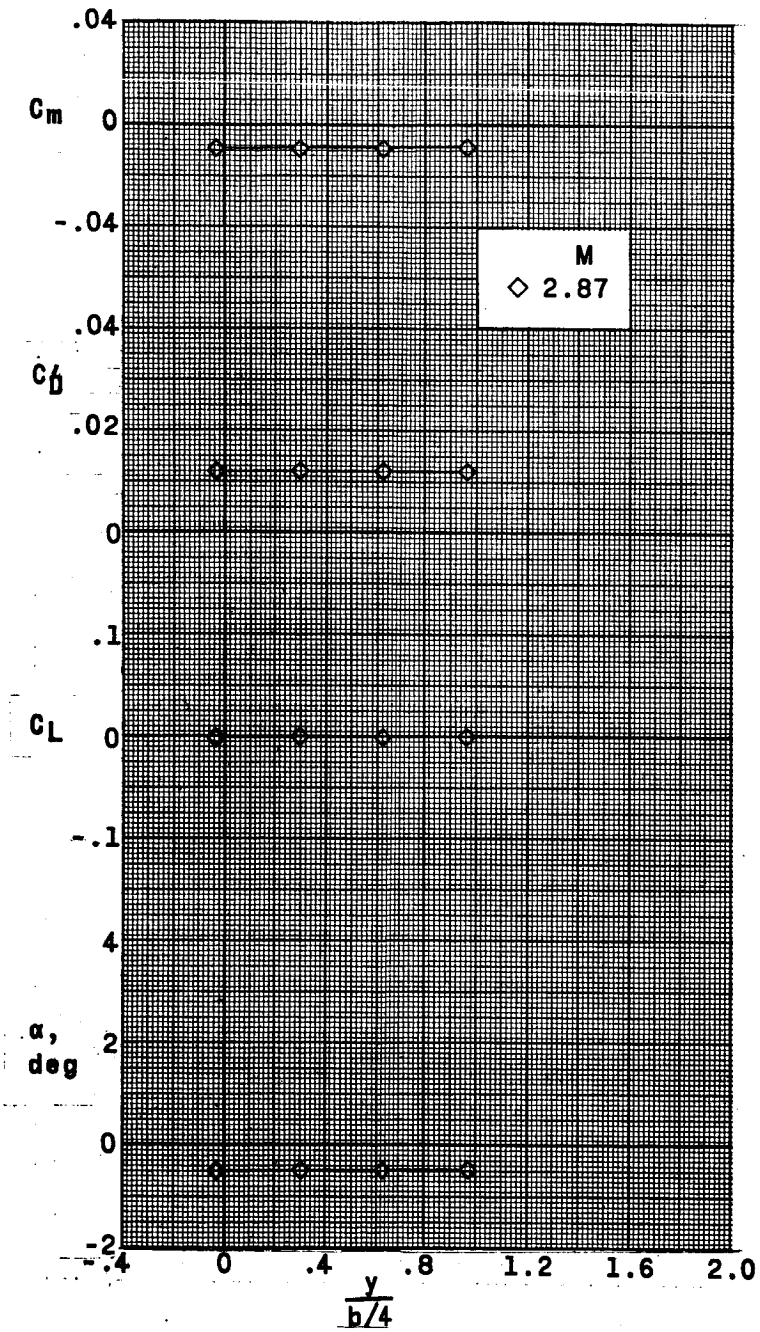

(j) $\frac{z}{b/4} = 2.90$; $\frac{x}{l/4} = 5.02$.

Figure 18.- Continued.

CONFIDENTIAL

CONFIDENTIAL

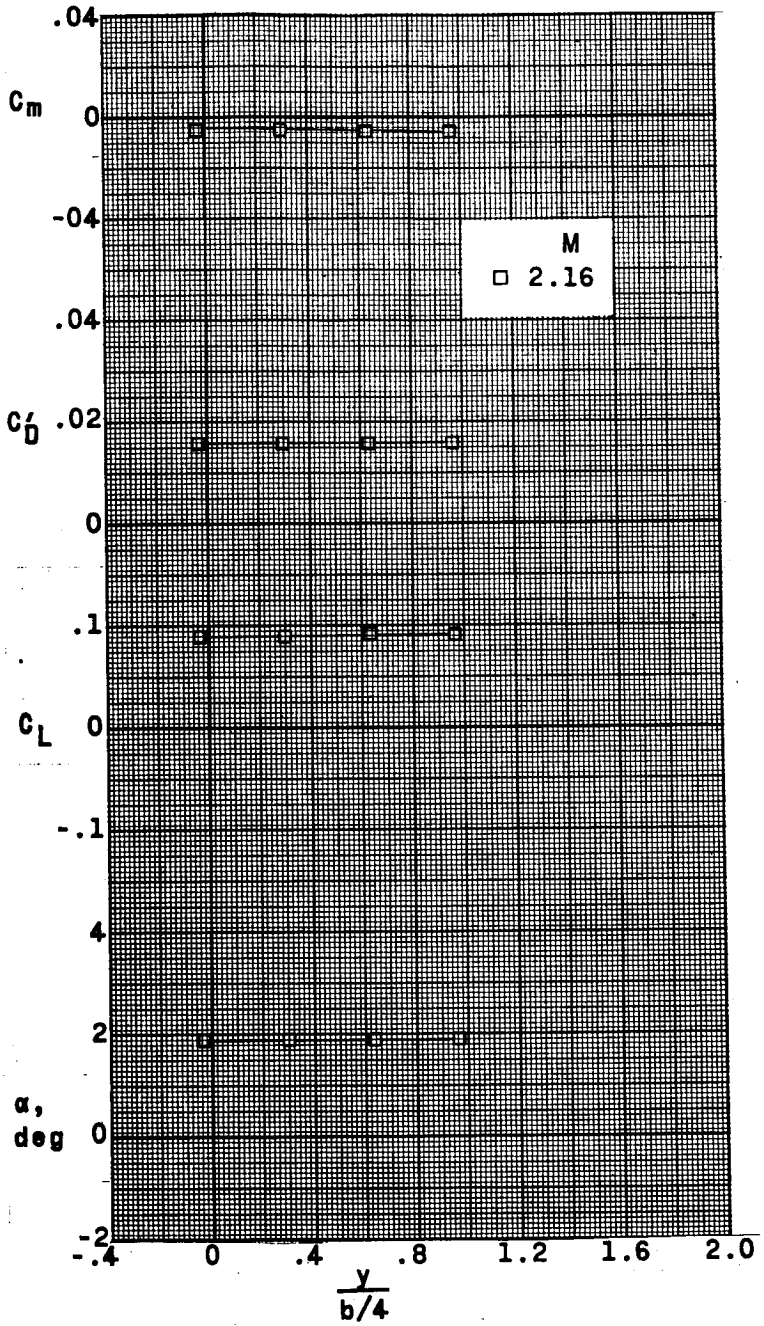

(k) $\frac{z}{b/4} = 3.90$; $\frac{x}{l/4} = 0.02$.

Figure 18.- Continued.

CONFIDENTIAL

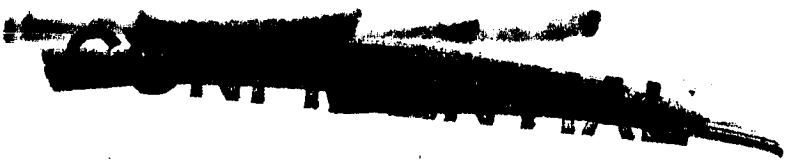

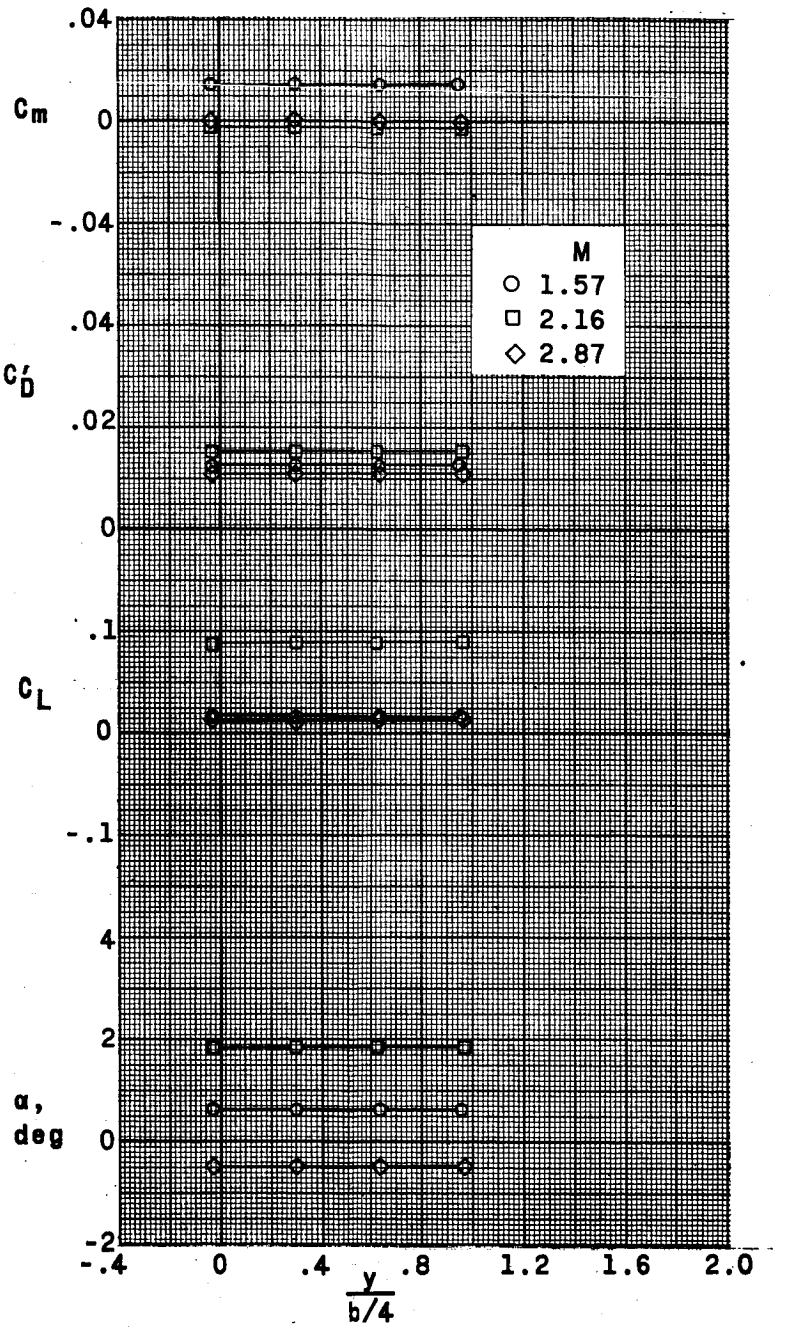

(l) $\frac{z}{b/4} = 3.90$; $\frac{x}{l/4} = 1.02$.

Figure 18.- Continued.

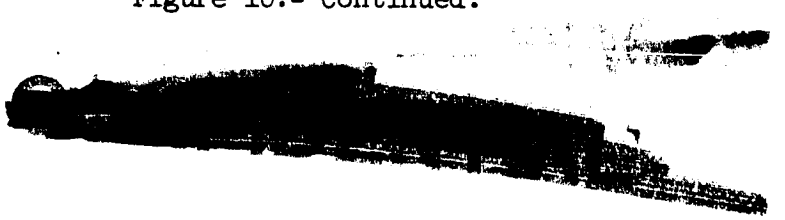

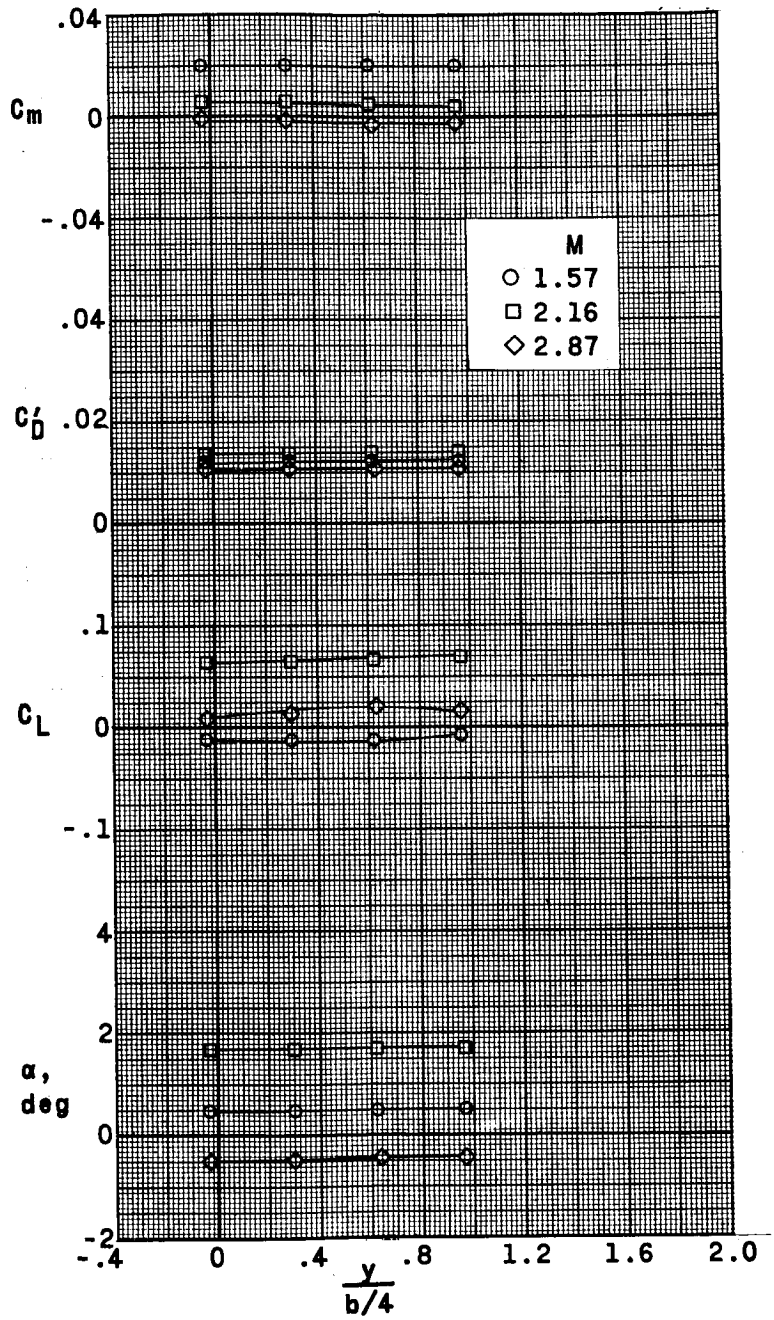

(m) $\frac{z}{b/4} = 3.90$; $\frac{x}{l/4} = 2.02$.

Figure 18.- Continued.

CONFIDENTIAL

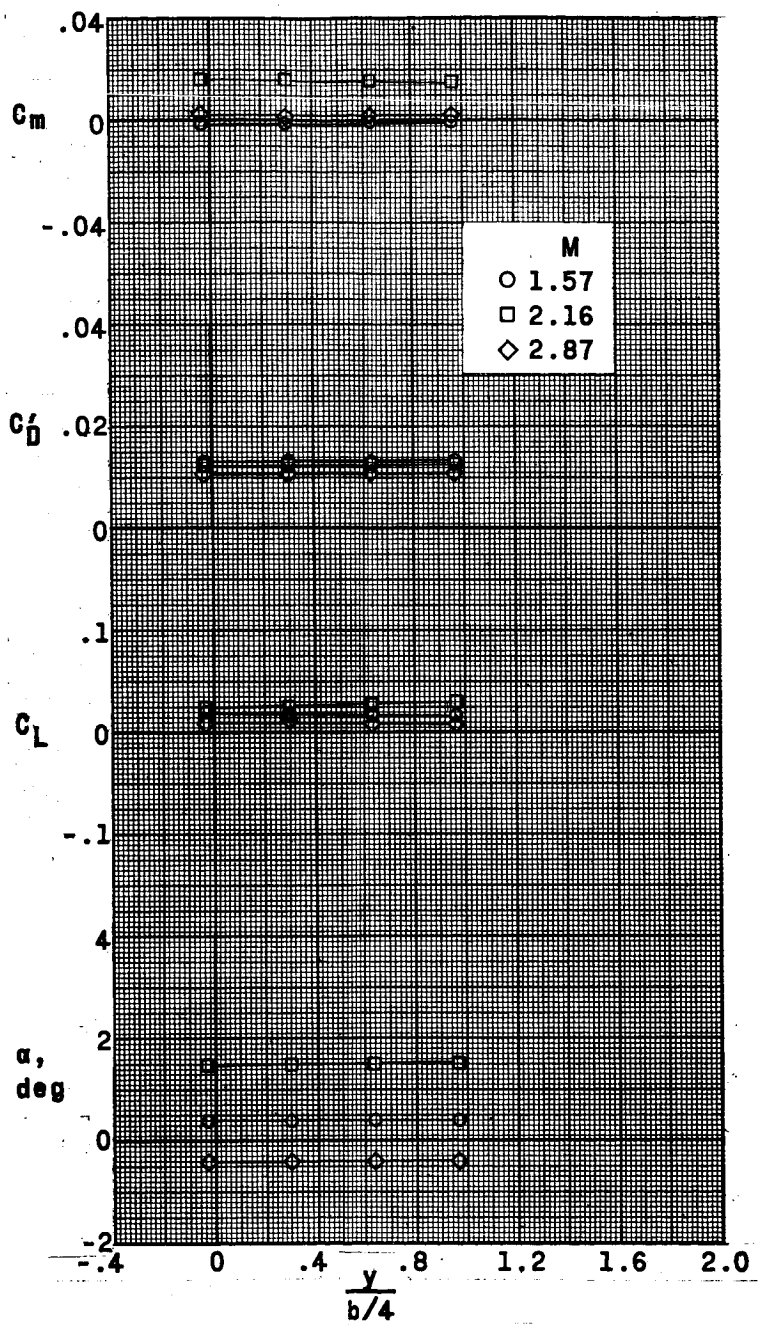

(n) $\frac{z}{b/4} = 3.90$; $\frac{x}{l/4} = 3.02$.

Figure 18.- Continued.

CONFIDENTIAL

CONFIDENTIAL

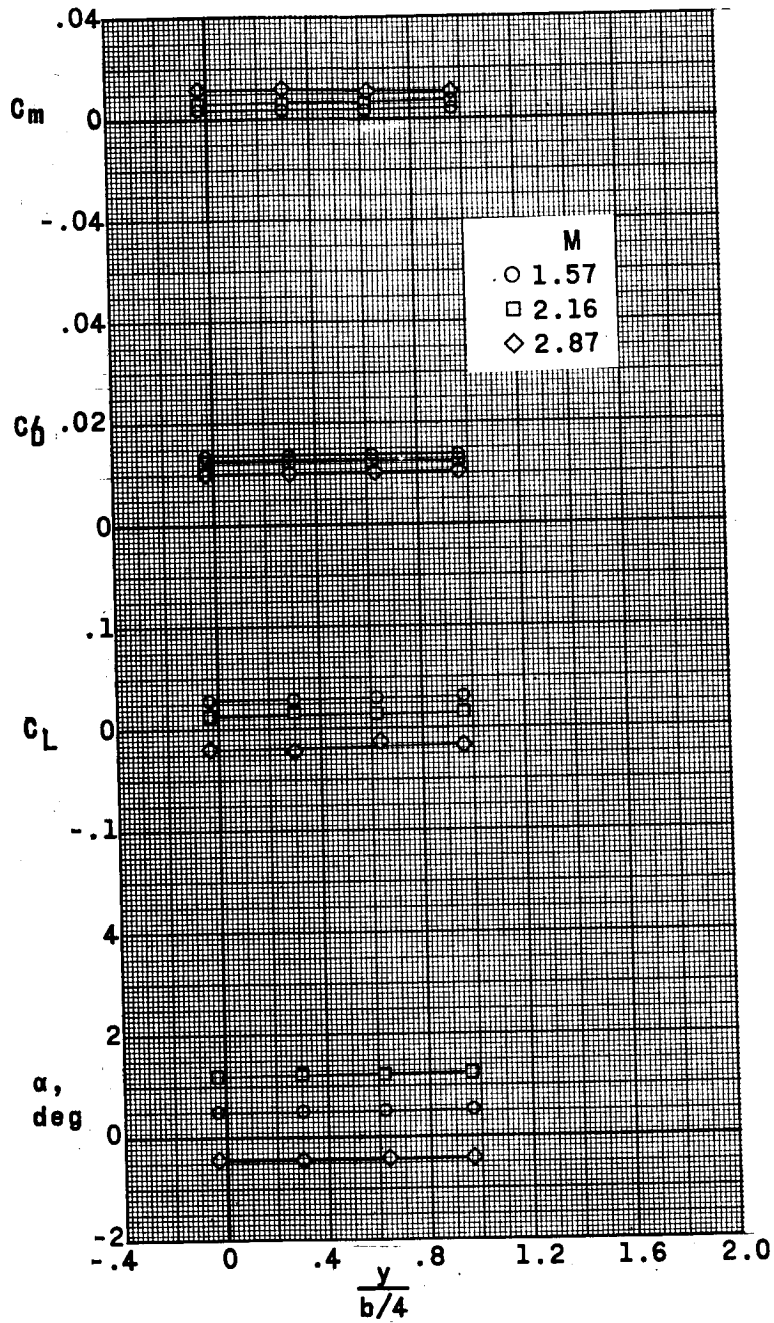

(o) $\frac{z}{b/4} = 3.90$; $\frac{x}{l/4} = 4.02$.

Figure 18.- Continued.

CONFIDENTIAL

L-591

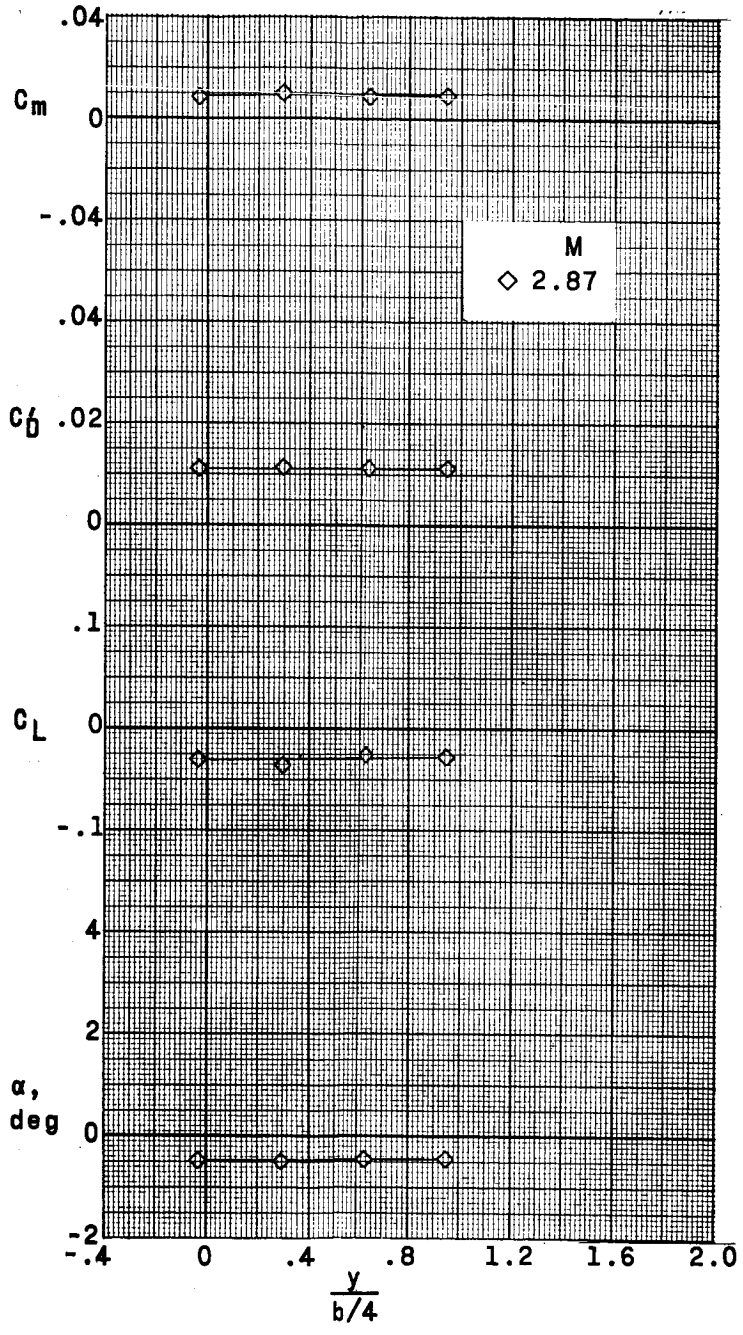

(p) $\frac{z}{b/4} = 3.90$; $\frac{x}{l/4} = 5.02$.

Figure 18.- Concluded.

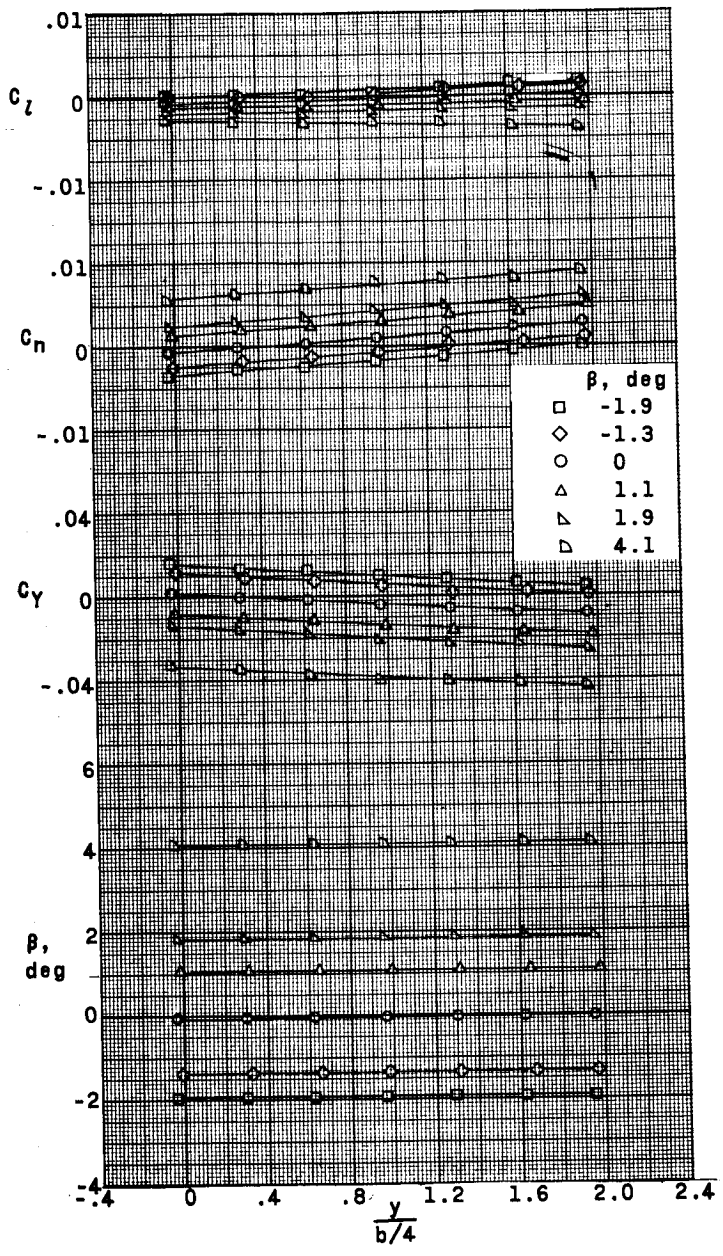

(a) $\frac{x}{l/4} = 1.02$; M = 1.57; $\alpha = 0.4^{\circ}$.

Figure 19.- The variation of aerodynamic lateral characteristics with lateral position of the receiver model in presence of tanker model. $\frac{z}{b/4} = 1.90$.

L-591

CONFIDENTIAL

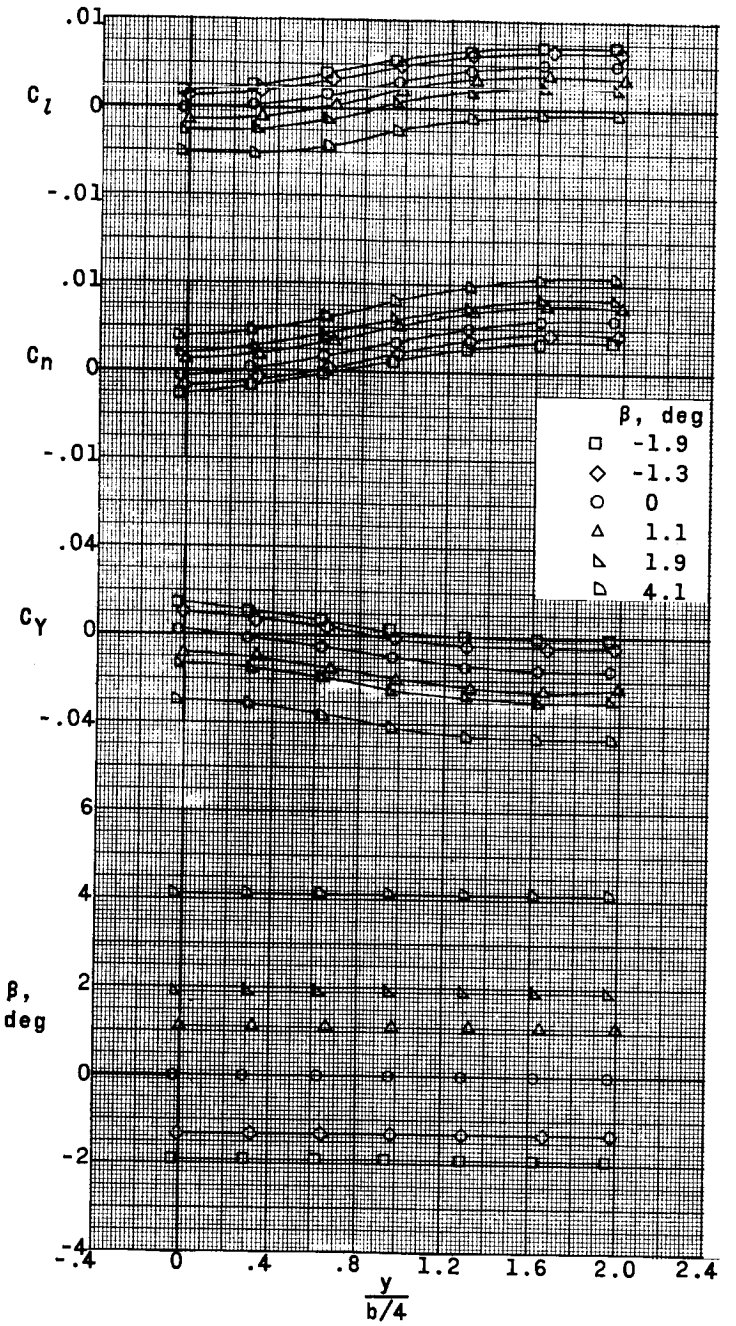

(b) $\frac{x}{l/4} = 1.02$; M = 2.16; $\alpha = 1.6^\circ$.

Figure 19.- Continued.

CONFIDENTIAL

CONFIDENTIAL

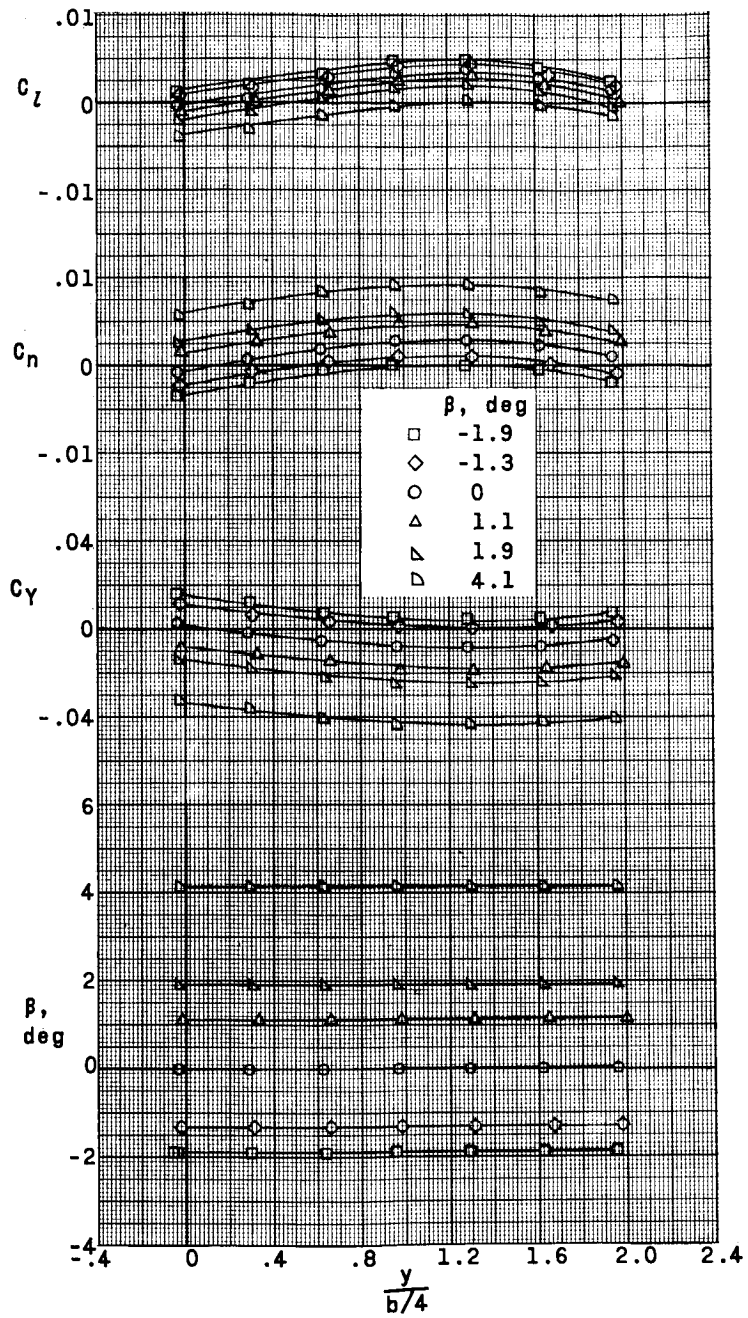

(c) $\frac{x}{l/4} = 2.02$; M = 1.57; $\alpha = 0.4^{\circ}$.

Figure 19.- Continued.

CONFIDENTIAL

CONFIDENTIAL

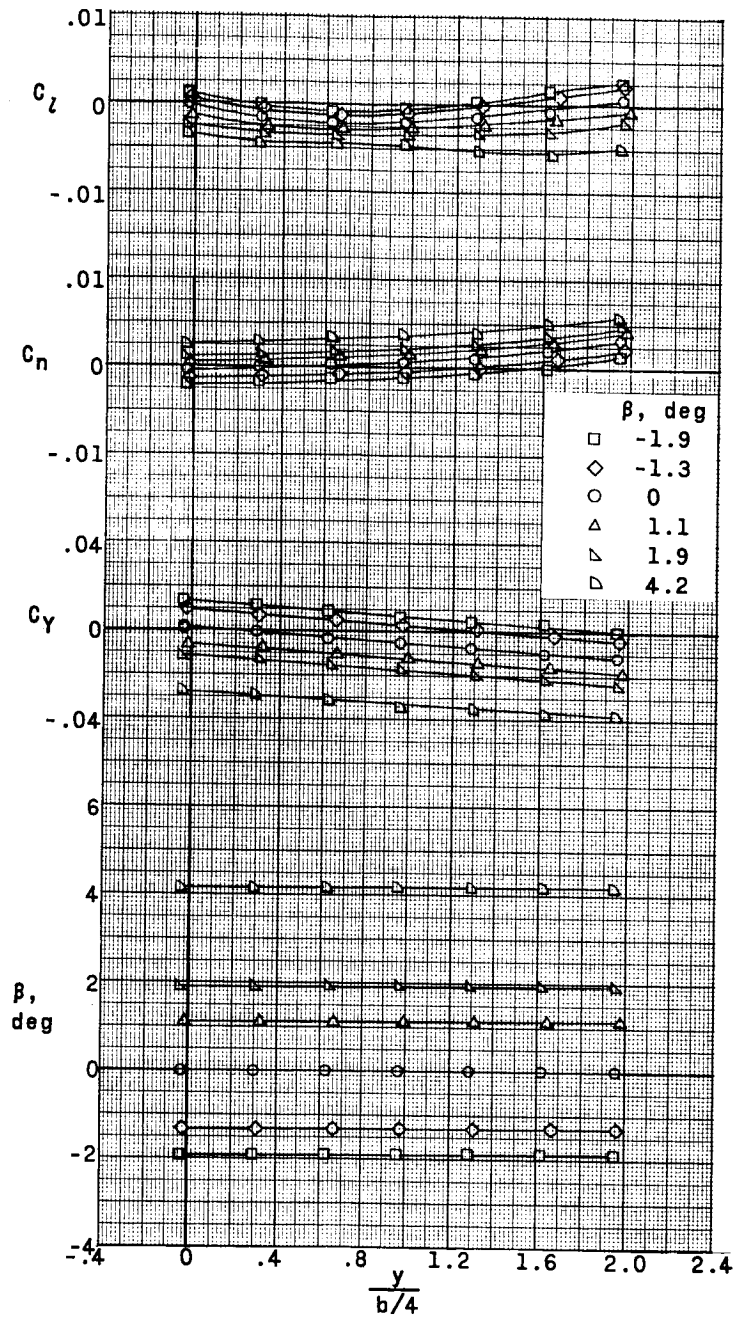

(d) $\frac{x}{l/4}$ = 2.02; M = 2.16; α = 1.3°.

Figure 19.- Continued.

CONFIDENTIAL

CONFIDENTIAL

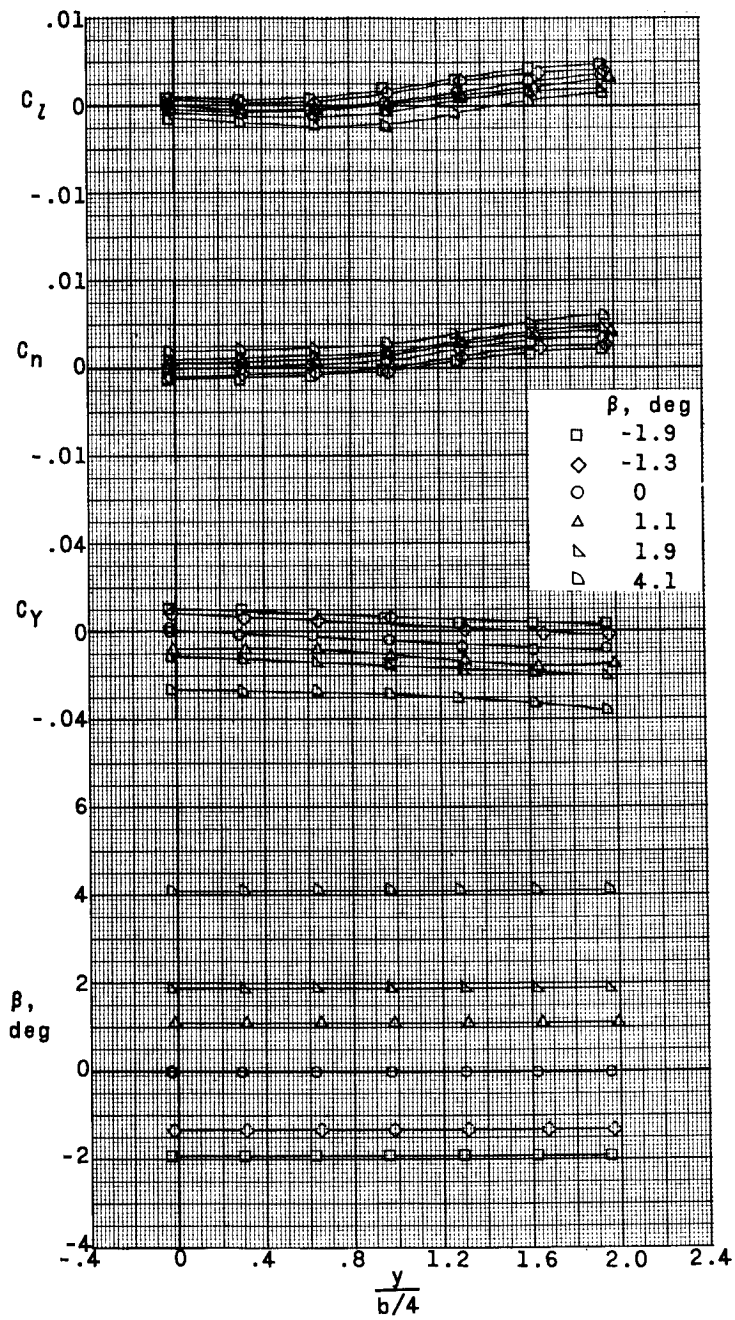

(e) $\frac{x}{l/4} = 2.02$; M = 2.87; $\alpha = -0.6^{\circ}$.

Figure 19.- Continued.

CONFIDENTIAL

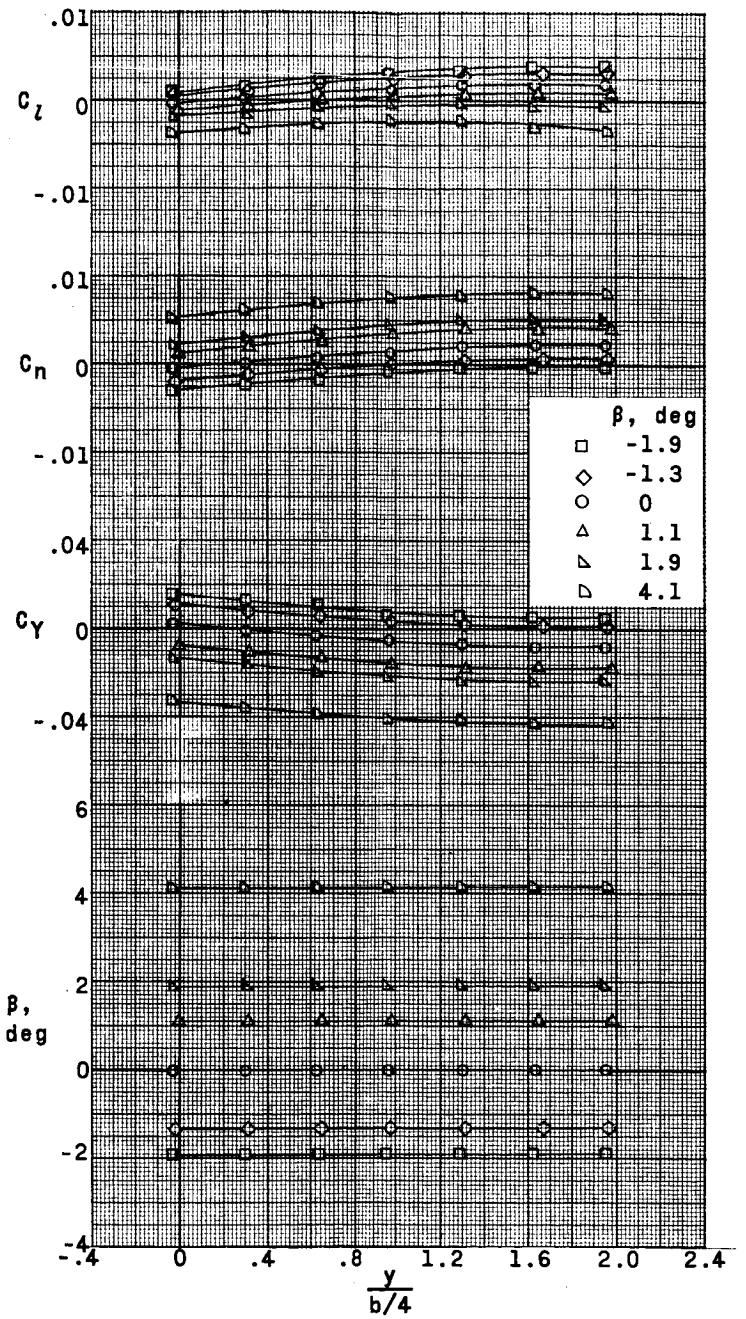

(f) $\frac{x}{l/4} = 3.02$; M = 1.57; $\alpha = 0.4^{\circ}$.

Figure 19.- Continued.

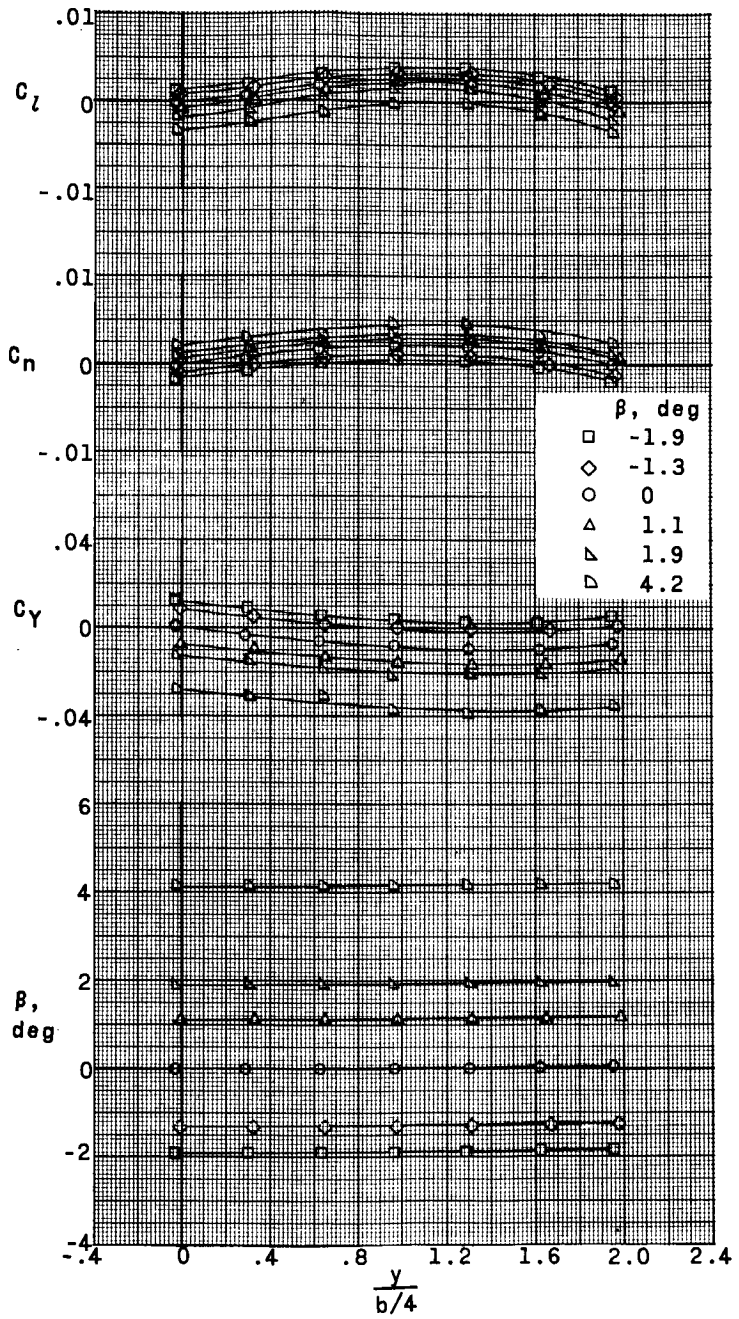

(g) $\frac{x}{l/4} = 3.02$; $M = 2.16$; $\alpha = 1.3^\circ$.

Figure 19.- Continued.

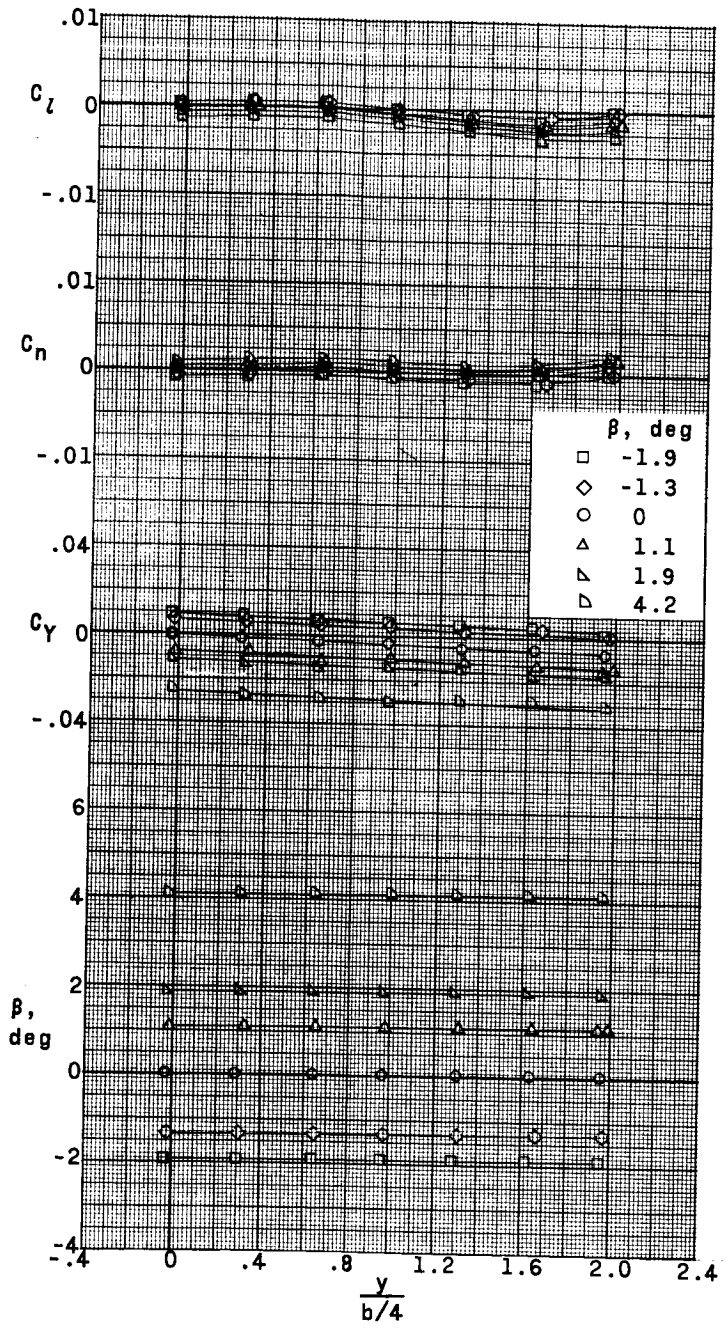

(h) $\frac{x}{l/4} = 3.02$; $M = 2.87$; $\alpha = -0.6^\circ$.

Figure 19.- Continued.

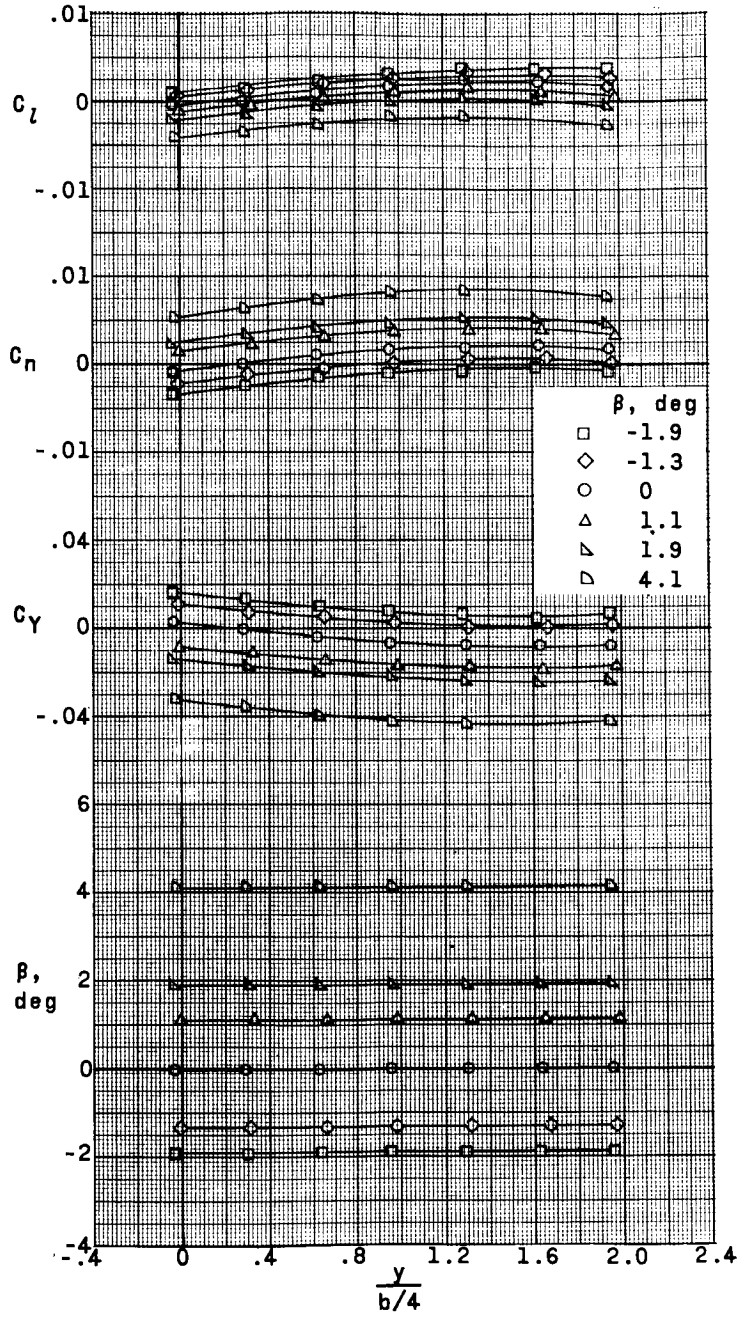

(i) $\frac{x}{l/4}$ = 4.02; M = 1.57; α = 0.5°.

Figure 19.- Continued.

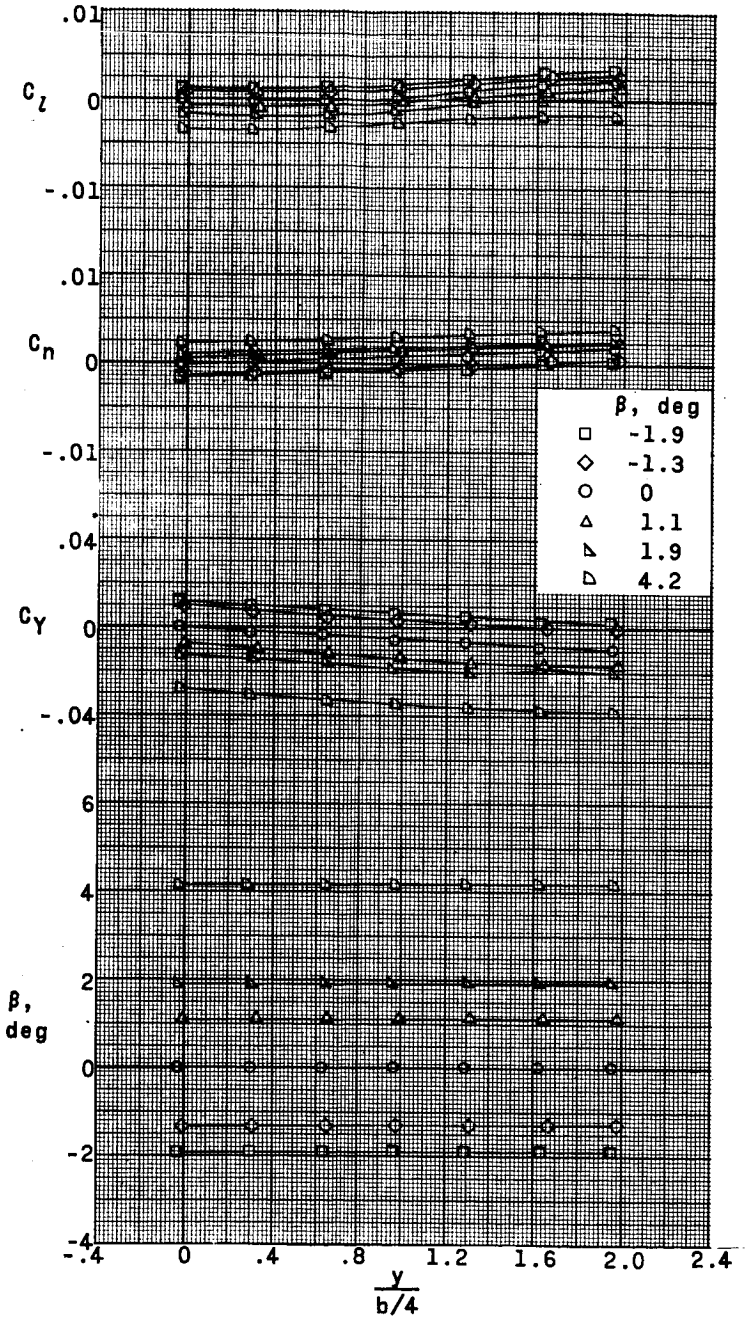

(j) $\frac{x}{l/4} = 4.02$; M = 2.16; $\alpha = 1.3^{\circ}$.

Figure 19.- Continued.

CONFIDENTIAL

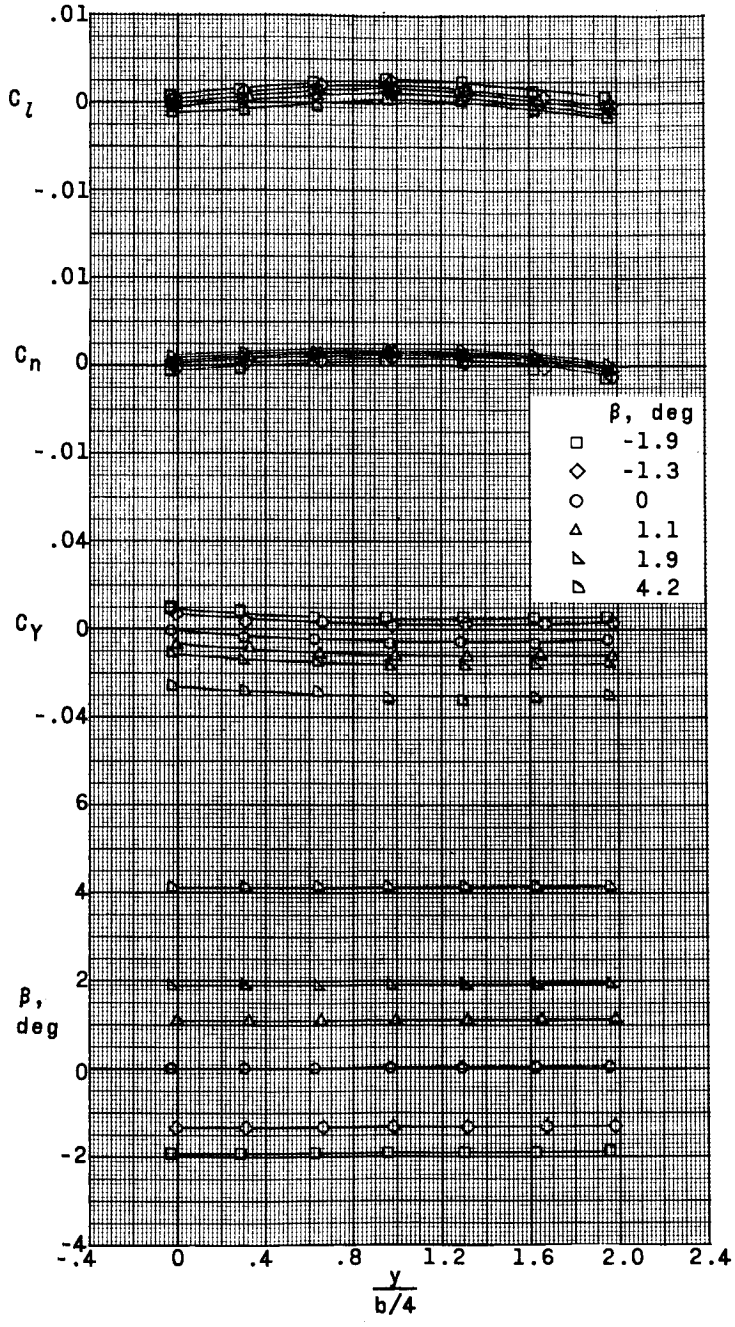

(k) $\frac{x}{l/4}$ = 4.02; M = 2.87; α = -0.5°.

Figure 19.- Continued.

CONFIDENTIAL

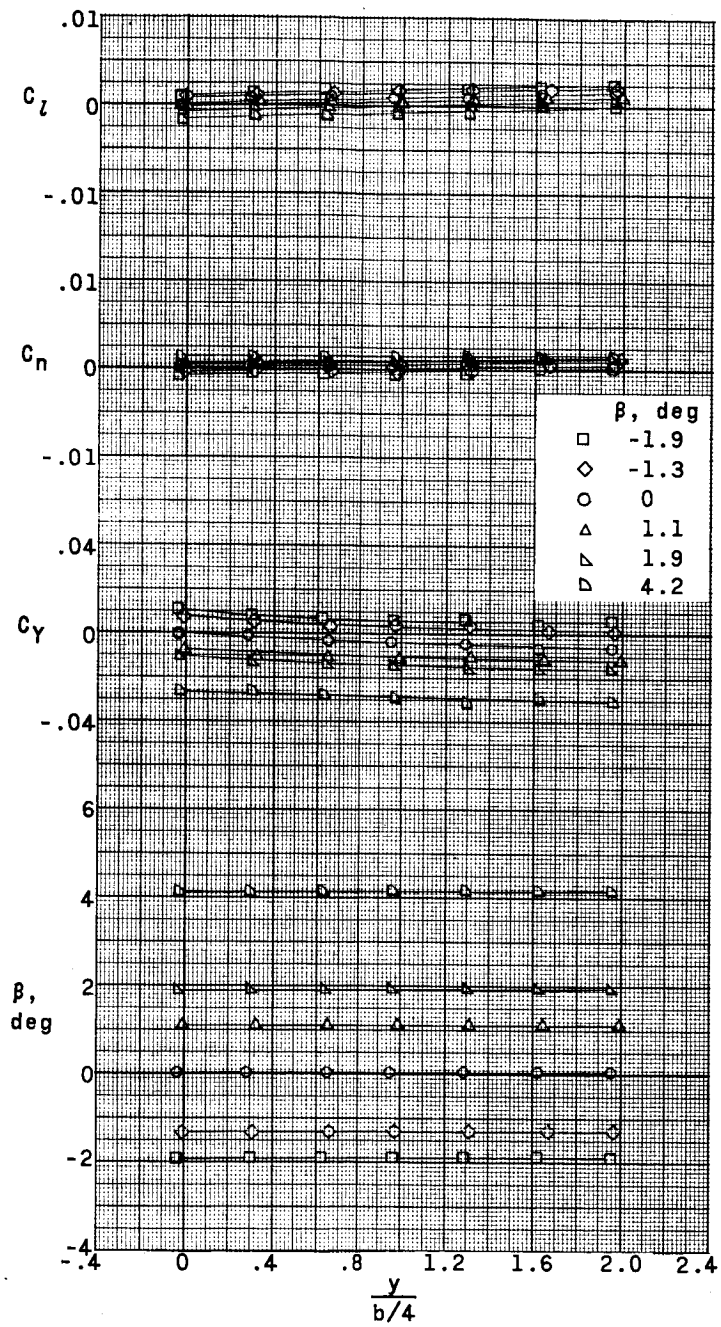

(l) $\frac{x}{l/4} = 5.03$; M = 2.87; $\alpha = -0.4^{\circ}$.

Figure 19.- Concluded.

CONFIDENTIAL

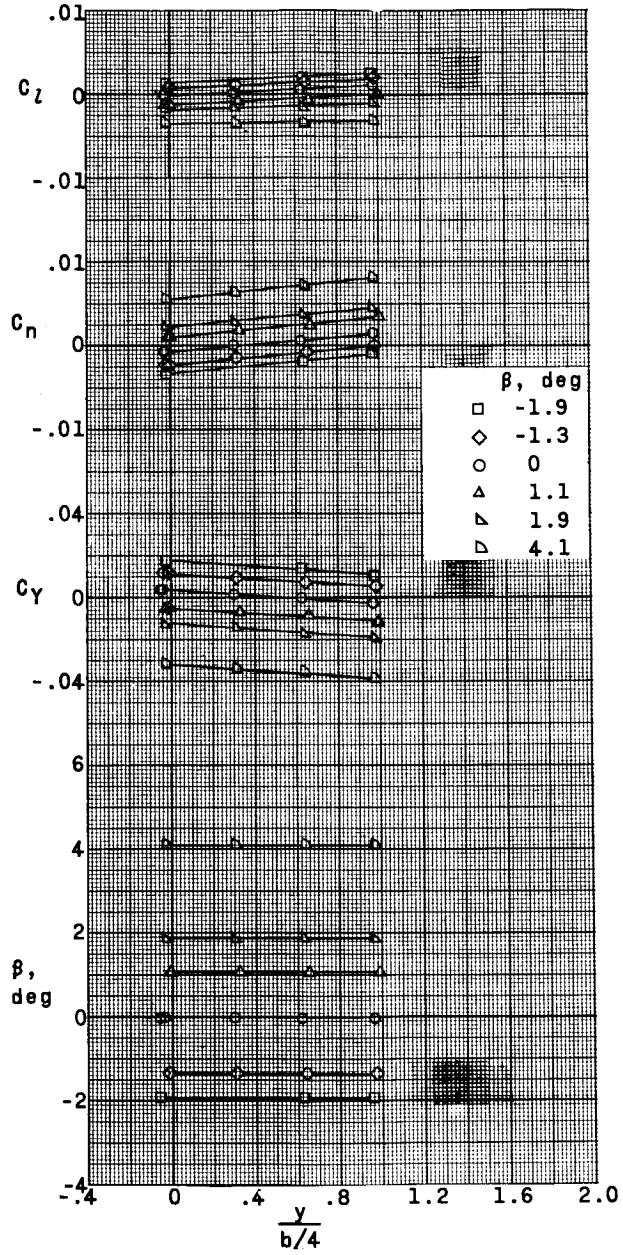

(a) $\frac{x}{l/4}$ = 1.02; M = 1.57; α = 0.5°.

Figure 20.- The variation of aerodynamic lateral characteristics with lateral position of the receiver model in presence of tanker model. $\frac{z}{b/4}$ = 2.90.

CONFIDENTIAL

CONFIDENTIAL

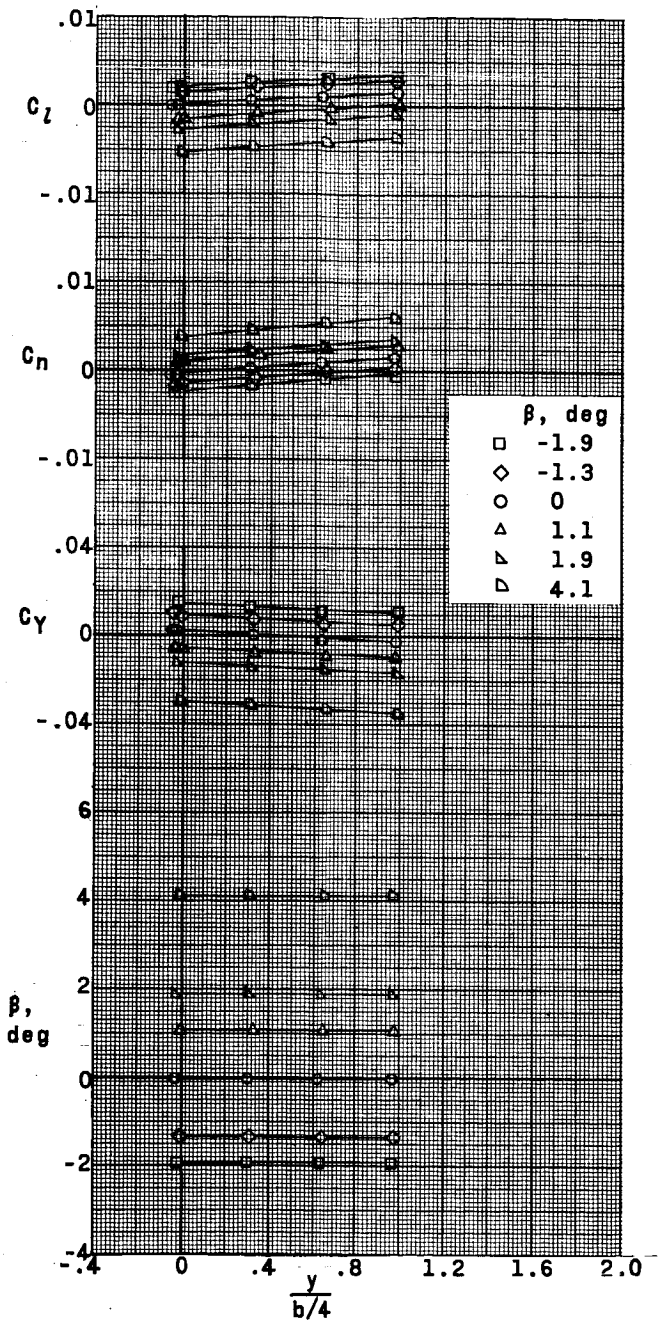

(b) $\frac{x}{l/4} = 1.02$; M = 2.16; $\alpha = 1.8^{\circ}$.

Figure 20.- Continued.

CONFIDENTIAL

CONFIDENTIAL

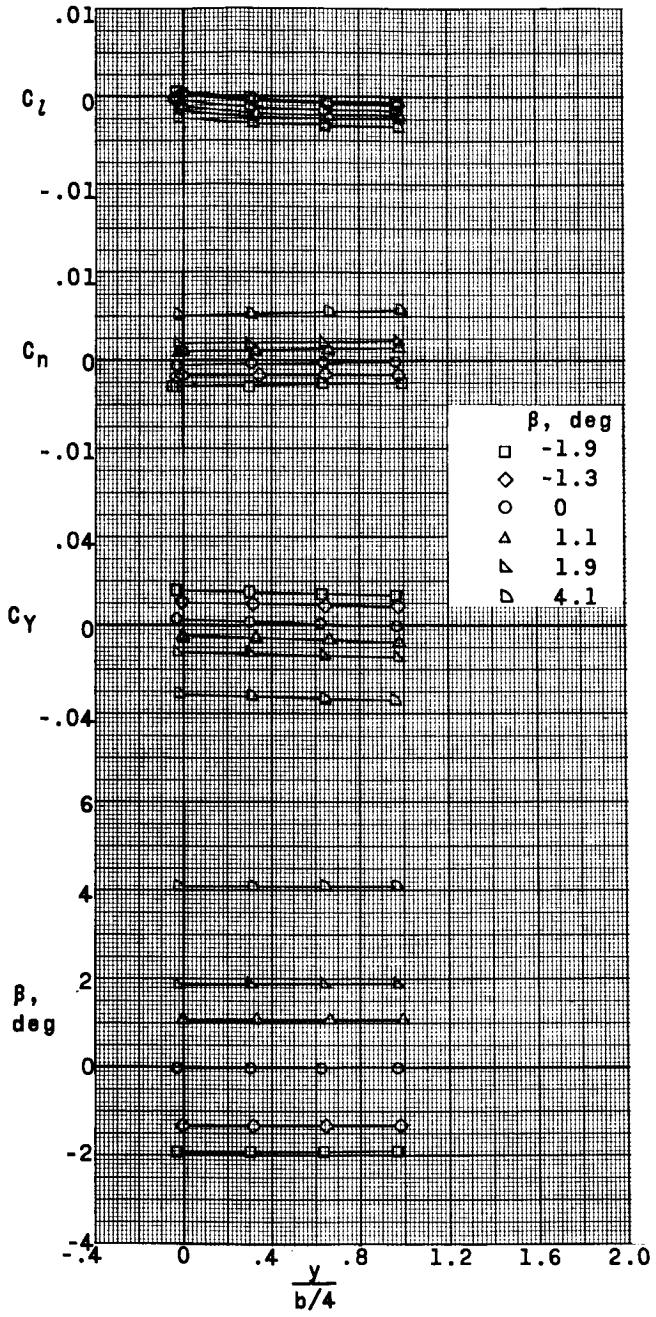

(c) $\frac{x}{l/4} = 2.02$; M = 1.57; $\alpha = 0.3^{\circ}$.

Figure 20.- Continued.

CONFIDENTIAL

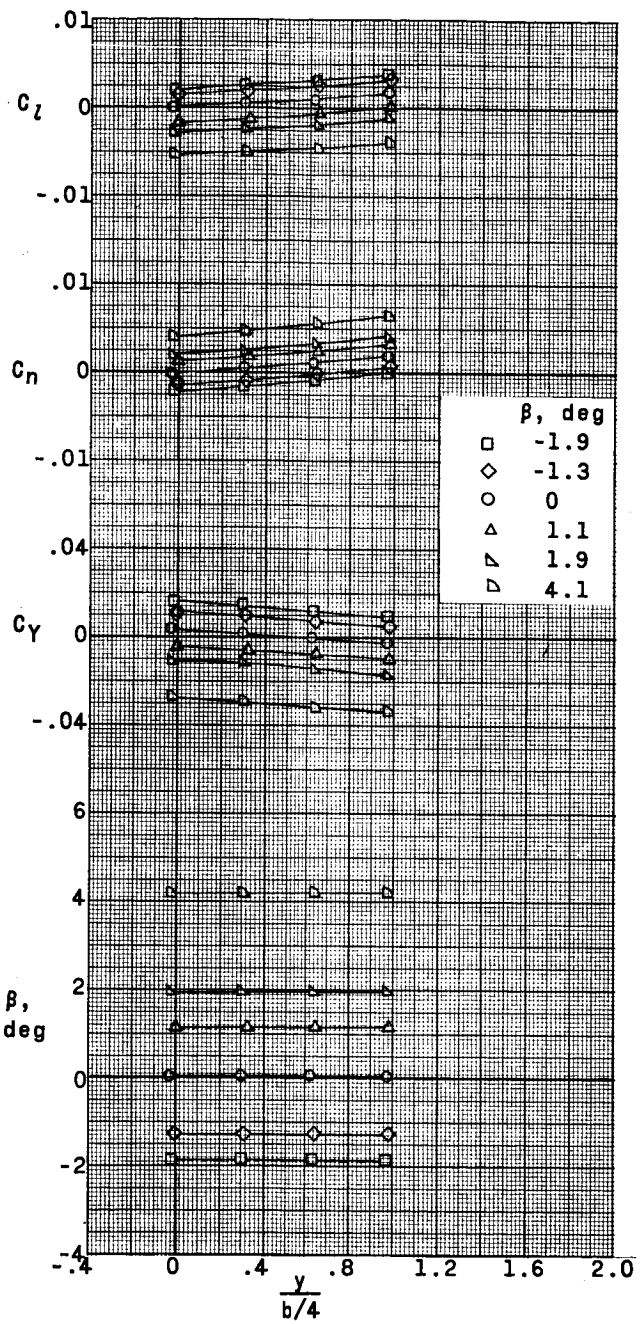

(d) $\frac{x}{l/4} = 2.02$; M = 2.16; $\alpha = 1.6^\circ$.

Figure 20.- Continued.

CONFIDENTIAL

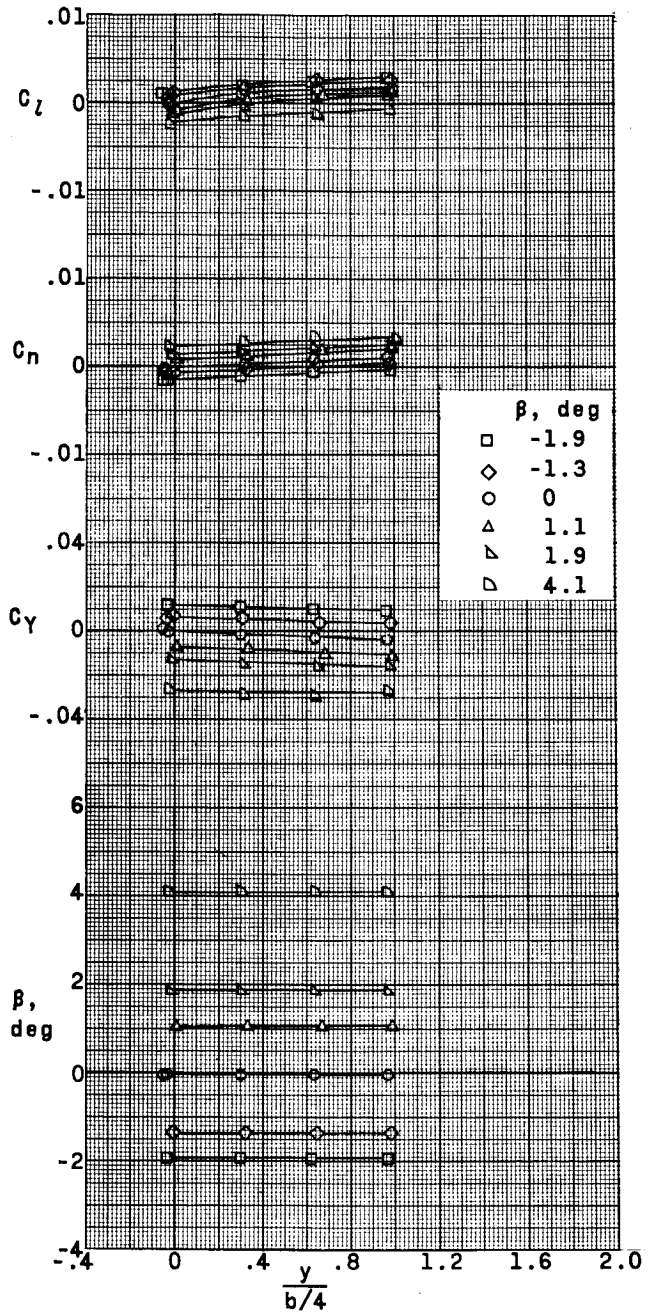

(e) $\frac{x}{l/4} = 2.02$; M = 2.87; $\alpha = -0.5^{\circ}$.

Figure 20.- Continued.

CONFIDENTIAL

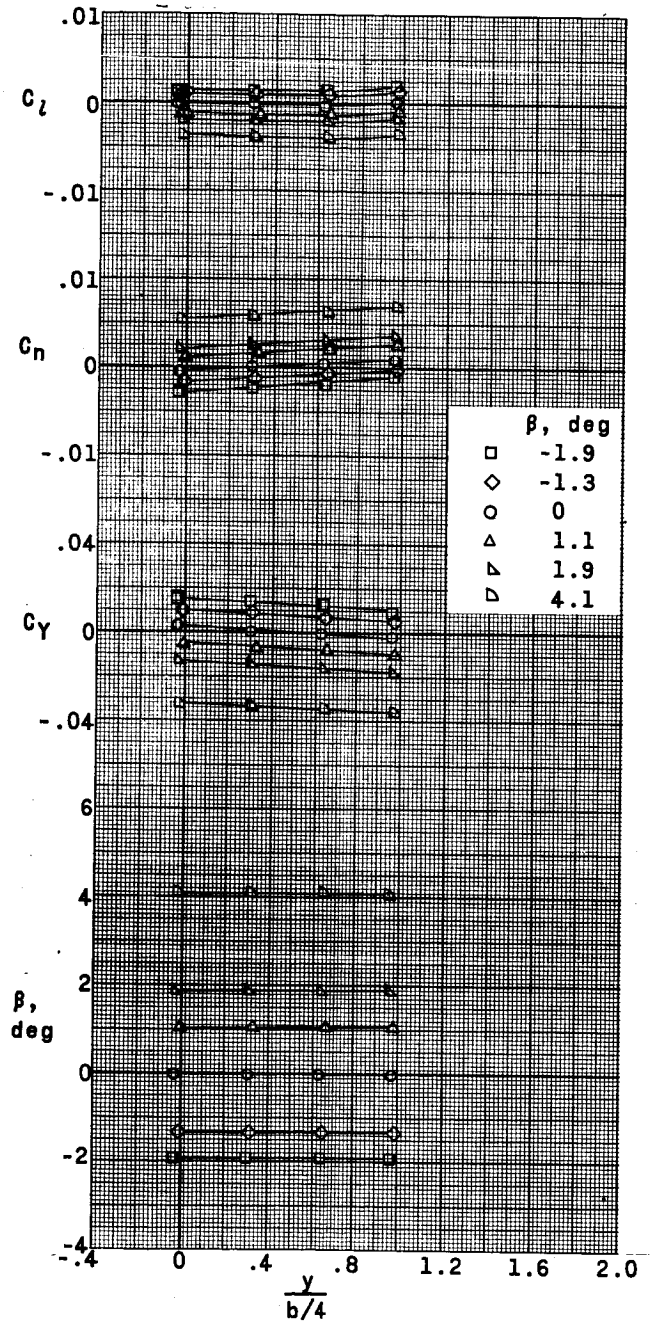

(f) $\frac{x}{l/4}$ = 3.02; M = 1.57; α = 0.4°.

Figure 20.- Continued.

CONFIDENTIAL

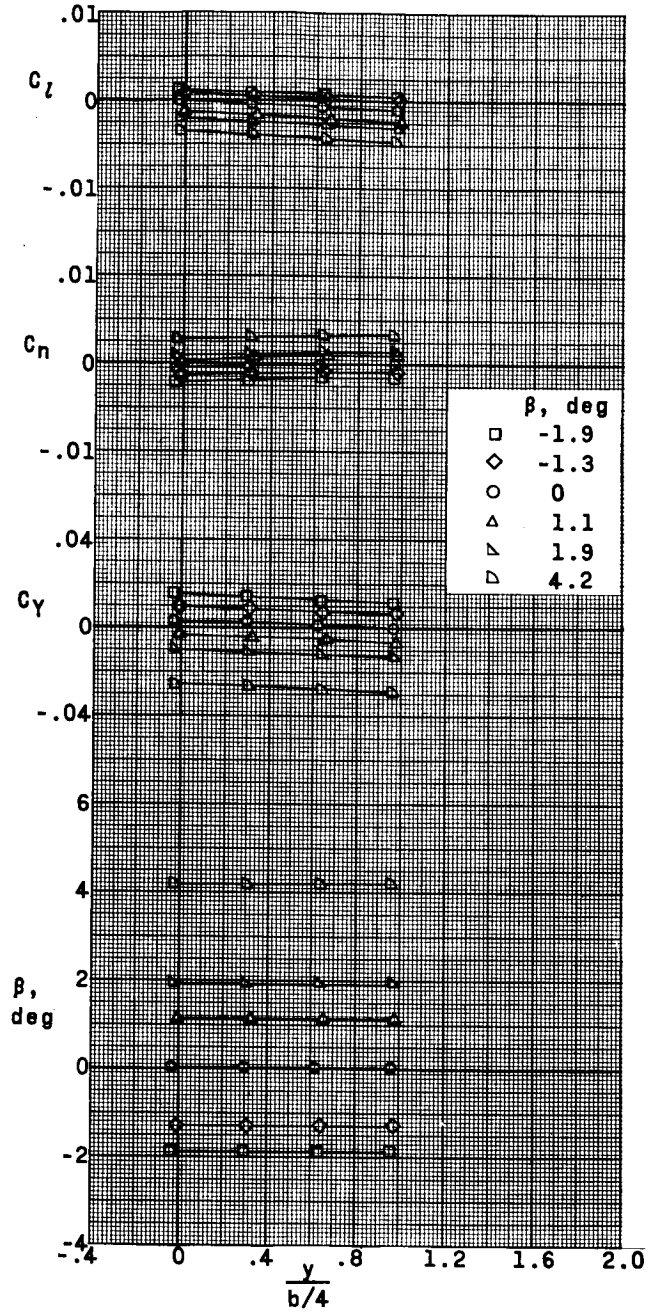

(g) $\frac{x}{l/4} = 3.02$; M = 2.16; $\alpha = 1.3^\circ$.

Figure 20.- Continued.

CONFIDENTIAL

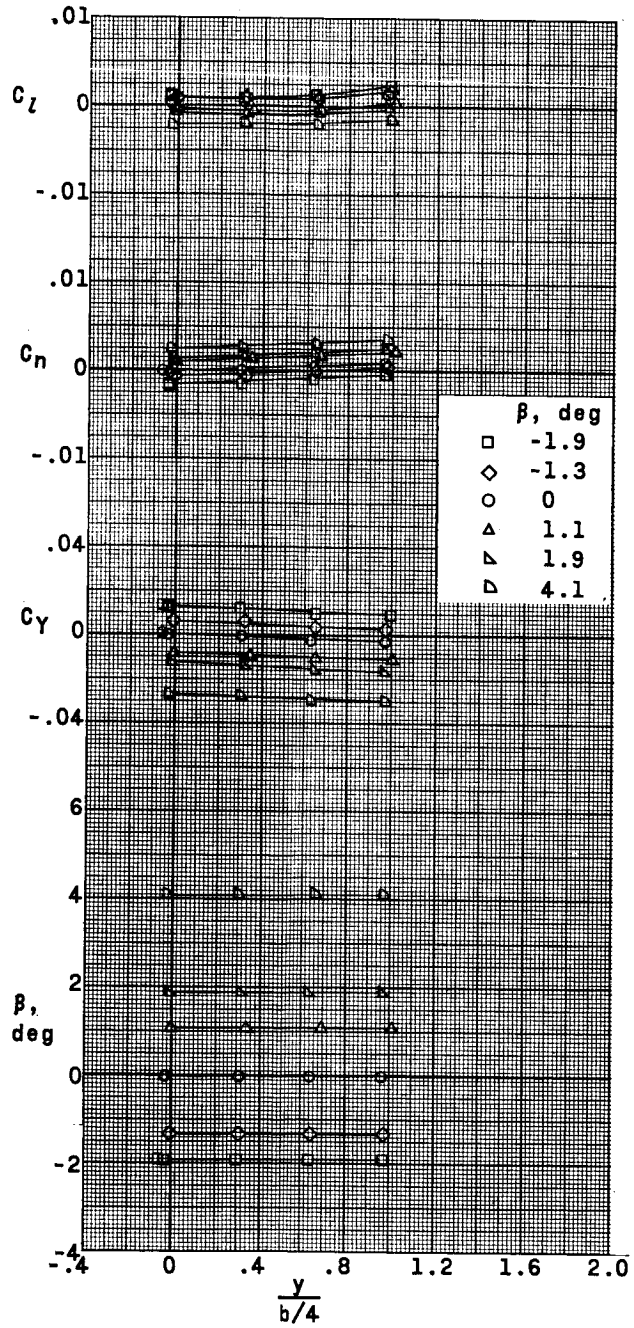

(h) $\frac{x}{l/4} = 3.02$; M = 2.87; $\alpha = -0.5^\circ$.

Figure 20.- Continued.

CONFIDENTIAL

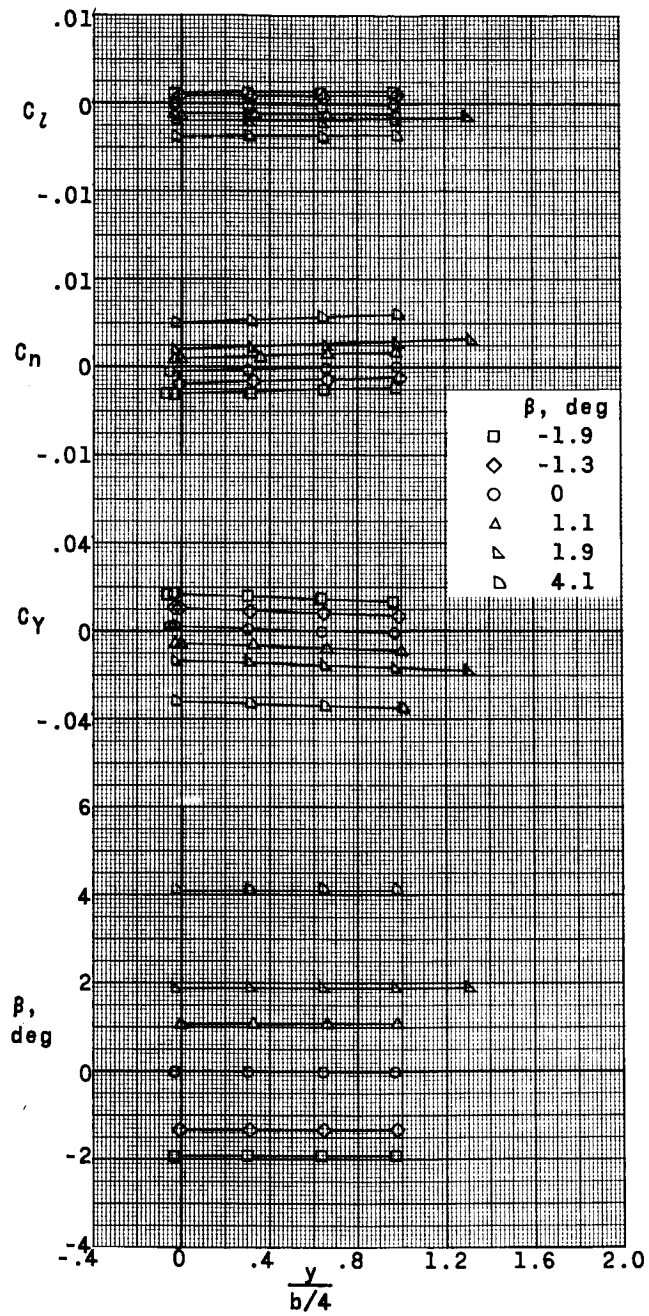

(i) $\frac{x}{l/4} = 4.03$; M = 1.57; $\alpha = 0.4^{\circ}$.

Figure 20.- Continued.

CONFIDENTIAL

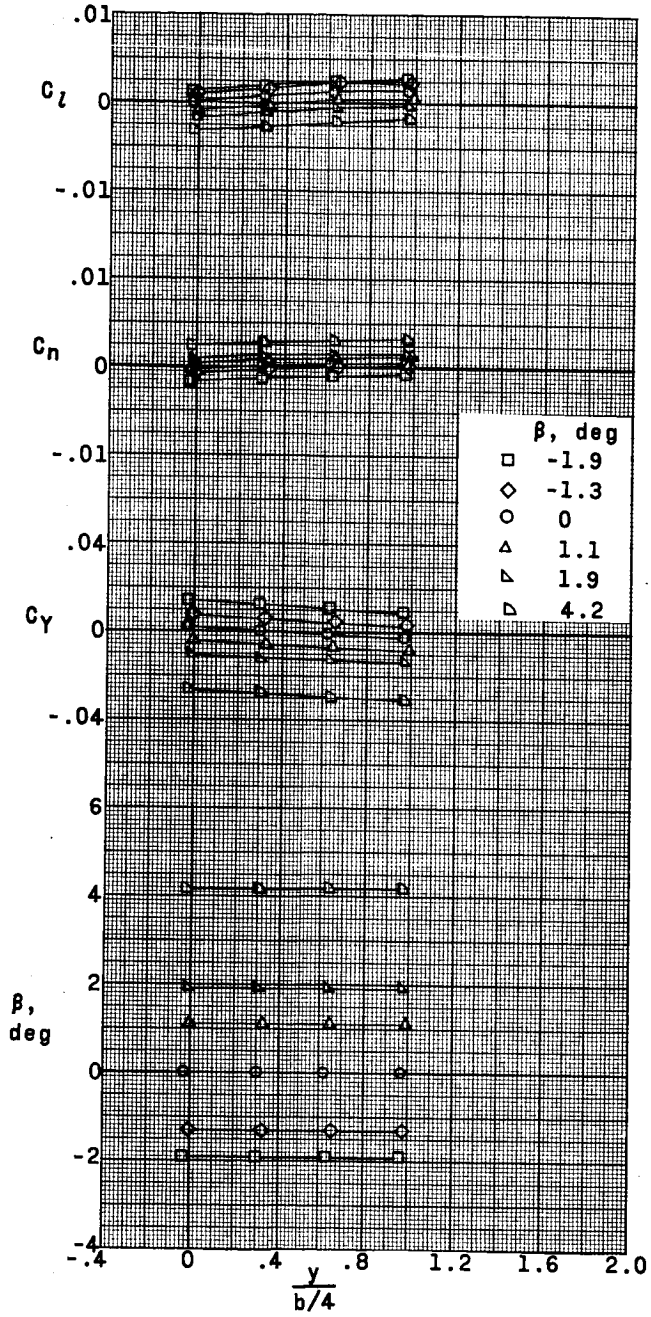

(j) $\frac{x}{l/4} = 4.03$; M = 2.16; $\alpha = 1.2^\circ$.

Figure 20.- Continued.

CONFIDENTIAL

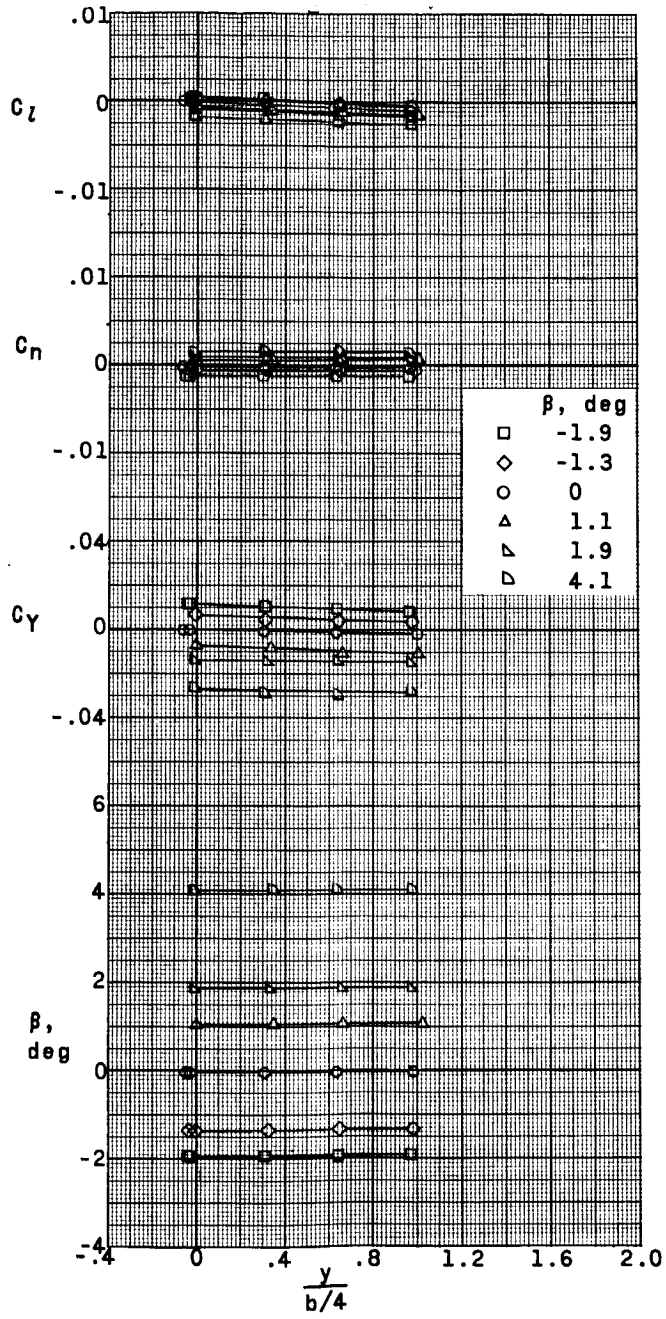

(k) $\frac{x}{l/4} = 4.03$; M = 2.87; $\alpha = -0.5^{\circ}$.

Figure 20.- Continued.

CONFIDENTIAL

L-591

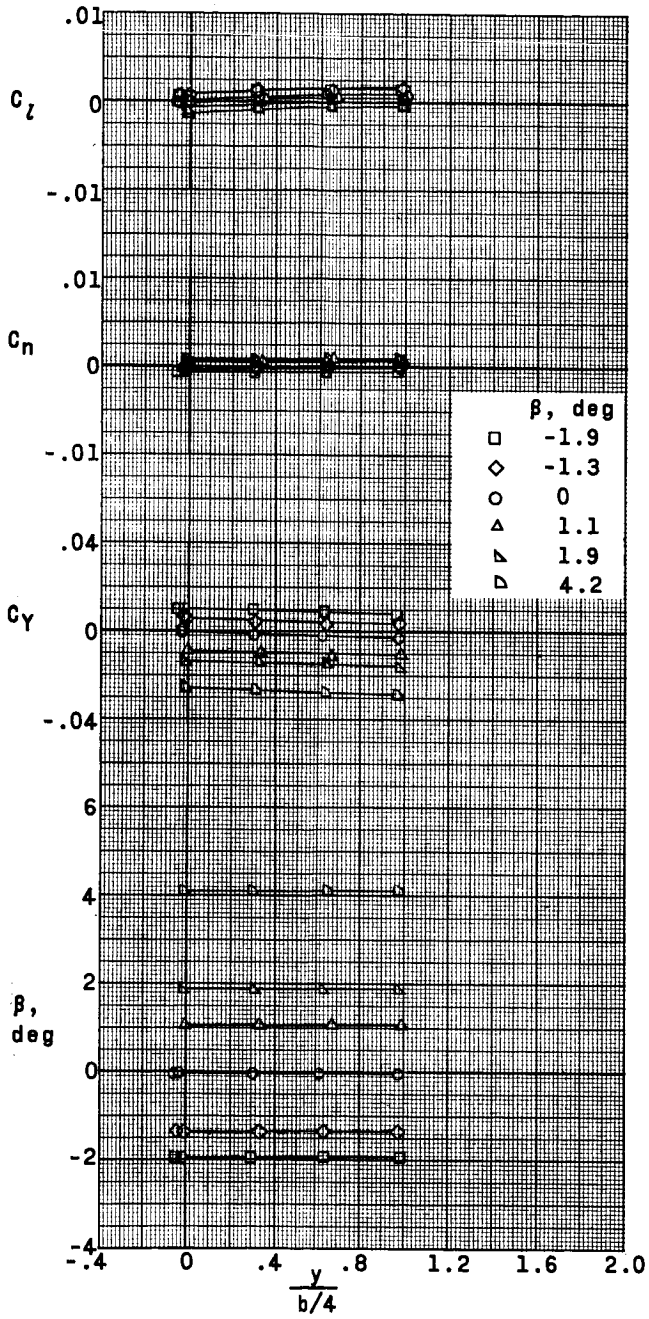

(l) $\frac{x}{l/4} = 5.03$; M = 2.87; $\alpha = -0.5^\circ$.

Figure 20.- Concluded.

CONFIDENTIAL

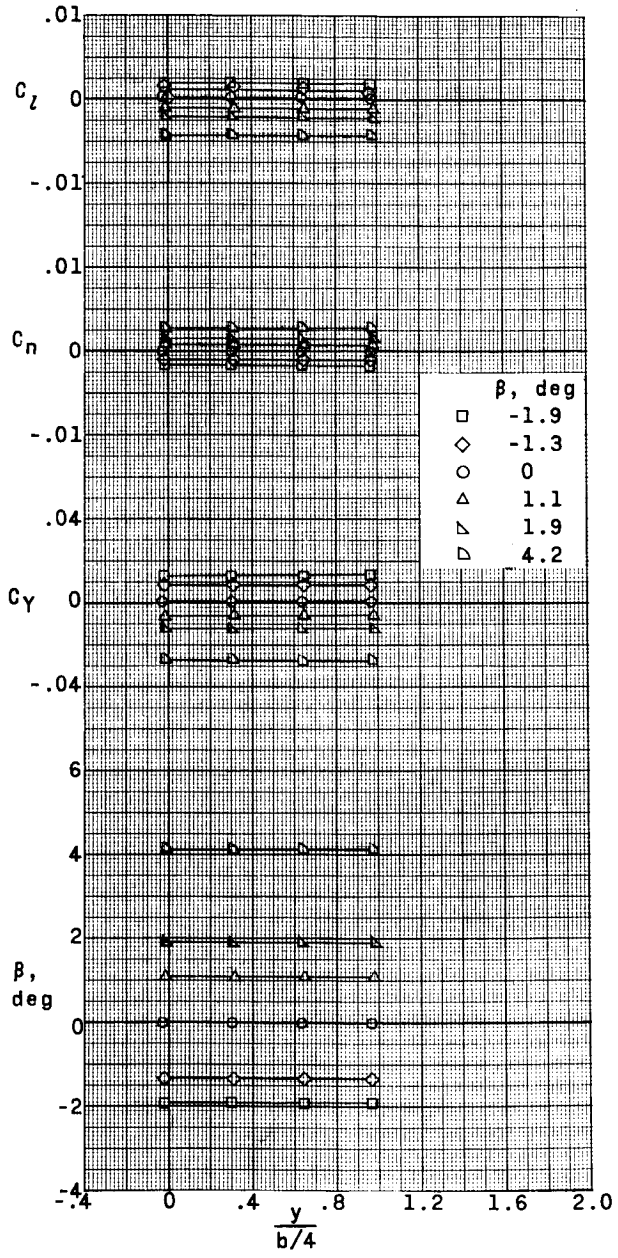

(a) $\frac{x}{l/4} = 0.02$; M = 2.16; $\alpha = 1.9^{\circ}$.

Figure 21.- The variation of aerodynamic lateral characteristics with lateral position of the receiver model in presence of tanker model. $\frac{z}{b/4} = 3.90$.

CONFIDENTIAL

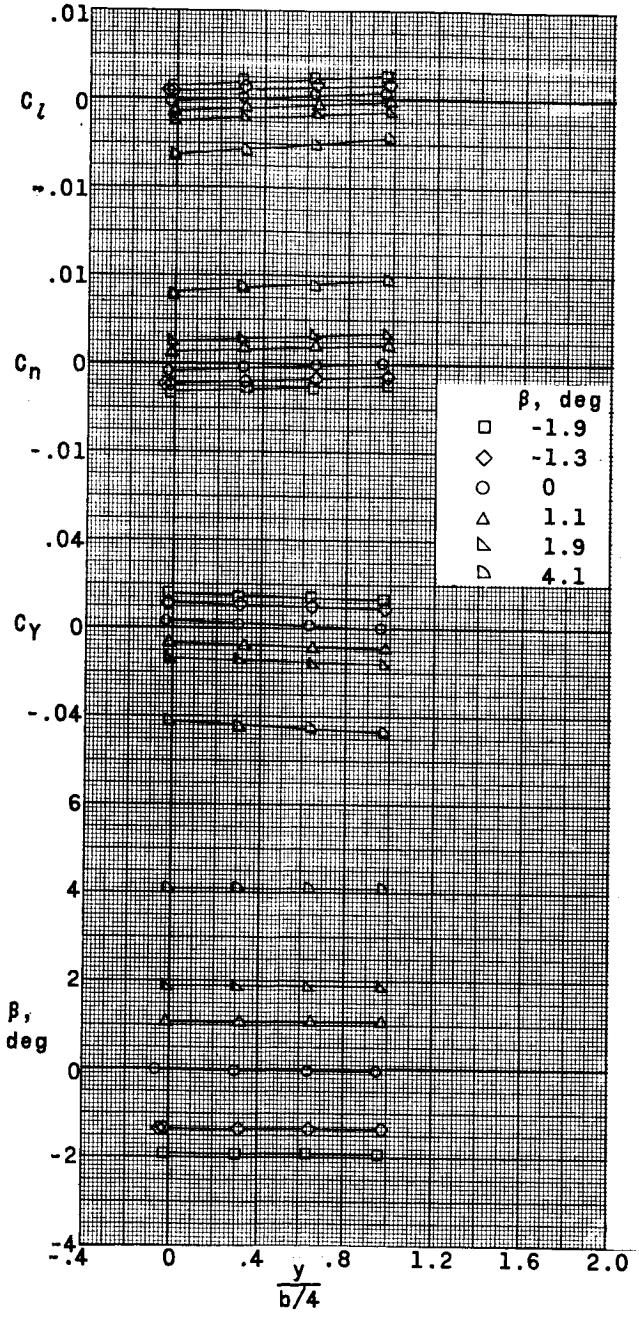

(b) $\frac{x}{l/4} = 1.02$; $M = 1.57$; $\alpha = 0.6^{\circ}$.

Figure 21.- Continued.

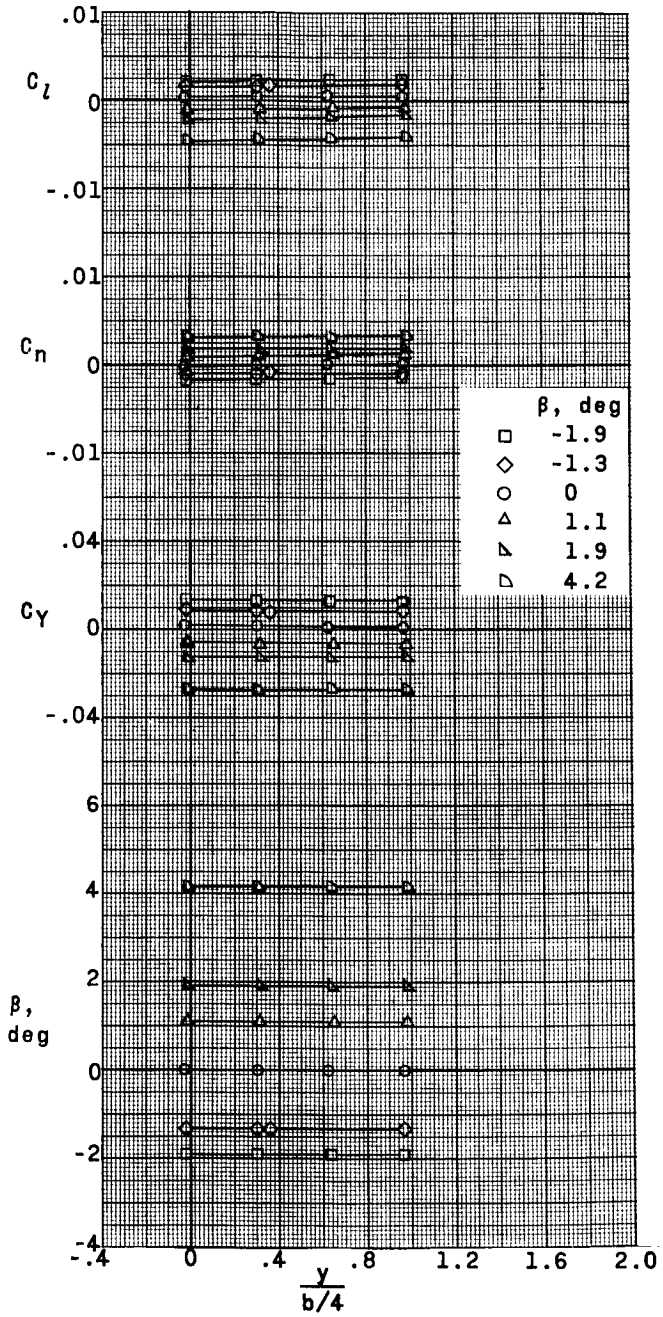

(c) $\frac{x}{l/4} = 1.02$; M = 2.16; $\alpha = 1.8^{\circ}$.

Figure 21.- Continued.

CONFIDENTIAL

L-591

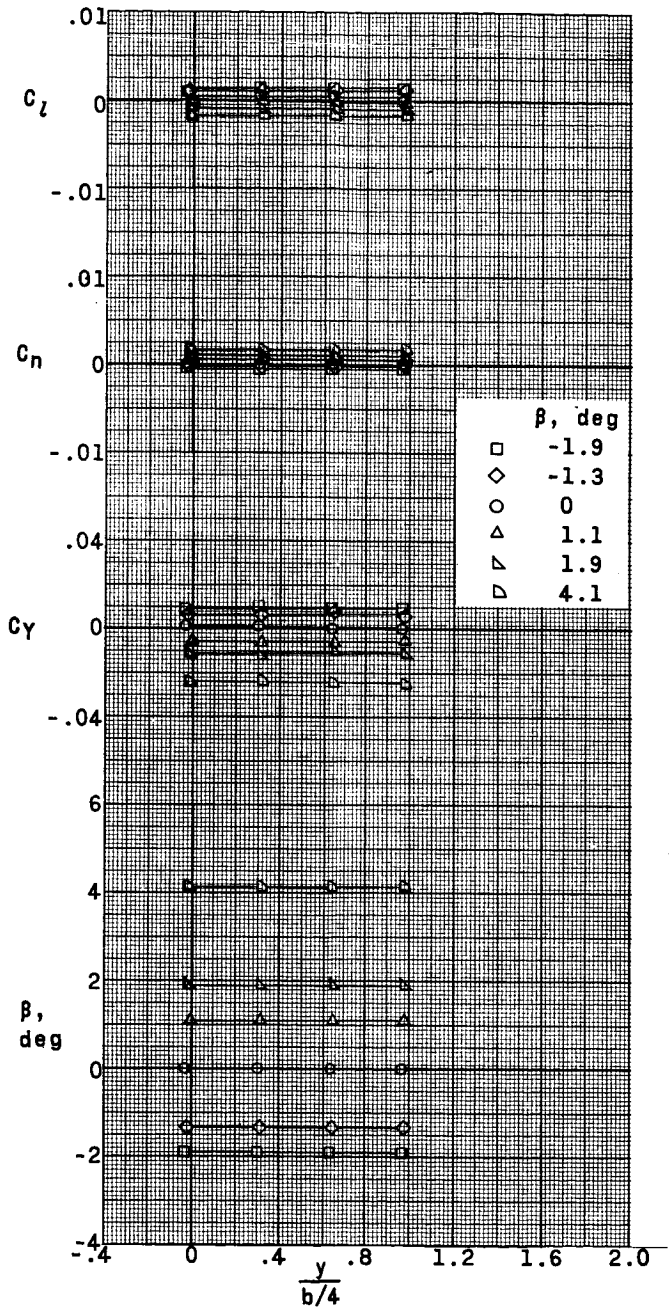

(d) $\frac{x}{l/4} = 1.02$; M = 2.87; $\alpha = -0.5^\circ$.

Figure 21.- Continued.

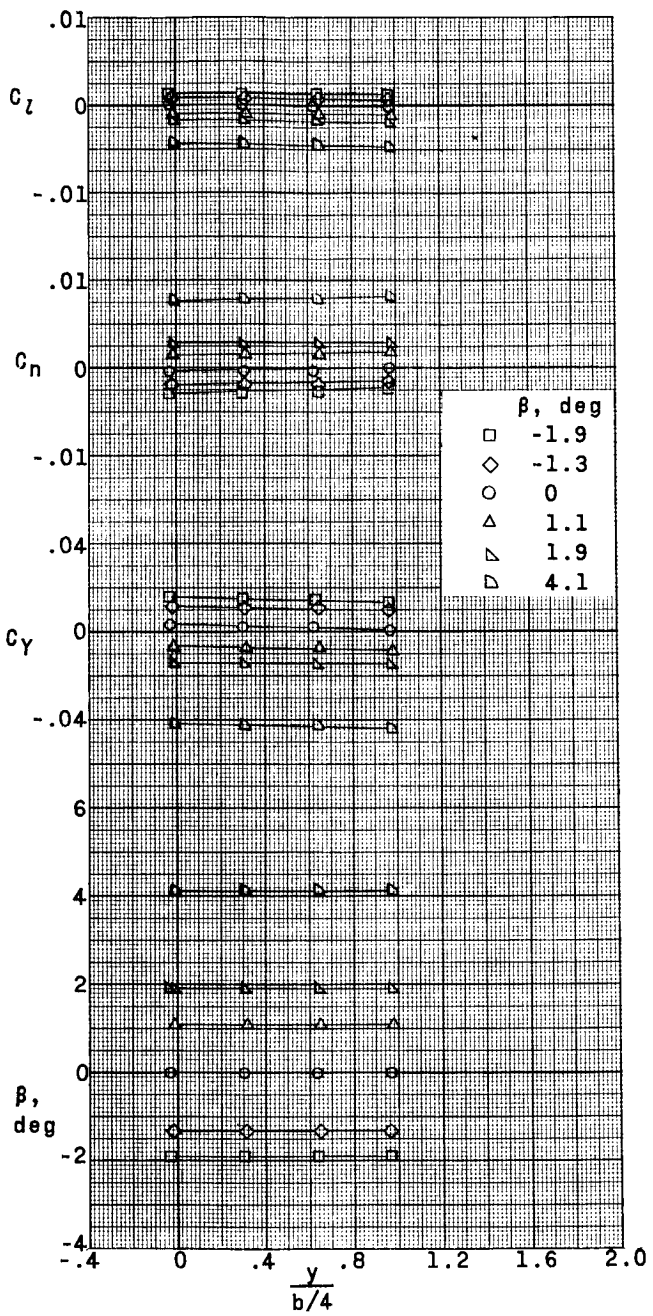

(e) $\frac{x}{l/4} = 2.02$; M = 1.57; $\alpha = 0.5^{\circ}$.

Figure 21.- Continued.

L-591

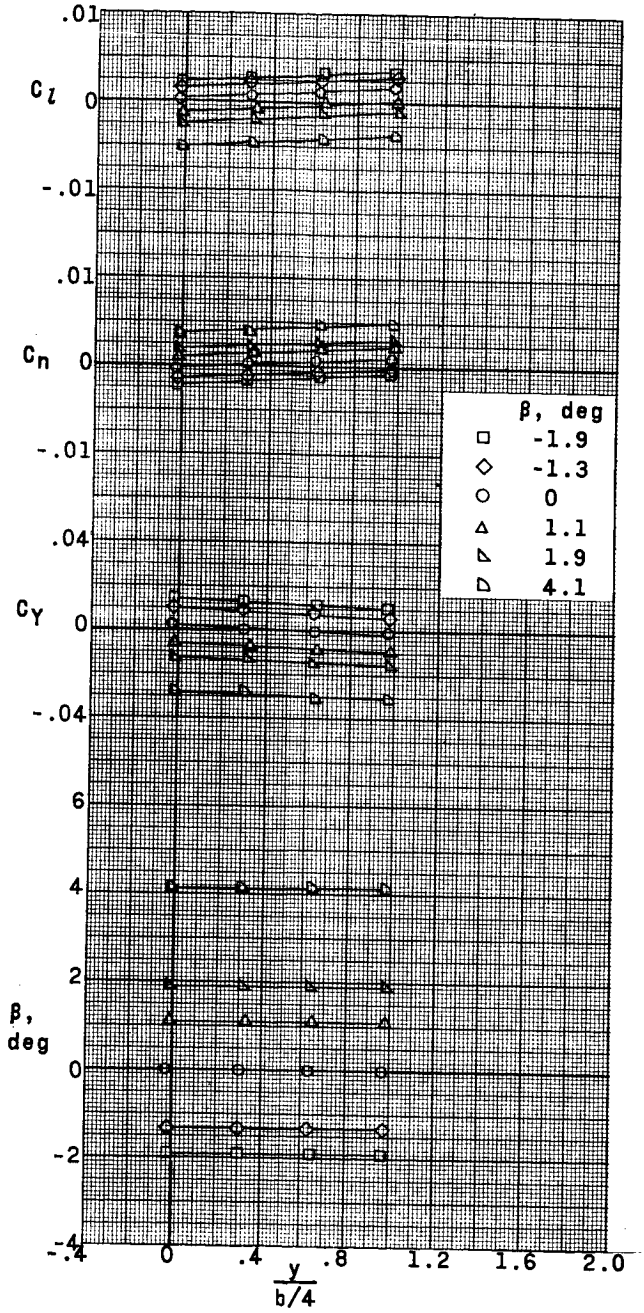

(f) $\frac{x}{l/4} = 2.02$; $M = 2.16$; $\alpha = 1.7^{\circ}$.

Figure 21.- Continued.

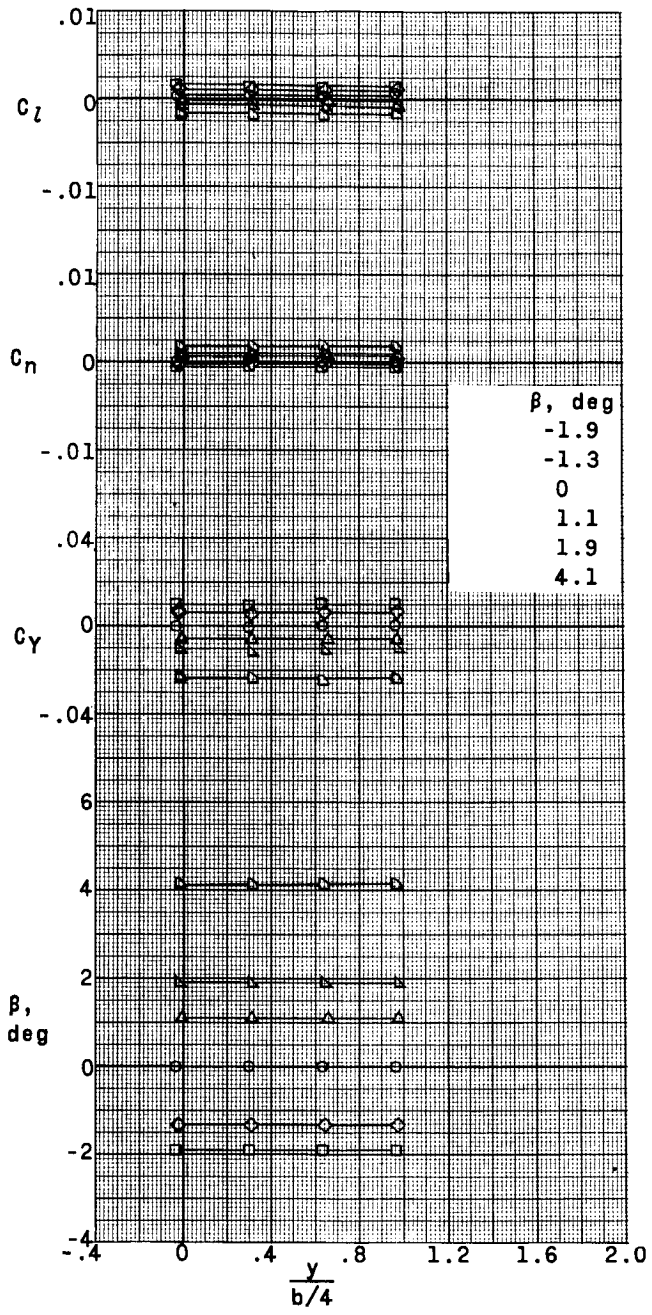

(g) $\frac{x}{l/4} = 2.02$; M = 2.87; $\alpha = -0.4^{\circ}$.

Figure 21.- Continued.

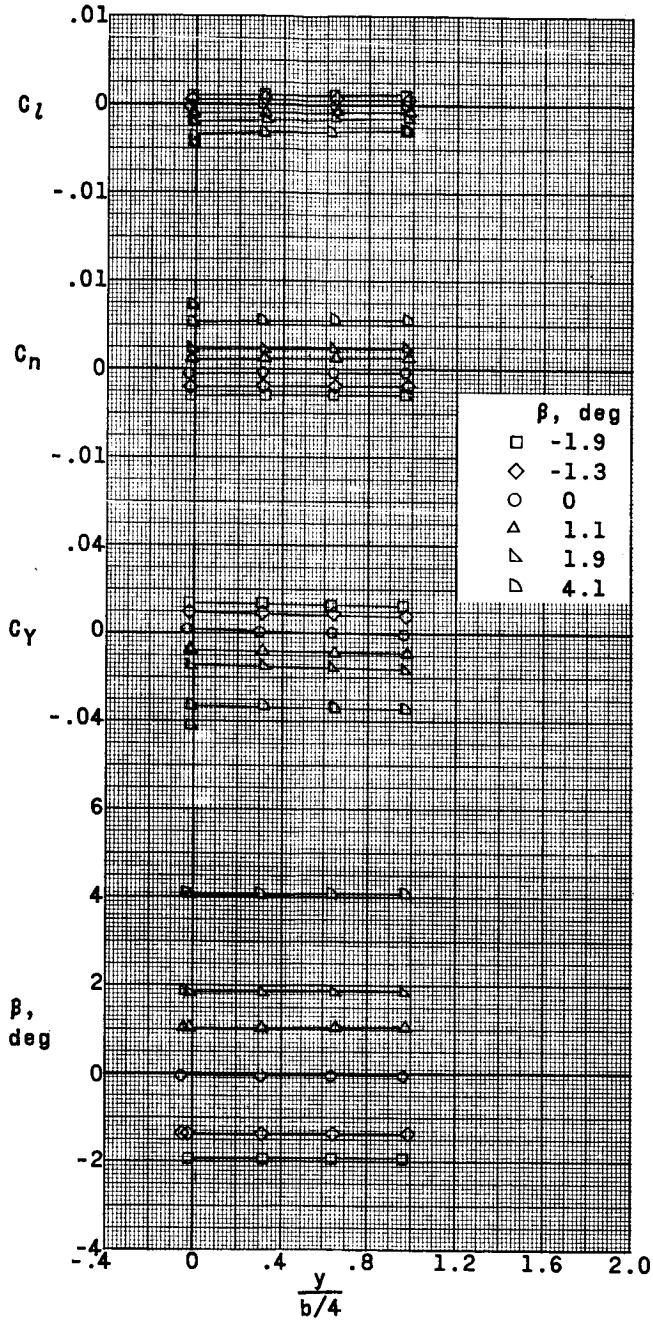

(h) $\frac{x}{l/4} = 3.03$; M = 1.57; $\alpha = 0.4^{\circ}$.

Figure 21.- Continued.

L-591

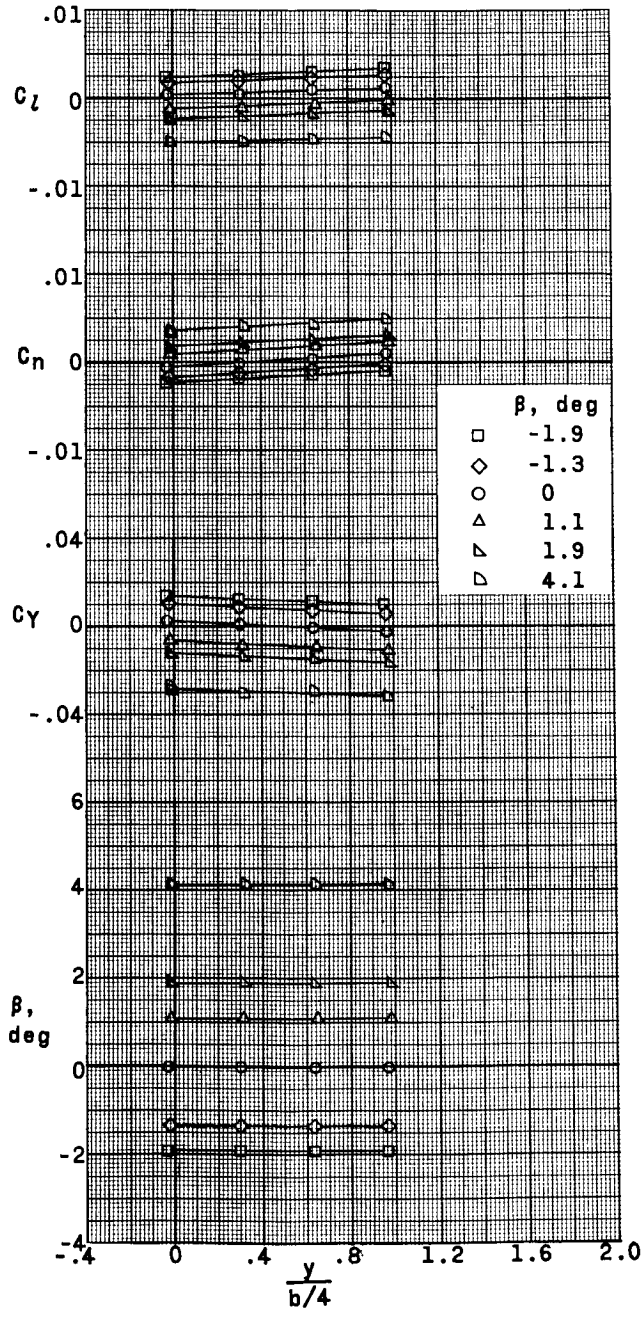

(i) $\frac{x}{l/4} = 3.03$; M = 2.16; $\alpha = 1.5^{\circ}$.

Figure 21.- Continued.

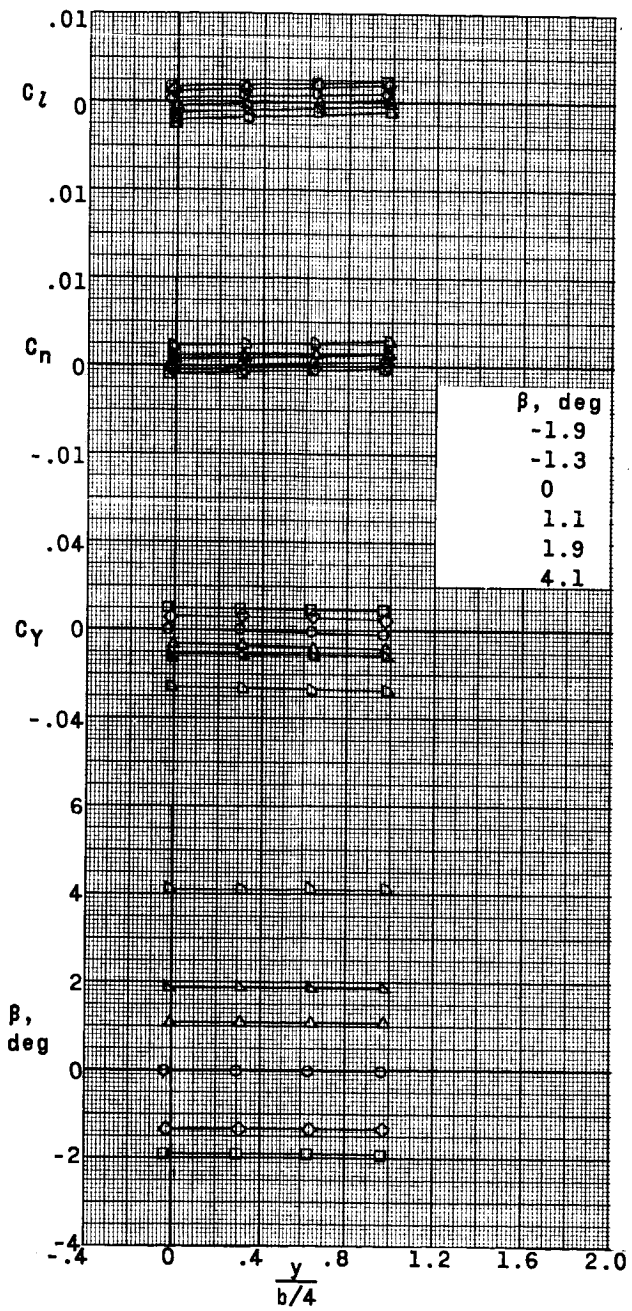

(j) $\frac{x}{l/4}$ = 3.03; M = 2.87; α = -0.4°.

Figure 21.- Continued.

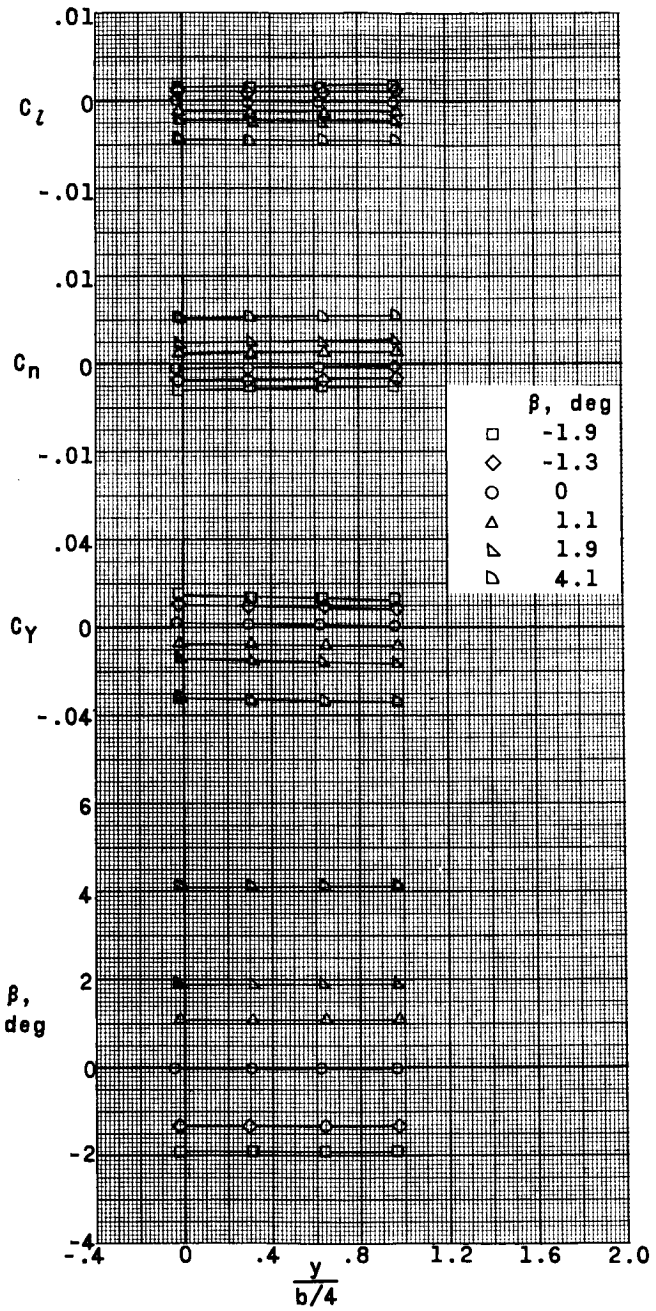

(k) $\frac{x}{l/4} = 4.03$; M = 1.57; $\alpha = 0.5^{\circ}$.

Figure 21.- Continued.

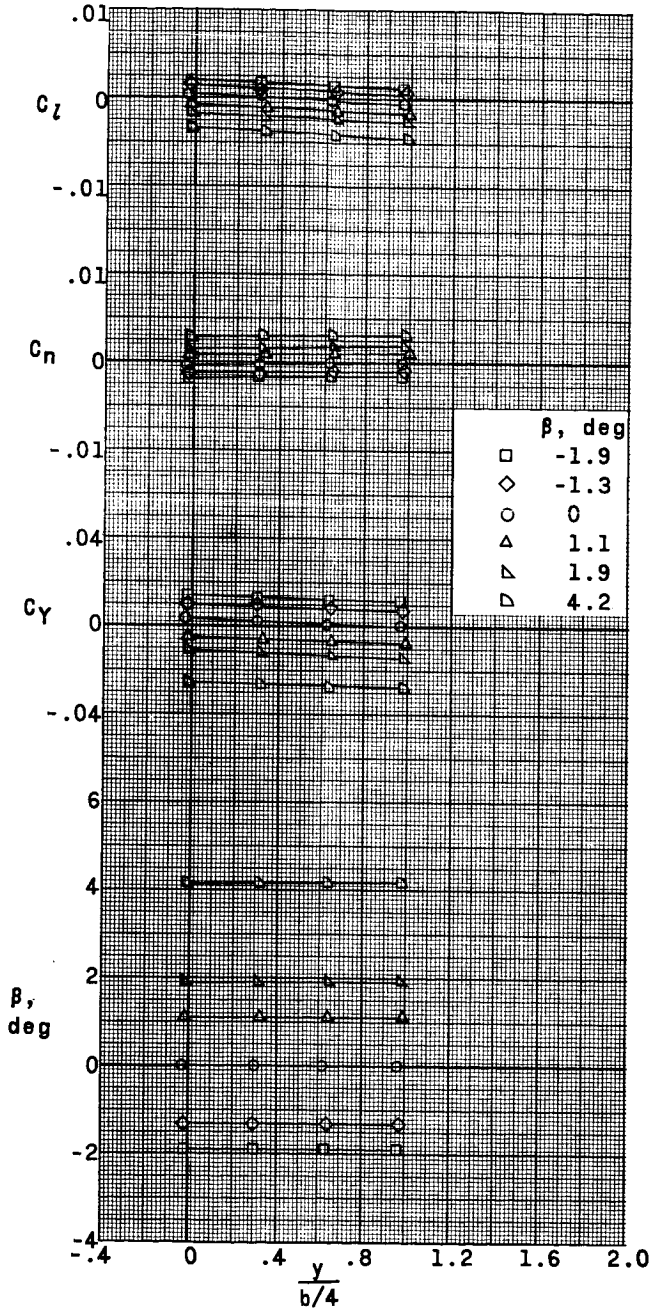

(l) $\frac{x}{l/4}$ = 4.03; M = 2.16; α = 1.3°.

Figure 21.- Continued.

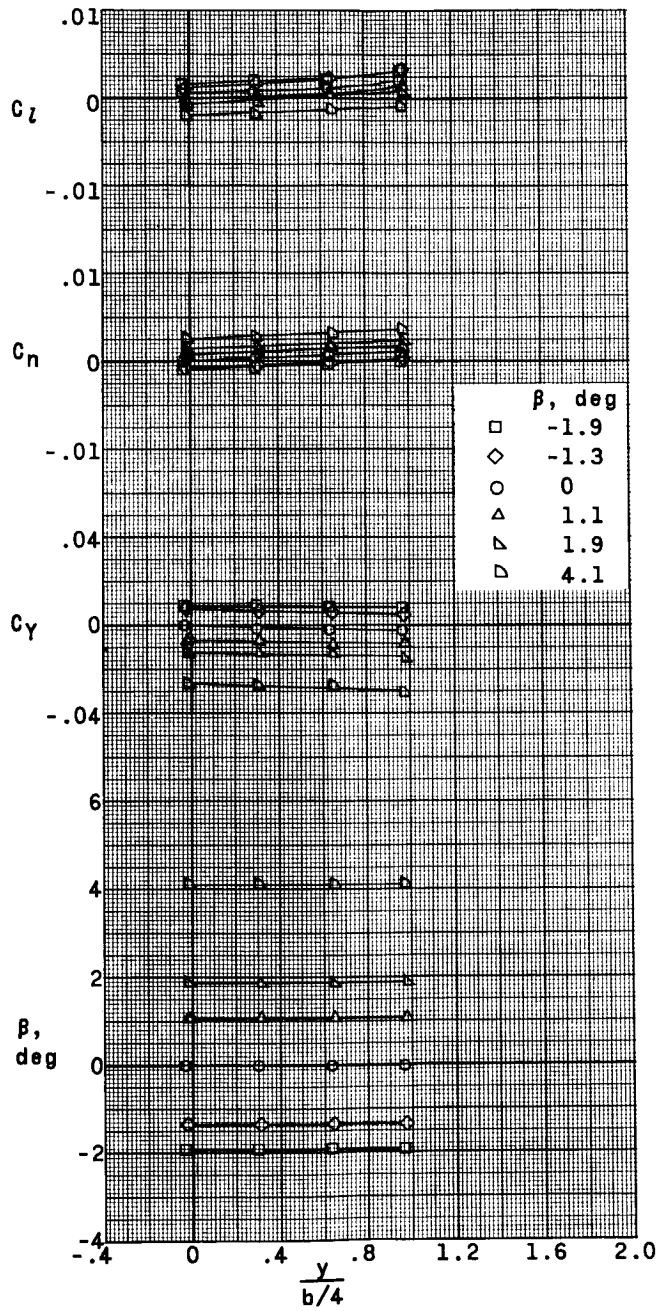

(m) $\frac{x}{l/4} = 4.03$; M = 2.87; $\alpha = -0.4^{\circ}$.

Figure 21.- Continued.

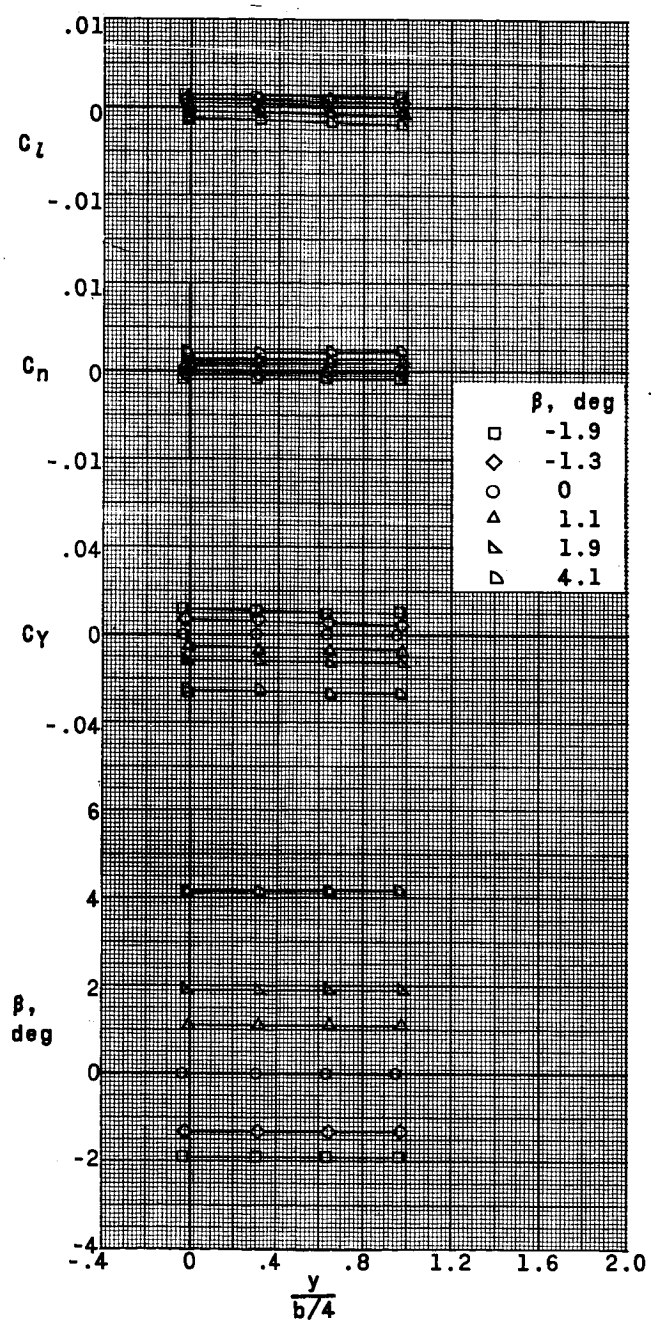

(n) $\frac{x}{l/4}$ = 5.03; M = 2.87; α = -0.5°.

Figure 21.- Concluded.

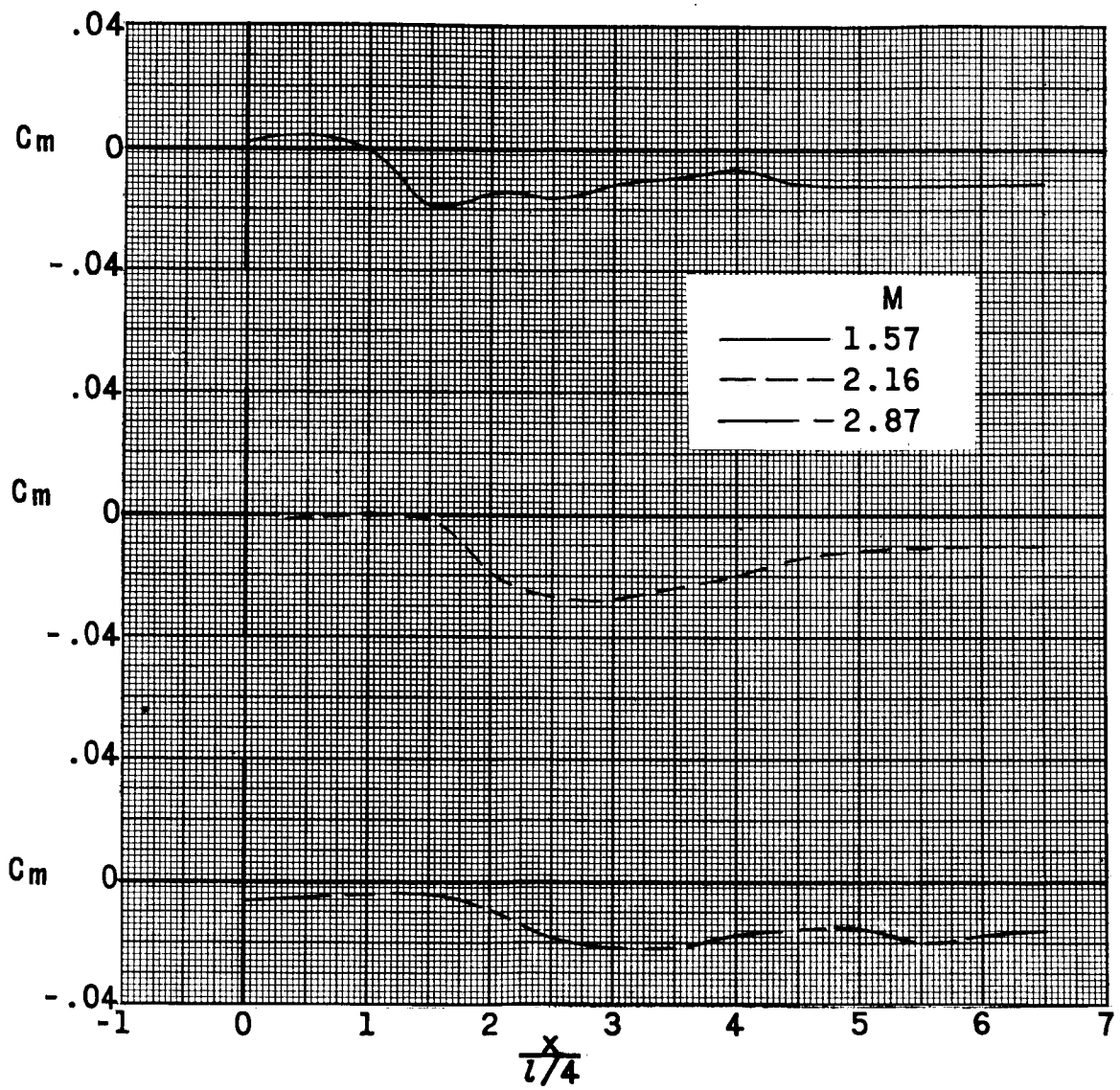

(a) $\left(\frac{z}{b/4}\right)_{nom} = 2.$

Figure 22.- Variation of pitching-moment coefficient at lift coefficient of 0.15 with longitudinal position of the receiver model in presence of tanker model. $\frac{y}{b/4} = 0$; $\beta = 0^{o}$.

CONFIDENTIAL

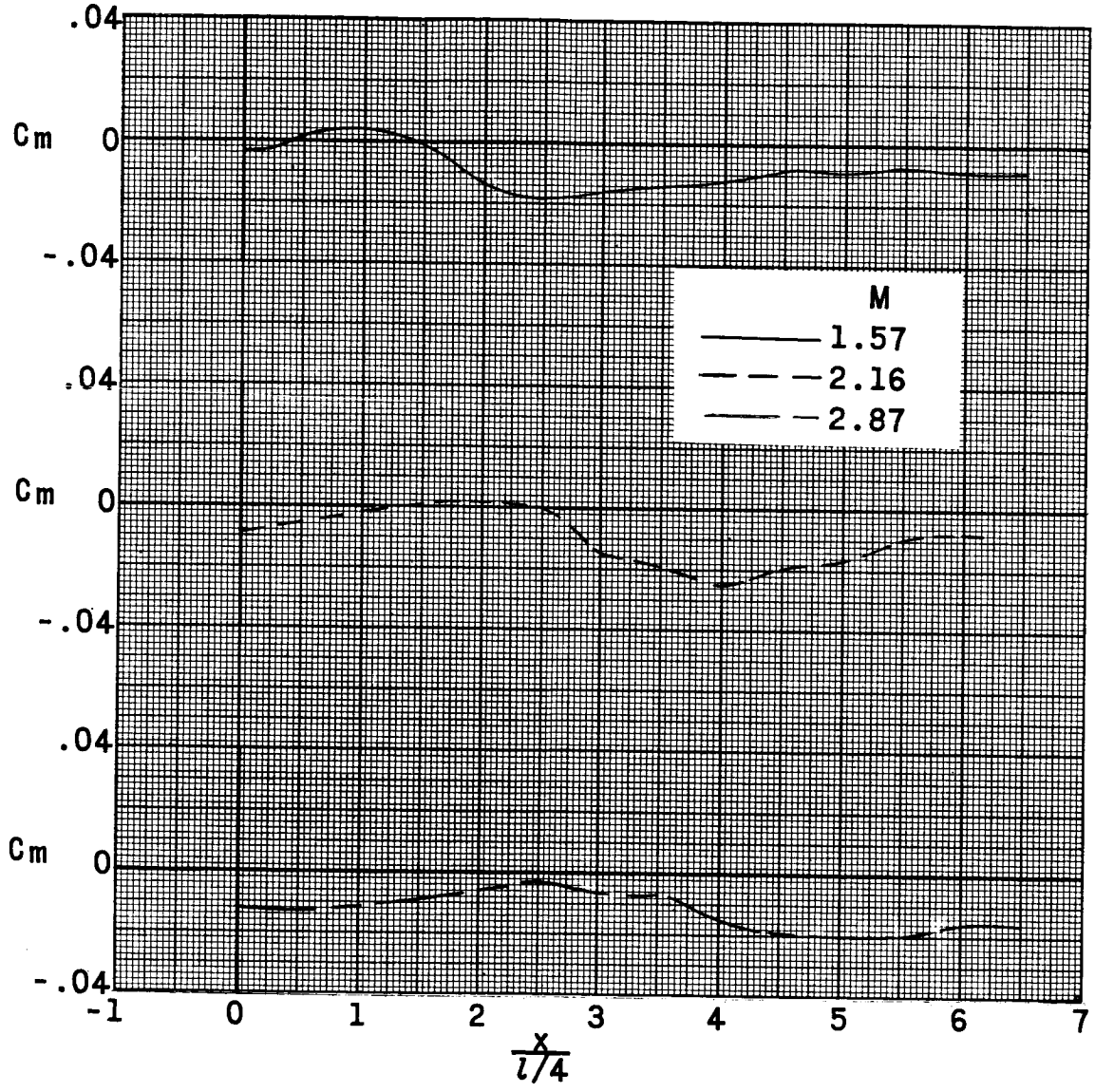

(b) $\left(\frac{z}{b/4}\right)_{nom} = 3.$

Figure 22.- Concluded.

CONFIDENTIAL

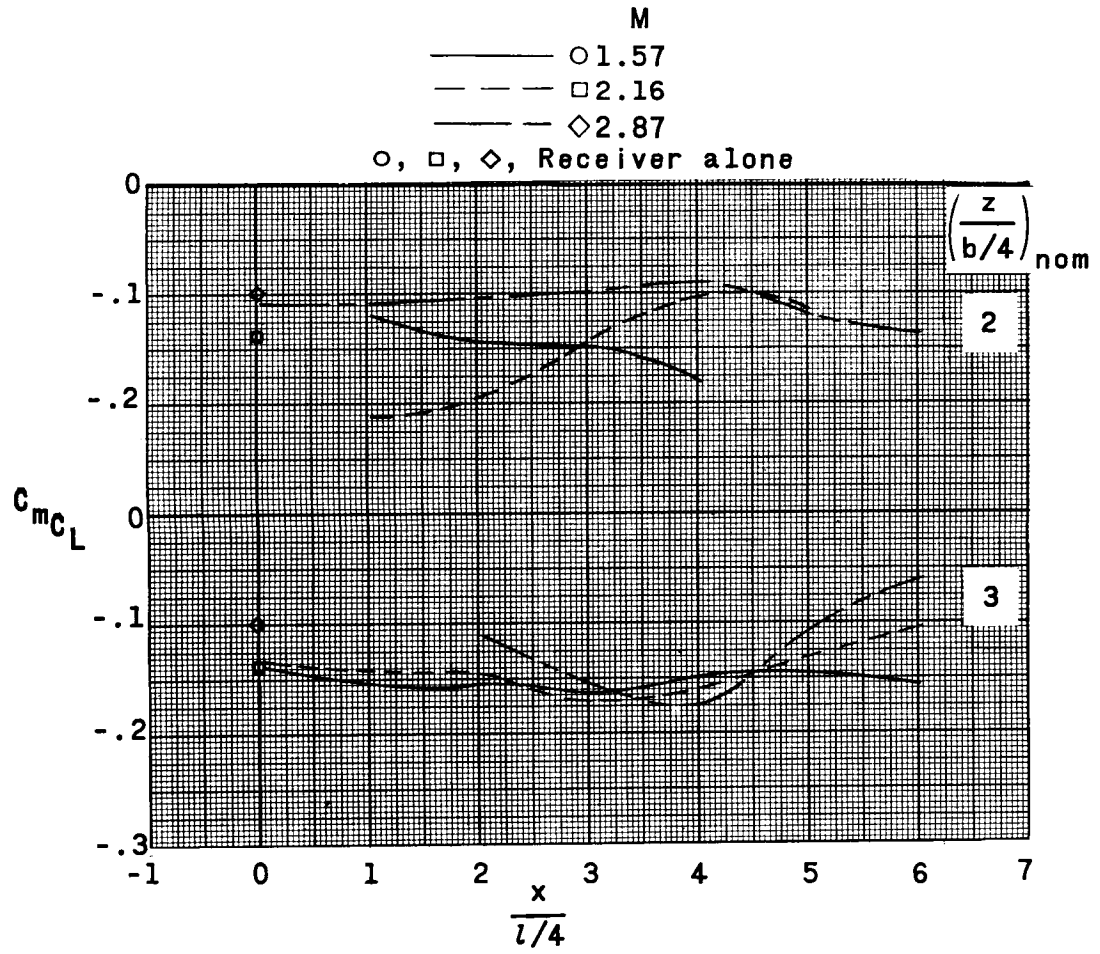

(a) Longitudinal-stability parameter.

Figure 23.- The variation of static-stability parameter with longitudinal position of the receiver model in the presence of the tanker model at two vertical positions. $\beta = 0^{\circ}$; $\frac{y}{b/4} = 0$.

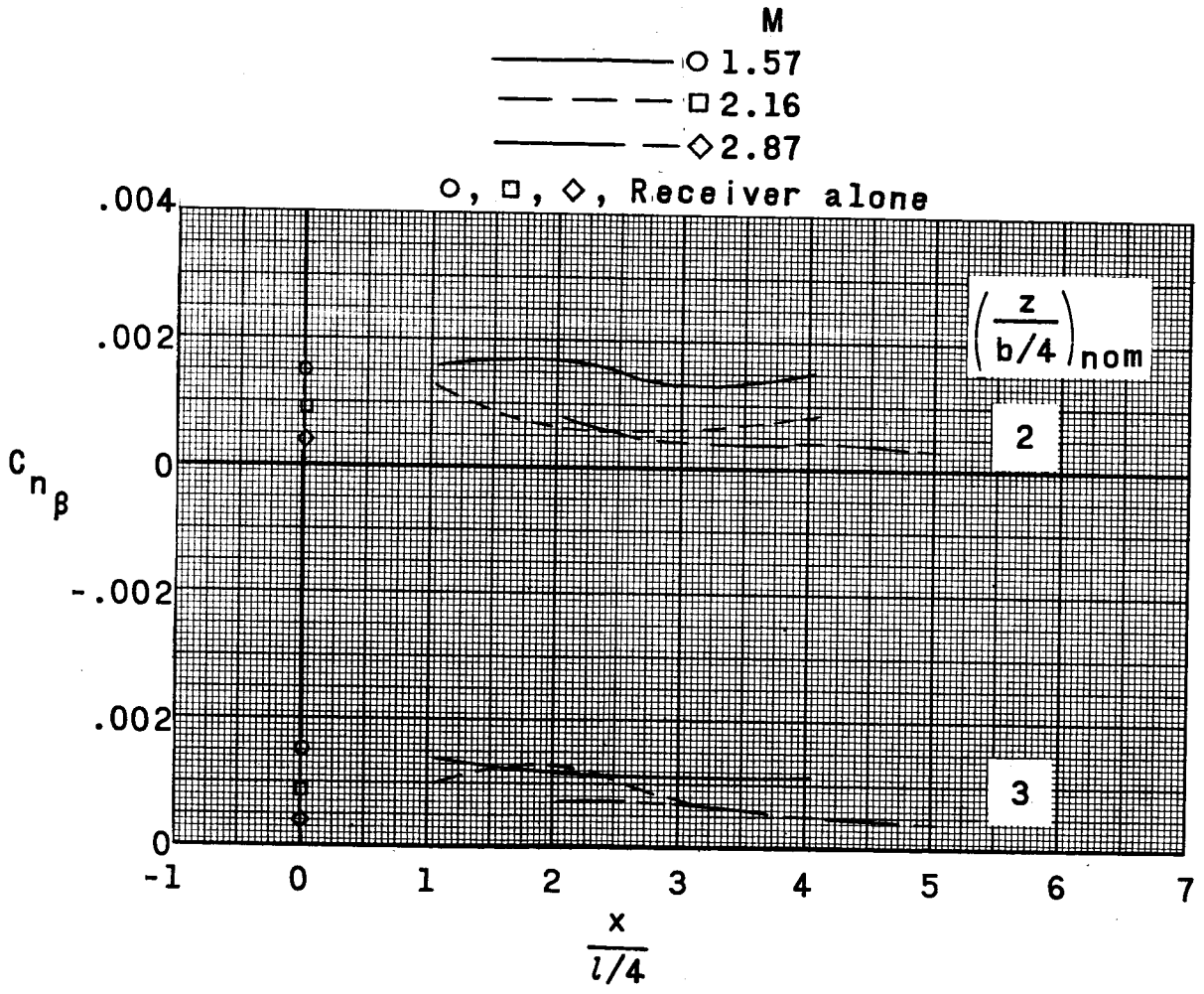

(b) Directional-stability parameter.

Figure 23.- Continued.

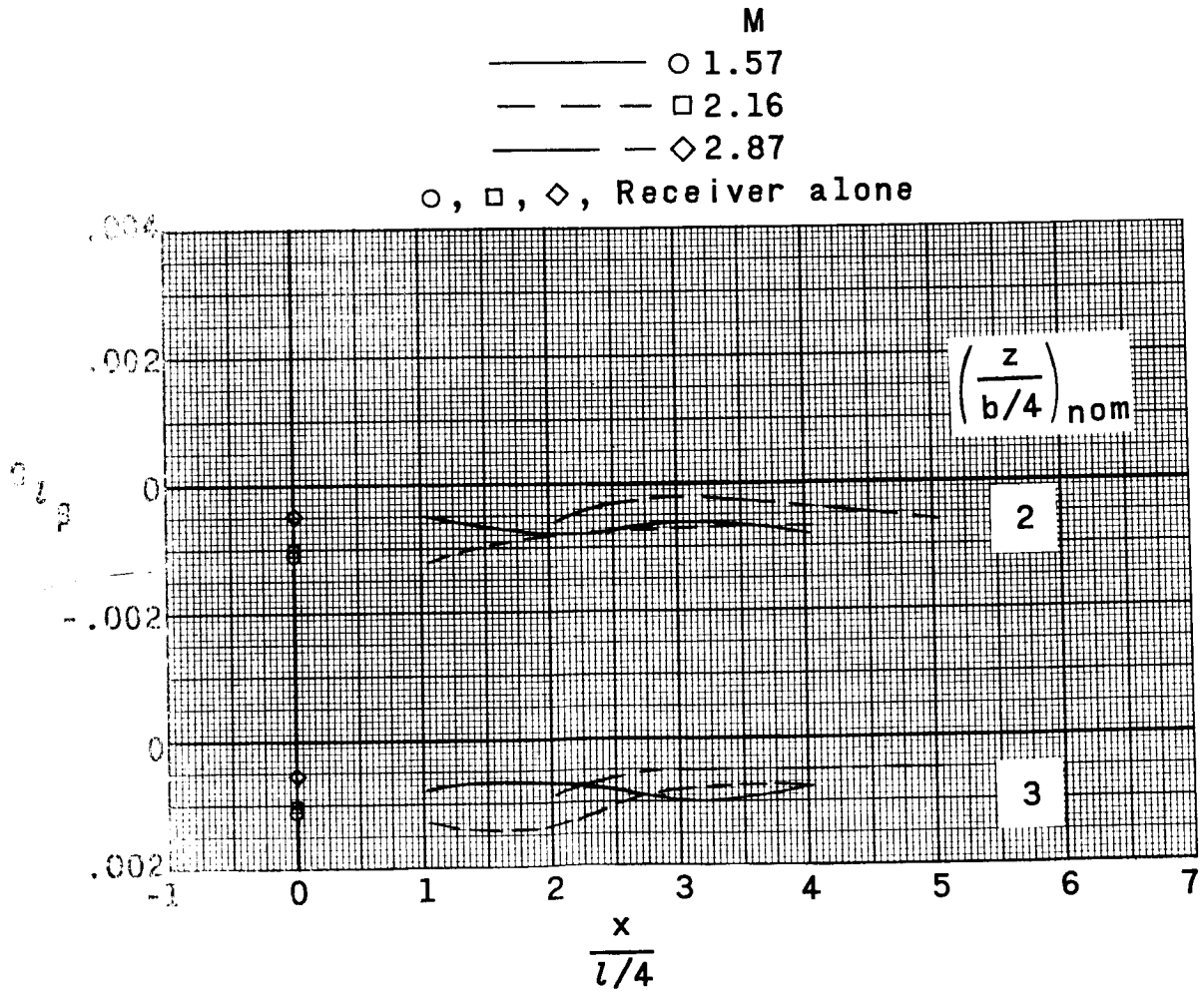

(c) Lateral-stability parameter.

Figure 23.- Concluded.